Université catholique de Louvain
Faculté des bioingénieurs
Earth and Life Institute
Applied Microbiology
Laboratory of mycology

Arbuscular mycorrhizal fungi impact metabolites production of *Anchusa officinalis* L. and *Alkanna tinctoria* Tausch.

Thèse de doctorat présentée par

Annalisa Cartabia

en vue de l'obtention du grade de Docteur en sciences agronomiques et ingénierie biologique

---

Promoteurs

Prof. Stéphane Declerck (UCLouvain, Belgium)
Dr. Ismahen Lalaymia (UCLouvain Belgium)

Membres du jury

Prof. Joëlle Quetin-Leclercq	UCLouvain, Belgium
Prof. Thierry Hance (Président)	UCLouvain, Belgium
Prof. Muriel Quinet (Secrétaire)	UCLouvain, Belgium
Dr. Carolin Schneider	Institut für Pflanzenkultur, Germany
Dr. Pierre-Emmanuel Courty	INRAE Dijon, France

Louvain-la-Neuve, 29 Juin 2023

Acknowledgements

I would like to thank Prof. Stéphane Declerck for having given me the opportunity and guidance to conduct this Ph.D. It was definitely one of the biggest challenges of my life, which included moving to another country. This Ph.D. brought me to the mycology lab of UCLouvain. Here, I found amazing people and colleagues that eventually became good friends and mentors. They never let me feel estranged, and I will always have good memories of the lab time. I truly thank Dr. Ismahen Lalaymia, your support was unlimited in any context since I arrived in Belgium. I would not be writing this part if it was for you. Also, I really want to acknowledge all the technical and affable support I received from the Myco team (Céline, Stephanie, Virginie, Francoise, François, Philip, Benoit, Isabelle, Silvie, Pierre), the postdocs (Maryline, Monica, Bryan, Marco) and my dear Ph.D. colleagues and friends (Marcé, Paola, and Yanyan), and all the others students/support staff that helped me through these years, the list would be too long.

This Ph.D. was mainly supported by the innovative training networks (ITN) project MICROMETABOLITE. Thanks to this ITN project, I had the opportunity to work with different teams all over Europe and to strengthen my work and friendship with many scientists and ESR colleagues, thank you all for the support and collaboration through these years, thanks Cintia, Elodie, Neb, Alicia, Ahmad, the list would be as well too long. The last year of my thesis was supported by the Special Research Funds (FSR) of UCLouvain, which of course I would like to thank.

I truly thank all the key collaborators who helped me in successfully deliver my research: Dr. Nikolaos Tsafantakis, Dr. Evangelia Tsiokanos, Dr. Virginia Sarropoulou, Dr. Katerina Grigoriadou, Dr. Sergio Ortiz, and Prof. Joëlle Quetin-Leclercq.

In 2017, I moved to Louvain-la-Neuve, alone, unaware of what the future had reserved for me. Indeed, I met amazing people who then became my Belgium family, and who supported me from the start of this journey and became dear friends. Thanks, Dani, Auri, Fusi, Presidente, Marti, Giuli, Alessio, Giacomo, and all the others, for the uncountable adventures and beers.

I want to thank also my Italian friends who were always there for me, even if the distance is becoming quite challenging, they remain next to me and always support me, thanks Chichi, Kio, So, Dany, Tommy, Kami, Lory, Nove, Silvia, Chicca. And thanks, as well, to the new friends I made here in Malta, and my dear colleagues "pastizzi" for all the support through this very difficult last year, you made me feel at home even in such a "crazy" country.

I want to dedicate my Ph.D. to my family. You always knew I was not going to come back home, but you had the strength to support me and understand my decision, which for an Italian family it is not an easy task. Thanks, mum and dad, you would do anything for me, and I should thank you more often for this. Thanks, sister, you were my rock through all these years and my first supporter. Thanks to my enlarged family, made of people I truly esteem and love.
(Voglio dedicare questo dottorato alla mia famiglia. Avete sempre saputo in cuor vostro che non sarai tornata a casa, ma avete comunque avuto la forza di sostenermi e capire la mia decisione, cosa non facile per una famiglia italiana. Grazie mamma e papà, fareste di tutto per me, e per questo vi dovrei ringraziare più spesso. Grazie sorella, sei stata la mia roccia in questi anni e la mia prima sostenitrice. Grazie alla mia famiglia estesa, composta da persone che ammiro e amo molto).

Thanks to this Ph.D., I met the most important person in my life, Marco. It was not predicted, but the common passion for science and, apparently, for mushrooms let us find each other. I discovered that Molise does exist and that you can find someone who completes and make you feel better and a better person every day. Home is wherever I'm with you.

The last years passed so fast, and now I'm thinking of all people I have met, and for which I reserved a place in my heart. Cheers to everyone who joined me on my pathway, even if for just a short while, and are still there walking with me. I miss you all and I hope I will see you in new adventures.

Thanks, Annalisa, you made it…

TABLE OF CONTENT

List of abbreviations

ABA	Abscisic Acid
ACP	Acyl Carrier Protein
A/Sd	Alkannin/Shikonin derivatives
AM	Arbuscular Mycorrhiza
AMF	Arbuscular Mycorrhizal Fungi
BA	6-BenzylAdenine
BAS	Branched Absorbing Structure
BCAAs	Branched-Chain Amino Acids
COs	Chitooligosaccharides
CO_4	Chitotetraose
CO_5	Chitopentaose
CMN	Common Mycorrhizal Network
CYP	Cytochrome P450
CSP	Common Symbiosis Signalling Pathway
Ct	Cycle threshold
DAD	PhotoDiode-Array Detector
DAPG	2,4-diacetylphloroglucinol
ECM	Ectomycorrhizae
ER	Endoplasmic Reticulum
ERM	Extraradical Mycelium
ESI	ElectroSpray Ionisation
GA_3	Gibberellic Acid
GABA	Gamma Amino Benzoic Acid
GB5	Gamborg B5
GBA	3-geranyl-4-hydroxybenzoic acid
G*10*H	Geraniol 10-hydroxylase
GHQ	Geranylhydroquinone
GHQ-3″-OH	3″-hydroxy-geranylhydroquinone
GHQH	Geranylhydroquinone 3”-hydroxylase
GINCO	Glomeromycota *IN vitro* COllection
GlcNAc	N-acetylglucosamine
GPAT	Glycerol-3-Phosphate Acyl Transferase
GPP	Geranyl diphosphate
GRSPs	Glomalin-Related Soil Proteins
GS/GOGAT	Glutamine Oxoglutarate Aminotransferase
HBA	p-HydroxyBenzoic Acid
HNQs	Hydroxynaphthoquinone enantiomers
HRCs	Hairy Root Cultures
HRMS	High Resolution Mass Spectrometry

HPLC	High Performance Liquid Chromatography
IAA	Indole-3-Acetic Acid
IBA	Indole-3-Butyric Acid
ISR	Induced Systemic Resistance
ICP-AES	Inductively Coupled Plasma - Atomic Emission Spectroscopy
LC-MS	Liquid Chromatography Mass Spectrometry
LysMs	Lysin Motifs
LPS	Lipopolysaccharides
JA	Jasmonic Acid
MAMP	Microbe Associated Molecular Patterns
MEP	Methylerythritol-4-phosphate
MIR	Mycorrhizal Induce Resistance
MPNS	Medicinal Plant Names Services
MS	Murashige-Skoog
MSR	Modified Strullu-Romand
MSTs	Monosaccharide Transporters
MUCL	Mycothèque de l'Université catholique de Louvain
MVA	Mevalonic acid
Myc-LCOs	Mycorrhizal-LipoChitoOligosaccharides
MS	Mass Spectrometry
NAA	α-Naphthalene Acetic Acid
NaDESs	Natural Deep Eutectic Solvents
NFT	Nutrient Film Technique
ORM	Orchid Mycorrhizas
PAs	Pyrrolizidine Alkaloids
PAI	Peri-Arbuscular Interface
PAL	Phenylalanine Ammonia Lyase
PAM	Peri-Arbuscular Membrane
PCA	Principal Component Analysis
PDA	PhotoDiode Array
PG	Pyroglutamic acid
PGPF	Plant Growth-Promoting Fungi
PGPR	Plant Growth-Promoting Rhizobacteria
PGRs	Plant Growth Regulators
PGT	4-hydroxybenzoate 3-geranyltransferase
PLS-DA	Partial Least Squares Discriminant Analysis
PMs	Primary Metabolites
PPA	Pre-Penetration Apparatus
PPF	Photosynthetic Photon Flux
PSII	Photosystem II

PTs	Phosphorous Transporters
RA	Rosmarinic Acid
RH	Relative Humidity
RLKs	Receptor-Like Kinases
ROS	Reactive Oxygen Species
RFW	Root Fresh Weight
RT	Retention Time
RT-qPCR	Real Time quantitative Polymerase Chain Reaction
RWC	Relative Water Content
SA	Salvianolic Acid
SAR	Systemic Acquired Resistance
S/N	Signal to Noise
SE	Standard Error
SFW	Shoot Fresh Weight
SPE	Solid Phase Extraction
SIMCA	Soft Independent Modelling of Class Analogy
SIS1	SL-Induced putative Secreted protein
SLs	Strigolactones
SMs	Secondary Metabolites
SPSS	Statistical Package for the Social Sciences
SSU	Small SubUnit
TAGs	Triacylglycerols
TCA	Tricarboxylic Acid Cycle
TDW	Total Dry Weight
TFW	Total Fresh Weight
UHPLC	Ultra-High Performance Liquid Chromatography
UV	Ultraviolet
VOCs	Volatile Organic Compounds
WHO	World Health Organization
WPM	Woody Plant Medium

Glossary

Abiotic elicitors: *substances that are of nonbiological origin and are grouped in physical, chemical, and hormonal factors, which induced or enhanced biosynthesis of metabolites* (Naik and Al–Khayri, 2016). See elicitor definition below.

Arbuscular mycorrhizas (AM): *widespread type of endomycorrhizal interactions involving fungi of the phylum Glomeromycota, the hyphae of which reach the root inner cortex and develop highly branched exchange structures called arbuscules* (Bonfante and Genre, 2010).

Bioactive compounds: *can be defined as nutrients and non-nutrients present in the food matrix (vegetal and animal sources) that can produce physiological effects beyond their classical nutritional properties* (Cazarin *et al.*, 2022).

Biotic elicitors: *substances of biological origin that include polysaccharides originated from plant cell walls (e.g., chitin, pectin, and cellulose) and microorganisms, which induced or enhanced biosynthesis of metabolites* (Naik and Al–Khayri, 2016). See elicitor definition below.

Chemometrics: *chemical discipline that uses mathematics, statistics and formal logic to design or select optimal experimental procedures, to provide maximum relevant chemical information by chemical data, and to obtain knowledge about chemical systems* (Brown, 1988).

Elicitor: *substance for stress factors which, when applied in small quantity to a living system, induces or improves the biosynthesis of specific compound which do have an important role in the adaptations of plants to a stressful condition* (Naik and Al–Khayri, 2016).

Endophytes: *important group of widespread and diverse plant symbionts that live asymptomatically and sometimes systematically within plant tissues without any harm or causing diseases in host plants* (Upadhyaya *et al.*, 2020).

Hydroponic systems: *include all systems that deliver the nutrients in a liquid form, with or without an aggregate medium to anchor the plant roots* (Hayden 2006).

Hyperhydricity: *formerly called vitrification, is considered a physiological, biochemistry and morphologic disorder due to abnormal*

accumulation of water inside the cells and tissues (Willadino *et al.*, 2012).

Medicinal plant: *plants that possess therapeutic properties or exert beneficial pharmacological effect on the human or animal body* (Namdeo, 2018).

Metabolite: *class of naturally occurring compounds, diverse in their chemical structure, that are less than 1 kDa in molecular mass. These compounds function as carriers, substrates or products in biochemical pathways* (Khoo and Al-Rubeai, 2007).

Metabolite profiling: *rapid analysis, often not quantitative, of a large number of different metabolites with the objective to identify a specific metabolite profile that characterizes a given sample* (Villas-Bôas *et al.*, 2005).

Metabolomics: *the quantitative measurement of the dynamic multiparametric metabolic responses of living systems to pathophysiological stimuli or genetic modification* (Khoo and Al-Rubeai, 2007).

Micropropagation or ***in vitro* propagation**: *is the clonal propagation of plants by tissue, cell and organ culture methods. It involves the aseptic culture of explants of tissues and organs in closed vessels using defined culture media in a controlled environment* (Debnath and Arigundam 2020).

Mycorrhiza: *is the symbiotic association between a mycorrhizal fungus and the root system of a compatible plant host* (Kokkoris *et al.*, 2020).

Obligate biotroph: *an organism that is unable to complete a reproductive cycle in the absence of a living host* (Parniske, 2008).

Primary metabolites/metabolism: *molecules (e.g., lipids, proteins, nucleic acids, and carbohydrates) that are common to all cells and are required for the proper functioning of cells and organisms* (Hopkins and Hüner, 2008).

Secondary metabolites or **natural products**: *are compounds which act as a defensive role in the interaction of the organism with its environment for survival in the ecosystem and are restricted to particular taxonomic group* (Verpoorte, 1999). *Recently renominated specialized plant metabolites (SPMs)* (Marone *et al.*, 2022).

Target analysis: *quantitative analysis of a class of compounds that are related to a specific pathway or to intersecting pathways, its analytical procedures must include identification and absolute quantification of the selected metabolites in the sample* (Villas-Bôas *et al.*, 2005).

Transcriptome: *full range of RNA molecules expressed by a cell, tissue, or organism in a certain physiological condition or at a specific stage of development* (Wang *et al.*, 2022).

Summary

Beneficial microorganisms (e.g., root or shoot endophytic bacteria or fungi, arbuscular mycorrhizal fungi – AMF) play key roles in plant growth and, for some, may induce/modify the production of primary and/or secondary metabolites (PMs and SMs, respectively) by plants. In this Ph.D., the main objectives were to determine whether AMF could modify the metabolites profiles of *Anchusa officinalis* (L.) and improve the SMs production (mainly alkannin/shikonin and their derivatives, A/Sd) of *Alkanna tinctoria* Tausch. Both plants belong to the Boraginaceae family and are well known to produce therapeutic metabolites.

In the first part of the thesis, the work was focused on *A. officinalis*. Two experiments were conducted. In the first one, plants were associated with *Rhizophagus irregularis* MUCL 41833 and grown in a circulatory semi-hydroponic (S-H) cultivation system. An up-down regulation of specific PMs and SMs was detected both in shoot and root tissues, as well as in the nutrient solution. In the second one, plants were associated with four different AMF strains: *Rhizophagus irregularis* MUCL 41833, *Rhizophagus intraradices* MUCL 49410, *Rhizophagus clarus* MUCL 46238, and *Rhizophagus aggregatus* MUCL 49408. The plants with their fungal associates were grown in a similar S-H cultivation system. A unique effect on the plant's metabolomic profile was demonstrated, which resulted in two differentiated fungal clusters. An enhanced accumulation of PMs and SMs was observed for *R. irregularis* and *R. intraradices*, showing a stronger effect on *A. officinalis* metabolome compared to *R. clarus* and *R. aggregatus*.

In the second part of the thesis, the work was focused on *A. tinctoria*. Four experiments were conducted. In the first one, a protocol for the mass production of *A. tinctoria* plants starting from *in vitro* shoot-tip explants was developed, as it has become an endangered species in several European regions and is difficult to grow artificially due, among others, to low seeds germination. In the second one, *A. tinctoria* plants were associated with *Rhizophagus irregularis* MUCL 41833 and grown in the S-H cultivation system. A significant higher relative expression of specific target genes was observed in mycorrhized plants as compared with the controls. Then, in the third one, plants were associated with four different AMF strains: two from the Glomeromycota *IN vitro* COllection (GINCO) - *Rhizophagus irregularis* MUCL 41833 and *Rhizophagus aggregatus* MUCL 49408

- and two isolated from the roots of wild-growing *A. tinctoria* - *Rhizophagus irregularis* and *Septoglomus viscosum*. The plants with their fungal associates were grown in a similar S-H cultivation system. In the fourth experiment, *A. tinctoria* were associated with three AMF strains (one from GINCO - *Rhizophagus irregularis* MUCL 41833 - and two natives - *Rhizophagus irregularis* and *Septoglomus viscosum*) and grown in pots under the same greenhouse conditions as for the S-H system above. Interestingly, *A. tinctoria* associated with the native AMF *Rhizophagus irregularis* were characterized by a higher content of total shikonin equivalent, which was also reported in the plants grown in the pot experiment.

In conclusion, this Ph.D. confirmed the key role of AMF in the metabolism modulation of two major medicinal plants (*A. officinalis* and *A. tinctoria*). *Anchusa officinalis* colonization by *R. irregularis* MUCL 41833 was followed by an enhanced production of PMs, including organic acids and key amino acids, and SMs, especially phenolic compounds and oleanane-types glycosidic derived from the phenylpropanoid and mevalonate pathways, respectively. Moreover, the production of two new derivatives of salvianolic acids (SA) and one new derivative of rosmarinic acid (RA), was reported in the roots of mycorrhized plants. Furthermore, specific biosynthetic pathways were demonstrated to be differently influenced by AMF through a qualitative and quantitative production of different metabolites. A higher accumulation of phenolic compounds and of saponins was detected in roots and shoots of *A. officinalis* associated specifically with *R. irregularis* and *R. intraradices*. Among them, six new SMs were tentatively identified including two acetyl- and four malonyl-phenylpropanoid and saponin derivatives. Finally, native AMF isolated from wild-growing *A. tinctoria*, were reported to be particularly efficient in enhancing the production of A/S derivates in *A. tinctoria* roots. As a conclusion, the best performing AMF strains should be further explored to better understand their regulatory mechanisms and their potential use in scale-up experiments. This could help improving the production of specific therapeutic compounds and to limit the exploitation of endangered plants from the wild. It would also be crucial to further study the application of circulating nutrient solutions, in order to set up *ad hoc* systems for the extraction of therapeutic compounds exuded by plant roots. For instance, innovative extraction methods, such as eco-friendly solvents (natural deep eutectic solvents – NaDESs)

or resin cartridges (e.g., amberlite XAD), could be implemented in hydroponic systems in a non-destructive extraction way.

Outline of the thesis

Within this thesis, different experiments were conducted to address the following three main objectives:

- Investigate whether AMF species from GINCO impact the metabolome of *A. officinalis* plants and determine which primary and secondary metabolites are up-down regulated.
- Develop an optimal protocol for the mass production of *A. tinctoria* plants starting from *in vitro* shoot-tip explants.
- Investigate whether AMF species sampled from the wild on *A. tinctoria* impact more markedly the production of important therapeutic compounds in *A. tinctoria* roots as compared to AMF species from GINCO.

The successive steps followed in this study are schematized here:

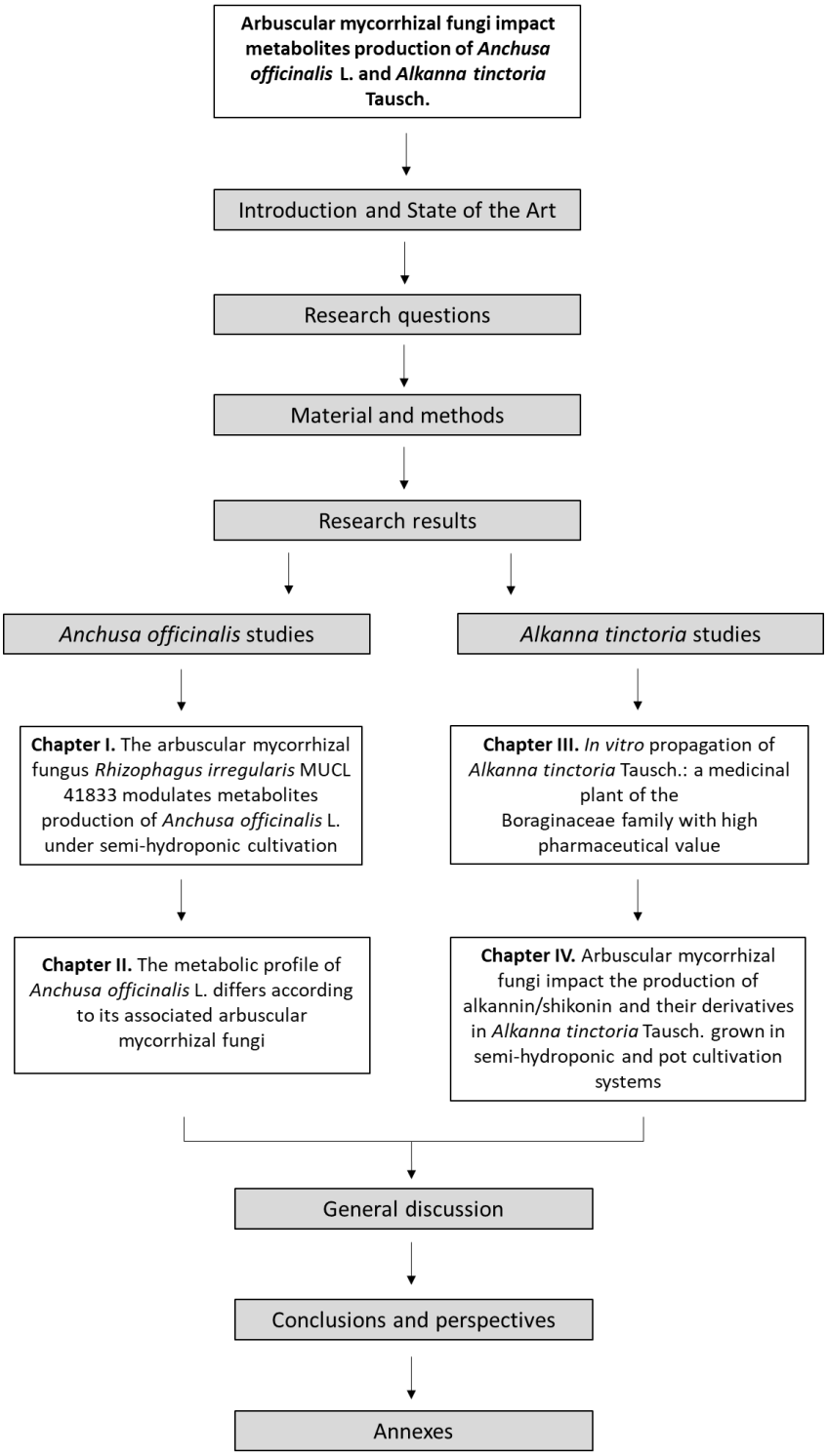
Arbuscular mycorrhizal fungi impact metabolites production of *Anchusa officinalis* L. and *Alkanna tinctoria* Tausch.
Introduction and State of the Art
Research questions
Material and methods
Research results
Anchusa officinalis studies
Alkanna tinctoria studies
Chapter I. The arbuscular mycorrhizal fungus *Rhizophagus irregularis* MUCL 41833 modulates metabolites production of *Anchusa officinalis* L. under semi-hydroponic cultivation
Chapter III. *In vitro* propagation of *Alkanna tinctoria* Tausch.: a medicinal plant of the Boraginaceae family with high pharmaceutical value
Chapter II. The metabolic profile of *Anchusa officinalis* L. differs according to its associated arbuscular mycorrhizal fungi
Chapter IV. Arbuscular mycorrhizal fungi impact the production of alkannin/shikonin and their derivatives in *Alkanna tinctoria* Tausch. grown in semi-hydroponic and pot cultivation systems
General discussion
Conclusions and perspectives
Annexes

In the **Introduction** section, the context and the general objectives of the study were presented.

In the **State of the Art** section, the most recent and relevant literature on AMF and their effects on metabolism of medicinal plants were reviewed.

In the **Materials and Methods** section, the biological materials were presented as well as the main methods and techniques used throughout the thesis.

The **Research results section** was divided in two parts focusing on *Anchusa officinalis* L. (**Part 1**) and *Alkanna tinctoria* Tausch. (**Part 2**).

Part 1 was divided in two chapters:

Chapter I aimed to assess the effects of the AMF *Rhizophagus irregularis* MUCL 41833 on the accumulation and exudation of PMs and SMs by *A. officinalis* grown in the S-H cultivation system.

Increased production of PMs and SMs, and detection of new SMs derivatives, were reported in mycorrhized *A. officinalis*.

The results of Chapter I were published in frontiers in Plant Science (2021) 12:724352.

Chapter II aimed to assess the impact of four AMF strains (i.e., *R. irregularis* MUCL 41833, *R. clarus* MUCL 46238, *R. aggregatus* MUCL 49408 and *R. intraradices* MUCL 49410) on the metabolomic profile of *A. officinalis* grown in the S-H cultivation system.

Increased production of phenolic and saponin metabolites was detected in *A. officinalis* associated specifically with *R. irregularis* and *R. intraradices.*

The results of Chapter II were published in *Metabolites* (2022) 12(7), 573.

Part 2 was divided in two chapters:

Chapter III aimed at developing an optimal protocol for the *in vitro* mass production of *A. tinctoria* plants.

The protocol allowed the production under *in vitro* culture conditions of a sufficient number of *A. tinctoria* plants with high levels of *ex vitro* survival.

The results of Chapter III were published in Industrial Crops & Products 182 (2022) 114860.

Chapter IV aimed at evaluating the effect of four AMF strains (two from GINCO - *Rhizophagus irregularis* MUCL 41833 and *Rizhophagus aggregatus* MUCL 49408 - and two natives - *Rhizophagus irregularis* and *Septoglomus viscosum*) on the production of A/Sd and their corresponding genes expression in *A. tinctoria* grown in S-H cultivation and pot systems.

The results of Chapter IV are submitted to frontiers in Microbiology section Microbe and Virus Interactions with Plants (2023).

Increased production of A/Sd was detected in *A. tinctoria* associated with native *R. irregularis*. Upregulation of specific target genes was reported in mycorrhized plant.

In the **General Discussion** section, the major findings of the thesis were summarized and discussed.

Finally, in the **Conclusions** and **Perspectives** section, the major outcomes of the thesis were given and commented. Further studies to improve our understanding of the impacts of AMF in the production of metabolites and their adequate application in the industry were proposed.

Author's contribution

The work presented here was realized during the time course of my Ph.D.

The Introduction and State of the Art as well as Material and Methods, General Discussion, Conclusions and Perspectives were written by me. These parts were not published.

Chapter I and **Chapter II** are research papers published in frontiers in Plant Science (2021) and in *Metabolites* (2022), respectively. My contribution for both papers was approximately 50%. The experiments set up and data collection on AMF-growth parameters and nutrients uptake were performed by me with the help of Ms. Maria Miguel and Dr. Ismahen Lalaymia (UCLouvain Earth and Life Institute - Applied Microbiology - Laboratory of Mycology). The data analysis with SPSS was performed by me with the help of Ms. Rebecca Marion (Statistical Methodology and Computing Service/Louvain Institute of Data Analysis and Modelling in Economics and Statistics, SMCS/LIDAM, UCLouvain). The extraction of plant metabolites and exudates were done by me in collaboration with Dr. Evangelia Tsiokanos and Dr. Nikolaos Tsafantakis (Department of Pharmacognosy and Natural Product Chemistry of the National and Kapodistrian University of Athens). They also provided the metabolomic data analysis and the tentative identification of up-down regulated compounds, with the supervision of Prof. Nikolas Fokialakis and in collaboration with Dr. Aikaterine Termentzi (Benaki Phytopathological Institute). Writing of the papers was conducted mostly by me and by Dr. Evangelia Tsiokanos. All the authors contributed to its revision and finalization.

Chapter III is a research paper published in Industrial Crops & Products (2022). My contribution to this work was approximately 50%. Part of the experimental set up, data collection of plant growth parameters, and statistical analysis were performed by me. Further experimentations, data collection and discussion of the results were provided by Dr. Virginia Sarropoulou (Institute of Plant Breeding and Genetic Resources, Hellenic Agricultural Organization, HAO-DEMETER). Writing of the paper was conducted mostly by me and by Dr. Virginia Sarropoulou. All the authors contributed to its revision and finalization.

Chapter IV is a research paper submitted to frontiers in Microbiology section Microbe and Virus Interactions with Plants

(2023). My contribution was approximately 50%. The experimental set up was done by me with the help of Ph.D. YanYan Zhao (UCLouvain Earth and Life Institute - Applied Microbiology - Laboratory of Mycology). Data collection on AMF-growth parameters, A/S derivates production and genes expression, data analysis and writing of the paper were conducted by me in collaboration with Ph.D. YanYan Zhao and Dr. Ismahen Lalaymia. Extraction of the metabolites and HPLC analysis (validation) were done in collaboration with Dr. Sergio Enrique Ortiz Aguirre (Faculty of Pharmacy and Biomedical Sciences Pharmacognosy lab, Louvain Drug Research Institute, UCLouvain). He also provided data from the mass spectrometry analysis and identification of A/Sd, with the help of Prof. Joëlle Leclercq. Help in the RNA extraction and genes expression analysis was provided by Ms. Stéphanie Huret (Technician at UCLouvain Earth and Life Institute - Applied Microbiology - Laboratory of Mycology). Primers utilized in the RT-qPCR were chosen with the help of Dr. Ahmad Muhammad (Austrian Institute of Technology, Center for Health and Bioresources, Tulln). Ms. Catherine Rasse (Statistical Methodology and Computing Service/Louvain Institute of Data Analysis and Modelling in Economics and Statistics, SMCS/LIDAM, UCLouvain) gave statistical support. Writing of the paper was conducted mostly by me and by YanYan Zhao. All the authors contributed to its revision and finalization.

For all the Chapters, Prof. Declerck gave substantial contributions to the conception and design of the experiments, interpretation of the data, draft corrections, final approval, and agreement with all aspects of the works.

INTRODUCTION

This Ph.D. was part of the innovative training networks (ITN) project MICROMETABOLITE[1], which has received funding from the European Union's Horizon 2020 research and innovation programme, under the Marie Skłodowska-Curie grant agreement [No 721635]. This project aimed to explore the impact of the plant-associated microbiome (i.e., bacteria and fungi) on the production of secondary metabolites that are of high value for industrial applications. It focused on members of the Boraginaceae plant family, more specifically on *Lithospermum erythrorhizon* and *Alkanna tinctoria*. These plants produce the naphtoquinones alkannin and shikonin and their derivatives (A/Sd), which are used in several pharmaceutical and cosmeceutical preparations that are already on the market or in the final stages of development. Due to the lack of plant material and poor seeds germination of *A. tinctoria*, another Boraginaceae plant, *Anchusa officinalis*, was also included in the study.

Plants are the basis of drug development and continually contribute to the discovery of new metabolites of pharmaceutical interest. Nowadays, around 25% of worldwide-prescribed drugs find their origin in plants (Sahoo *et al.*, 2010) and many more are inspired from plant metabolites. Several interesting pharmaceutical-relevant plant species belong to the Boraginaceae family [e.g., *Anchusa officinalis* (L.) and *Alkanna tinctoria* Tausch.]. Their therapeutic properties are due to the content of various biologically-active substances such as naphthoquinones, flavonoids, terpenoids and phenols (Ali *et al.*, 2014).

Anchusa officinalis is characterized by the predominant presence of phenolic compounds, especially caffeic acid esters, such as rosmarinic acid (RA), which gives its extracts antioxidant, antibacterial, and anti-inflammatory activities (Dresler *et al.*, 2017). *Alkanna tinctoria* produces the naphthoquinones alkannin/shikonin and their derivates (A/Sd), which are well known small molecules with a wide range of biological properties, such as tissue regeneration, wound healing, antimicrobial, anti-inflammatory, anti-HIV-1, and anticancer activities (Papageorgiou *et al.*, 1999).

[1] http://micrometabolite.eu/

A growing body of evidence suggests that plant-associated microorganisms (i.e., endophytes or symbionts) have a marked impact on the chemical composition of their host (Goh *et al.*, 2013; Mitter *et al.*, 2013). Among them are the arbuscular mycorrhizal fungi (AMF). These soil inhabitants form the most ancient and widespread plant-fungal symbiosis on earth. They receive carbohydrates and lipids from the plant, necessary for the completion of their life cycle, in exchange for minerals and water (Smith *et al.*, 2011; Begum *et al.*, 2019). This relationship improves plant resistance/tolerance to unfavourable environmental conditions (e.g., drought, salinity) and to pests and diseases (Gianinazzi *et al.*, 2010). Interestingly, a number of studies have reported that AMF influence the production of primary metabolites (PMs) in plants, and impact various biosynthetic pathways involved in the production of secondary metabolites (SMs) in leaves, roots or fruits/tubers of different crops used as food or for medicinal purpose (Pedone-Bonfim *et al.*, 2015; Avio *et al.*, 2018; Pandey *et al.*, 2018; Kaur and Suseela, 2020).

So far, metabolomics studies on AMF-associated plants have mainly been conducted in pots or fields under semi-controlled conditions. However, the development of highly controlled and up-scalable bioreactors or semi-hydroponic (S-H) cultivation systems have gained importance, allowing in particular the discovery of biotic elicitors for the production of metabolites of interest (Malik *et al.*, 2016). These systems, in addition to supporting the biosynthesis of bioactive compounds (Gontier *et al.*, 2002; Sgherri *et al.*, 2010), could include microorganisms of interest (e.g., AMF). Moreover, most of the studies applying a full metabolomics profile approach have been limited to the AMF *R. irregularis* and/or *Funneliformis mosseae* (Hill *et al.*, 2018). Though, it is known that not all plant-AMF associations are mutually beneficial and that host plant productivity is highly dependent on the identity of the AMF symbiont (Kaur and Suseela, 2020). Thus, diverse AMF species or strains can affect differentially the production of specific phytochemicals in the same plant species (Rivero *et al.*, 2015).

Until today, no study has reported the beneficial effects of AMF on the production of metabolites of interest in *A. officinalis* and *A. tinctoria*. Therefore, the objective of this Ph.D. was to investigate the effects of AMF on the metabolic reprogramming of *A. officinalis* and on the A/Sd production of *A. tinctoria* growing under a S-H cultivation system. This study was not limited to a single AMF (i.e., *R. irregularis*),

but was extended to three AMF (*R. intraradices*, *R. clarus*, and *R. aggregatus*) from the GINCO collection and two AMF (*R. irregularis* and *S. viscosum*) isolated from *A. tinctoria* growing wild in Greece. Moreover, for *A. tinctoria*, two cultivation systems were compared: the semi-hydroponic and a conventional pots system.

STATE OF THE ART

I. Medicinal plants

1. Pharmaceutical "bioreactors"

Plants have been exploited by humans for food, shelter, fuel, clothing, art, and health since ancient times. Moreover, humans depend on many complex substances produced by plants, such as dyes, tannins, waxes, resins, flavourings, medicines, and drugs (Shoemaker, 1994). In fact, they have been used as an important source of medicine in pharmaceutical biology since thousands of years. Scripts reporting on medicinal plants date back nearly 5000 years in India, China and Egypt, and at least 2500 years in Greece and Central Asia (Jamshidi-Kia *et al.*, 2018). According to estimates by the World Health Organization (WHO), even today, up to 80% of the world's population depends on traditional medicines for primary health care needs (Pandey *et al.*, 2018a).

Medicinal plants are a rich source of bioactive compounds, which are widely used as drugs for their therapeutic properties (Kilam *et al.*, 2017). Different plant parts can be exploited, such as seeds, roots, leaves, fruits, skin, flowers or even the whole plant. The bioactive compounds have direct or indirect therapeutic effects (Jamshidi-Kia *et al.*, 2018). Clinical, pharmaceutical, and chemical studies of these compounds are the basis of many early drugs, digoxin (from *Digitalis sp*.), morphine (from *Papaver somniferum*), quinine (from skin of *Cinchona sp.*) and pilocarpine (from *Pilocarpus microphyllus*) (Jamshidi-Kia *et al.*, 2018). Natural medicines have gained popularity among consumers as they are effective and safe to use and have moderate side effects (Kilam *et al.*, 2017). Demand for wildlife sources has increased by 8-15% per year in Europe, North America, and Asia over the past decades (Jamshidi-Kia *et al.*, 2018). Since medicinal plants are mostly harvested from the wild, are not evenly distributed around the world, and are increasingly in demand, large-scale production methods using modern tools have been developed (Kilam *et al.*, 2017). The number of plants covered by "pharmacopoeias", which are official publications providing detailed descriptions and tests to

identify and assess the quality of plants used in herbal drugs, represents only a small percentage of the plant diversity used in traditional medicines. Kew's Medicinal Plant Names Services (MPNS), collated information on the names of 28,187 species recorded as being used medicinally, but found that only 4,478 are cited in official regulatory publications (Allkin, 2017). Increasing demand for herbal medicines threatens wild populations of many of these plants. Of the 28,187 species recorded in MPNS, approximately 1,280 are under protection under the Convention on International Trade in Endangered Species of Wild Fauna and Flora (CITES).

2. Metabolism and relevant compounds

The wide assortment of phytochemicals produced by plants falls into two categories: primary and secondary metabolites[2]. At the biosynthetic level, PMs and SMs share many identical intermediates and are derived from the same core metabolic pathways (**Figure 1**). However, in the strictest sense, SMs are not part of the essential molecular structure or function of the cells. They are usually, but not always, produced in relatively small quantities and may be widespread or restricted to particular plant families, genera, or even species (Hopkins and Hüner, 2008). Secondary metabolites are often coloured, fragrant, or flavourful compounds and they are generally involved in the interaction of plants with other organisms and the environment.

[2] Recently renamed specialized plant metabolites (SPMs) to highlight their importance in a broad range of biological functions (Marone *et al.*, 2022).

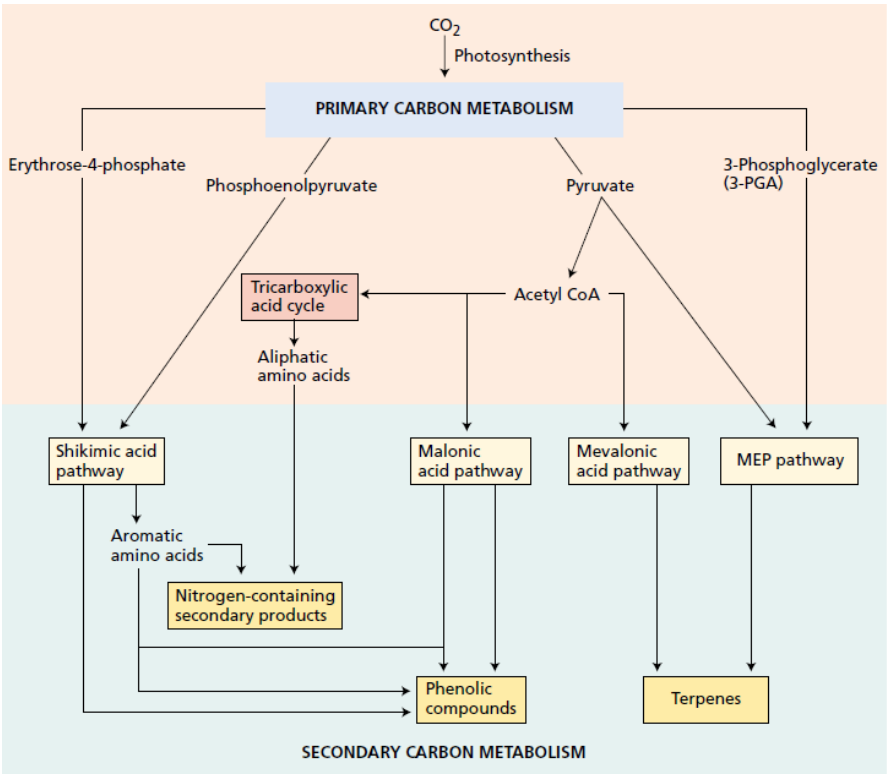

Figure 1. Simplified view of the major biosynthetic pathways of secondary metabolites and their relationship to primary metabolism (from Taiz and Zeiger, 2010).

Primary metabolites comprise many different types of organic compounds, including, but not limited to, carbohydrates, lipids, proteins, and nucleic acids. They are found in all plants because they are the components or products of fundamental metabolic pathways or cycles, such as glycolysis, the tricarboxylic acid cycle (TCA) and Calvin cycles.

Carbohydrates (e.g., glucose**,** sucrose, trehalose) are well known for their essential role as vital sources of energy and carbon skeletons for organic compounds and storage components. Hence, as they interact with diurnal changes, abiotic and biotic stresses, and hormone signalling, carbohydrates are considered as actors of a complex communication system necessary for the coordination of metabolism with growth, development, and responses to environmental changes and stresses. In addition, there is growing evidence for a role of carbohydrates, especially the disaccharides sucrose and trehalose, as

antioxidants because they possess reactive oxygen species (ROS) scavenging properties (Trouvelot *et al.*, 2014).

Lipids are essential for the integrity of cells and organelles by acting as hydrophobic barriers for the membranes. Moreover, they are stored in the form of chemical energy in seeds, and they act as signal molecules to regulate cell metabolism. Fatty acids, the major lipids in plants, are synthesized in plastid and assembled by glycerolipids or triacylglycerols in endoplasmic reticulum (Kim, 2020).

Organic acids (e.g., citrate, malate, oxalate) are intermediates of the TCA cycle and their main site for intracellular biosynthesis is the mitochondria. They are of fundamental importance at the cellular level for several biochemical pathways, including energy production, and as precursors for amino acids biosynthesis, and at the whole plant level for modulating adaptation to environment (Panchal *et al.*, 2021).

Amino acids are precursors of proteins synthesis. They participate in both primary and secondary metabolic processes associated with plant development and stress responses. For example, glutamine, glutamate, aspartate, and asparagine serve as pools and transport forms of nitrogen, as well as in balancing the carbon/nitrogen ratio (Galili *et al.*, 2008). Other amino acids (e.g., tryptophan, methionine, proline, arginine) contribute to plant tolerance against biotic and abiotic stresses directly or indirectly by serving as precursors to secondary products and hormones (Galili *et al.*, 2008). In fact, as reported in more details below, the biosynthesis of most phenylpropanoids (e.g., lignols, flavonoids, coumarins, stilbenes, catechin) begins with the aromatic amino acids phenylalanine, tyrosine, and tryptophan, which are synthesized from phosphoenolpyruvate and erythrose-4-phosphate by a sequence of reactions known as the shikimic acid pathway.

The shikimic acid pathway is common to bacteria, fungi, and plants, but is not found in animals. Phenylalanine and tryptophan are consequently among the ten amino acids considered essential for animals (including humans) and represent the principal source of all aromatic molecules in animals (Hopkins and Hüner, 2008). The ‘‘essential amino acids’’ (e.g., lysine, methionine, threonine) indicate the nutritional quality of plants as foods and feeds. Humans as well as most livestock, cannot synthesize these compounds and therefore depend on their diets to obtain them. Thus, the therapeutic use of amino acids (e.g., branched-chain amino acids – BCAAs – leucine, isoleucine,

valine, and glutamine) present a viable and important option for natural medicine (Tamanna and Mahmood, 2014). In addition to the shikimic acid pathway, the mevalonic acid (MVA) as well as the methylerythritol-4-phosphate (MEP) pathways give rise to both PMs and SMs.

Secondary metabolites were thought, for many years, to be simply functionless end products of metabolism, or metabolic wastes. Studies of these substances were initiated in the 19th and early 20th centuries by organic chemists who became interested in them because of their importance as medicines, poisons, flavourings and industrial materials (Taiz and Zeiger, 2010). Secondary metabolites extracted from plants are broadly classified into three major classes namely phenolics, alkaloids, and terpenoids.

Phenolic compounds or ***phenolics*** are chemically defined as compounds containing or derived (esters, ethers, etc.) from hydroxylated aromatic rings. They represent a chemically heterogeneous group of nearly 10,000 compounds. Two major groups of plant phenols are phenolic acids (C6-C1 skeleton) and phenylpropanoids (C6-C3 skeleton). Plant phenolics are synthesized by several different routes and thus constitute a heterogeneous group from a metabolic point of view. Two basic pathways are involved: the shikimic acid pathway (as reported above) and the malonic acid pathway (Taiz and Zeiger, 2010). Deamination of phenylalanine to cinnamic acid, catalyzed by the enzyme phenylalanine ammonia lyase (PAL), effectively diverts carbon from primary metabolism into the synthesis of a wide range of SMs based on simple phenolic acids (Hopkins and Hüner, 2008a). They are widespread in plants and subdivided into seven groups according to their structure: simple phenolics, tannins, coumarins, flavonoids, chromones/xanthones, stilbenes and lignans (Hussein and El-Anssary, 2019).

Some phenolics are valued pharmacologically for their anti-inflammatory activities, such as quercetin, or antihepatotoxic properties, such as silybin. Others exert a phytoestrogenic activity as genistein and daidzein, and some are insecticidal as naringenin. Many of the phenolic compounds are also effective antioxidants and free radical scavengers, especially flavonoids (Hussein and El-Anssary, 2019). In addition, many phenolic compounds appear to be involved in plant/herbivore interactions, serve as attractants for pollinators and to function as agents of plant-plant competition and plant-microbe

symbioses. Finally, some (e.g., lignin) are important structural compounds (Taiz and Zeiger, 2010).

Alkaloids are SMs characterized, as a general chemical feature, by the presence of at least one nitrogen. They have extremely divergent chemical structures including heterocyclic ring systems and they encompass more than 20,000 different molecules in organisms (Eguchi *et al.*, 2019). Despite the extensive variation in structure, alkaloids are generated from a limited number of simple precursors. Most are synthesized from a few common amino acids, such as tyrosine, tryptophan, ornithine or argenine, and lysine (Hopkins and Hüner, 2008a).

Alkaloids demonstrate a diverse array of pharmacological actions (e.g., analgesia, local anaesthesia, cardiac stimulation, respiratory stimulation, and relaxation) as well as activity against herbivores and toxicity in vertebrates. Moreover, antibacterial, antifungal, antiviral and allelopathic properties have been reported in the literature (Hussein and El-Anssary, 2019).

Terpenoids are a class of SMs with nearly 15,000 structures known. They derive from the MVA and MEP pathways that give rise to isopentenyl pyrophosphate and dimethylallyl pyrophosphate, which form the basis for the terpenoid family (Hopkins and Hüner, 2008a). Terpenes can be grouped into several classes, based on the number of carbon atoms. Moreover, they include PMs such as phytol (a portion of the chlorophyll molecule), membrane sterols, carotenoid pigments, and the hormones gibberellin and abscisic acid (ABA), and many of the essential oils that give plants their distinctive odours and flavours.

Terpenoids have significant commercial value as well as important physiological roles. In fact, the terpenoids derivatives considered as PMs play significant roles in plant growth and development. Nonetheless, the vast majority of terpenoids are SMs, many of which appear to act as toxins or feeding deterrents to herbivorous insects (Hopkins and Hüner, 2008).

Other SMs or group of SMs having therapeutic properties.

Saponins are triterpenoids or steroids containing one or more sugar units. The combination of a relatively hydrophobic triterpene with a hydrophilic sugar gives to saponins the properties of a surfactant or detergent. Saponins from the bark of *Quillaja saponaria* Molina have

been used as surfactants in photographic film, in shampoos, liquid detergents, etc., while saponin glyscyrrhizin from licorice (*Glyscyrrhiza glabra* L.) has been used in medicines and as a sweetener and flavour-enhancer in foods and cigarettes (Hopkins and Hüner, 2008).

Naphthodianthrones such as hypericin and pseudohypericin (anthraquinone derivatives), are mainly extracted from *Hypericum* species, characterized by various pharmaceutical properties (e.g., sedatives, antiseptics, and antispasmodics).

Naphthoquinones are natural products that are widespread in nature. The chemical structure of monomeric naphthoquinones is based on the naphthalene skeleton with carbonyl groups in positions C1 and C4 (1,4-naphthoquinones) or in C1 and C2 (1,2-naphthoquinones). In addition to a great variety of possible substituent groups, monomeric naphthoquinones may be joined together forming dimers, trimers and, more rarely, tetramers. Most of them are coloured compounds, varying from yellow to orange and brown (Babula *et al.*, 2009). The known spectrum of activity of naphthoquinones includes antibiotic, antiviral, anti-inflammatory, and antiproliferative effects. These properties have been attributed to their ability to produce oxygen free radicals as well as their electrophilicity, which allows them to form adducts with cellular constituents (Papageorgiou *et al.*, 2008). Naphthoquinones, specifically isohexenylnaphthazarins (alkannin/shikonin derivatives), are found in the root periderm of several Boraginaceous plants (Durán *et al.*, 2017).

3. The Boraginaceae family

The Boraginaceae family comprises approximately 2,000 species distributed mainly in Europe and Asia (Dresler *et al.*, 2017). They produce and accumulate bioactive compounds that comprise naphthoquinones, flavonoids, terpenoids and phenols (Sharma *et al.*, 2009). These SMs have specific therapeutic effects such as antimicrobial, antitumor, antiviral, anti-inflammatory and cardiotonic. Most Boraginaceae produce the red pigments naphthoquinone enantiomers A/S, which have been used since ancient times as dye and remedy with a wide range of effects (Papageorgiou *et al.*, 2008).

Therefore, traditional and modern medicine have explored the pharmacological potential of various species of Boraginaceae.

a. *Anchusa officinalis* (L.)

Anchusa officinalis, commonly known as blush, duck nest or common bugloss, is a perennial herbaceous weed with a tendency to a biennial lifecycle. It is native to the Mediterranean region, mainly distributed in the southern part of the Balkan Peninsula (Selvi and Bigazzi, 1998) (**Figure 2a**), in sunny warm places such as fields, meadows, and river sediments. It is also found in northern regions of Europe.

In the first year of growth, young plants bear a rosette of narrow lanceolate shaped leaves from which, in subsequent years, shoots (10-80 cm high) covered with bristly hairs develop. Flowering occurs from May to September and each inflorescence develops tubular purplish-blue flowers (Chwil and Weryszko-Chmielewska, 2012) (**Figure 2b**).

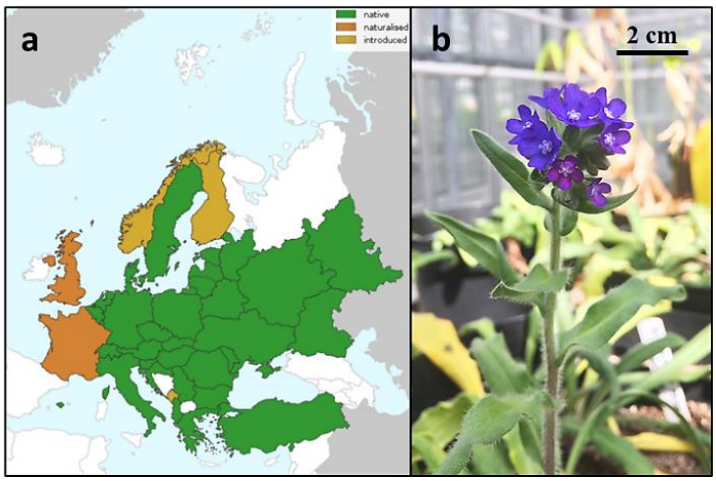

Figure 2. **(a)** Distribution of *Anchusa officinalis* plants (from Euro+Med PlantBase-ww2.bgbm.org/EuroPlusMed/). **(b)** *Anchusa officinalis* plants growing in the greenhouse of UCLouvain, detail of the inflorescence.

A phytochemical screening, performed on wild plants by Jakovljević *et al.* (2016) and Boskovic *et al.* (2018), demonstrated the presence of an abundant content of phenolic compounds, among which the most dominant were rosmarinic acid (RA), chlorogenic acid (CGA),

naringenin (NG), lutein-glycoside and rutin. These compounds exhibit several health-related properties (Dresler *et al.*, 2017) conferring antioxidant, antibacterial and anti-inflammatory activities to *A. officinalis* extracts. The polyphenol rosmarinic acid (**Figure 3**), is an efficient antagonist of lipid peroxidation and is able to insert spontaneously in lipid membranes, with a higher affinity for unsaturated than for saturated lipids (Fadel *et al.*, 2011). However, a review from El-Shazly and Wink (2014), described the presence of pyrrolizidine alkaloids (PAs), toxic compounds that can alkylate DNA after metabolization by hepatic enzymes, causing mutations and even cancer mainly in humans and livestock liver.

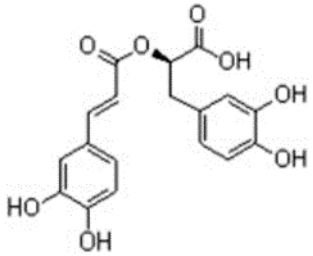

Figure 3. Chemical structure of rosmarinic acid (from Fadel *et al.*, 2011).

Regarding specifically the PAs content in *A. officinalis*, 7-acetyllycopsamine, curassavine, intermedine, and lycopsamine have been described. Nevertheless, a great interest emerged for the use of this plant species as source of high value therapeutic compounds. However, the phytochemical characterisation of *A. officinalis* is limited, and, to our knowledge, no studies exist regarding symbiotic relationships between this species and beneficial microorganisms, such as AMF.

b. *Alkanna tinctoria* Tausch.

Alkanna tinctoria, commonly known as alkanet or dyers' bugloss/alkanet, is a perennial herbaceous plant belonging to the Boraginaceae family. It is found across southern Europe, northern Africa, and southwestern Asia, with a central distribution in the Mediterranean region (Valdés, 2011) (**Figure 4a**). It blooms between March and May, giving rise to small flowers with a bright blue colour (**Figure 4b**). The germination rate is very low, and seeds may take up

to four weeks to germinate. It has an extensive root system, exhibiting a dark reddish colour, which has attracted the attention of botanists and philosophers for centuries (**Figure 5**).

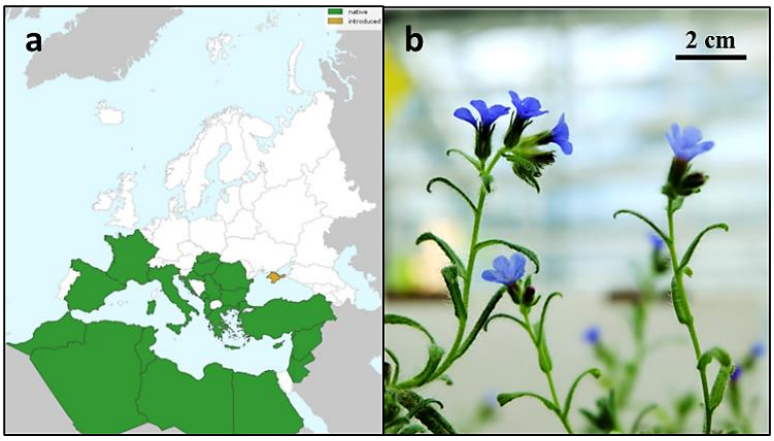

Figure 4. **(a)** Distribution of *Alkanna tinctoria* plants (from Euro+Med PlantBase-ww2.bgbm.org/EuroPlusMed/). **(b)** *Alkanna tinctoria* plants growing in the greenhouse of UCLouvain, detail of the inflorescence.

Figure 5. Details of the characteristic reddish colour of the root system of *Alkanna tinctoria* due to the presence of naphthoquinone enantiomers A/S (greenhouse, UCLouvain).

This plant has a long history of medicinal (e.g., treatment of ulcers) and dye uses, already mentioned more than 2000 years ago by Hippocrates and Theophrastus (Papageorgiou *et al.*, 1999). Dioscorides, who can be considered the founder of pharmacognosy, described in more details the properties of *A. tinctoria* in his *De Materia Medica* around 77 AD. Some references to these benefits were still found in the 17th century, but later drifted into folklore (Papageorgiou *et al.*, 1999). Modern science has credited the ancient texts with

scientific explanations and, in 1976, the major active components were chemically isolated and identified as the naphthoquinone enantiomers A/S: a new class of drugs (**Figure 6**) (Papageorgiou *et al.*, 2008).

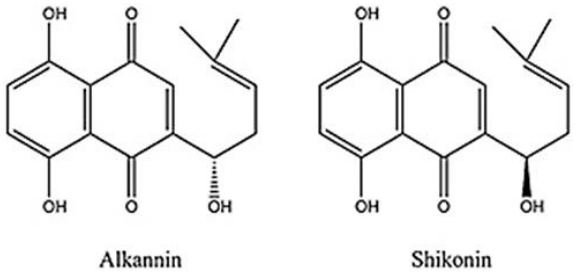

Figure 6. Chemical structures of the enantiomeric pair of naphthoquinones alkannin and shikonin, representing major bioactive compounds in diverse *Alkanna* species (from Tappeiner *et al.*, 2014).

Nowadays, A/S and their derivatives (A/Sd) are known to possess a wide range of pharmaceutical/medicinal properties (e.g., wound healing, antioxidant, antimicrobial, anti-inflammatory and anti-cancer) (Assimopoulou *et al.*, 2004; Papageorgiou *et al.*, 2008; Sengul *et al.*, 2009; Huu Tung *et al.*, 2013; Kheiri *et al.*, 2017). They are also used as cosmetics, food additives or natural dyes to color silk (Malik *et al.*, 2016; Ozer *et al.*, 2010). Although studies have been carried out to assess the phytochemical potential of extracts of *A. tinctoria*, they mainly focused on naphthoquinone content, detection, and extraction techniques. So far, only a limited number of studies have focused on the roles played by plant symbiotic microorganisms (e.g., endophytic bacteria *Chitinophaga* sp., *Allorhizobium* sp., *Duganella* sp., and *Micromonospora* sp.) on SMs production in *A. tinctoria* and none have considered the impact of AMF on this important plant species (Rat *et al.*, 2021).

More details on the general effects on AMF associated to medicinal plants, specifically Boraginaceae, are reported below in section III paragraph 2.

4. Alkannin/shikonin derivatives metabolic pathway

Hydroxynaphthoquinones (HNQs) shikonin, or its enantiomer, alkannin, and dozens of other acylated A/Sd, are synthesized in the root periderm of *A. tinctoria* and several other Boraginaceae species (Auber

et al., 2020). They are released either by tissue degradation/sloughing or by other membrane-bound transport proteins. They play multiple roles in the rhizosphere: plant-microbe interaction, defence, interference with the growth of competing plants (allelopathy) (Papageorgiou *et al.*, 2008; Weston *et al.*, 2012; Auber *et al.*, 2020). Brigham *et al.* (1999) observed that the ratio of shikonin derivatives in *Lithospermum erythrorhizon* (Sieb. and Zucc.) varies depending on the level of stress and species of microorganism present in the rhizosphere. A brief metabolic pathway describing the biosynthesis of these metabolites is shown in **Figure 7**.

Shikonin is derived from p-hydroxybenzoic acid (HBA) and geranyl diphosphate (GPP), originating from the shikimic acid and MVA pathways, respectively (Song *et al.*, 2020). The coupling of these two key precursors is catalysed by geranyl diphosphate: 4-hydroxybenzoate 3-geranyltransferase (*PGT*) to yield the important intermediate 3-geranyl-4-hydroxybenzoic acid (GBA), which is subsequently converted to geranylhydroquinone (GHQ) by unknown enzymes (Yazaki *et al.*, 2002; Wu *et al.*, 2017; Song *et al.*, 2020). A cytochrome P450 (CYP) monooxygenase was identified from *L. erythrorhizon* suspension cultures catalysing the C-3″ hydroxylation of GHQ to form a key intermediate 3″-hydroxyl-geranylhydroquinone (GHQ-3″-OH) (Yamamoto *et al.*, 2000). Recently, two CYP enzymes catalysing the oxidation of GHQ were identified: CYP76B100 catalysed the 3″-hydroxylation of GHQ to form GHQ-3″-OH, and CYP76B101 catalysed the oxidation of GHQ at the C-3″ position to synthesize 3″-carboxyl-geranylhydroquinone (GHQ-3″-COOH) besides one-step oxidation product GHQ-3″-OH (Song *et al.*, 2020). This latest CYP has been previously reported has geranylhydroquinone 3”-hydroxylase (*GHQH*) (Wang *et al.*, 2014) or geraniol 10-hydroxylase unigene (*G10H*; P-450 monooxygenase) (Wu *et al.*, 2017). Cyclization of GHQ-3″-OH, yielding a naphthoquinone structure, was followed by several oxidation steps to form deoxyshikonin/shikonin. Although several studies have attempted to identify the genes responsible for the activation of these last reactions, none have been identified to date (Takanashi *et al.*, 2019). Moreover, no reference genome is available so far for *A. tinctoria* (Ahmad *et al.*, 2021), which could have been used to develop suitable primers for the Quantitative-Real Time PCR (RT-qPCR) and, therefore, for the expression analysis of the genes involved in the shikonin biosynthesis.

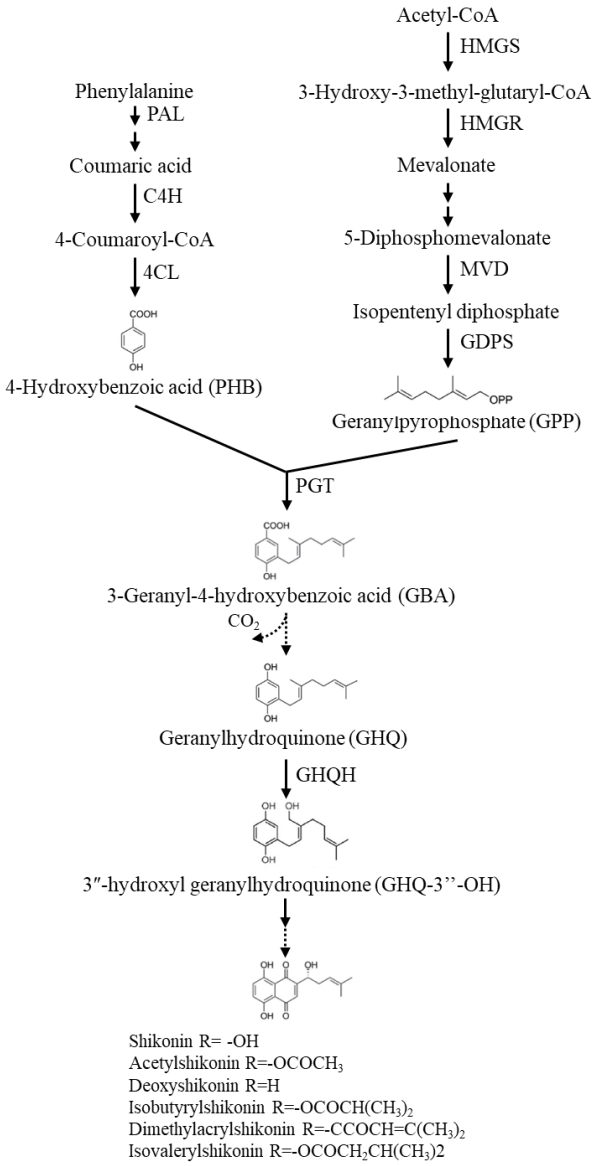

Figure 7. An abridged schema of the shikonin derivatives biosynthesis pathway. Single arrows represent one step reaction, while double arrows represent multiple step reactions. Dotted arrows mean undefined steps or enzymes have not yet been verified. Abbreviations: *HMGS*, 3-hydroxy-3-methylglutaryl-CoAsynthase; *HMGR*, 3-hydroxy-3-methylglutaryl-CoAreductase; *MVD*, mevalonatediphosphate decarboxylase; *GDPS*, geranyldiphosphate synthase; *PAL*, phenylalanine ammonialyase; *C4H*, cinnamicacid4-hydroxylase; *4CL*, 4-coumaroyl-CoAligase; *PGT*, 4-hydroxybenzoate-m-geranyltransferase; *GHQH*, geranylhydroquinone 3"-hydroxylase (from Wang *et al.*, 2014).

II. Plants-microbes associations

Symbiosis is a close, prolonged physical and/or metabolic association between two or more distinct organisms (Dattagupta and Zielinski, 2011). Specifically, a mutualistic symbiosis involves a reciprocal enhancement of fitness that can be represented by a bilateral nutrient flux and/or by any protective effect of one partner toward the other, enhancing the latter's survival or reproduction (Selosse *et al.*, 2004). Some of the most intriguing forms of symbioses happen in the microbial world and especially in hidden places like soil. The root system is a chemical factory releasing organic compounds, which act as signalling agents to attract beneficial microorganisms such as rhizobia, mycorrhizal fungi, bacterial and fungal endophytes, plant growth-promoting rhizobacteria or fungi (PGPR and PGPF, respectively) to form mutualistic interactions (Mitter *et al.*, 2013). In fact, bacteria and fungi are capable of invading host organisms, modify genetic and metabolic processes along the way. The microbiome of the rhizosphere and root periderm is particularly important for plant nutrition, abiotic stress tolerance and defence against pathogen attack (Mitter *et al.*, 2016). A myriad of metabolites often mediates the interactions between plants and beneficial microorganisms as they facilitate partner recognition, colonization success, and hence the benefits gained by both partners. Thus, the plants-microorganisms associations induces changes in the transcriptome, proteome, and finally, the metabolome of the plants and microorganisms (Kaur and Suseela, 2020).

1. Mycorrhizal symbiosis

The mycorrhizal symbiosis is probably the most ancient and widespread symbiosis on earth being present in almost all ecosystems, from deserts to tropical forests and arable lands (Heijden *et al.*, 2015). This symbiosis dates back 400 million years and gave rise to four main types of mycorrhizae that emerged at different times in plant evolution: arbuscular mycorrhizas (AM), ectomycorrhizas (ECM), orchid mycorrhizas (ORM), and ericoid mycorrhizas (ERM) (Genre *et al.*, 2020). The great majority of land plants (72%) associate with the AM dominant type belonging to the phylum Glomeromycota, followed by

the other types [i.e., ORM, ECM, and ERM, forming associations with 10%, 2% and 1.4% of plants species, respectively] belonging to the Basidiomycota or Ascomycota fungal phyla (Heijden *et al.*, 2015; Feijen *et al.*, 2018; Tedersoo *et al.*, 2020).

Arbuscular mycorrhizas and ECM associations differ in their structural characteristics (**Figure 8**) and in the plant and fungal species involved. In arbuscular mycorrhizal symbiosis, the fungus penetrates intercellularly and intracellularly into the root cortex (endomycorrhizae), whereas in ECM symbiosis, the fungus only penetrates intercellularly into the root cortex (ectomycorrhizae) (Bucking *et al.*, 2012a). The arbuscular mycorrhizal fungi will be described profusely in the next paragraph, as they represent the key microorganisms of this Ph.D. As for the ECM fungi, they develop a network close to the roots, with a mantle that surrounds short bifurcated or monopodial roots and a Hartig net that penetrate between the cortical cells. Ascomycetous and basidiomycetous fungi form ECM with Gymnosperms [e.g., Pinaceae (all genus), Cupressaceae, Gnetaceae] and a few families of Angiosperms (e.g., Fagaceae, Betulaceae, Salicaceae) (Strullu-Derrien and Strullu, 2007). Ericoid and ORM also show intracellular colonization with fungal hyphae penetrating inside the host's tissues. Dense hyphal coils are produced inside each epidermal cell in ERM, while the hyphae reach the cortical parenchyma of the roots, where they form large hyphal coils, called "pelotons", in the OCM (Genre *et al.*, 2020) (**Figure 8**). Ascomycetous fungi are associated with members of the order Ericales and a few liverworts, while Basidiomycetous associations are found in Orchidaceae and also a few liverworts (Strullu-Derrien and Strullu, 2007).

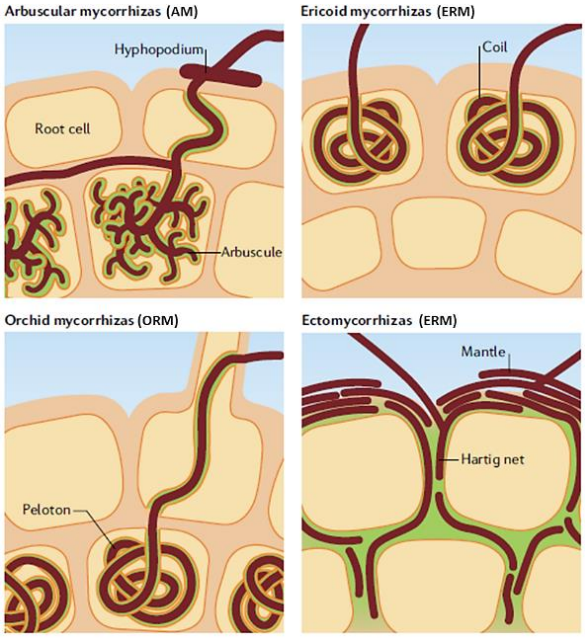

Figure 8. Main cellular features of arbuscular (AM), ericoid (ERM), orchid (ORM), and ectomycorrhizas (ERM) (Genre *et al.*, 2020).

2. Arbuscular mycorrhizal fungi: an obligate root symbiont

Arbuscular mycorrhizal fungi are among the oldest living asexual eukaryotes. Indeed, structures resembling arbuscules in extant AMF species have been detected in subterranean organs of fossil plants from the 400 million-year (Ma) old Rhynie Chert formation (Stürmer *et al.*, 2018). Moreover, the origin of AMF is estimated to coincide with the evolution of land plants between the Ordovician (510-439 Ma) and the Devonian (409-354 Ma), suggesting their role in the colonization of terrestrial ecosystem by aquatic plants (Stürmer *et al.*, 2018; Chen *et al.*, 2018). They are today classified in a monophyletic phylum, the Glomeromycota, based on phylogenetic analyses of the small subunit (SSU) rRNA gene sequence. Four orders of AMF, namely, Glomerales, Archaeosporales, Paraglomerales, and Diversisporales, have been identified in this phylum, which also includes 25 genera (Redecker *et al.*, 2013). These obligate root symbionts supply the plant with mineral nutrients, especially phosphate and nitrogen, and water (Smith and Read, 2008b). In return, they receive carbohydrates (Bago *et al.*, 2003)

and lipids (Keymer *et al.*, 2017). The exchange of nutrient for carbohydrates and lipids takes place in the arbuscules, which are highly branched hyphal structures, which form in the inner cortical cells of the roots (Luginbuehl *et al.*, 2017). In addition, AMF form an extensive hyphal network within the roots as well as vesicles, in the majority but not all AMF genera. They also produce spores and hyphae, and in some genera auxiliary cells, outside the root, forming a continuum separating an intraradical (intraradical mycelium-IRM) from extraradical (extraradical mycelium-ERM) phase (**Figure 9**). The coenocytic hyphal network of AMF contains hundreds of nuclei sharing the same cytoplasm (Parniske, 2008).

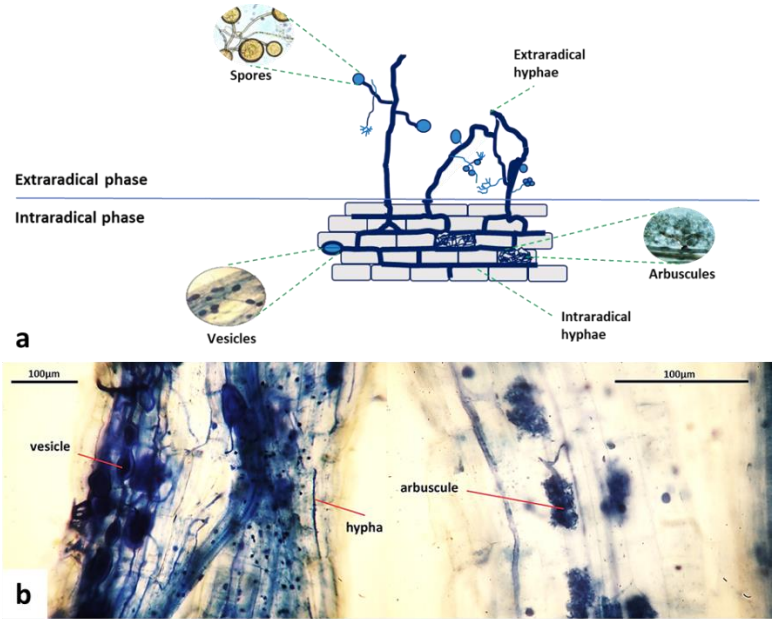

Figure 9. (a) Schematic illustration of major AMF structures formation in the extraradical and intraradical phase. **(b)** Microscopic image of stained roots of *Anchusa officinalis* with red lines indicating the AMF intraradical structures (i.e., vesicles, arbuscules, and hyphae).

3. AMF life cycle

Although spores of AMF can germinate in the absence of host plants, they are obligate biotrophs, and therefore depend on a living photoautotrophic partner to complete their life cycle and produce the

next generation of spores (Parniske, 2008). In soil, they produce asexual spores, and, for some genera, vesicles (inside) and auxiliary cells (outside) the roots. These structures are named propagules because they are able to germinate and colonize new roots.

The development of the AMF symbiosis is a highly dynamic process that can be divided into three distinct phases: (a) asymbiotic, (b) pre-symbiotic, and (c) symbiotic.

a. Asymbiotic phase

The development of the AMF starts with the germination of propagules (i.e., spores, auxiliary cells, vesicles, or colonized root fragments). These structures produce a limited amount of branched, coenocytic hyphae. In absence of host plant, their growth is restricted. The hyphae septate, with an intense vacuolisation and retraction of nuclei, cytosol and mitochondria (Parniske, 2008).

b. Pre-symbiotic phase

In presence of root signals (i.e., strigolactones - Akiyama *et al.*, 2005), the growth and branching of hyphae is strongly stimulated and the fungus switch its development from the asymbiotic to the pre-symbiotic phase. This phase is characterized by mutual recognition between the plant and fungus prior to physical contact. A complex signalling process is initiated between the plant and the AMF generating physiological changes in both partners (**Figure 10**). These changes stimulate hyphal-branching elicited by plant-derived exudates and plant gene expression induced by diffusible fungal-signalling molecules (Gutjahr and Parniske, 2013). The bioactive compounds in root exudates include carlactones, strigolactones (SLs), flavonoids and 2-hydroxy fatty acids (2-OH-FA) (Akiyama *et al.*, 2005; Mori *et al.*, 2016; Xue and Wang, 2020).

Strigolactones are derived from the carotenoid metabolism. Despite their multiple roles as endogenous phytohormones (e.g., suppression of shoot branching, regulation of root architecture and acceleration of leaf senescence) (Waters *et al.*, 2017), they contribute as exogenous signals

at different stages of AMF formation, such as stimulation of AMF spore germination, hyphal branching and promotion of hyphopodium formation (Xue and Wang, 2020). Moreover, cutin monomers have been involved as a specific class of plant signalling factors, which play a crucial role for AMF stimulation. Two loci, RAM1 and RAM2 ("required for arbuscular mycorrhization"), have been identified in *Medicago truncatula* Gaertn. mutants seriously affecting AM symbiosis. They encode a GRAS domain transcription factor and a acyl transferase involved in the production of cutin monomers (Venturi and Keel, 2016).

Upon perception of SLs, AMF release at least two types of oligosaccharides, known as Myc-factors: mycorrhizal-lipochitooligosaccharides (Myc-LCOs) (Maillet *et al.*, 2011) and short-chain chitooligosaccharides (COs), namely chitotetraose (CO_4) and chitopentaose (CO_5) (Genre *et al.*, 2013). These signals share the same β-1-4-linked N-acetylglucosamine (GlcNAc) backbone and they both have structures closely related to chitin. This aspect suggests that molecules related to fungal cell wall biogenesis play a role as inter-kingdom messengers that only host plants for AMF recognize as symbiotic signals (Bonfante and Genre, 2015). Therefore, both Myc-LCOs and COs are chemically linked to the Nod-factors of symbiotic rhizobium bacteria, which are indispensable for the establishment of the interactions between rhizobia and legumes (Oldroyd, 2013).

Myc-factors induce the expression of plant genes, calcium spiking in rhizodermal cells, starch accumulation in roots, and lateral root formation prior to colonization (Gutjahr and Parniske, 2013). Specifically, nuclear calcium spiking in the rhizodermis is associated with the activation of the common symbiosis signalling pathway (CSP), which regulates gene expression required for rhizodermal penetration (Choi *et al.*, 2018). In addition to Myc-factors, the AMF *R. irregularis* has been reported to exude the putative SL-induced secreted protein (SIS1) into the rhizosphere upon SLs treatment (Tsuzuki, 2016). Similarly, *Glomus intraradices* (now *Rhizophagus intraradices*) has been shown to secrete the protein 7 (SP7) reducing the level of host defence responses (Kloppholz *et al.*, 2011).

Perception of GlcNAc oligosaccharides by the plant is mediated at the root cell surface by receptor-like kinases (RLKs) containing lysin motifs (LysMs) in their extracellular domain that are capable of GlcNAc binding (Choi *et al.*, 2018). The specificity of each receptor for

each chitin oligomer remains to be fully understood (Bonfante and Genre, 2015).

c. Symbiotic phase

Following signal exchange between the host plant and AMF, the fungal hyphae contact the root epidermal cells, and differentiate into an hyphopodium, before entry in the root cortex (Luginbuehl and Oldroyd, 2017) (**Figure 10**). Upon attachment to an epidermal cell, the plant cell nucleus moves to the site of hyphal contact before migrating across the cell to the opposite side (Genre *et al.*, 2005), creating a specialized tube-like intracellular structure, called the pre-penetration apparatus (PPA) (Choi *et al.*, 2018). This apparatus is derived from the accumulation of a dense network of endoplasmic reticulum (ER) cisternae, actin filaments and microtubules. Once the PPA has assembled and spans the whole width of the cell, the fungal hypha enters the cell lumen through this pre-formed cytoplasmic bridge and is guided across the cell on this pre-defined path (Genre *et al.*, 2005).

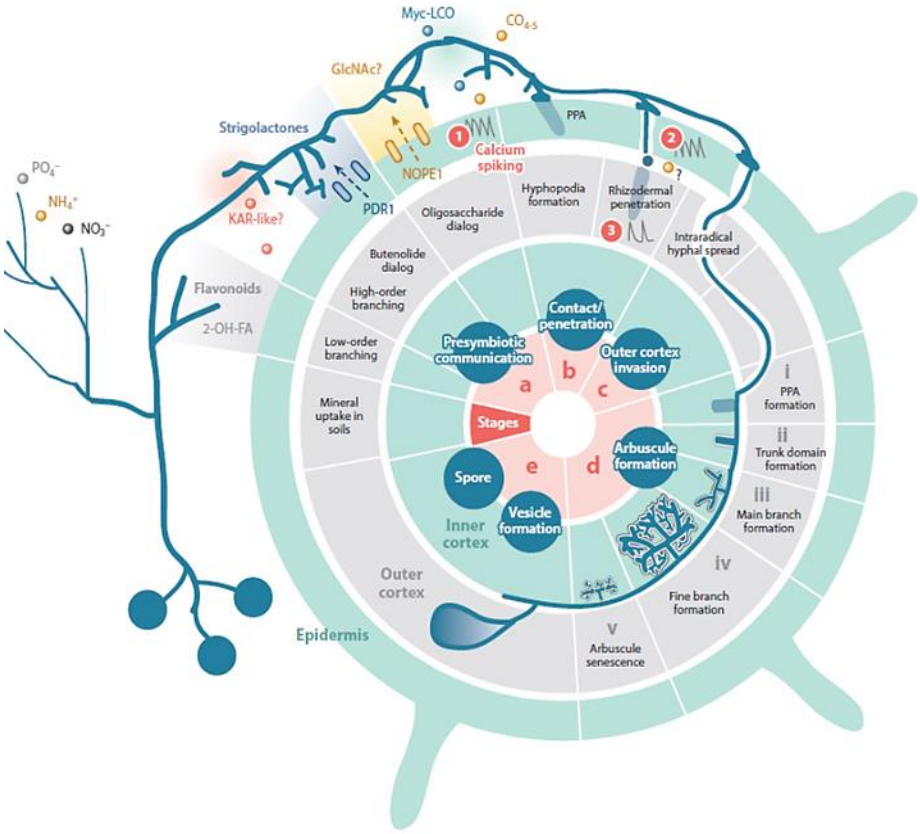

Figure 10. Arbuscular mycorrhizal fungi life cycle representation: symbiotic mechanism through which AMF colonize the interior of plant roots. Under optimal environmental conditions, fungal spores germinate, and hyphae grow toward the host root. **(a)** Prior to contact, both organisms detect diffusible signals released by the partners, namely butenolides (common feature of all bioactive strigolactones) and oligosaccharides. Perception of fungal oligosaccharides such as CO_{4-5} and Myc-LCOs triggers nuclear calcium spiking in the rhizodermis to activate the Common Symbiosis Signalling Pathway - CSP (steps 1,2, and 3), which regulates gene expression required for rhizodermal penetration. **(b)** Fungal attachment structures, called hyphopodia, form on the epidermal surface, while the host cell produces a PPA to intracellularly accommodate the fungus. **(c)** Fungal hyphae grow toward the inner cortex to initiate arbuscule formation. **(d)** Arbuscule development can be divided into five substages featuring development and collapse of arbuscules (stages i–v). **(e)** Successful arbuscule formation enables carbon uptake in exchange for mineral nutrients delivered by the fungus, leading to the formation of nutrient storage vesicles, in the majority of AMF species, and daughter spores (from Choi *et al.*, 2018).

Following epidermal penetration, fungal hyphae proliferate inter- and intracellularly through the outer cortical layer *via* continuous formation of PPA. Upon reaching the inner cortex, AMF develop highly branched, tree-shaped structures, the **arbuscules** (**Figure 10**) (Choi *et al.*, 2018). Although the fungus penetrates the cell wall to enter cortical cells, the host plasma membrane does not rupture. Instead, it expands to envelop the hyphal branches and forms the so-called periarbuscular membrane (PAM), which separates the fungal hyphae from the host cytoplasm (Luginbuehl and Oldroyd, 2017). Thereby, a large membrane surface area and periarbuscular interface (PAI) is created for the exchange of nutrients and signals between the two partners of the symbiosis (Choi *et al.*, 2018) (see section II paragraph 4).

Root colonization follows two distinct patterns: the *Arum* and *Paris*-types (**Figure 11**) (Smith and Read, 2008). The first one is characterized by the spread of intercellular hyphae and, as described above, by the formation of arbuscules in cortical cells, whereas the *Paris*-type entails hyphal passage from cell to cell as well as intercalary coils or arbuscules formation (Gutjahr and Parniske, 2013). Most plants support intermediate forms of these patterns, which have led to the formation of the term "*Arum*-*Paris*-type continuum" (Dickson, 2004). The formation of terminal arbuscules by the most-studied *Arum*-type AMF, is preceded by cellular reorganization, nuclear repositioning, and localized cytoplasmic aggregations.

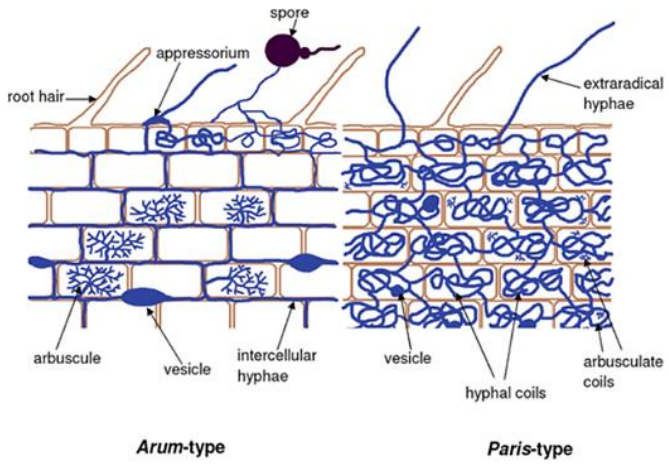

Figure 11. Arbuscular mycorrhizal fungi structures showing Arum- and Paris-types (from Priyadharsini and Muthukumar, 2015).

Upon contact with intracellular hyphae, separated PPA-like ER aggregates form in the inner cortical cells (Genre *et al.*, 2008). Moreover, extensive cytoskeleton modifications are induced in cells containing arbuscules (Gutjahr and Parniske, 2013). The plant vacuole is deformed to accommodate the growing arbuscule, and the ER, peroxisome, Golgi apparatus, nucleus, and plastids are densely compacted within the cytoplasm. A marked proliferation of plastids and plant mitochondria is observed, probably necessary to satisfy the increased demand for fatty acids and amino acids during biosynthesis of the PAM (Pumplin and Harrison, 2009; Gutjahr and Parniske, 2013). Recently, it has been reported that host plant lipids are needed for arbuscules growth, probably to provide material for the extensive plasma-membrane of the highly branched fungal structure (see section II paragraph 4). This suggests that the arbuscules dictate the AMF development as a whole, since lipids uptake is required for vesicle formation, full exploration of the root and development of extraradical mycelia and spores (Keymer *et al.*, 2017). Moreover, they typically have a relatively short life span of about two to eight days before a rapid collapse. This degeneration can be followed by recolonization of the root and the formation of new arbuscules, sometimes in the same cells, resulting in simultaneous cycles of arbuscules formation and degradation (Luginbuehl and Oldroyd, 2017). Moreover, the mutation of the arbuscule-specific phosphate transporter PT4 suggests that the lifetime of arbuscules is influenced by their ability to deliver phosphate and probably other nutrients (Parniske, 2008).

Upon the successful establishment of AM symbioses, AMF produce lipid storage **vesicles** (**Figure 11**), which are thick-walled lobes formed intraradically within or between host cells (Choi *et al.*, 2018). In *Scutellospora* and *Gigaspora* species, vesicles are absent, but these species possess distinct extraradical structures called **auxiliary cells** (**Figure 12**) that contain a handful of nuclei. The function of auxiliary cells is not known to this day and it is possible that they are remnants of a former functional structure (Declerck *et al.*, 2004; Kokkoris *et al.*, 2020). The extraradical mycelium network proliferates in the soil through a straight-growing thick-walled hyphae called runner hyphae and it could develop **branched absorbing structures** (BAS), which are supposedly involved in the uptake of minerals (Bago *et al.*, 1998). However, no detailed information on BAS longevity or activity are available (Kokkoris *et al.*, 2020). Adequate feeding of the fungus by the host plant leads to the production of **asexual spores** containing many

nuclei as well as lipids, which will support spore germination and asymbiotic growth of the germ tube (Marleau *et al.*, 2011; Choi *et al.*, 2018) (**Figure 12**).

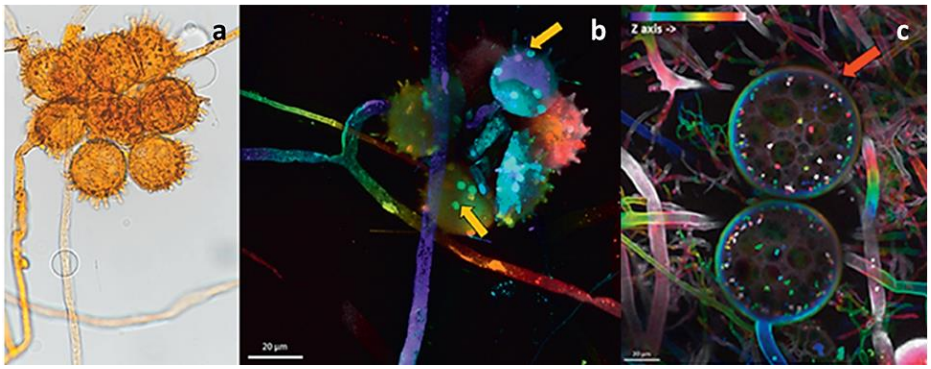

Figure 12. **(a)** Auxiliary cells observed with an optical microscope. **(b)** Confocal microscopy of the same auxiliary cells observed in image **a** with nuclei stained with SYTO 13 green, fluorescent nucleic acid dye (orange arrows). **(c)** Localization of nuclei peripheral to the innermost spore wall (red arrow). Lipid droplets are also visible within the spores, along with abundant hyphae in the background (from Kokkoris *et al.*, 2020).

4. Plant-AMF nutrient exchanges

One major attribute of AMF is the supply of nutrients (e.g., P, N) to plants. They play important roles in terrestrial ecosystems, contributing to an increase in agricultural productivity and crop quality (Kameoka *et al.*, 2019; Genre *et al.*, 2020). Therefore, it is important to understand the regulation of nutrient transport and metabolism associated with the AMF symbiosis.

Plants colonized by AMF have two pathways for nutrient uptake (**Figure 13**): the direct pathway *via* the root epidermis and root hairs and the indirect or mycorrhizal pathway *via* the uptake in the soil, transport along the hyphae and transfer from the arbuscule to the root cells (Wang *et al.*, 2017).

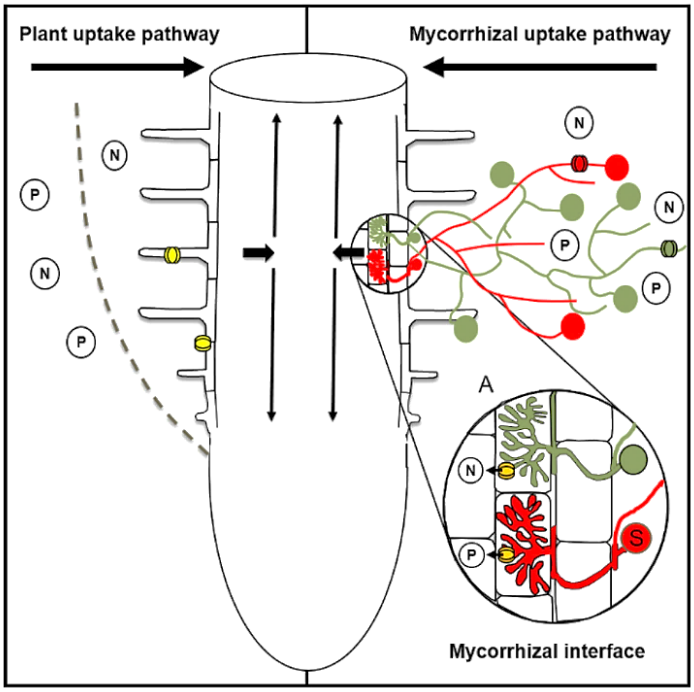

Figure 13. Plants can take up nutrients by transporters that are in their epidermis or root hairs (yellow symbols) or *via* mycorrhizal structures that comprises the uptake of nutrients by fungal transporters in the extraradical mycelium (red or green symbols). The plant nutrients uptake in the mycorrhizal interface is regulated by mycorrhiza-inducible plant transporters present in the periarbuscular membrane (orange symbols) (from Bücking and Kafle, 2015).

The thin ERM is able to reach and uptake soil nutrients much more efficiently than plant roots/hairs, improving significantly the nutrient status of the plant (Luginbuehl *et al.*, 2017). A recent study by Jiang *et al.* (2021) has demonstrated that the AMF extraradical hyphae can transport phosphate solubilizing bacteria (PSB) to organic phosphorous (P) patches and enhance organic P mineralisation.

Using high-affinity P transporters (PTs), the ERM acquires **inorganic phosphorus** (Pi) from the soil and converts it into polyphosphates for storage and translocation to the intraradical fungal structures, where they are hydrolysed into the inorganic form to be unloaded into the PAI. From here, symbiosis-specific phosphate transporters, belonging to the MtPT4 (*M. truncatula*)/OsPT11 (*Oryza sativa* L.) type, acquire the phosphate across the PAM (Choi *et al.*, 2018). The host plant is capable of measuring the delivery of phosphates from arbuscules and, if the fungus does not provide

adequate levels, it sanctions the symbiosis through premature arbuscules degeneration (Javot *et al.*, 2007). Interestingly, the mycorrhizal phenotype of MtPT4 mutants can be suppressed by low-nitrogen conditions, indicating that also nitrogen transfer to the plant acts as a signal to support arbuscules survival and maintenance (Luginbuehl *et al.*, 2017).

The **inorganic nitrogen** (NO_3^- and NH_4^+) absorbed by the fungal ERM can be incorporated into amino acids *via* the glutamine synthetase, glutamine oxoglutarate aminotransferase (GS/GOGAT) cycle, and converted into glutamine, and then into arginine. After their conversion into urea and ammonia, the latter is released into the PAI. Plant NH_4^+ transporters take up ammonia across the PAM (Luginbuehl *et al.*, 2017; Wang *et al.*, 2017; Choi *et al.*, 2018; Kameoka *et al.*, 2019).

The induction of many other mineral nutrient transporters in mycorrhizal roots, and the fact that mycorrhizal plants contain increased amounts of various mineral nutrients, suggests that other macronutrients, such as **calcium**, **sulphur**, **potassium** and micronutrients, such as **copper** and **zinc**, may also be transferred *via* the arbuscules (Cardini *et al.*, 2021). However, for most AM-induced predicted nutrient transporters, the expression pattern, protein localization, and function remain to be established (Wang *et al.*, 2017; Chen *et al.*, 2018).

Conversely, AMF depend on their host for **carbon** supply, which is essential for the fungal growth. It is thought that up to 20% of photo-assimilates in host plants flow to the AMF to support the mutualistic interaction (Bago *et al.*, 2000). The main form of carbon delivered to AMF is **glucose**, which is taken up from the PAI by a high-affinity fungal monosaccharide transporters (MSTs) and then catabolized, *via* the glycolytic pathway and TCA cycle, into glycogen and trehalose for export to the rest of the fungal mycelia (Choi *et al.*, 2018).

Recent studies have revealed a direct transfer of **lipids** from plants to AMF (Luginbuehl *et al.*, 2017; Keymer *et al.*, 2017). It has already been reported that AMF store carbon mainly in the form of lipids, triacylglycerol (TAG), and that the major proportion of fatty acids found in AMF is composed of 16:0 (palmitic) and of 16:1ω5 (palmitvaccenic acids) (Trépanier *et al.*, 2005; Keymer *et al.*, 2017). However, thanks to the availability of the whole AMF genome sequence, it has recently been shown that AMF can elongate and

desaturate fatty acids but not synthesize them, because they lack cytosolic fatty acid biosynthesis genes (encoding FA synthase I subunits) (Luginbuehl *et al.*, 2017; Keymer *et al.*, 2017). Thus, these fungi might lack the ability for *de novo* fatty acids synthesis, even when associated with roots, but they do encode the enzymatic machinery for 16:0 fatty acids elongation to higher chain length and for fatty acids desaturation (Trépanier *et al.*, 2005; Keymer *et al.*, 2017). During the AMF symbiosis, the fatty acids provided by the plant are converted into triacylglycerols (i.e., lipids presumably C16:0 β-MAG) and transferred to AMF via arbuscules to be used in the fungal metabolism (Sugiura *et al.*, 2020).

The active transport of nutrients across a plant membrane requires energy, which is usually provided by an electrochemical gradient generated *via* proton transport (Luginbuehl *et al.*, 2017). It has been shown that plasma membrane H^+-ATPases, specifically induced in arbuscule-containing cells, are required for enhanced proton pumping activity in membrane vesicles from AMF-colonized roots of *O. sativa* (rice) and *M. truncatula* (Wang *et al.*, 2014). This bidirectional nutrient exchange is regulated by both partners in order to maintain a stable symbiotic relationship. For instance, it appears that host plants are able to discriminate the best fungal partners and reward them with more carbohydrates. In return, AMF transfer increased mineral nutrients to those roots providing more carbohydrates (Wang *et al.*, 2017).

5. General benefits of the AMF symbiosis

Arbuscular mycorrhizal symbiosis offers a plethora of benefits to their hosts and the ecosystem in which they live. These benefits are important for the sustainable management of agricultural ecosystems, which have been put under pressure by intensive practices (e.g., mechanisation, monocultures, increased use of fertilizers and pesticides) (Gianinazzi *et al.*, 2010). Arbuscular mycorrhizal fungi contribute to a wide range of ecosystem functions such as **soil aggregation**, **litter decomposition**, and **reduced nutrient losses**, which may lead to a lower need for fertilizers and directly influence the profitability and environmental impact of AMF-based agricultural practices, even in the absence of a net yield increase (van der Heijden *et al.*, 2015).

The dense hyphal network of the highly ramified AMF mycelium creates a three-dimensional matrix that tangles and links soil particles without compacting the soil (Chen *et al.*, 2018). A glycoprotein, glomalin, secreted by AMF has been identified as an additional important agent in the **aggregation of soil particles** (Rillig, 2004). In addition, glomalin-related soil proteins (GRSPs) (2-5% of total organic soil carbon) can contribute significantly to soil carbon sequestration (Chen *et al.*, 2018). The hyphal network and its stimulating effect on plant growth and root system development protects the soil from wind and water erosion (Gutjahr and Parniske, 2013). Therefore, AMF have been shown to increase **soil water retention**, thanks to GRSPs, which protect soil from desiccation by improving soil water holding capacity, increasing water accessibility for plants (Gianinazzi *et al.*, 2010; Begum *et al.*, 2019).

Moreover, AMF have a selective influence on microbial communities in the rhizosphere. The increased microbial activity surrounding mycorrhizal roots compared to non-mycorrhizal roots is, in fact, called the "mycorrhizosphere effect" (Cameron *et al.*, 2013).

The common mycorrhizal network (CMN), established between two or more plants and one or more ERM, can strongly interconnects plant communities and potentially increases their stability as weaker individuals can take advantage of mineral nutrients supplied *via* the CMN at the expense of stronger plants that support the CMN (Jakobsen and Hammer, 2015; Chen *et al.*, 2018). Moreover, the AMF hyphal network can transmit **resistance induction to neighbouring plants**, acting as an underground plant-plant communication system (Jung *et al.*, 2012).

As described above, the ERM, which extend from the colonized roots into the soil, functions as an efficient uptake system, given the high surface area to volume ratio of the mycelium, which is able to **take up nutrients from the soil** beyond the depletion zone around the roots, and the presence of nutrient transporter genes in the hyphae (Giovannini *et al.*, 2020) (**Figure 14**). The resulting improved nutrient uptake, primarily in soils poor in nutrients, often lead to an increased plant growth and development [although negative effects on plant biomass have also been repeatedly reported in natural and agricultural ecosystems (van der Heijden *et al.*, 2015)], as well as growth related functions. For example, stomatal conductance, leaf water potential, relative water content (RWC), photosystem II (PSII) efficiency, and

CO_2 assimilation (Begum *et al.*, 2019) (**Figure 14**) were increased in mycorrhizal plants. All these beneficial effects, along with the high degree of coordination required between both partners, can lead to a modification in the content of health-promoting phytochemicals in plants, as detailed in section III. Furthermore, AMF increase plant tolerance to biotic (e.g., fungal and bacterial pathogens) and abiotic (e.g., drought, salinity, heavy metals) stresses.

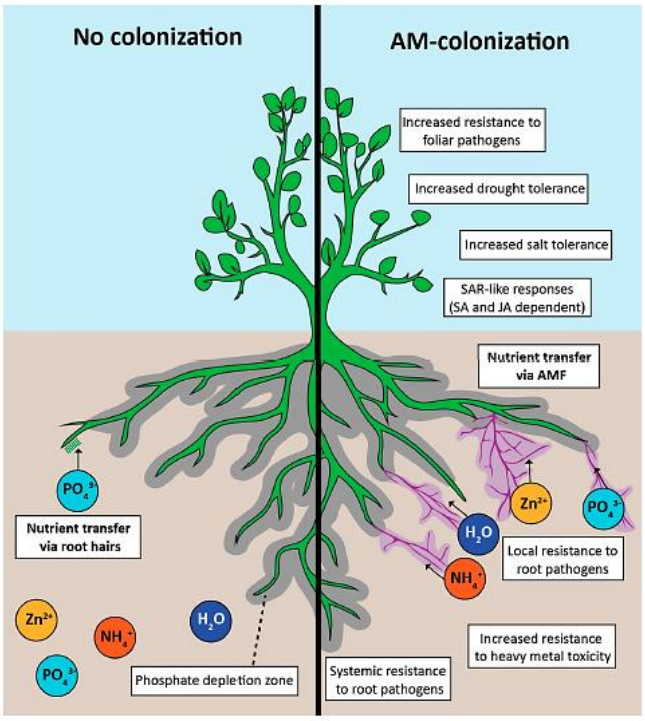

Figure 14. General benefits of arbuscular mycorrhizal colonization (on the right) as compared to non-colonized (on the left) root system (from Jacott *et al.*, 2017).

a. Mitigation of biotic stress by AMF

Colonization by AMF has been repeatedly shown to increase plant resistance to belowground pests and diseases, such as parasitic plants, fungi, bacteria and nematodes, as well as generalist belowground herbivores (Hill *et al.*, 2018). In contrast, few studies have reported the control of aboveground pets and diseases and results were less conclusive. In addition to nutritional effects (i.e., the improvement of

plant nutrition and the consequent compensation of damages caused by pathogens), changes in plant root architecture, root exudation, microbial populations in the rhizosphere, and the activation of plant defence mechanisms are all relevant aspects in the protection induced by AMF (Pozo *et al.*, 2010).

The protective effects by AMF have been mainly attributed to the induction of several defence pathways in mycorrhizal plants, *via* the so-called mycorrhiza-induced resistance (MIR) mechanism (Pozo *et al.*, 2010). This provides systemic protection against a wide range of attackers (e.g., biotrophic pathogens, necrotrophic pathogens, nematodes, and herbivorous arthropods) and shares characteristics with the systemic acquired resistance (SAR) after infection with pathogens, and the induced systemic resistance (ISR) following root colonization by non-pathogenic rhizobacteria (Cameron *et al.*, 2013). The initial induction of plant immunity is based on host recognition of microbe associated molecular patterns (MAMPs) from the AMF by pattern-recognition receptors. This elicits a series of signalling cascades resulting in the enhanced production of plant defence hormone salicylic acid (SA) and expression of MAMP-triggered immunity (Zhang and Zhou, 2010). The initial SA response is suppressed during successive stages of AMF colonization. Localised MAMP recognition and SA production can lead to the production of long-distance SAR signals and cause systemic priming of SA-dependent defences (Cameron *et al.*, 2013). To maintain their functionality, AMF promote the production of abscisic acid (ABA) by plants, which suppress SA-dependent defences against biotrophic pathogens (Ton *et al.*, 2009). Moreover, ABA promotes defence mechanisms, such as MAMP-induced stomatal closure, induction of reactive oxygen species (ROS), and cell wall reinforcements, and its mobility through both xylem and phloem makes this hormone an attractive candidate to act as a complementary long-distance MIR signal to the shoot (Ton *et al.*, 2009). From a phytochemical point of view, the AMF-protection results from passive and active activation of the plant's secondary metabolism. Passively, AMF cause host plants to produce and store highly potent defensive compounds (e.g., alkaloids and terpenoids) in trichomes and vacuoles, which can be released at will. More actively, external and internal fungal hyphae may sense pathogen effectors and other secondary compounds in the surrounding environment and "warn" host cells by producing LCOs and COs (French, 2017). Being a type of low-cost induced resistance, this could explain why root associations with AMF

have been conserved through evolution and are widespread among plant species worldwide (Pozo and Azcón-Aguilar, 2007). The impact of the AMF symbiosis on resistance/tolerance of plants to biotic stresses differs among AM fungal isolates for a given plant-pathogen interaction and can be modulated by environmental conditions (Pozo *et al.*, 2010).

b. Alleviation of abiotic stress by AMF

Arbuscular mycorrhizal fungi are able to alter plant physiology in a way that confers the plant the ability to more efficiently grow under stress conditions and cope with stresses (Miransari *et al.*, 2008). These soil fungi can alleviate various stresses or combination of stresses (e.g., drought, salinity, temperature, nutrients, and heavy metals), using various mechanisms, such as improved photosynthetic rate, uptake and accumulation of mineral nutrients, accumulation of osmoprotectants, upregulation of antioxidant enzyme activity, and change in the rhizosphere ecosystem (Plouznikoff *et al.*, 2016; Begum *et al.*, 2019).

Arbuscular mycorrhizal fungi considerably mitigate the negative effects of **drought stress** in various plants, including sugarcane, citrus, mung bean, apple, tomato, maize, wheat, wild jujube, trifoliate orange (Wu and Zou, 2017). This attenuation could be due to changes in root morphology (e.g., higher length of root system, surface area, volume, and number of first-, second-, and third-order lateral roots) and improved leaf area index and biomass under drought conditions (Begum *et al.*, 2019). In addition, AMF regulate other mechanisms such as improved cell turgor *via* osmotic adjustment in shoots (Wu and Xia, 2006), neutralization of ROS in tissues *via* the synthesis of enzymes (e.g., superoxide dismutase) (Ruiz-Lozano *et al.*, 1996), increased transport of water to the root cells *via* the extraradical mycelium (Gianinazzi *et al.*, 2010), increased root hydraulic conductivity through modulation of aquaporin expression (Quiroga *et al.*, 2018), and stomatal regulation by controlling ABA metabolism (Ludwig-Müller, 2010).

Several studies have reported an increased **salt tolerance** of plants colonized by AMF. Several mechanisms have been suggested: greater root hydraulic conductivity and osmotic adjustment, maintenance of enhanced K^+/Na^+ ratios, and lower accumulation of sodium in host plant shoots (Ruiz-Lozano *et al.*, 2012). However, the intimate

mechanisms that confer a higher tolerance of mycorrhizal plants to salinity are far from being totally understood.

Arbuscular mycorrhizal fungi protect plants from **heavy metals** by their sequestration in the hyphae and consequently decreased translocation to plants (Miransari, 2017). The presence of AMF in nickel hyperaccumulating plant species found naturally on metal-rich soils offers possibilities of using heavy metal hyperaccumulating plants together with AMF for phytoremediation strategies (Gianinazzi *et al.*, 2010). In addition, the ERM has been shown to buffer the effects on cadmium uptake, often found as a trace element in rock phosphates used as fertilizer, reducing its toxic effects on plant (Lugon-Moulin *et al.*, 2006; Gianinazzi *et al.*, 2010). Arbuscular mycorrhizal fungi activate various mechanisms, such as immobilization/restriction of metal compounds, precipitation of polyphosphate granules in the soil, adsorption to chitin in the fungal cell wall, and heavy metal chelation inside the fungi (Begum *et al.*, 2019).

III. Focus: AMF-plant association modulates plant metabolic profile

A functional mycorrhizal association requires a high degree of coordination between plant and AMF. On the one side, the AMF has to deal with the plant's immune system, contend with the defence mechanisms and overcome them for successful colonization of the host. On the other side, the plant has to regulate the level of fungal development within the root to maintain an adequate mutualistic level (Jung *et al.*, 2012). These regulations imply important changes in the plant primary and secondary metabolism, and consequently in the regulation of plant defence mechanisms (**Figure 15**). Furthermore, AMF impact various plant physiological characteristics: it increases the photosynthetic rate, alters the distribution of photosynthates in shoot and root parts, and affects the uptake of nutrients from the soil resulting in modified nutrient concentrations in plants (Begum *et al.*, 2019).

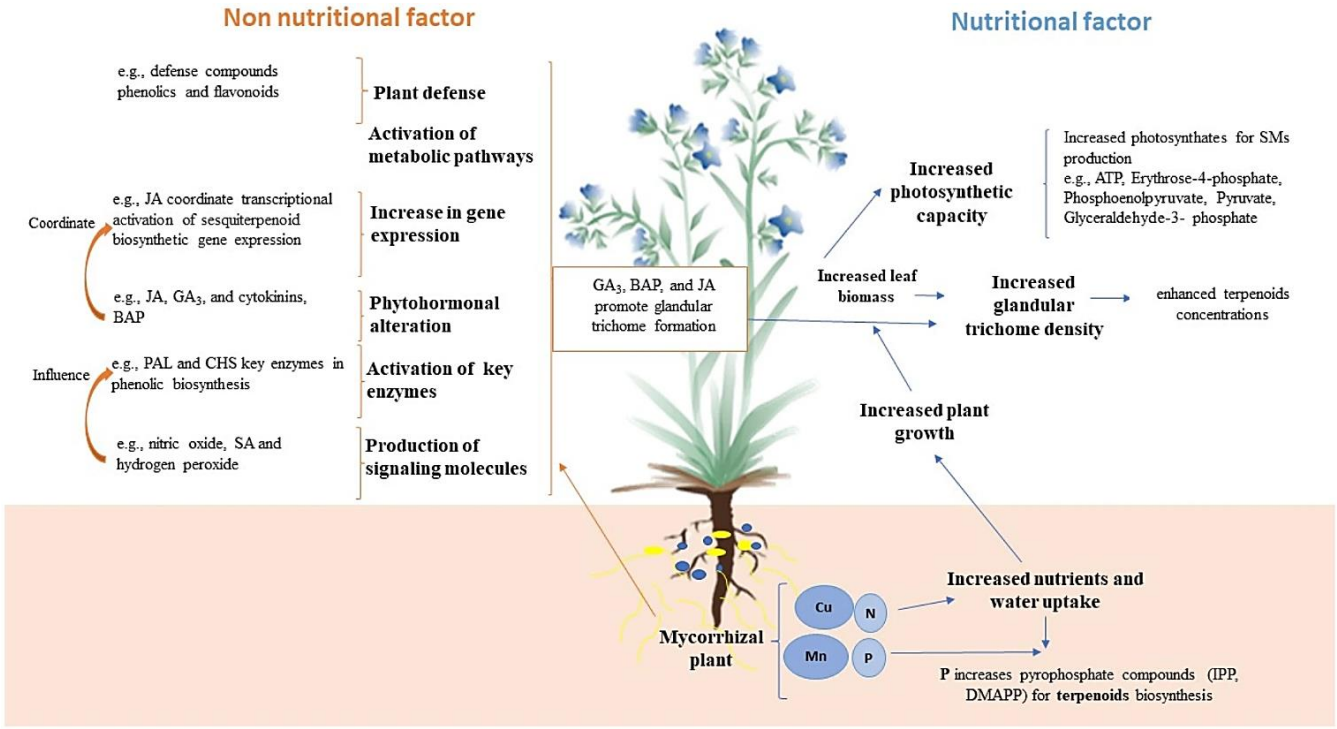

Figure 15. Schematic representation of the potential pathways by which AMF reprogram the plant metabolome. Reprogramming of SMs autoregulates AMF colonization in the plant by modulating the production of signalling compounds. Interaction of plants with AMF primes plant defence *via* changes in secondary metabolic pathways, which increases plant tolerance to biotic and abiotic stresses (from Zhao *et al.*, 2022).

In the AMF life-cycle description (see section II paragraph 3), the molecules produced exogenously to recognize partners and to establish a functional symbiosis have been reported (e.g., SLs, flavonoids, LCOs). Plants routinely "communicate" with conspecific organisms in the rhizosphere by PMs and SMs from their roots to recruit beneficial microbes including AMF (Cameron *et al.*, 2013). Upon mycorrhizal colonization, a fast but transient increase of endogenous SA occurs in the roots with a concurrent accumulation of defensive compounds, such as ROS, specific isoforms of hydrolytic enzymes, and the activation of the phenylpropanoid pathway (Jung *et al.*, 2012). A shared, permeable membrane is created between the arbuscule and root cell which allows the exchange of nutrients and carbohydrates (Parniske, 2008). Consequently, the AMF symbiosis causes specific physiological changes in the host cells: the number of mitochondria increases threefold and they migrate toward the arbuscule, the nucleus increases in size, and nuclear chromatin decondenses (allowing for increased transcriptional activity) (French, 2017). In addition, plastids increase in number and stromules become more abundant, and can move toward arbuscules, forming a net-like structure over the fungus (Lohse *et al.*, 2005). These modifications trigger metabolic changes in root cortical cells, such as increased energy production from the TCA cycle and production of plastid metabolites (e.g., fatty acids, amino acids, carotenoids, and terpenoids) (Jung *et al.*, 2012; Sbrana *et al.*, 2014). The tricarboxylic acid cycle and its intermediaries are important for cellular respiration and adenosine triphosphate (ATP) synthesis (Kaur and Suseela, 2020). In the cytosol, sugar levels increase due to the aforementioned increased photosynthesis in the leaves, which promotes high efflux rates between the arbuscule and host cell (French, 2017). Amino acids (e.g., tyrosine and phenylalanine) act as nitrogen donors and they are related to stress and defence mechanisms, and serve as a pool for the synthesis of other compounds, especially SMs (e.g., RA and caffeic acid) (Zeng *et al.*, 2013; Gaude *et al.*, 2015). Arbuscular mycorrhizal symbiosis can enhance the synthesis of these compounds by promoting inorganic nitrogen uptake and facilitating its transport. Indeed, the increased production of PMs and SMs is linked to the transfer of mineral nutrients in exchange for fatty acids, amino acids, sugars, and lipids from AMF to the host cell (Gaude *et al.*, 2015a). The role of Pi in the synthesis of terpenoids precursors via the MVA (acetyl-CoA, ATP and NADPH) as well as the MEP (glyceraldehyde phosphate and pyruvate) pathways is widely recognized (Kapoor *et al.*, 2017). Levels of JA, derived from linoleic acid produced in the plastids, also

increase and trigger the production of phytoalexins (i.e., defensive compounds), while the production of antifungal compounds (e.g., gallic acid) by the host plant decreases (Gaude *et al.*, 2015; French, 2017). Moreover, defensive compounds in AMF-foliar tissues increase (e.g., rutin, HBA), not only due to the enhanced plant Pi content, but also to the aforementioned hormonal changes, and can trigger these metabolic modifications (Toussaint, 2007; Kapoor *et al.*, 2017). The impact of AMF on the production of various SMs in leaves, roots or fruits/tubers of different crops used as food or for medicinal purposes has been extensively reported (Gianinazzi *et al.*, 2010; Zeng *et al.*, 2013; Pedone-Bonfim *et al.*, 2015; Pandey *et al.*, 2018; Agnolucci *et al.*, 2020; Zhao *et al.*, 2022). Few examples: artemisinin in leaves of *Artemisia annua* L. (Chaudhary *et al.*, 2008), caffeic acid and RA in shoots of *Ocimum basilicum* L. (Toussaint *et al.*, 2007), and triterpene and phenolics in *Dioscorea* spp. (Lu *et al.*, 2015) were increased in plants colonized by AMF. Indeed, AMF increase the content of polyphenols and carotenoids, the activity of antioxidant enzymes, mevalonate, malonyl-CoA, and shikimate pathways, enhancing isoprenoids, polyketides, and polyphenols biosynthesis (Agnolucci *et al.*, 2020). These compounds are indicators of different functions in the plant-AMF symbiosis such as signalling, nutrient uptake, and resistance against biotic and abiotic stresses (**Figure 15**) (Kaur and Suseela, 2020).

1. Metabolomic studies on AMF-plant associations

Arbuscular mycorrhizal fungal symbiosis causes both global (species-independent) and local (species-specific) changes in plant metabolism. Global changes include increased production of PMs such as amino acids (e.g., glutamic, aspartic, and asparagine acid), fatty acids (e.g., palmitic and oleic) or SMs such as phenyl alcohols, linolenic acid, apocarotenoids, isoflavonoids, and plant hormones (e.g., oxylipin, cytokinins, and JA) (Rivero *et al.*, 2015; French, 2017). In contrast, the levels of specific SMs increase with plant and AMF species (see section III paragraph 2). An increasing number of studies have reported the "full picture" of AMF impact on PMs and SMs production in various plant species and crops (Hill *et al.*, 2018; Kaur and Suseela, 2020). Indeed, *via* a non-targeted metabolomics approach, it has been possible to separate and detect a wide range of molecules providing a global fingerprint of the quantitative and qualitative changes in the metabolism

of AMF colonized plants (Rivero *et al.*, 2015) (**Table 1**). Metabolomics represents a close link between genotype and has been proposed also for the comprehension of plant-environment interactions (Bernardo *et al.*, 2019).

An early study by Lohse *et al.* (2005), focused on the compounds referring to plastid and mitochondrial metabolism and on phosphate and trehalose in *M. truncatula* roots associated or not with *R. irregularis*[3]. They noticed a significant increase in the levels of certain amino acids (e.g., aspartate, glutamate, glutamine) and lower increases in others (e.g., asparagine, tyrosine, and tryptophan). In addition, two compounds involved in the mitochondrial TCA cycle (e.g., fumarate and malate) markedly decreased. Moreover, the production of fatty acids (e.g., palmitate, oleate, stearate, palmitvaccenoate, and vaccenoate) was increased in mycorrhized roots. A few years later, Schliemann *et al.* (2008), used a metabolomics approach to demonstrate that *R. irregularis* impacted both PMs and SMs production in *M. truncatula* roots. Indeed, during the most active stages of root colonization, elevated levels of amino acids (e.g., asparagine, aspartic and glutamic acid) and fatty acids (e.g., palmitic and oleic acids) were observed. Stimulation of certain SMs biosynthesis (e.g., isoflavonoids, apocarotenoids, saponins, cell wall-bound tyrosol) was also noticed, but mostly at the late stages of root colonization (Schliemann *et al.*, 2008). A similar work was performed with *Lotus japonicus* L. colonized or not with *Funneliformis mosseae*, but this time through a comprehensive analysis of aboveground tissues (Fester *et al.*, 2011). These authors observed a decrease in organic acids either connected to the central catabolic pathways in general (e.g., malic acid, citric acid, succinic acid), to the amino acids (e.g., glutamic acid, aspartic acid, glycine, asparagine, 4-aminobutanoic acid, 2-methyl-malic acid), or to the fatty acids (octadecanoic acid), carbohydrate (ribonic acid) or ascorbic acid (threonic acid) metabolisms in the AMF-colonized plants. These effects were particularly prominent in sink leaves, while flowers and source leaves showed additional increase in sugars (kestose), sugar alcohols (e.g., xylitol, myo-inositol), certain polyols and carbohydrates (e.g., fructose, altrose, galactose, trehalose) related to the abiotic stress (Fester *et al.*, 2011). In another study, Laparre *et al.* (2014), detected 71 mycorrhiza-associated SMs (e.g., isoflavonoids and apocarotenoids)

[3] It is to be noticed that the species names of AMF follow the nomenclature of today not the one at the time of publication.

exclusively present or at least 10-fold more abundant in *M. truncatula* roots associated with *R. irregularis*. Regarding specifically the aboveground metabolome of plants, the analysis of leaves of several dicots and monocots colonized by *R. irregularis*, showed an up/downregulation of different PMs (e.g., amino acids, organic acids) and SMs (e.g., catalpol, verbascoside) (Schweiger *et al.*, 2014). This study demonstrated that systemic phytometabolome responses to root colonization by the same AMF species with similar extent of symbiotic establishment are highly plant species-specific with only low degrees of conservation across species (Schweiger *et al.*, 2014). Gaude *et al.* (2015), presented the specific metabolites composition of colonized root cortex cells of *M. truncatula* associated with *R. irregularis*. In this study, among the 56 identified PMs, 14 were classified as amino acids (e.g., aspartate, asparagine, glutamate, and glutamine) and all of them were upregulated in colonized roots cells. Moreover, elevated amounts of sucrose and steady-state of hexose levels indicated a direct assimilation of monosaccharides by the fungal partner (Gaude *et al.*, 2015). In another study, Saia *et al.* (2015), evaluated the effects of AMF inoculation, either alone or in combination with PGPR, on the metabolic changes in roots of *Triticum durum* Desf. (durum wheat) grown under N-limited conditions in a P rich environment. These two treatments were compared with the association by the natural AMF population. Roots inoculated with a pool of different AMF species (*Scutellospora calospora, Acaulospora laevis, Glomus aggregatum, R. irregularis, F. mosseae, Glomus fasciculatum, Glomus etunicatum, Glomus deserticola,* and *Gigaspora margarita*) showed a decrease of amino acids, saturated fatty acids, whereas inoculation with AMF and PGPR increased the concentrations of such compounds. These results support the hypothesis that N availability is crucial for the benefit of AMF to the plant and that soil fungi can compete with the plant for N from organic matter. Because most N taken up directly in organic form from AMF is sequestered in AM structures, the result obtained by the authors is likely due to the increase in soil inorganic N in AMF associated to PGPR compared to AMF treatments. Nonetheless, compounds involved in C fixation (e.g., malic acid) were increased in mycorrhized roots as well as xilitol, which is crucial in the AMF-plant interaction (Saia *et al.*, 2015). Conversely, Rivero *et al.* (2015), presented, through a detailed metabolomics analysis, clear metabolites difference in *Solanum lycopersicum* L. (tomato) roots associated with two different AMF species (*F. mosseae* and *R. irregularis*). Their untargeted metabolomics analysis showed a notable increase of several

signals in AMF-colonized versus non-colonized plants referring to sugars, carboxylic acids, amino acids (e.g., glutamate, aspartate), compounds from the phenylpropanoid pathway (e.g., ferulic acid, cumaryl and coniferyl alcohols), and 13-LOX branch of the oxylipin pathway that leads to the biosynthesis of the phytohormone JA and derivatives. As reported in more details in the next paragraph, the two AMF species induced specific modifications in the metabolism of plants; *F. mosseae* had a stronger impact on amino acids, sugars, and phenolics as compared with *R. irregularis* (Rivero *et al.*, 2015). All the studies reported so far did not consider the metabolic variations of shoot and roots concomitantly. For this reason, Hill *et al.* (2018), investigated the metabolites profile in both foliar and root tissues of *Senecio jacobae* Gaertn. associated with *R. irregularis*. Their untargeted metabolomic approach revealed a significant upregulation of SMs belonging mainly to blumenol derivates and anti-herbivore defence compounds as PAs. Nevertheless, the changes were found mostly in the root system, while a slight or nonsignificant metabolic modification was observed in the shoot parts (Hill *et al.*, 2018). Shtark *et al.* (2019), studied the metabolomic profile changes in *Pisum sativum* L. associated with *R. irregularis* at different growth stages. Their analyses revealed that leaves of colonized plants, at different growth stages, contained higher levels of amino acids (e.g., glutamate, glutamine, glycine, homoserine, phenylalanine, proline, threonine, valine), unsaturated fatty acids, other N-containing compounds (e.g., urea and Gamma Amino Benzoic Acid-GABA), organic acids (e.g., aconitate, lactate, malonate), and SMs (e.g., 4-hydroxycinnamic acid). Sterol levels were accordingly lower than in non-colonized plants. Thus, AMF partially slows down the aging process and makes the leaf profiles of old M plants a little "younger". This effect was associated with prolongation of the vegetation period and the increase in seed biomass of the inoculated plants (Shtark *et al.*, 2019). Moreover, Bernardo *et al.* (2019), elucidated the metabolomic responses triggered by *F. mosseae* once associated with two different wheat genotypes (*Triticum durum* Desf. and *Triticum aestivum* L.) under full irrigation or water deficit regimes. Metabolomics results indicated a similar regulation of secondary metabolism in both genotypes under water limiting conditions. Nonetheless, *T. aestivum* was more affected by AMF colonization, with discriminant compounds mostly related to sugars and lipids, both being positively modulated by AMF colonization under water stress. Moreover, a regulation of metabolites related to oxidative stress (e.g., flavonoids, brassinosteroids, lignans) and a tuning of crosstalk between

phytohormones were also observed. A few more studies were conducted on *Vitis vinifera* L. (grape vine). For instance, in a study by Torres *et al.* (2019), the association of a AMF consortium (*Septoglomus deserticola, F. mosseae, R. intraradices, Rhizophagus clarus,* and *Glomus aggregatum*) modified the metabolites' in Tempranillo cv. berries, especially those belonging to the primary metabolism. The levels of glucose and amino acids (including those of the aromatic precursor amino acids) clearly increased in berries of mycorrhized Tempranillo grapevines, while the total amount and the profiles of anthocyanins and flavonols were barely influenced (Torres *et al.*, 2019). Recently, a detailed picture on metabolic changes induced by *R. irregularis* in both the roots and leaves of *Vitis vinifera* cv. Gewurztraminer was provided by Goddard *et al.* (2021). In their study, AMF triggered major reprogramming of primary metabolism in the roots, especially sugar and fatty acids' metabolism, with a significant increase in several fatty acids (e.g., C16:1, linoleic and linolenic acids, C20 arachidonic and eicosapentaenoic acids). Conversely, mycorrhizal roots had decreased contents of most sugars (e.g., galactose, glucose, mannose, sucrose, erythronic, and threonic acids), sugar acids, myoinositol, shikimic acid, and epicatechin. Metabolic changes were less marked in leaves, but involved higher levels of linoleic, linolenic, ribose, pyroglutamic, aspartic, and glyceric acids, and decreased sucrose, quinic, and shikimic acid, and putative caffeoylglycerol contents (Goddard *et al.*, 2021).

Table 1. Detailed summary of the metabolomic studies on AMF-plant associations.

Plant species	AMF[1]	Plant organ	Harvest time (days)	Experimental conditions	Analytical techniques[2]	No. of compounds detected	Change in PMs	Change in SMs	Reference
Medicago truncatula Gaertn.	*Rhizophagus irregularis*	roots	40	greenhouse (expanded clay)	GC-MS, GC-TOF-MS	170 polar	increased amino acids and fatty acids	NA	Lohse *et al.*, 2005
Medicago truncatula Gaertn.	*Rhizophagus irregularis*	roots	different growth stages (7-56)	greenhouse (expanded clay)	GC-TOF-MS, LC-MS	81 polar and 74 non-polar	increased amino acids and fatty acids	increased isoflavonoids, apocarotenoi, saponins, cell wall-bound tyrosol	Schliemann *et al.*, 2008
Lotus japonicus L.	*Funneliformis mosseae*	flowers, sink, source leaves	different growth stages (70-84)	greenhouse (sand:expanded clay mixture)	GC-MS	70-100 in total	decreased organic acids, amino acids, fatty acids, ribonic acid, threonic acid, increased sugars, polyols, carbohydrates	NA	Fester *et al.*, 2011

Medicago truncatula Gaertn.	*Rhizophagus irregularis*	excised hairy roots	70	laboratory (sterile culture medium)	UHPLC-HRMS (Q-TOF)	71 in total	NA	isoflavonoids, apocarotenoids (propionyl- and butyryl-carnitines)	Laparre *et al.*, 2014
Plantago lanceolata L., *Plantago major* L., *Veronica chamaedrys* L., *Medicago truncatula* Gaertn., *Poa annua* L.	*Rhizophagus irregularis*	leaves	62	climate chamber (sterilized leached swelling clay:sand mixture)	GC-MS, UHPLC-ToF-MS	NA	increased/decreased amino acids, organic acids	increased/decreased catalpol, verbascoside	Schweiger *et al.*, 2014
Medicago truncatula Gaertn.	*Rhizophagus irregularis*	arbuscule-containing cells	21	greenhouse (clay:silica sand: vermiculite mixture)	GC-EI/TOF-MS	56 polar	increase amino acids, sucrose, hexose	NA	Gaude *et al.*, 2015

Continue in the next page…

Triticum durum Desf.	mix AMF[3], mix AMF + PGPR, NAT	roots	110	field	GC-TOF-MS, HILIC-Q-TOF-MS	127 in total	decreased amino acids, carbohydrate, fatty acids. Increased malic acid, xylitol	NA	Saia *et al.*, 2015
Solanum lycopersicum L.	*Funneliformis mosseae*, *Rhizophagus irregularis*	roots	56	greenhouse (sterile sand:soil mixture)	LC-ESI-Q-TOF-MS	1876 signals in total. 300 signals (M treatments)	increased/decreased amino acids	increased phenolic alcohol derivatives, vitamins, plant hormones, oxylipins, cytokinins	Rivero *et al.*, 2015
Senecio jacobae Gaertn.	*Rhizophagus irregularis*	leaves, roots	70	greenhouse (sterile silver sand:Terragreen® mixture)	UPLC-Q-TOF-MS	NA	no effect	increased blumenol apocarotenoids, phenolics, PAs	Hill *et al.*, 2018
Pisum sativum L.	*Rhizophagus irregularis*	leaves	Different growth stages (7-56)	Climate chamber (sterile soil:quartz sand mixture)	GC-MS	300 in total	increased amino acids, unsaturated fatty acids, organic acids, decreased sterol	increased phenylpropenoic acid	Shtark *et al.*, 2019

Triticum durum Desf., *Triticum aestivum* L.	*Funneliformis mosseae*	roots	43	climate chamber (sterile sand:pasteurized field soil mixture)	UHPLC-ESI/QTOF-MS	115 in total	increased phosphate sugars, glycerol-heptoses, lipids	increased glutathione, homotaurine, brassinosteroids, flavonoids, lignans	Bernardo *et al.*, 2019
Vitis vinifera L.	mix AMF[4]	berries	93-95	greenhouse (sterile vermiculite:sand :light peat)	HPLC, UHPLC	NA	increased glucose, amino acids	no effect	Torres *et al.*, 2019
Vitis vinifera L.	*Rhizophagus irregularis*	leaves, roots	56	climate chamber (sterile sand:perlite mixture)	GC-MS, LC-MS	494 in total	increased sugars, fatty acids, decreased sugars	increased JA, SA, decreased shikimic acid, epicatechin, catechin, putative resveratrol	Goddard *et al.*, 2021

[1]It is to be noticed that the species names of AMF follow the nomenclature of today not the one at the time of publication.
[2]Gas Chromatography Time-of-Flight Mass Spectrometry (GC-TOF-MS), UltraHigh-Performance Liquid Chromatography (UHPLC), High-Resolution Mass Spectrometry (HRMS), Quadrupole Time-of-Flight (Q-TOF), Gas Chromatography-Electron impact ionisation/Time-of-Flight-Mass Spectrometry (GC-EI/TOF-MS), Hydrophilic Interaction Chromatography Time-of-Flight Mass Spectrometry (HILIC-Q-TOF-MS), Liquid Chromatography-Electrospray Ionisation-Quadrupole Time-of-Flight Mass Spectrometry (LC-ESI-Q-TOF-MS).
[3]*Scutellospora calospora, Acaulospora laevis, Glomus aggregatum, Rhizophagus irregularis, Fulleniformis mosseae, Glomus fasciculatum, Glomus etunicatum, Glomus deserticola, and Gigaspora margarita.*
[4]*Septoglomus deserticola, Funneliformis mosseae, Rhizophagus intraradices, Rhizophagus clarus, and Glomus aggregatum*.

2. Functional specificity in AMF interactions

Most available commercial inocula are composed of only a few AMF species, mostly those that are easily maintained and mass cultured. However, commercial inocula are far from accomplishing the potential benefits offered by AMF in each specific situation (Brito *et al.*, 2019). In fact, there is considerable functional diversity among AMF and, depending on the host plant or the environmental conditions, the symbiosis has different effects on the host. This aspect is also reflected in the metabolomic studies mentioned above, which focused mainly on two AMF species, *R. irregularis* and *F. mosseae*. These soil fungi are easily available as commercial products and are considered generalist symbionts, widespread all over the world in almost all soils and climatic zones (Giovannini *et al.*, 2020). In addition, *R. irregularis* is used as a model organism in AMF research, because it is easily and massively grown *in vitro* on root organs (Declerck *et al.*, 2005) and its genome has been fully sequenced (Rivero *et al.*, 2015). Even if molecular approaches have considerably improved the identification and traceability of AMF, their functional diversity is still poorly understood. Indeed, plant growth promotion and phosphorus uptake may vary between AMF species as well as between isolates of a same species (Munkvold *et al.*, 2004). As already mentioned, depending on the host plant or environmental conditions, the symbiosis has different effects, thus not all plant-AMF associations are mutually beneficial and the productivity of the host plant (i.e., the outcome of the association) is highly dependent on the identity of the AMF symbiont (Brito *et al.*, 2019; Kaur and Suseela, 2020).

Additionally, diverse AMF species or strains can affect differently the production of specific phytochemicals in the same or different plant species. For instance, Rivero *et al.* (2015), reported that, although the metabolic pathways altered by the mycorrhizal symbiosis were common to both *S. lycopersicum* roots associated with *F. mosseae* and *R. irregularis*, many compounds showed specific responses to one of the symbionts. For example, bioactive forms of JA, methyl-JA (Me-JA) and JA-Ile conjugates were accumulated in significantly higher amounts only in the roots associated with *F. mosseae*. Thus, a fine-tuned developmental regulation of these pathways was suggested to be dependent on the AMF species. Moreover, Schweiger *et al.* (2014), demonstrated that different plant species associated with the same generalist AMF (*R. irregularis*) share the same “core metabolome”.

However, the specific phytometabolomes were highly dependent on plant species/taxon. For instance, *M. truncatula* was most responsive to AMF with 14.7% of its metabolic features being modulated, whereas the Plantaginaceae species (e.g., *P. lanceolata*: 5.8%, *P. major*: 5.4%, *V. chamaedrys*: 5.7%) exhibited an intermediate response and *P. annua* was the least responsive (1.7%) to AMF symbiosis. As a more specific examples, the pool size of the SM catalpol was highly increased in mycorrhized *P. lanceolata*, whereas it was slightly decreased in *V. chamaedrys.* Several organic acids from the TCA cycle (e.g., citrate, malate, fumarate) decreased in pool sizes in *P. lanceolata*, *P. major*, *V. chamaedrys* and *M. truncatula* associated to AMF, but increased in the grass *P. annua*. Thus, Schweiger *et al.* (2014) concluded that phytometabolome modulation by an identical AMF symbiont is severely limited even between closely related plant species. This was also observed by Bernardo *et al.* (2019), with two different wheat genotypes (i.e., *T. durum* and *T. aestivum*) associated with *F. mosseae*. Their unsupervised analysis revealed an AMF x cultivar interaction on root secondary metabolome, with *T. aestivum* cultivar more affected by AMF colonization. They hypothesized that the AMF colonization had a strong impact in reprogramming the wheat roots metabolism of sugars, lipids and plant phytohormones, besides flavonoids, metabolites related to histidine biosynthesis and lignans that were known to accumulate in mycorrhizal roots.

A systematic combinatorial study on mycorrhizal benefits using a large panel of plant and fungal species from different geographical locations showed that the mycorrhizal growth response (i.e., difference between the weights of colonized and non-colonized plants) ranged from growth depression of 50% to growth promotion of 50%, with almost half of the combinations resulting in growth depression (Klironomos, 2003). The mutualistic potential did not correlate with phylogenetic patterns in either partner, indicating adaptive mechanisms independent from lineage. Interestingly, combinations of partners isolated from the same location performed better, suggesting co-adaptation (Chen *et al.*, 2018). Indeed, indigenous AMF have been demonstrated to be equally or even better performing than isolates from commercial products or culture collections (Berruti *et al.*, 2016). For instance, Estrada *et al.* (2013) demonstrated how, under saline stress conditions, maize plants inoculated with native AMF had a higher shoot dry weight, efficiency of photosystem II, stomatal conductance, and accumulation of glutathione than those inoculated with AMF from

culture collections. Another study by Wu *et al.* (2021), showed that inoculation of *Salvia miltiorrhiza* Bge. with native AMF promoted roots growth and increased SMs production (especially phenolic acids).

Regarding Boraginaceae plants, they are frequently described based on their therapeutic properties. However, the literature involving their AMF microbial associates' remains poor. A recent study by Sinegani and Yeganeh (2016) reported the presence of AMF in *Echium amoenum* Fisch. & C.A. Mey. and *Borago officinalis* L. Moreover, fungal endophyte and AMF root colonization were reported for *Anchusa orientalis* L. and *A. officinalis* (Zubek *et al.*, 2011; Zubek et al., 2016). However, no direct studies, to the best of our knowledge, have investigated the effects of these symbionts in *A. officinalis* and/or *A. tinctoria*.

Since different AMF can promote the accumulation of bioactive compounds to varying degrees in medicinal plant species, as reported in detail in the review by Zhao *et al.* (2022), large scale screening of a range of AMF is necessary in order to utilise an ideal strain. In this review, more details on the effects of AMF on the production of specific bioactive compounds in various medicinal plant species can be found as well.

IV. Methods of production of bioactive compounds in Boraginaceae plants

The production of bioactive compounds *via* cultivation of Boraginaceae plants under conventional agricultural practices is difficult due to poor seed germination, low-availability of planting material, extensive time needed for noticeable bioactive compounds production, and high harvesting costs (Malik *et al.*, 2016). For these reasons, direct plant regeneration and micropropagation are options that have been considered in the recent years. In addition, several efforts have been made to produce important compounds (e.g., A/Sd, RA) from plants grown under controlled conditions and in the synthesis of pharmaceutically important compounds. As described in the next paragraphs, most of the trials did not succeed or were not economically viable (Sharma and Shahzad, 2013). Yet, for what concern specifically A/Sd, they remain mostly extracted from roots of plants (e.g., *A. tinctoria*) grown in nature, resulting in an unconsidered exploitation and

risk of extinction of important medicinal plants. For instance, in some European countries such as Slovakia and Hungary, *A. tinctoria* is considered as very rare (Yazaki, 2017; Yaman *et al.*, 2019; Ahmad *et al.*, 2021). The risk of extinction has also been documented for *L. erythrorhizon* in Japan, *Alkanna sieheana* Rech. Fil. and *Alkanna orientalis* (L.) Boiss. in Turkey.

Finally, the production of bioactive compounds in plants is usually low (i.e., less than 1% of the plant dry weight) and is greatly dependent on the physiological and development stage of the plant (Halder *et al.*, 2019). Their production is often subjected to uncontrollable factors (e.g., biotic/abiotic stresses), which affect the overall plant biomass and production of metabolites. To overcome these problems, several cultivation techniques have been developed to induce the biosynthesis of compounds and their direct production under controlled conditions (Ji *et al.*, 2019).

1. Production of bioactive compounds under *in vitro* conditions

Biotechnological developments give us the possibility to use cells, tissue or organs of economically important plants by growing them under *in vitro* culture conditions or modifying their genome to obtain the desired compounds. Additionally, *in vitro* cultures (e.g., callus, cell suspension, shoot, and hairy roots) could replace the extraction of valuable compounds from wild or cultivated plants (Malik *et al.*, 2016). Indeed, these cultivation techniques offers a number of advantages: (i) interfering compounds that occur in field-grown plant can be avoided *in vitro*, (ii) phytochemicals can be produced in large volumes; (iii) secondary products can be generated on a continuous year-round basis without seasonal constraints, (iv) production is independent of environment conditions (Park *et al.*, 2008). For instance, over the last decades, several efforts have been made to produce A/S from plants grown under controlled conditions. Cell tissues and root cultures of *A. tinctoria* have been attempted (Urbanek *et al.*, 1996; Gerardi *et al.*, 1998). Studies on the effects of growth medium ingredients on the production of shikonin by *L. erythrorhizon* callus cells were conducted, and a two-stage culture system composed of a growth medium (Linsmaier and Skoog or Murashige and Skoog, LS or MS) and a production medium (M9) has been established (Fujita, 1988). Indeed,

N source in the growth medium, with an ammonium-to-nitrate ratio, is important to induce the growth of callus cells, but is negatively correlated with the biosynthesis of A/Sd. Thus, applying only M9 medium with no ammonium is unsuitable for the growth of hairy roots (Fu *et al.*, 2020). The two-stage culture system was then applied for shikonin biosynthesis in tissue cultures of *Echium plantagineum* L. (Fu *et al.*, 2020) (**Figures 16 a-b**), *L. erythrorhizon* (Zhao *et al.*, 2015), and *Arnebia euchroma* (Royle) Johnston (Singh *et al.*, 2010). However, the only successful example of shikonin scaling up from cell cultures was with *L. erythrorhizon* by Mitsui Petrochemical Industries Ltd. (now Mitsui Chemicals Inc., Tokyo, Japan) in 1984 (Yazaki, 2017). A few other attempts have been made with cell suspension cultures of *Arnebia* spp. in stirred-tank (New Brunswick Scientific Company Inc., Edison, NJ) and in air-lift bioreactors, but no further commercial success has been reported (Gupta *et al.*, 2014; Malik *et al.*, 2016) (**Figure 16c)**.

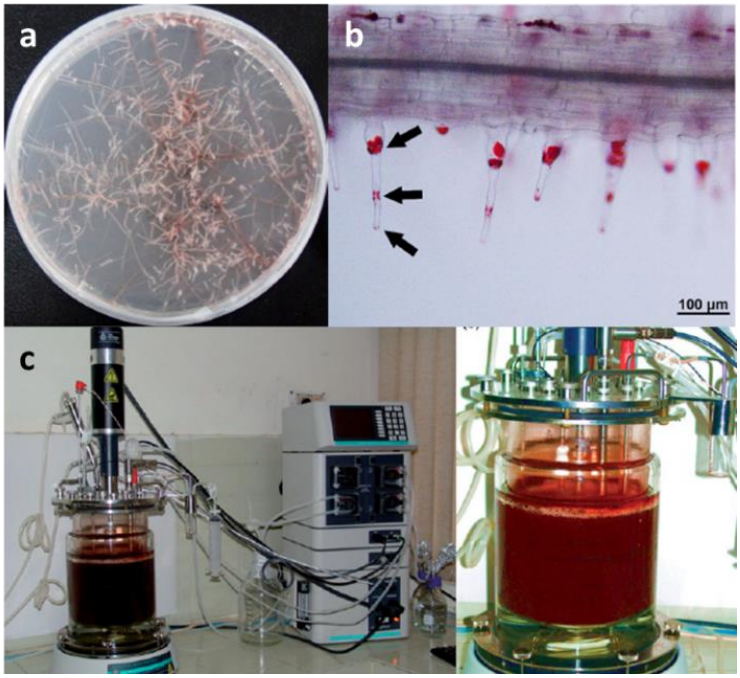

Figure 16. **(a)** Hairy root culture of *Echium plantagineum* and **(b)** microscopy image of the transformed hairy roots culture with arrows pointing to the red naphthoquinones (from Fu *et al.*, 2020). **(c)** Shikonin derivatives production from cell suspension cultures of *Arnebia euchroma* in 7.5 L bioreactor and a close up of the same (from Malik *et al.*, 2016).

Production of RA, up to 4 g dry weight L^{-1}, by *A. officinalis* was obtained in shake-flask cultures using a cultivation strategy that involved intermittent medium change (Su *et al.*, 1994). Implementation of this cultivation strategy in 2.5-L stirred-tank bioreactor cultures was further investigated, and similar results were obtained with a maximum cell density of 35 g dry weight L^{-1} and a RA concentration of 3.7 g L^{-1} (Su *et al.*, 1995). However, to our knowledge, no recent study or reference to successful industrial applications could be found. The reasons for failure and limited scaling up can have several origins: low yield of bioactive compounds from plant tissues cultures, unpredictably variable yields, limited benefits due to long procedures in selecting high yielding cell lines, inappropriate nutrient media and culture conditions (Park *et al.*, 2008; Malik *et al.*, 2016).

Direct plant regeneration and micropropagation are options that have been considered in the recent years for several Boraginaceae such as *Arnebia hispidissima* (Lehm). DC. (Pal and Chaudhury, 2010), *Sericostoma pauciflorum* Stocks ex Wight (Satish *et al.*, 2014), and *Mertensia maritima* L. (Park *et al.*, 2019). For instance, the total content of shikonin from 1 g of induced *A. hispidissima* root tissue was 0.50 mg after 50 days of *in vitro* culture (Pal and Chaudhury, 2010).

Increasing production of bioactive compounds has also been obtained by using elicitors (i.e., chemical compounds from abiotic and biotic sources), which stimulate the stress responses in plants (Naik and Al-Khayri, 2016). A recent review by Zhao *et al.* (2022), reported numerous examples of successful biotic elicitation for production of SMs in hairy root cultures (HRCs). For instance, Zou *et al.* (2011) reported a 30-fold increase of A/S accumulation in *L. erythrorhizon* HRCs treated by fungal elicitors isolated from *Rhizoctonia solani*. Moreover, A/Sd increase was reported in cell cultures of *L. erythrorhizon*, *A. tinctoria*, and *A. euchroma,* after application of exogenous jasmonate (Gaisser and Heide, 1996; Urbanek *et al*., 1996). Finally, in a recent study by Rat *et al.* (2021), isolated bacterial endophytes were tested for their ability to induce A/S production in HRCs of *A. tinctoria*. Four strains belonging to *Chitinophaga*, *Allorhizobium*, *Duganella*, and *Micromonospora* species, significantly increased A/S production compared to uninoculated controls.

2. Production of bioactive compounds in hydroponic systems

Because of high costs, slow growth, possible lack of metabolites excretion from cells or tissues and preservation of the axenic conditions, hydroponic cultivation systems have been tested for the production of bioactive compounds by medicinal plants (Gontier *et al.*, 2002). Dayani and Sabzalian (2017), reported more than 20 examples of improved SMs yield in medicinal plants cultivated in hydroponic systems (e.g., caffeic acid derivatives and RA in *O. basilicum*, essential oils in *Coriandrum sativum* L., and in *Mentha x piperita* L.). Hydroponic cultivation systems are conducted under highly controlled and up scalable conditions and are suitable for the adoption of a new technology named Plant Milking® [4]. This allows the direct extraction of important bioactive compounds in a non-destructive way using the same plants material multiple times (Gontier *et al.*, 2002; Sgherri *et al.*, 2010). By using the Plant Milking® technology for *Morus alba* L. (i.e., an emblematic tree of the traditional Chinese medicine rich in alkaloids and flavonoids), Chajra *et al.* (2020), obtained an extract enriched in prenylated flavonoids that was 18-fold higher as compared to commercial root extracts (**Figure 17a**). Interestingly, the hydroponic cultivation systems are adapted to the use of metabolites elicitors, like AMF (IJdo *et al.*, 2011; Garcés-Ruiz *et al.*, 2017; Cartabia *et al.*, 2021) (**Figure 17b**). Therefore, the combination of highly controlled hydroponic cultivation systems with AMF represents an interesting avenue to assess and understand the increase/modulation of bioactive compounds produced by our plants of interest.

[4] https://www.plantadvanced.com/home

Figure 17. (a) *Morus alba* trees cultivated in aeroponic conditions and a close-up of the same (from Chajra *et al.*, 2020). **(b)** Plant based bioreactor system for the mass production of AMF (from IJdo *et al.*, 2011).

RESEARCH QUESTIONS

The State of the Art section encompassed, to the best of our knowledge, most of the literature available to support this study. Nonetheless, significant gaps in the study of the beneficial effects of AMF on the production of metabolites of interest in *A. officinalis* and *A. tinctoria,* as well as the availability of plant material mainly concerning *A. tinctoria,* have been identified. These gaps have been taken into consideration in this thesis through five main research questions which are presented below, and the answers are reported in the relevant chapters of the thesis:

1- Does the AMF *R. irregularis* MUCL 41833 modulate the production of metabolites in shoot and root tissues as well as in the nutrient solution of *A. officinalis* plants grown in a semi-hydroponic cultivation system? What specific biosynthetic pathways are up or down regulated as compared to uncolonized plants? Results reported in Chapter I.

2- Is the metabolome of *A. officinalis* dependent on AMF species (*R. irregularis* MUCL 41833, *R. intraradices* MUCL 49410, *R. clarus* MUCL 46238, and *R. aggregatus* MUCL 49408) and are PMs and SMs productions species specific? Results reported in Chapter II.

3- What is the best protocol to mass produce healthy *ex vitro A. tinctoria* plants starting from *in vitro* shoot-tip explants? Results reported in Chapter III.

4- Does the AMF *R. irregularis* MUCL 41833 increase the production of A/Sd and the relative expression of genes in the root tissues of *A. tinctoria* plants growing in a semi-hydroponic cultivation system? Results reported for Experiment 1 in Chapter IV.

5- Does the association of *A. tinctoria* plants with different AMF strains from GINCO (*R. irregularis* MUCL 41833, *R. aggregatus* MUCL 49408) and isolated from wild-growing *A. tinctoria* (*R. irregularis* and *S. viscosum*) results in similar effects on the production of A/Sd and relative genes expression? Results reported for Experiments 2 and 3 in Chapter IV.

MATERIAL AND METHODS

I. Biological materials

1. Arbuscular Mycorrhizal Fungi

- *Rhizophagus irregularis* (Błaszk., Wubet, Renker & Buscot) (Schüßler and Walker) as [‘irregulare'] MUCL 41833, formerly named *Glomus intraradices/irregulare* (Redecker *et al.*, 2013), was isolated from a soil in the Canary Island (Spain). It is used as a model organism in AMF research, since it is considered a generalist symbiont, widespread all over the world in almost all soils and climatic zones (Giovannini *et al.*, 2020). In addition, it is easily grown *in vitro* on root organs (Declerck *et al.*, 2005) and is widely used in commercial products (Rivero *et al.*, 2015).
- *Rhizophagus intraradices* (N.C. Schenck & G.S. Sm.) C. Walker & Schuessler) MUCL 49410, formerly named *Glomus intraradices* (Walker *et al.*, 2021), was isolated from a soil in Clermont-Minneola (Florida, Orlando, USA). A recent study by Walker *et al.* (2021) confirmed that sequences from all *R. intraradices* formed a monophyletic clade well separated from, and not representing a sister clade to, *R. irregularis*.
- *Rhizophagus clarus* (T.H. Nicolson & N.C. Schenck) C. Walker & A. Schüßler) MUCL 46238, formerly named *Glomus clarum*, was originally isolated from soils in La Palma (Pinar del Rio, Cuba).
- *Rhizophagus aggregatus* (N.C. Schenck & G.S. Sm.) C. Walker MUCL 49408, formerly named *Glomus aggregatum* (Schenck and Smith, 1982), was isolated from a soil in Brittany (France). Further analyses are needed to clarify its phylogenetic position, as this fungus is firmly believed to be simply a small variant of *R. intraradices* (source INVAM)[5].

All these AMF strains have been used in various studies proving their effect on the metabolism and growth of plants (Zhao *et al.*, 2022).

[5] https://amf-phylogeny.jimdofree.com/

The AMF strains have been supplied by the Glomeromycota *IN vitro* COllection (GINCO)[6] in Petri plates, associated to Ri T-DNA transformed roots of *Daucus carota* L. or *Cichorium intybus* L. The strains were further maintained and sub-cultured *in vitro* on the modified Strullu-Romand (MSR) medium (Declerck *et al.*, 1998), solidified with 3 g L^{-1} GelRite® (Carl Roth, Karlsruhe, Germany). Petri plates were incubated in an inverted position in the dark at 27°C. After 4-5 months, several hundred to thousands of spores were obtained from each Petri plate. The AMF were then proliferated in the greenhouse in association with *Zea mays* L. plants to produce a sufficiently established mycelium network and colonized roots that will then serve as inoculum.

- *Rhizophagus irregularis* and *Septoglomus viscosum* strains isolated, purified, and identified by Ph.D. YanYan Zhao from *A. tinctoria* plants collected in Northern Greece (Evaggelistria, Seih Sou, Thessaloniki).

These two AMF strains were also proliferated in the greenhouse in association with *Zea mays* L. plants. To our knowledge, this is the first time that AMF have been isolated from *A. tinctoria* roots (further details in Chapter and Annex IV).

2. Plants

- *Anchusa officinalis* L. and *Alkanna tinctoria* Tausch., Boraginaceae, were chosen based on their well-known and reported production of bioactive compounds. Seeds of *A. officinalis* were purchased from Rühlemann's herbs & aromatic plants (Horstedt, Germany), while *A. tinctoria in vitro* plants were provided by the Institute of Plant Breeding and Genetic Resources, Hellenic Agricultural Organization (HAO)-DEMETER, Thessaloniki, Greece. Growth conditions and plants development are reported in further details in Chapters I and II for *A. officinalis*, and Chapters III and IV for *A. tinctoria*.
- *Zea mays* L. cv. ES Ballade (maize) seeds were purchased from Euralis (Lescar, France). This plant was used for AMF mass production in the greenhouse due to its high colonization rate under controlled greenhouse conditions (IJdo *et al.*, 2011). The method

[6] http://www.mycorrhiza.be/ginco-bel

reported below was applied throughout the entire study. Bleach soaked and water washed maize seeds were germinated in sterilized lava (DCM, Grobbendonk, Belgium) substrate (120°C for 15 min) in 10 L size pot. One-week old maize seedlings were inoculated with propagules of the GINCO AMF strains described above (i.e., transformed roots and spores). Regarding the native AMF, one-week old maize seedlings were inoculated with spores produced on single trap plant in pots (more details to be found in Chapter IV and Annex IV). All the pots were watered every three weeks and kept under greenhouse condition at 20°C, 50% relative humidity (RH), photoperiod of 16 h day^{-1} and photosynthetic photon flux (PPF) of 96 µmol $m^{-2}s^{-1}$. About every 6 months, the maize plants were replaced (older plants were cut at the base and new surface-disinfected maize seeds were sown in the established AMF mycelium network). Before associating the plants of interest (i.e., *A. officinalis* and *A. tinctoria*) with the above-mentioned AMF strains, maize roots were checked for effective AMF colonization.

II. Evaluation of root colonization by AMF

Root colonization in this study was estimated by the method of McGonigle *et al.* (1990). Roots were first stained with ink (Parker Blue Ink, United States), following the protocol below, to reduce the use of noxious and dangerous chemicals (Walker, 2005) (**Figure 18**).

Two slightly different procedures were followed for *A. officinalis* and *A. tinctoria* roots in this study. For both plants, 25 mL of potassium hydroxide (KOH) 10% was added before incubation at 70°C in a hoven for 40/45 min for clearing the cells. The KOH solution was then removed and replaced with hydrochloric acid (HCl) 1% for 1 min at room temperature, to neutralize the pH and increase the affinity with the ink solution. Regarding *A. tinctoria* roots, an extra step was added since the roots of this plant are characterized by a high content of pigments (i.e., naphthoquinones responsible for the red colour of the roots). The HCl 1% solution was replaced with hydrogen peroxide (H_2O_2) 3.5% solution before incubation at 70°C for 5 min. The roots were then rinsed with deionized water. Similar staining step consisted in adding blue ink 2% in HCl 1% and again incubate in the hoven at

70°C for 30 min. Finally, the roots were rinsed with deionized water and kept in acidified glycerol before observation.

For colonization assessment, the root fragments were placed on microscope slides and covered with a 40×22 mm coverslip before observation under a bright field light microscope (Olympus BH2-RFCA, Japan) at ×10 magnification (**Figure 18**). Around 200 intersections were observed per plant. The percentage of total colonization (TC%) of roots (e.g., hyphae, arbuscules, and vesicles), and percentage of arbuscules (AC%) was further calculated using the formulas below:

$$TC\% = \frac{\text{tot n. intersections examined} - \text{“negative-intersect”}}{\text{tot n. intersections examined}} \times 100$$

$$AC\% = \frac{\text{n. intersections with presence of arbuscules}}{\text{tot n. intersections examined}} \times 100$$

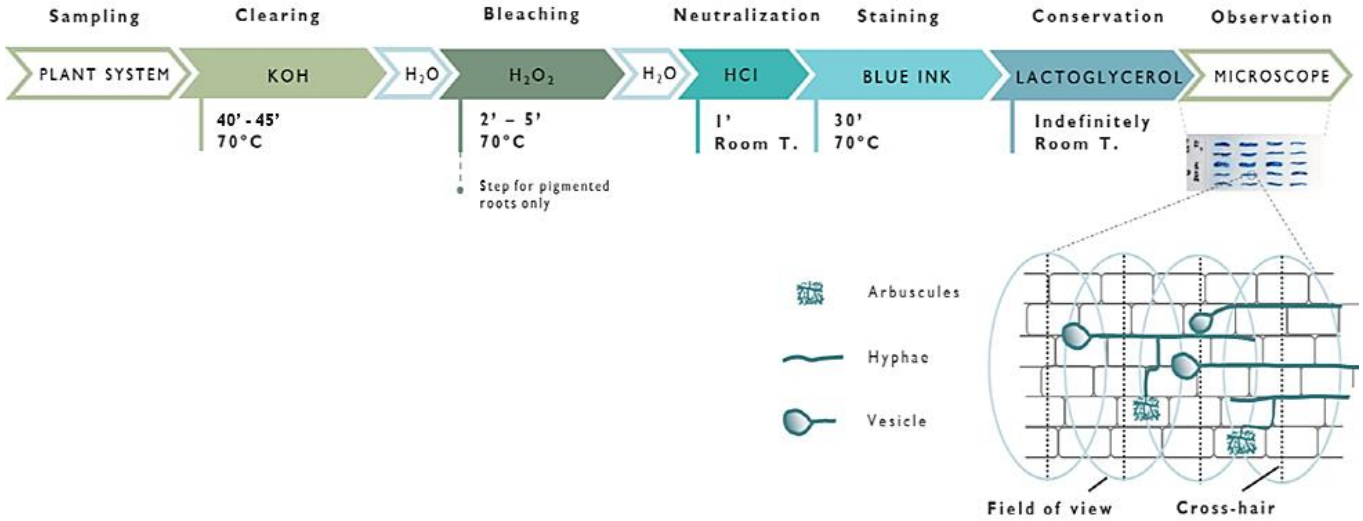

Figure 18. Schematic representation of the staining procedure and AMF colonization assessment in Boraginaceae roots. The bleaching step was only used for *A. tinctoria* whose roots are pigmented due to the presence of naphthoquinone compounds (from Maria Miguel master thesis).

III. The Semi-Hydroponic cultivation system

The semi-hydroponic (S-H) cultivation system (**Figure 19**), developed by Garcés-Ruiz *et al.* (2017), was applied in Chapters I and II to detect profile modifications in PMs and SMs produced in shoots and roots, as well as exudated in the nutrient solution, of AMF-colonized or non-colonized *A. officinalis* plants. It was further applied in Chapter IV to detect differences in the production of A/Sd and to study targeted gene expression in roots of AMF-colonized or non-colonized *A. tinctoria* plants.

a) The nutrient solution – A 90% P-impoverished (Phosphorus = 6.245 mg L^{-1}) modified Hoagland solution (**Supplementary Table 1**, **Annex I**) was used at two different concentrations: diluted by 200× (referred as Hoagland^{dil200X}) during the acclimatization phase and diluted by 100× (referred as Hoagland^{dil100X}) during the circulation phase. The pH of the solutions was always adjusted to 5.6 ± 0.2 beforehand.
b) Set-up – Boraginaceae plants were placed in 500 mL wash plastic bottles (VWR INTERNATIONAL, Leuven, Belgium) cut at the base and placed bottom-up. A 100 µm size pore nylon mesh (Prosep B.V.B.A., Zaventem, Belgium) was glued on the top of the bottles (called containers thereafter) to prevent loss of substrate and roots growing out of the containers. Each container was filled with 32 g of sieved (1-mm diameter), rinsed (with deionized water), and dried (48 h at 50°C) perlite. The perlite was covered with a superficial layer of black lava rock (1-3 mm) and the containers were wrapped in aluminium foil to avoid algae development. The containers were transferred randomly in holes made in flex foam supports and were maintained under greenhouse (specific plant growth conditions reported in the relevant Chapters).
c) Acclimatization – Boraginaceae plants were acclimatized for 7 days, receiving 200 mL Hoagland^{dil200X} solution every 48 h. The containers were closed with screw caps at the bottom, which were opened to discard the old solution before replacement with fresh solution.
d) Flushing – Following the acclimatization phase, an initial flushing was performed to establish an equal nutrient concentration in all the containers. Each plant container received 200 mL of Hoagland^{dil100x}

solution, which was circulated at a velocity of 44 mL min^{-1} through the containers and then discarded.

e) Circulatory system – Following the acclimatization and flushing phases, the circulatory system was set up as follows. Each container was connected to a 1 L glass bottle (SCHOTT DURAN, Landshut, Germany), covered with aluminium foil containing Hoagland^{dil100X} solution. A 3 mm diameter silicon tube (VWR INTERNATIONAL, Leuven, Belgium) connected a dropper cap fixed on the bottom of the plant container with the glass bottle, and another silicon tube of the same diameter connected the glass bottle to the upper part of the plant container via a multichannel peristaltic pump (Gilson's Minipuls Evolution, Villers le Bel, France). Once the circulation started, the nutrient solution was pumped from the glass bottle into the plant container and the liquid flowed back by gravity into the bottle (specific circulation durations reported in the relevant Chapters).

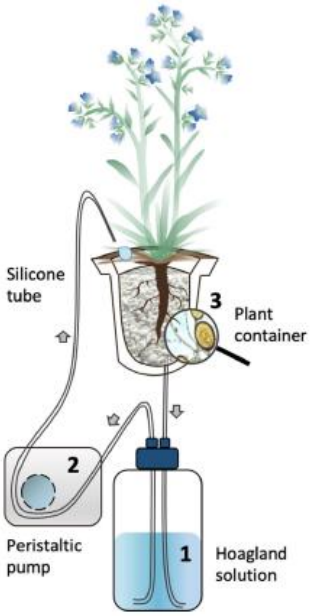

Figure 19. Schematic representation of the circulatory semi-hydroponic cultivation system. The Hoagland solution circulated through the containers supporting the Boraginaceae plants. The nutrient solution in the glass bottle **(1)** is pumped using a peristaltic pump **(2)** to the upper part of the plant container **(3)** *via* silicon tubes. The solution percolate through the plant container back into the glass bottle. The arrows indicate the flow direction of the nutrient solution in the tubing (adapted from Cartabia *et al.*, 2022).

IV. Metabolic profiling workflow

Metabolic profiling focuses on small molecules or metabolites present in an extract that reflect the metabolome at a specific time (Kim *et al.*, 2010). The metabolome itself consists of the larger collection of all metabolites in a biological system including both PMs and SMs. A typical metabolomic workflow (**Figure 20**) includes the design of analytical experiments, followed by sample preparation, data acquisition (i.e., metabolites analysis), data pre-processing, data annotation, statistical analysis, and data visualization for biological interpretations (Ernst *et al.*, 2014; Fenaille *et al.*, 2017). Further details on the specific workflow conditions can be found in Chapters I and II for the metabolites analysis of shoot and roots of *A. officinalis* as well as exudates in the nutrient solution. In Chapter IV, further details can be found on the A/Sd analysis in roots of *A. tinctoria*.

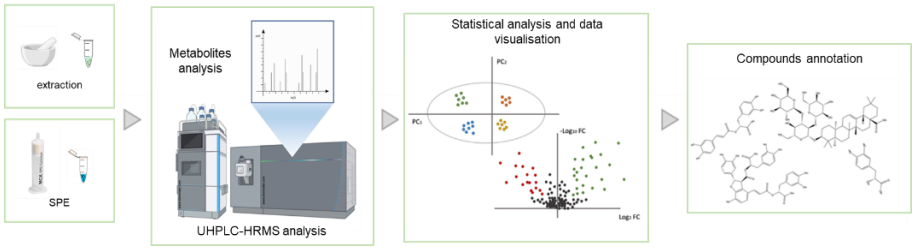

Figure 20. Diagram representing the metabolomic workflow applied in Chapters I and II (adapted from Tsiokanos *et al.*, 2022).

1. Samples preparation

This stage can be subdivided in the following four general steps (Ernst *et al.*, 2014):

i. **Harvesting of the plant materials**. The metabolome of plants may vary depending on the time or environmental conditions of harvest. The influence of environmental conditions is extremely important for plant material collected in the wild, while it may be considered minor for plants cultivated in the greenhouse. The main sources of variability to be considered during harvesting are light, plant circadian cycle, plant growth stage, plant organ.

ii. **Processing before extraction**. Stressing the plant during the harvesting could causes metabolome alterations. Thus, harvesting should be done as quickly as possible, and the metabolism should be stopped immediately by freezing or freeze-drying plant material in liquid nitrogen or storing samples at low temperature. Further processing before extraction may include pulverizing the plant material into small particles to improve the extraction process through, for example, the use of a mortar and pestle (**Figure 21a**).

iii. **Extraction**. Because metabolomic studies are usually large-scale experiments, extraction methods should be as simple and fast as possible. Solvent extraction was the method applied in this study (**Figure 21b**). Degradation, modification, and loss of metabolites during extraction should be minimised. However, there is no ideal method for extraction of all metabolites without formation of artifacts or degradation of compounds. Also, plant tissue metabolites are highly diverse: non-polar compounds (e.g., terpenoids and fatty acids from cell membranes), medium polarity compounds (most of the SMs), and polar compounds (most of the PMs). Several critical factors must be considered during extraction: ratio of solvent and plant material, solvent characteristics, time of extraction, temperature, and choice of appropriate method for desired goals. Although a completely non-compound-specific sample preparation, as required in metabolomic experiments, is not possible, the preparations of the analysed samples must be identical for accurate comparisons.

iv. **Pre-analytical samples preparation**. In some cases, pre-analytical procedures are required to prepare a sample for the analytical method. This preparation may avoid sample carryover in chromatographic systems, concentrate the analytes of interest or remove interfering substances.

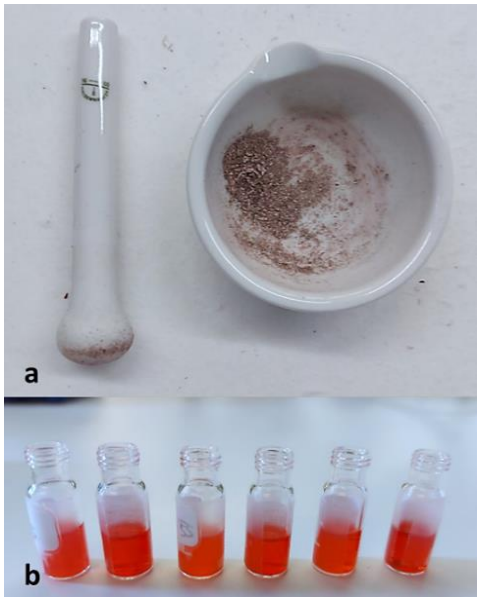

Figure 21. (a) Pulverization of *A. tinctoria* roots material using mortar and pestle. **(b)** Solvent extraction of *A. tinctoria* roots material, characteristic red colour due to the extraction of naphthoquinones (A/Sd) (Chapter IV).

1.2 Solid Phase Extraction

The Solid Phase Extraction (SPE) technique is a rapid, simple, sensitive technique developed for extracting either polar or nonpolar organic compounds from small volumes of liquid (Sbrana *et al.*, 2014). It is highly reproducible and allows quantitative determinations, often by its coupling with other analytical strategies, such as HPLC coupled with MS and LC-MS (Simpson, 2000). In this study, cartridges characterized by a silica fiber coated with polymeric compounds (i.e., stationary phase or packing) were applied to detect plants exudates from the nutrient solutions circulating in the S-H cultivation system. Further details on the experimental conditions can be found in Chapter I for *A. officinalis*, and Chapter IV for *A. tinctoria*.

The general steps of the SPE process could be summarized as follows (**Figure 22a**):

i. **Conditioning**: rinsing the SPE cartridge with a solvent similar to the matrix of the sample. It serves to "activate" the stationary phase and to (a) remove some of the impurities and avoid system

pollution/influence on the sample loading effect, (b) spread out more orderly the functional groups on the surface of the packing, (c) increase the contact area of the loading liquid to play a better role in retention.

ii. **Loading**: the sample is loaded onto the cartridges. Usually, a vacuum manifold (**Figure 22b**) is applied to speed up the separation process. The target analyte molecules will be firmly retained on the SPE stationary phase. However, some interfering components (i.e., impurities) with similar properties to the target will also be retained on the SPE.

iii. **Washing**: elute the impurities to avoid the pollution of chromatographic columns and instruments and reduce the interference of impurities to the detection of target molecules (i.e., reduction of matrix effect).

iv. **Elution**: disrupt hydrophobic interactions between the analyte and sorbent functional groups with an organic solvent or solvent combination of sufficient non-polar character, so as to separate and collect the target from stationary phase.

Once the sample has been collected, the cartridge can be rinsed with 100% H_2O to remove unretained compounds.

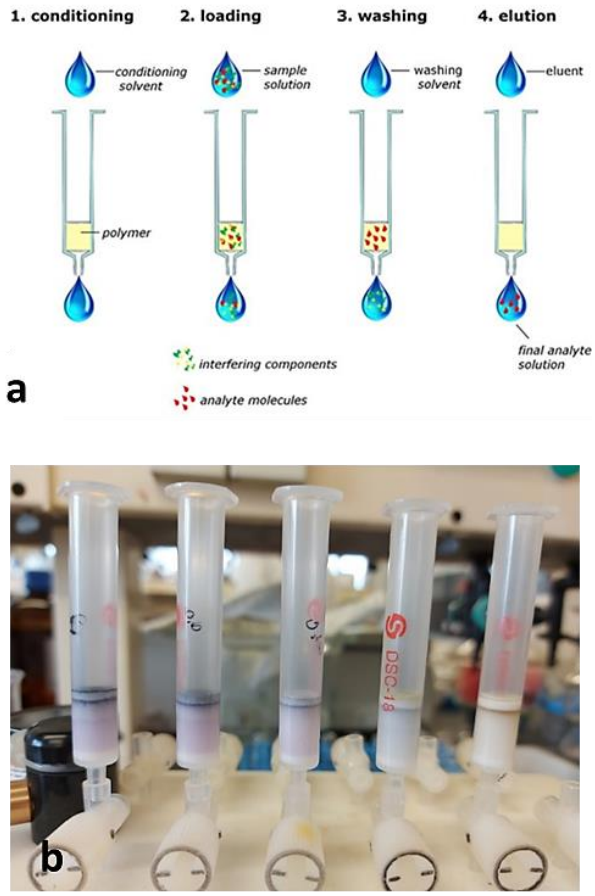

Figure 22. (a) General steps for solid phase extraction (SPE) modified from Sandoval (2017). (**b**) SPE-cartridges after the elution phase of nutrient solution samples from the S-H cultivation system with *A. tinctoria* (Chapter IV).

2. Metabolites analysis

Data acquisition applying High Resolution MS analysers (e.g., time of flight, Orbitrap and Fourier transform ion cyclotron resonance instruments) fitted with atmospheric pressure ionisation sources are more and more often used in metabolomic studies with at least two complementary LC stationary phases (Fenaille *et al.*, 2017). Hyphenated mass spectrometry methods are so-called separation-based methods coupled with mass spectrometry. Prior to MS analysis, metabolites are separated by a separation-based method (e.g., GC, LC),

and by exploiting different interactions of the compounds with the stationary phase (Ernst *et al.*, 2014). The basic components of HPLC-UHPLC analytical techniques are: mobile phase, column, pump, and detector. Further details on the experimental conditions are given in the corresponding Chapters.

Mass spectrometers operate by converting the analyte molecules to a charged (ionised) state, with subsequent analysis of the ions and any fragment ions that are produced during the ionisation process, based on their mass to charge (*m/z*) ratio. The basic components of a UHPLC-HRMS system are: sample inlet, ionisation source, mass analyse, detector, and data analysis system (**Figure 23a**).

The **electrospray ionisation** (**ESI**), ionisation source applied in this study, allows to analyse a wide array of metabolites (i.e., both small and large molecules of various polarities) in a complex biological sample, and it imparts very small amounts of energy to the analytes that results in minimal source fragmentation (Ho *et al.*, 2003). Specifically, the solution containing the analyte (i.e., chemical constituent that is of interest in an analytical procedure) crosses a metallic capillary, where an electric potential is applied (between 2 to 4.5 kV). This promotes a migration of charges to the interface of the capillary with the solution, which results in an electric double layer, and thus, droplets with charged surfaces are formed. The process of solvent evaporation starts within a chamber with a slight reduction of pressure under a nebuliser gas. With the reduction of droplet sizes, an approximation of the charges occurs, and consequently, the electrostatic repulsive forces are increased, which leads to a decrease in the surface tension of the droplets until rupture. This results in the release of ions into the gas phase by a spray of charged particles (Ernst *et al.*, 2014). With ESI, protonation/deprotonation is the main source of charging for biologically relevant ions (**Figure 23b**). Different types of adducts with salts or solvent molecules may also be generated according to the nature of the analytes. In a good approximation, acidic molecules (e.g., carboxylic acids or phenolics) will mainly produce $[M-H]^-$ in negative ionisation, while bases (e.g., alkaloids, amines) will generate $[M+H]^+$ in positive ionisation. Thus, the comprehensive coverage of most metabolites requires the use of both modes (Wolfender *et al.*, 2013).

The ions then travel through the **mass analyser** and arrive at different parts of the **detector** according to their mass to charge (*m/z*) ratio. Some mass analysers, such as Orbitrap and time-of-flight (TOF)

instruments, give the *m/z* ratio with a high resolution, allowing to obtain the molecular formula of the compounds detected and hence proposed identification. They allow to detect the largest possible number of features and, thus, obtain a full picture of the plant metabolome (Wolfender *et al.*, 2013).

After the ions contact the detector, useable signals are generated and recorded by a **computer system** (i.e., data analysis system). The computer displays the signals graphically as a mass spectrum showing the relative abundance of the signals according to their *m/z* ratio.

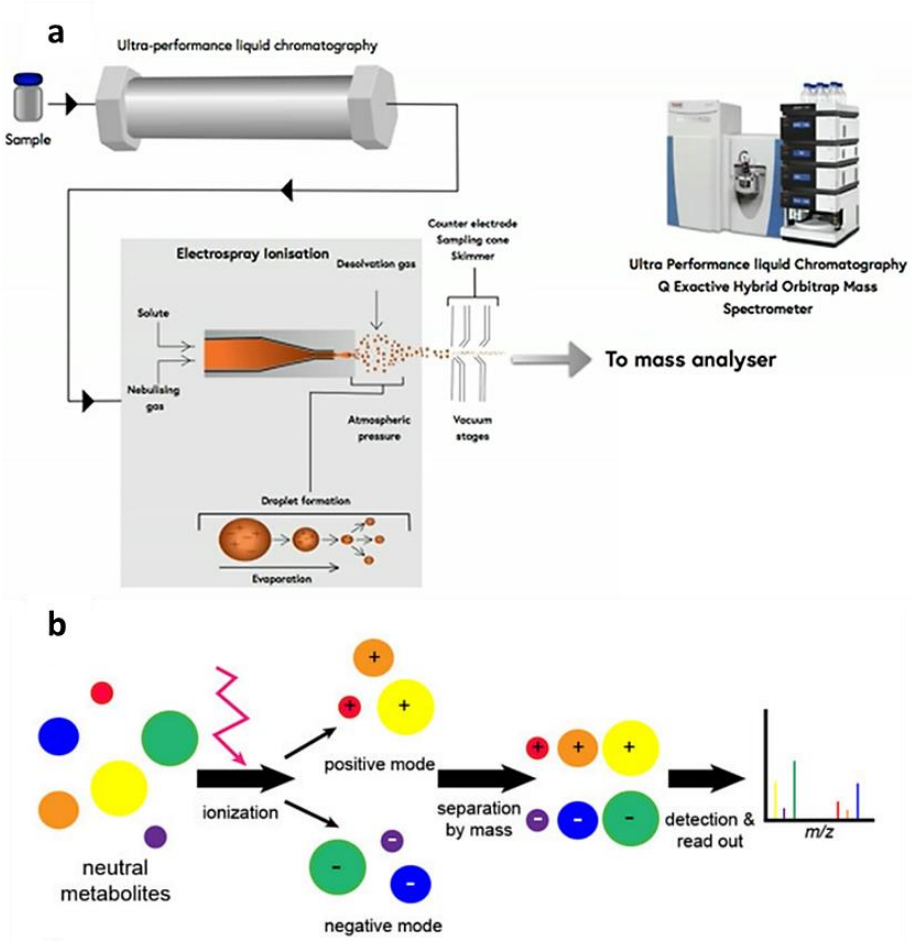

Figure 23. **(a)** Diagram representing the equipment required to conduct UHPLC-HRMS analysis (from FutureLearn in Metabolomics: Understanding Metabolism in the 21st Century course by the University of Birmingham**)**. **(b)** Illustration of what happens to molecules during LC-MS analysis. Following ionisation, negatively and positively charged compounds are generated (from Stringer *et al.*, 2016).

3. Data processing

The multivariate nature of data obtained from metabolomics experiments requires several steps to extract relevant information. The typical workflow includes: pre-processing and pre-treatment of the raw data, variable selection, modelling of the data and statistical validation (Wolfender *et al.*, 2013). Data pre-processing stage is required to eliminate the variance and bias, introduced during the analysis of the samples by MS methods, by reducing the complexity and extract the most important features of the raw data (Ernst *et al.*, 2014). Different softwares are available; vendor specific and commercial software, freeware like XCMS and mzMine are often used (Engskog *et al.*, 2016). This stage includes different general steps as follow (Castillo *et al.*, 2011; Engskog *et al.*, 2016):

- **Noise filtering**: designed to separate compound signals from background signals originating from chemical or instrumental interference.
- **Normalisation**: applied to correct the systematic variation and for direct comparison of different samples (i.e., removal of unwanted differences between samples due to intensity variations owing to technical or analytical reasons. It can be applied either using internal standards or a factor based on e.g., sum, mean or median intensity across samples).
- **Peak detection** or **deconvolution**: used to correct identification of a compound signal and its intensity, which involves the transformation of three-dimensional (retention time, *m/z*, intensity) MS data into a two-dimensional matrix of features with corresponding values.
- **Gap-filling:** used to integrate missing peak section of the chromatogram or missing value imputation, where the absent data is estimated.
- **Deisotoping algorithms**: applied to group isotopic peaks that originate from the same compound. Isotopes would otherwise be considered different compounds during data analysis and would consequently falsify data interpretation. In different samples, slightly different *m/z* values may be obtained for the same compound.
- **Alignment**: aimed to compensate for small variations in the position of corresponding peaks between spectra.

To handle the large data set obtained during the metabolites analysis (i.e., chromatogram or spectrum obtained comprising hundreds of signals), suitable chemometric methods are required (Cornejo-Báez *et al.*, 2020). Multivariate modelling provides a powerful tool to assess the large and complex data sets obtained from profiling experiments. Through unsupervised analysis it is possible to assess the distribution of samples and detect potential outliers. Principal Component Analysis (PCA), Partial Least Squares Discriminant analysis (PLS-DA), and orthogonal PLS-DA are used for data overview and visual identification of potential outliers as well as to make biological interpretations related to the study objective(s) through pinpointing discriminating features responsible for group separations. These models should be reported along with various parameters including number of components, the measurement of the overall fit of the model (R2) as well as prediction power of the model (sometimes referred to as Q2) (Engskog *et al.*, 2016). Data transformations are used to compensate for feature heteroscedasticity and deviations from normal distribution, while scaling balances fold change differences between features. Pareto scaling is the common and recommended method for multivariate approaches for the detection of biologically significant features and classification purposes (Engskog *et al.*, 2016).

The data for the PCA must be collected in a two-way matrix or matrix, called X, in which the column vectors represent loadings (e.g., absorbances, wavelengths, retention times, peaks, area under the peaks) and row vectors represent 'objects' for which these loadings are measured (e.g., samples). Principal Component Analysis reduces the number of loadings and allows to visualize the information included in the matrix. By linear combinations of the original loadings, PCA produces the so-called latent variables or principal components (PC) in a way that they describe the greatest possible variation in X. The score plot gives information regarding the (dis)similarity of the objects, for example, on their tendency to group, whereas the loading plot provides information on the contribution of the original loadings (Cornejo-Báez *et al.*, 2020). While the unsupervised nature of the PCA algorithm provides a means to achieve unbiased dimensionality reduction, its application only reveals group structure when within-group variation is sufficiently less than between-group variation. Therefore, supervised forms of discriminant analysis, such as PLS-DA, that rely on the class membership of each observation are also commonly applied in

metabolic fingerprinting experiments (Worley and Powers, 2012). Further details can be found in Chapters I and II.

For the **identification** of compounds, the main strategies are (a) tandem mass spectrometry, also known as MS/MS or MS^2, which covers various screening methods (e.g., product ion, neutral loss and precursor ion scanning) and (b) accurate mass-based identification using high-resolution instruments (Orbitrap). In order to deal with the computational challenge, various databases and software tools have been developed for the identification of mass signals. Straight elucidation and annotation of the compounds can be done by comparing their accurate mass, potential adducts, and isotopes in correlation with MS/MS fragmentation spectra, with commercial and non-commercial databases (e.g., Dictionary of Natural Products, library mzCloud, Chemspider, Masslist) as well as with data from literature. In Chapter IV, a molecular network computational strategy was applied to identify similarities among MS/MS spectra within the dataset and to propagate annotation to unknown but related molecules (Wang *et al.*, 2016). This approach exploits the assumption that structurally related molecules produce similar fragmentation patterns, and therefore they should be related within a network. In the molecular network, MS/MS data are represented in a graphical form, where each node represents an ion with an associated fragmentation spectrum. The links among the nodes indicate similarities of the spectra. By propagation of the structural information within the network, unknown but structurally related molecules can be highlighted and successful dereplication can be obtained (Vincenti *et al.*, 2020).

V. Molecular analysis

Genes expression analysis allows the identification of genes active in biosynthetic pathways in plants and also allows the expression assessment, providing qualitative and quantitative information related to specific genes (Skoneczny *et al.*, 2017). The metabolites present in plant extracts reflect the end products of gene expression at a specific point of time and often include both plant and microbial metabolites, corresponding to complex regulatory systems in the genome of a living plant (Weston *et al.*, 2015). Gene expression profiles coupled to metabolic profiles can provide key information on plant response to

environmental conditions, including biotic stress, and therefore the production of specific metabolites.

1. Total RNA extraction

In Chapter IV, *A. tinctoria* frozen roots were first ground in liquid nitrogen (-196°C) with a pestle and mortar. Total RNA extraction was done on 0.2 g starting root material using the protocol of Xu *et al.* (2010) slightly modified.

1) Prewarm the extraction buffer [100 mM Tris-HCl (pH 8.0), 20 mM ethylenediaminetetraacetic acid (EDTA), 1.4 M sodium chloride - NaCl, 2% cetyltrimethylammonium bromide (CTAB) (w/v), 2% polyvinylpyrrolidone (PVP) (w/v)] to 65°C.
2) Quickly transfer the frozen powder to the prewarmed extraction buffer (0.6 mL) and vortex. Add 12 µl of β-mercaptoethanol. Incubate at 65°C for 15 min, vortexing several times.
3) Add 0.5 mL of chloroform, vortex well and centrifuge at 13,000 rpm for 10 min at 4°C.
4) Transfer the viscous supernatant to a new tube, add 0.1 mL 5 M NaCl and 0.3 mL chloroform, vortex well and centrifuge at 13,000 rpm for 10 min at 4°C.
5) Transfer the upper phase to a new tube and repeat the above step.
6) Collect the supernatant very slowly and carefully into a new tube and add a half volume of isopropanol and a half volume of high salt solution (0.38 M trisodium citrate dihydrate + 1.2 M NaCl) and store at room temperature for 15 min.
7) Recover the RNA by means of centrifugation at 13,000 rpm for 10 min at 4°C.
8) Completely discard the viscous supernatant, wash the pellet with 70% ethanol to remove the remaining mucilage, and air dry it for 10 min.
9) Dissolve the RNA in 55 µL diethyl pyrocarbonate (DEPC)-treated water.

The total RNA was treated with TURBO DNA-freeTM Kit (Thermo Fisher Scientific, San Jose, USA), according to the manufacturer protocol. The RNA from all samples was loaded onto a 1.5% agarose gel, electrophoresed to separate RNA, stained with GelRed® (Biotium, USA), and visualised under UV light to assess the

integrity of ribosomal bands. In addition, concentration of each RNA sample was measured using NanoDrop®-ND 1000 UV-vis Spectrophotometer (NanoDrop Technologies, United States) and RNA purity estimated from the A260/A280 and A260/A230 absorbance ratios. Finally, a 1 μg aliquot of total RNA was used for the first-strand cDNA synthesis according to the protocol of the Transcriptor High Fidelity cDNA Synthesis Kit (Roche, Montreal, QC, Canada). For each RNA sample, a reaction without Transcriptor High Fidelity Reverse Transcriptase (Hifi RT) enzyme was performed as a control for contamination by genomic DNA.

2. Selection of genes for Real-Time quantitative PCR (RT-qPCR) analysis

a) Reference/housekeeping gene

One reference/housekeeping gene, which is expressed constitutively and level of expression is not affected by the different treatments (i.e., AMF strains) or during time, was applied in this study. This gene was selected from Wu *et al.* (2009), and it was used to make the normalization of genes expression obtained in the RT-qPCR analysis (**Table 2**):

Glyceraldehyde 3-phosphate dehydrogenase (*GADPH*) – this gene is encoding for an enzyme involved in glycolysis and glyconeogenesis.

b) Target genes

Three target genes involved in the shikonin (A/Sd) biosynthesis pathway were selected (**Figure 7**):

Geranylhydroquinone 3"-hydroxylase (***GHQH***) – is a CYP enzyme catalysing the oxidation of GHQ at the C-3″ position to synthesize 3″-carboxyl-geranylhydroquinone (GHQ-3″-COOH) besides one-step oxidation product GHQ-3″-OH (Wang *et al.*, 2014; Song *et al.*, 2020).

4-hydroxybenzoate-m-geranyltransferases (***PGT1*** and ***PGT2***) – these genes are coupling two key precursors, p-hydroxybenzoic acid (HBA) and geranyl diphosphate (GPP), to catalyse an important intermediate the 3-geranyl-4-hydroxybenzoic acid (GBA) (Yazaki *et al.*, 2002).

Table 2. Primers used for RT-qPCR to quantify the relative expression of genes.

Name (abbreviation)	Primer sequence 5'-3' (forward)	Primer sequence 5'-3' (reverse)	Accession number or reference used for primer designing
GAPDH	ACCGTCCACTCCATTACCG	ATGAGGCAGCCCTTCCACC	Wu *et al.*, 2008
GHQH/G10H	ATTGCTGGGACTGATACAAC	CGTGCAACATCGGATTCTTC	MH077962 (Wang *et al.*, 2019) MN056184 (Song *et al.*, 2020)
LePGT1	CTCTTAGGCTCCTCTGCT	CGTCGTCCACCTTATCTT	Wu *et al.*, 2008
LePGT2	AGAAAGGCAAGCAACCATC	CCCACCATCCAAATATTGCC	KT991522 (Liu *et al.*, 2016) AB055079.1 (Yazaki *et al.*, 2002)

3. Relative quantification in RT-qPCR analysis

Since no published genomic resources are available for *A. tinctoria*, a previously published primer for amplification of *PGT1* in *Onosma paniculatum* Bur. *et* Franch was used, while for *PGT2* and *GHQH* new primer pairs were designed. Sequences of each gene (*PGT2* or *GHQH*) from two phylogenetically distant Boraginaceae species [*L. erythrorhizon* and *Arnebia euchroma* (Royle) Johnston] were obtained from NCBI, aligned, and primers were generated from conserved regions (**Supplementary Figure 8, Annex IV**). Once reference and targets primer genes have been designed, their efficiency and specificity have been analyzed by RT-qPCR. Material (i.e., cDNA) from different treatments (i.e., control, mycorrhized plants, from different time points) were mixed to serve in the standard curve. Six levels of dilution were used, from pure mix to a dilution of 1/1,000. To increase the stability of the standard curve, chain dilution was made through these dilutions: 1/5, 1/10, 1/50, 1/100, 1/500. For all primer genes tested, three technical replicates of each level of standard curve were made. Additionally, three replicates of negative control (i.e., water instead of DNA template) were used. Efficacy of the reaction was assessed for each gene, normally around efficacy (E) = 2 with curve slop of -3.3.

Selected primers were then used on all tested treatments. One plate was used by gene for each treatment: biological replicate tested, negative control, std/positive control.

Normalization was achieved for each experiment separately using the reference gene (i.e., *GAPDH*) and the "Pfaffl" method (Pfaffl, 2001). Relative quantification analysis results were expressed as a ratio: the relative amount (fold change) of a target nucleic acid (test)

compared to a control sample (calibrator). The advantage of using a reference gene is that this method prevents the need for accurate quantification and loading of the starting material. The drawback is that this method requires the availability of a known reference gene or genes, with constant expression in all samples tested and whose expression is not changed by the treatment under study.

Average cycle threshold ("Average Ct") for each gene in each sample analyzed is calculated. Control treatment (i.e., non-mycorrhized plants) is selected and the Ct average of all control samples calculated ("control average"). Then, **ΔCt** is calculated separately for each gene in each sample (i.e., subtract the "Control average" value from the "Average Ct" of each sample including all of the control samples).

Finally, these values are used to calculate the gene expression ratio (fold change compared to a calibrator) applying the formula of Pfaffl (2001):

$$\textit{Gene expression ratio} = \frac{(E_{target})^{\Delta Ct,\ target}}{(E_{ref})^{\Delta Ct,\ ref}}$$

RESEARCH RESULTS

PART 1

ANCHUSA OFFICINALIS STUDIES

Chapter I

The Arbuscular Mycorrhizal Fungus *Rhizophagus irregularis* MUCL 41833 modulates metabolites production of *Anchusa officinalis* L. under semi-hydroponic cultivation

Adapted from the research article published in:

frontiers in Plant Science (2021) 12:724352

doi: 10.3389/fpls.2021.724352

Annalisa Cartabia, Evangelia Tsiokanos, Nikolaos Tsafantakis, Ismahen Lalaymia, Aikaterini Termentzi, Maria Miguel, Nikolas Fokialakis and Stéphane Declerck

Preface

The first part of this Ph.D. focuses on *Anchusa officinalis* L. This important medicinal plant belongs to the Boraginaceae family and is characterized by the production of therapeutic metabolites, among which phenolic compounds, especially caffeic acid esters, such as rosmarinic acid, and saponins. The effects of AMF on modulating the metabolism of various plants have been extensively reported and discussed in the literature. However, whether these soil fungi can modulate the metabolism of *A. officinalis* is still unknown. Moreover, highly controlled and up-scalable conditions, such as bioreactors or hydroponic cultivation systems, have never been applied to AMF-medicinal plant associates.

Therefore, in this first Chapter, *A. officinalis* plants were associated with the AMF standard strain *R. irregularis* MUCL 41833 and grown in a controlled circulatory semi-hydroponic cultivation system. An untargeted metabolomics analysis, allowing simultaneous detection of a wide variety of primary and secondary metabolites, was performed on shoot and root tissues as well as on the nutrient solution flowing over the roots.

Abstract

Anchusa officinalis is recognized for its therapeutic properties, which are attributed to the production of different metabolites. This plant interacts with various microorganisms, including the root symbiotic arbuscular mycorrhizal fungi (AMF). Whether these fungi play a role in the metabolism of *A. officinalis* is unknown. In the present study, two independent experiments, associating *A. officinalis* with the AMF *Rhizophagus irregularis* MUCL 41833, were conducted in a semi-hydroponic (S-H) cultivation system. The experiments were intended to investigate the primary and secondary metabolites (PMs and SMs, respectively) content of shoots, roots, and exudates of mycorrhized (M) and non-mycorrhized (NM) plants grown 9 (Exp. 1) or 30 (Exp. 2) days in the S-H cultivation system. Differences in the PMs and SMs were evaluated by an untargeted ultrahigh-performance liquid chromatography high-resolution mass spectrometry metabolomics approach combined with multivariate data analysis. Differences in metabolite production were shown in Exp. 1. Volcano-plots analysis revealed a strong upregulation of 10 PMs and 23 SMs. Conversely, in Exp. 2, no significant differences in PMs and SMs were found in shoots or roots between M and NM plants whereas the coumarin scoparone and the furanocoumarin byakangelicin, accumulated in the exudates of the M plants. In Exp. 1, an enhanced production of PMs was noticed, including organic acids and amino acids, with the potential to act as precursors of other amino acids and as building blocks for the production of macromolecules. Similarly, SMs production was significantly affected in Exp 1. In particular, the phenolic compounds derived from the phenylpropanoid pathway. Fifteen di-, tri-, and tetrameric C_6-C_3 derivatives of caffeic acid were induced mainly in the roots of M plants, while four oleanane-types saponins were accumulated in the shoots of M plants. Two new salvianolic acid B derivatives and one new rosmarinic acid (RA) derivative, all presenting a common substitution pattern (methylation at C-9”’ and C-9’ and hydroxylation at C-8), were detected in the roots of M plants. The accumulation of diverse compounds observed in colonized plants suggested that AMF have the potential to affect specific plant biosynthetic pathways.

Keywords

Arbuscular mycorrhizal fungi; *Rhizophagus irregularis*; *Anchusa officinalis*; semi-hydroponic cultivation system; metabolomics; primary and secondary metabolites

Introduction

The plant kingdom is an incredible source of structurally and functionally diverse metabolites (e.g., phenolic compounds, amino acids, peptides, terpenes, and alkaloids) useful for human life (Wang *et al.*, 2019). Many of these (called primary or secondary metabolites) are of commercial interest, and currently exploited in fields such as cosmetics, pharmaceuticals, nutraceuticals, agrochemicals, food and fine chemicals (Charles Dorni *et al.*, 2017; Neelam *et al.*, 2020). Interestingly, plants have evolved with highly complex assemblages of microorganisms (called the microbiota), having roles in plant development and health (Rivero *et al.*, 2015). Many of these microorganisms produce metabolites of interest but, in numerous cases, also influence the metabolism of plants and thus their qualitative and quantitative production of metabolites (Kaur and Suseela, 2020). Among the microorganisms that interact intimately with plants are the AMF. These soil fungi, belonging to the Glomeromycota Phylum, are obligate symbionts that live in association with nearly 72% of plant species (Brundrett and Tedersoo, 2018). They provide their hosts with nutrients (especially N and P) in exchange for carbon and lipids (Smith *et al.*, 2011; Chen *et al.*, 2018) and increase their resistance to a/biotic stresses (Gianinazzi *et al.*, 2010).

In the recent decade, a number of studies have reported the impact of AMF on the production of plant PMs, and on various biosynthetic pathways involved in the production of SMs in the leaves, roots, or fruits/tubers of different crops used as food or for medicinal purposes (Gianinazzi *et al.*, 2010; Zeng *et al.*, 2013; Pedone-Bonfim *et al.*, 2015; Pandey *et al.*, 2018). Most studies involving metabolic analysis of AMF colonized plants were focused on few chemical groups, and it is only in the last decade that the first untargeted metabolomics analysis, allowing a simultaneous detection of a wide variety of compounds, was conducted (Rivero *et al.*, 2015; Hill *et al.*, 2018). Interestingly, most of these studies reported a nonnegligible impact of AMF on PMs and SMs production by plants. For instance, Schliemann *et al.* (2008)

investigated the metabolic changes in the roots of the model plant *M. truncatula* colonized with *R. irregularis*. Their study, conducted over a nearly 2-month period, showed a strong effect of AMF on polar and nonpolar PMs and SMs. More precisely, PMs such as amino acids, fatty acids or alcohols and alkanes, and SMs, such as isoflavonoids, phenylpropanoid derivatives, and apocarotenoids, were accumulated in higher proportion in the roots of AMF-colonized plants than in those of the noncolonized controls. More recently, Saia *et al.* (2015) have shown a decrease in amino acids and saturated fatty acids content of *Triticum durum* roots inoculated with a pool of different AMF species, while Rivero *et al.* (2015) presented through a detailed metabolomics analysis clear metabolites difference in tomato roots associated with two different AMF species (*Funneliformis mosseae* and *R. irregularis*). Their untargeted metabolomics analysis showed a notable increase of several signals referring to sugars, carboxylic acids, amino acids, and compounds from the phenylpropanoid pathway in AMF-colonized versus noncolonized plants. Regarding the aboveground metabolome, the analysis of leaves of several plants, both dicots and monocots, colonized by *R. irregularis*, has shown an up/downregulation of different PMs (e.g., amino acids, organic acids) and SMs (e.g., catalpol, verbascoside); hence, many species-specific responses were reported (Schweiger *et al.*, 2014).

The majority of the studies considered the foliar or the aboveground metabolic variations, without taking into consideration both parts (shoot and roots) concomitantly. For this reason, Hill *et al.* (2018) investigated the metabolites profile in both foliar and root tissues of *Senecio jacobae*. Their untargeted metabolic approach revealed a significant upregulation of SMs belonging mainly to blumenol derivates and anti-herbivore defence compounds as pyrrolizidine alkaloids. Nevertheless, the changes were found mostly in the root system, while a slight or nonsignificant metabolic modification was observed in the shoot parts of the plants.

So far, the metabolomics studies on plants associated with AMF were, to the best of our knowledge, conducted in pot cultures or field trials under semi-controlled conditions. However, for medicinal plants, metabolites production is more often conducted under highly controlled and up-scalable conditions, such as bioreactors or hydroponic cultivation systems (Gontier *et al.*, 2002; Sgherri *et al.*, 2010; Malik *et al.*, 2016), both being never applied to AMF-medicinal plant associates. Therefore, moving to hydroponics could represent a step forward to

study the metabolomics reprogramming of plants (medicinal or others) associated with AMF under highly controlled conditions. Recently, a semi-hydroponic (S-H) cultivation system with perlite as inert substrate has been developed by Garcés-Ruiz *et al.* (2017) to study the dynamics of inorganic phosphorus (Pi) uptake from a circulating nutrient solution by maize plants colonized with the AMF *R. irregularis* MUCL 41833. After 25 days of experiment, a considerable increase in plant growth, Pi uptake, and strong root colonization (e.g., 90%) was observed, suggesting that the S-H cultivation system is adequate for growing AMF-colonized plants.

Anchusa officinalis L. belongs to the Boraginaceae family. This plant is mostly encountered in the southern part of the Balkan Peninsula (Selvi and Bigazzi, 1998) in sunny warm places, such as fields, meadows, and river sediments. A phytochemical screening, performed on wild plants by Jakovljević *et al.* (2016) and Boskovic *et al.* (2018), demonstrated the presence of an abundant content of phenolic compounds, especially caffeic acid esters such as rosmarinic acid (RA). This compound presents several health-related properties, conferring antioxidant, antibacterial, and anti-inflammatory activities to *A. officinalis* extracts (Dresler *et al.*, 2017). The association between *A. officinalis* and AMF has been reported by Zubek *et al*. (2011), but no study has ever reported the effects of these beneficial soil-borne fungi on the metabolites profile of this plant.

In the present chapter, two independent experiments conducted under a S-H cultivation system and applying *A. officinalis* associated with the AMF *R. irregularis* MUCL 41833 are described. The experiments were intended to investigate the PMs and SMs content of shoots, roots, and exudates of mycorrhized (M) or non-mycorrhized (NM) plants grown 9 (Exp. 1) or 30 (Exp. 2) days in the S-H cultivation system. In both experiments, UHPLC-HRMS analysis was used. The untargeted metabolomics approach was further conducted to shed light on the overall effects of AMF on *A. officinalis* plants grown under highly controlled S-H culture conditions.

Material and Methods

Chemicals

HPLC grade methanol (MeOH) was obtained from Fisher Chemical (Fisher Scientific, Loughborough, UK), acetonitrile LC-MS grade (LiChrosolv® hypergrade) (ACN), and formic acid LC-MS grade (LiChropur®) (FA) from Merck (Merck KGaA, Darmstadt, Germany) and ethyl acetate (ExpertQ®, 99.8%) (EtOAc) from Scharlau Basic (a.r. grade, Scharlab S.L., Barcelona, Spain). Ultrapure water was received from LaboStar apparatus (Evoqua LaboStar® 4, Evoqua Water Technologies, Pittsburgh, USA). Discovery® DSC-C18 Supelco SPE cartridges of 500 mg bedweight and 6 mL volume were purchased from Sigma-Aldrich (Taufkirchen, Germany).

Biological material

Seeds of *Anchusa officinalis* L. were surface disinfected by immersion in sodium hypochlorite (8% active chloride) for 5 min and rinsed three times with sterilized (121°C for 15 min) deionized water. The seeds were then germinated in plastic seed trays (37.5×23×6 cm) filled with a mix (w/w 1:2) of sterilized (121°C for 15 min) perlite (Perligran Medium, KNAUF-GMBH, Dortmund, Germany) and turf (DCM, Grobbendonk, Belgium). The trays were placed in the greenhouse set at 25°C/18°C (day/night), relative humidity (RH) of 38%, a photoperiod of 16-h day^{-1} and photosynthetic photon flux (PPF) of 120 μmol m^{-2} s^{-1}.

The AMF *Rhizophagus irregularis* MUCL 41833 was proliferated on plants of *Zea mays* L. in a 10 L plastic box containing sterilized lava as previously described. The plants were grown under the same greenhouse conditions as above.

Colonization of *A. officinalis*

Two-week-old *A. officinalis* plants were transferred in 10 L pots containing a sterilized (121°C for 15 min) mix of lava and perlite (w/w 2:1). For the mycorrhizal (M) treatment, the substrate was half mixed with the AMF-inoculum substrate above (final-ratio lava: perlite w/w 5:1). For the non-mycorrhizal (NM) treatment (i.e., the control), the substrate was half mixed with the AMF inoculum substrate above but sterilized (121°C for 15 min) in the same final ratio (5:1). The plants were grown under the same greenhouse conditions as above.

Metabolites profile of *A. officinalis* associated with *R. irregularis* in a 9-day experiment conducted in a S-H cultivation system (Exp. 1)

Experimental setup

In the first experiment, the objective was to evaluate the metabolites profile of M and NM *A. officinalis* plants grown for 9 days in the S-H cultivation system. The metabolites released in the circulating nutrient solutions were also assessed.

Two-month-old plants (7 M and 6 NM) were gently removed from the 10-L pots above and their roots cleaned with deionized water to eliminate lava and perlite debris. They were subsequently transferred to the S-H cultivation system as previously described. The containers were maintained in the greenhouse set at the same conditions as described above. After the acclimatization and initial flushing, a regular circulation was initiated and maintained at 7.5 mL min^{-1} for 42 h (T1).

The metabolites profile of *A. officinalis* associated with *R. irregularis* in a 30-day experiment conducted in an S-H cultivation system (Exp. 2)

Experimental setup

In the second experiment, the objective was to evaluate the metabolites profile of M and NM *A. officinalis* plants grown for 30 days in the S-H cultivation system. The metabolites released in the circulating nutrient solutions were also assessed. In addition, the concentrations of Pi and nitrate (NO^{-3}) in the nutrient solutions were analysed at regular intervals to ascertain the uptake by the plant-AMF associates and thus vitality of the system and to verify that the concentration of minerals remains sufficient for adequate plant growth.

The same procedure as in Exp. 1 was applied. Briefly, after cleaning the roots system, two-month-old plants (7 NM and 7 M) were transferred in the S-H cultivation system, and the containers were randomly placed in the holes made in the flex foam supports. Then, after the acclimatization period (7 days), four successive circulations were performed for different durations: 42 h at day 9 (T1) and 8 h at day 15 (T2), day 22 (T3), and day 30 (T4).

Monitoring minerals depletion in Hoagland^{dil100X} low-P solution

In this experiment exclusively, Pi and NO^{-3} concentrations were monitored in the Hoagland^{dil100X} solution of the M and NM plants grown in the S-H cultivation system. Twenty mL of Hoagland^{dil100X} solution was sampled from each bottle after each circulation (T1, T2, T3, and T4). At each sampling time, the solution was collected in 50-ml Falcon Tubes (Sarstedt, Germany) and then stored at 4°C in the dark before proceeding with the analysis. Concentration of Pi was evaluated as described by Garcés-Ruiz *et al.* (2017). Briefly, 2 mL of each nutrient solution sampled was diluted 5 times with Milli-Q water. The solution was then acidified with 20 µL of nitric acid - HNO_3 at 65% (Merck, Darmstadt, Germany) and subsequently analysed via inductively coupled plasma atomic emission spectroscopy (ICP-AES) (ICAP 6500, Thermo Fisher Scientific, San Jose, USA). The inorganic phosphorus content was determined with axial viewing of the emitted radiation. A peristaltic pump was used to introduce the solutions into the ICP-AES at a flow rate of 1.5 mL min^{-1}. Operating parameters for the instrument included forward power 1,150 W, coolant gas flow rate 12 L min^{-1}, auxiliary gas flow rate 1 L min^{-1} and nebulizer gas flow rate 0.6 L min^{-1}. Inorganic phosphorus quantification was analysed under a wavelength of 177.495 λ nm^{-1}. The limit of detection was < 100 ppb. Data obtained (in ppm) were converted in mg L^{-1}.

For nitrate, samples were first diluted 50 times with Milli-Q water and then analysed via ionic chromatography system (IC, DIONEX, DX 120, Thermo Fisher Scientific, San Jose, USA). The nitrate quantification was analysed under ultraviolet-visible (UV/VIS) spectrophotometry detection between 200 and 220 nm. The limit of detection was <100 ppb.

Plant harvest and AMF root colonization

The *Anchusa officinalis* plants were harvested at days 9 and 30, in Exp. 1 and 2, respectively. The nutrient solutions were also kept in the bottles at 4°C in the dark before proceeding with the phytochemical content analysis.

In both experiments, total fresh weight (TFW, e.g., the sum of shoots and roots), as well as root colonization of M and NM plants, was assessed at the start and the end of the experiments. Root colonization

was evaluated as previously described by McGonigle *et al.* (1990) method on one-third of the root system. Before proceeding, the roots were first cut into small pieces (circa, 1 cm) and placed into 50 mL Falcon tubes.

Analysis of PMs and SMs of *A. officinalis* plants and nutrient solutions

Sample Preparation

The remaining two-third root systems, as well as the shoot parts of six randomly chosen M and NM plants of both experiments, were separated and subjected to freeze-drying during 24 h. The freeze-dried samples were then reduced into powder, using liquid nitrogen. Twenty mg of each plant material was subsequently subjected to a 30-min exhaustive ultrasound-assisted extraction (three cycles), using a mixture of EtOAc and MeOH (35:65 v/v) at room temperature. The samples were finally centrifuged at 3,500 rpm for 3 min, and the supernatants of each cycle were combined.

In parallel, four randomly chosen nutrient solutions of M and NM plants from both experiments, sampled after 9 and 30 days, were prepared for analysis as follows: 50 mL of each nutrient solution was subjected to a solid phase extraction process, using a C18 cartridge (500 mg/6mL) previously preconditioned with 6 mL of MeOH, followed by an equilibration step with 6 mL of Milli-Q water. The SPE cartridges were loaded with the nutrient solutions, washed with Milli-Q water, and dried under a slight vacuum. Finally, the elution was performed, using 12 mL of MeOH, and the resulting solutions were dried under a nitrogen stream. In total, six independent M and NM plants grown in different S-H systems and their corresponding nutrient solution eluates were considered.

Each sample was analysed in triplicate. Prior to analysis, the nutrient solution eluates and plant extracts were filtered through a 45-µm pore size hydrophilic polyvinylidene fluoride membrane. Each sample was adjusted to the final concentration of 300 µg mL^{-1}, using 50% H_2O: MeOH of LC-MS grade.

UHPLC-HRMS analysis

High-resolution metabolomic profiling of M and NM samples was performed on an UHPLC-HRMS/MS Orbitrap Q-Exactive platform (Thermo Fisher Scientific, San Jose, USA). A full scan with a mass

range of 100-1,200 Da on a centroid mode was applied, while HRMS data (70,000 resolution) were collected in both negative and positive ESI ionisation modes under the following conditions: capillary temperature, 320°C; spray voltage, 2.7 kV; S-lense Rf level, 50V; sheath gas flow, 40 arb. units; aux gas flow, 5 arb. units; aux. gas heater temperature, 50°C. The HRMS/MS spectra (35,000 resolution) were recorded for the most intense three peaks, keeping a 10-s exclusive window. Stepped normalized collision energy was set at 40, 60, and 100. An hypersil Gold UPLC C18 (2.1×100 mm, 1.9 μm) reversed phase column (Thermo Fisher Scientific, San Jose, USA) was used for the separations. The mobile phase consisted of solvents A: ultra-pure H_2O.1% (v/v) FA and B: ACN. A 16-min gradient method was used, varying as follows: 0-1 min, 5% B (isocratic gradient); 1-11 min, 5-95% B (linear gradient); 11-14 min, 95% B (isocratic gradient, column cleaning); 14-14.1 min, 95-5% B (linear gradient); 14.1-16 min, 5% B (isocratic, column equilibration). The flow rate was 0.260 mL min^{-1}, and the injection volume was 5 μL. The column temperature was kept at 40°C, while the sample tray temperature was set at 10°C. All experiments were performed in triplicate.

Untargeted metabolomics data processing

HRMS and MS/MS data were processed with Thermo Xcalibur and Compound Discoverer 3.1.1.12 (Thermo Fisher Scientific, San Jose, USA). For the untargeted metabolomics analysis, customizable processing workflow, including selection of spectra, retention time (RT) alignment and signal correction, peak detection, and grouping and annotation of compounds, was applied to all the data set and described as follows: after the selection of imported raw files, RT alignment was performed from 1 to 12 min as an upper limit with a maximum time shift alignment set at 2 min with 10-ppm mass tolerance. The peak-picking procedure was conducted on a full HRMS data scan between 0 and 1,100 Da, adopting criteria, such as minimum peak intensity (1,000,000), mass tolerance set up at 5 ppm but also by integrating selected isotopes and adducts. Finally, the straight elucidation and the annotation of compounds were performed according to the accurate mass, the potential adducts, and isotopes in correlation with MS/MS fragmentation spectra by comparing with commercial and non-commercial exported or implemented databases (e.g., Dictionary of Natural Products, library mzCloud, Chemspider, Masslist) as well as data from literature.

Statistical analysis

In both experiments, the TFW of plants was subjected to a mixed model for repeated measurements fit by restricted maximum likelihood (REML) estimation. "ID plants" were regarded as a random factor while "time" of sampling (T0 and T1- Exp.1 and T0 and T4 - Exp. 2) and "treatments" (NM and M) as fixed factors. Similarly, AMF colonization parameters (TC% and AC%) were subjected to the mixed model, as described above, with "ID plants" as a random factor and "time" as a fixed factor. For all parameters, normal distribution of residuals variance and normality was checked before analyses.

In the second experiment, the concentrations of Pi and NO^{-3} in the nutrient solutions were analysed with a mixed model for repeated measurements, where "ID plants" were regarded as a random factor and "time" of sampling (T1, T2, T3, and T4) and "treatments" (M and NM) as fixed factors. To fulfil the assumptions of normality and homoscedasticity, Pi concentration from two NM plants was excluded from the statistical analysis. When the interaction between the fixed factors was not significant, a pairwise comparison test ($p < 0.05$) was computed on each significant principal effect ("time" and/or "treatments" factors). Data analyses were performed by IBM SPSS Statistics for Windows, version 26 (IBM Corp., Armonk, N.Y., USA).

The interpretation of metabolomics HRMS data involved a multivariate data analysis. The pre-processed datasets remaining after filtering criteria were imported into SIMCA 14.1 software (Soft Independent Modelling of Class Analogy, Umetric, Malmo, Sweden) for the assignment of the metabolic changes between M and NM plants at the end of both experiments. Principal component analyses (PCA), as well as the partial least squares discriminant analyses (PLS-DA), were performed according to Pareto correlation, while UV scaling was applied for the interpretation of clustering results between nutrient solutions of M and NM treatments at the end of the second experiment. To exclude the overfitting of the aforementioned PLS-DA models, a permutation test with n = 100 was performed. The discriminant variables were highlighted through Volcano-plots analyses generated with GraphPad Prism 7 (GraphPad Software, California, USA) and Compound Discoverer 3.1.1.12 (Thermo Fisher Scientific, San Jose, USA) on the basis of criteria such as $p < 0.05$ and fold change > 1.5. The dereplication and the matching of differential compounds were performed as described above.

Results

The metabolite profile of *A. officinalis* associated with *R. irregularis* in a 9-day experiment conducted in an S-H cultivation system (Exp. 1)

Plant total fresh weight and root colonization by AMF

The total fresh weight of the M and NM plants was evaluated at T0 and T1. No significant interaction ($p = 0.167$) was reported between the two fixed factors "treatments" and "time". Conversely, a significant effect was noticed for the fixed factor "treatments" ($p < 0.001$), as well as "time" ($p = 0.004$) separately. A significantly higher TFW of M plants was found as compared with NM plants. Moreover, the overall TFW of the two plant groups (M and NM) increased significantly between T0 and T1 (**Table 3**).

Root colonization of the M and NM plants was evaluated prior to their transfer in the containers (T0) and at the end of the experiment (i.e., after 9 days of growth in the S-H cultivation system – T1). A significant effect ($p < 0.05$) of the fixed factor "time" was noticed for TC% and AC%. Both parameters significantly decreased between the start and the end of the experiment. No root colonization was observed for the NM plants (**Table 4**).

Metabolite profiles of M and NM *A. officinalis* plants and of nutrient solution

The metabolite profiles of shoots and roots of M and NM plants as well as of nutrient solutions were assessed *via* UHPLC-HRMS mass spectrometry. Sample analyses revealed 220 and 420 different mass signals for shoot and root samples, respectively, and the unsupervised PCA with Pareto correlation revealed a clear contrast and discrimination between M and NM plants for both plant parts (**Figure 24**). Interestingly, root and shoot parts showed a similar clustering pattern without any overlapping between M and NM individuals from the same dataset. Furthermore, higher proximity and similitude of individuals were observed for the NM plants in both shoots and roots, in comparison to the M plants, which were found more widespread in the model. Curiously, the root metabolic profile of one NM plant was closer to the M plants than to the NM plants (**Figure 24 A**), while the corresponding shoot part was considered as an outlier and was removed from the PCA model (**Figure 24 B**).

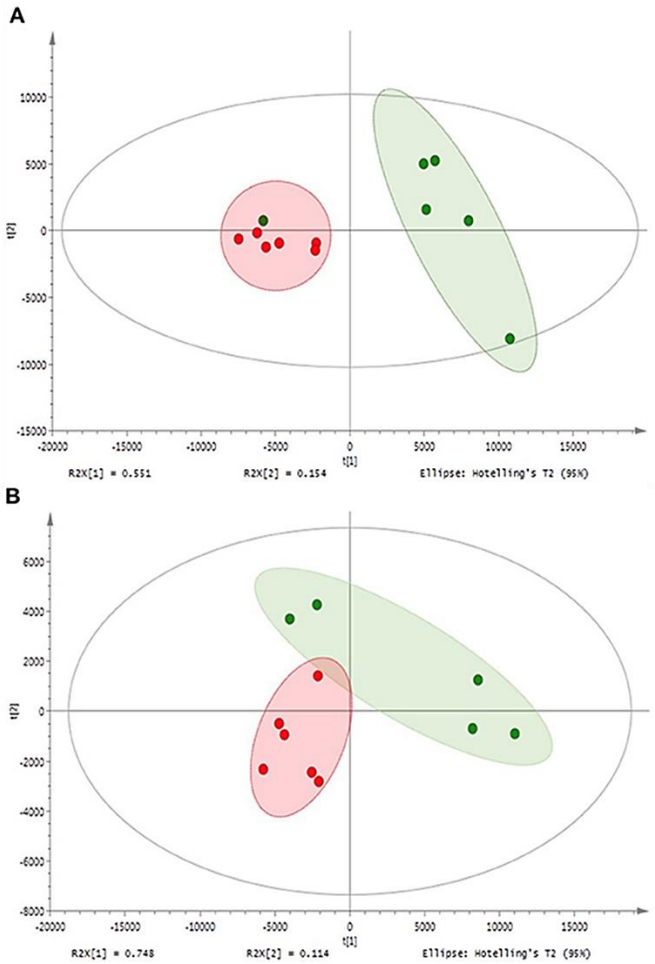

Figure 24. Principal component analysis (PCA) – comparison of UHPLC-HRMS metabolic profiles from M and NM root **(A)** and shoot **(B)** samples after 1 week (T1) of growth in the S-H cultivation system (M_T1: green dots; NM_T1: red dots).

Preliminary PCA analyses showed that AMF colonization significantly affected plant metabolism in both root and shoot samples. The partial least squares-discriminant analysis of M and NM shoots and roots confirmed the results obtained by PCA, showing clear differentiation between M and NM samples. The statistical significance test obtained from 100 possible rearrangements of data points confirmed the aforementioned model (**Supplementary Figure 1,** Annex I). Variables of importance were highlighted in the Volcano-plot analyses obtained with specific data-filtering criteria such as $p < 0.05$ and FC > 1.5. Among the 220 and 420 mass signals identified for shoot and root samples of M and NM plants, 55 and 49, respectively, passed

the defined threshold (**Figures 25 A-B**). Afterwards, those compounds were tentatively identified by matching the corresponding accurate mass and MS/MS spectra pattern with already published data from literature and compound libraries (see paragraph Dereplication of PMs and SMs).

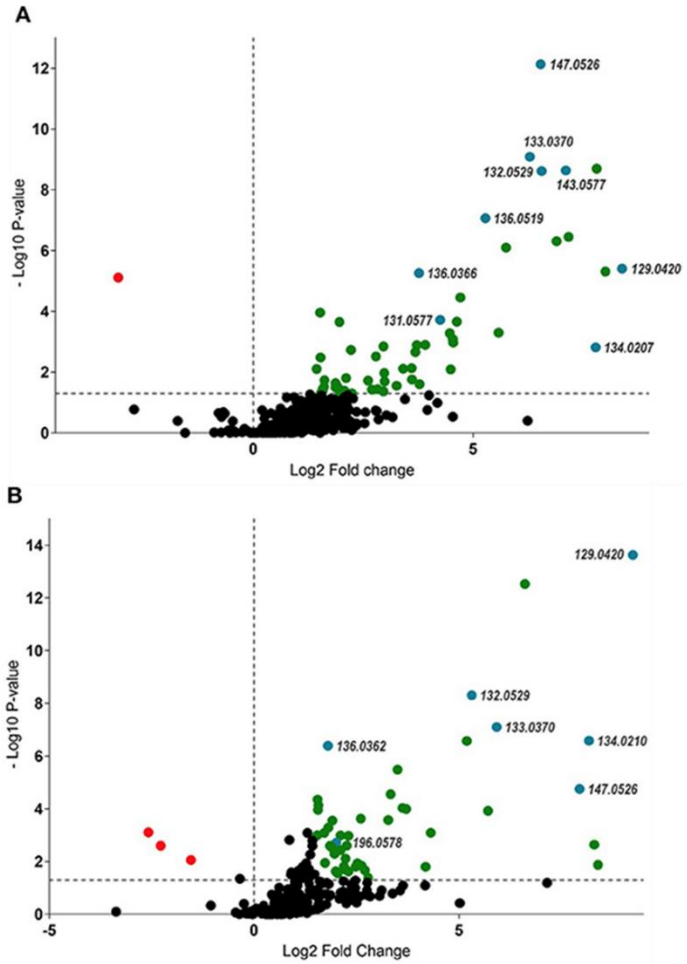

Figure 25. Volcano-plot analysis - identification of up and downregulated compounds ($p < 0.05$ and fold change > 1.5) between M and NM root **(A)** and shoot **(B)** samples after 1 week (T1) of growth in the S-H system. Statistically significant upregulated SMs were represented in green, while PMs were highlighted in blue (right side of the plots). Downregulated compounds were represented in red (left side of the plots). Numbers represent pseudomolecular ions (*m/z*).

In contrast to plant samples, PCA and PLS-DA analyses of the nutrient solutions from M and NM plants did not follow the same clustering pattern as in shoots and roots. In particular, no significant

differences in mass signals were underlined in the different HRMS-(-) ESI profiles, meaning that the association of plants with the AMF did not affect the root exudation and the release of compounds in the nutrient solution within a period of 9 days. As a result, metabolic profiles observed in nutrient solutions of M and NM plants were represented in a single cluster in the plot (**Figure 26**). Volcano-plot analysis of post-processing HRMS data confirmed PCA and PLS-DA models. In fact, despite the higher number of mass signals (> 500) detected in the nutrient solution of M and NM plants, no significant difference was observed according to the same data-filtering criteria ($p < 0.05$ and fold change > 1.5).

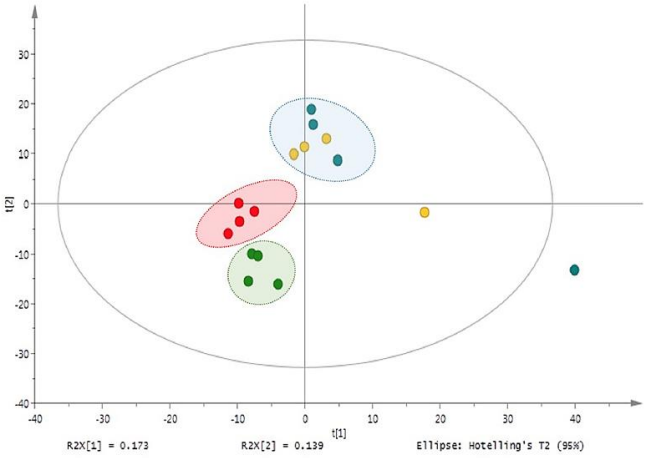

Figure 26. Principal component analysis (PCA) of M and NM nutrient solutions - UHPLC-HRMS-based metabolite variation after 1 week (M_T1: blue dots; NM_T1: yellow dots) and 4 weeks (M_T4: green dots; NM_T4: red dots) of plant growth in the S-H cultivation system.

The metabolites profile of *A. officinalis* associated with *R. irregularis* in a 30-day experiment conducted in an S-H cultivation system (Exp. 2)

Plant total fresh weight and root colonization by AMF

The total fresh weight of the M and NM plants was measured at T0 and T4. No significant interaction ($p = 0.926$) was reported between the two fixed factors "treatments" and "time", while only a significant effect was found for the fixed factor "time" ($p < 0.001$). The overall

TFW of the two groups (M and NM) of plants increased between T0 and T4 (**Table 3**).

Root colonization of the M and NM plants was evaluated prior to the transfer in the containers (T0) and at the end of the experiment (i.e., after 4 weeks of growth in the S-H cultivation system - T4). A significant effect of the fixed factor "time" was reported only for TC% (p = 0.032), with a decrease between the start and the end of the experiment. The AC% remained stable during the experiment. No root colonization was observed for the NM plants (**Table 4**).

Table 3. Total fresh weight (TFW) of *A. officinalis* inoculated (M) or not (NM) with *R. irregularis* MUCL 41833 before (T0) and after 1 (T1) and 4 (T4) weeks of growth in the S-H cultivation system.

Treatments	Exp. 1	Exp. 2	Time	Exp. 1	Exp. 2
NM	2.3 ± 0.7 a	7 ± 1 a	**T0**	3.7 ± 0.5 *	6 ± 0.8 *
M	5.8 ± 0.7 b	9.6 ± 1 a	**T1**	4.4 ± 0.5 *	-
			T4	-	10.6 ± 0.8 *

The parameters are expressed as mean ± standard errors (SE) of 7 M and 6 NM (Exp. 1) and 7 M and 7 NM (Exp. 2) replicates. Values within the same column followed by different lowercase letters, for fixed factor "treatment," and by *, for fixed factor "time", are significantly different according to the mixed model for repeated measurements ($p < 0.05$).

Table 4. Total colonization (TC%) and arbuscules colonization (AC%) of *A. officinalis* inoculated (M) with *R. irregularis* MUCL 41833 before (T0) and after 1 (T1) and 4 (T4) weeks of growth in the S-H cultivation system.

Fixed factor	Exp. 1		Exp. 2	
Time	**TC**	**AC**	**TC**	**AC**
T0	62 ± 2*	35 ± 2*	57 ± 2*	26 ± 2
T1	55 ± 2*	18 ± 2*	-	-
T4	-	-	50 ± 2*	24 ± 2

The parameters are expressed as mean ± standard errors (SE) of 7 M replicates. Values within the same column followed by * are significantly different according to the mixed model for repeated measurements ($p < 0.05$).

Minerals depletion in Hoagland^{dil100X} low-P solution

The concentration of Pi and NO^{-3} in the bottles of the M and NM plants followed a similar decrease over time (**Supplementary Figure 2**, Annex I). The depletion of both minerals in the circulating solution resulted in a concomitant uptake/immobilization by the plant-AMF associates. No significant interactions (p = 0.704 and p = 0.866) were

noticed between the fixed factors "treatments" and "time" for both Pi and NO^{-3}. Conversely, a significant effect ($p < 0.001$) of the fixed factor "time" was noticed. According to the pairwise comparison test ($p < 0.05$), a significant difference in the Pi and NO^{-3} concentration, represented as the average of M and NM plants at the different time points, was noticed at T4 as compared with the other time samplings. A decrease by 88 and 35% of [Pi] and [NO^{-3}], respectively, was noticed at the end of the experiment.

Metabolite profiles of M and NM *A. officinalis* plants and of nutrient solution

The metabolite profiles of shoots and roots of M and NM plants, as well as of nutrient solutions, were assessed *via* UHPLC-HRMS. Clustered analysis was illustrated through an unsupervised PCA model (**Figure 27**) with Pareto correlation and confirmed by PLS-DA analysis (**Supplementary Figure 3,** Annex I). Shoot and root samples of M and NM plants were clustered as a single group in the plot, and no significant differences in mass signals were observed between metabolic profiles of M and NM plants. However, roots of M and NM plants were closely clustered (**Figure 27 A**), with the exception of 2 NM individuals plotted at the upper limits of the model. Conversely, shoot samples from both M and NM plants were widespread in the model, reflecting the higher metabolic variability in the shoots, independent of AMF colonization (**Figure 27 B**).

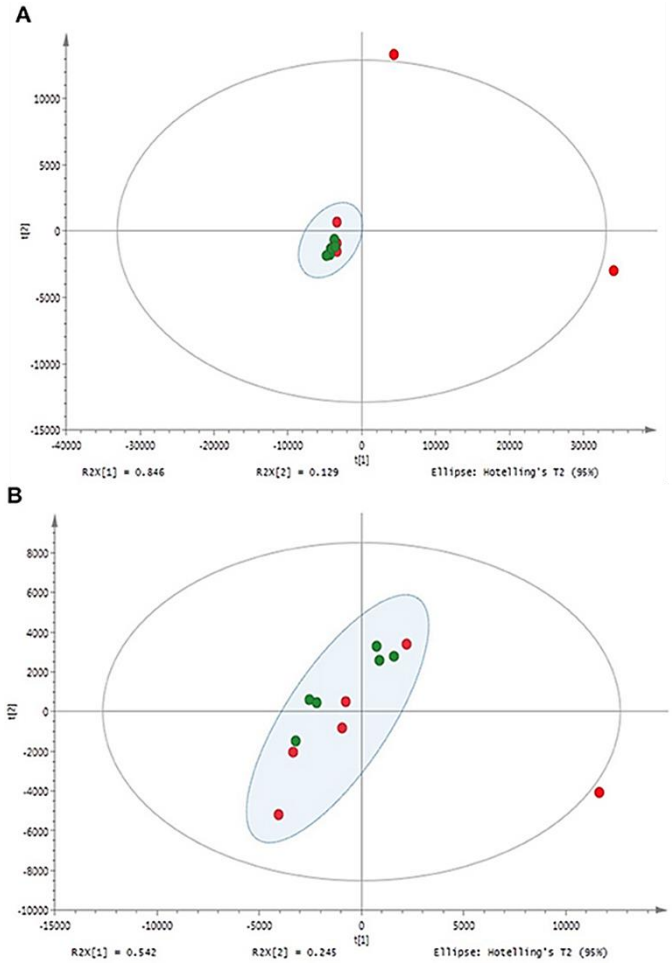

Figure 27. Principal component analysis (PCA) - comparison of UHPLC-HRMS metabolic profiles from M and NM root **(A)** and shoot **(B)** samples after 4 weeks (T4) of growth in the S-H cultivation system (M_T4: green dots; NM_T4: red dots).

Regarding the metabolic analysis of the nutrient solutions from M and NM treatments at the end of the experiment (T4), more than 600 mass signals were detected. Interestingly, distinguishable clustering between nutrient solutions of M and NM plants was noticed through an unsupervised UV scaling PCA analysis (**Figure 26**). Results were confirmed by PLS-DA analysis (**Supplementary Figure 4,** Annex I).

UHPLC-HRMS data were further interpreted by Volcano-plot analysis (**Supplementary Figure 5,** Annex I), with the same criteria as described earlier ($p < 0.05$ and FC > 1.5). Two compounds with *m/z* 206.0570 and *m/z* 334.1049 were significantly induced in the nutrient

solutions of the M plants. A tentative annotation was proposed by matching the corresponding accurate mass and MS/MS spectra pattern with already published data from literature and compound libraries (see Section Dereplication of PMs and SMs).

Besides the AMF key role in the induction of specific compounds, the nutrient solutions at T1 and T4 significantly differed in the abundance of exuded metabolites. Among them, 37 compounds were mostly accumulated at T1, while 45 metabolites were induced at T4 ($p < 0.05$ and FC > 1.5) (**Supplementary Figure 6**, Annex I). Results of Volcano-plot analysis suggested that the PMs and SMs exudation rate significantly changed according to the time spent by the plants in the S-H culture system. However, for most of them, it was not related to the AMF colonization.

Dereplication of PMs and SMs

The untargeted metabolic analysis of M and NM shoots, roots, and nutrient solutions of both experiments revealed the up and downregulation of several different mass signals. The dereplication process was performed with commercial and non-commercial databases and by comparison with available literature data, leading to the identification of 36 upregulated and downregulated fragments tentatively assigned to PMs and SMs. These up and downregulated compounds were showed only in negative ESI ionisation mode, thus compounds from the positive mode were not reported.

Ten compounds from the primary metabolism were tentatively identified according to their $[M-H]^-$ pseudomolecular ions and by their full MS/MS fragmentation patterns (**Table 5a**). Six amino acids, among which were aspartic and glutamic acids, were significantly increased, especially in M root parts, and four organics acids, tentatively annotated as threonic acid, malic acid, gluconic acid, and phenylacetic acid, were only identified in shoots of M plants.

Secondary metabolites production in shoots and roots was also modulated by AMF (**Table 5b**). Twenty-four different compounds, belonging to different chemical groups, were tentatively characterized. Among them, 16 peaks were annotated as C_6-C_3 mono-, di-, tri, and tetramers derivatives of caffeic acid, two compounds as C_6-C_1 benzoic acid derivatives, and four compounds were characterized as triterpenes

saponins according to the $[M-H]^-$ pseudomolecular ion and their corresponding MS/MS fragments. In addition, compound 26 was found to be the most upregulated metabolite from the AMF symbiosis. This compound presented a pseudo molecular ion at *m/z* 745.1430 $[M-H]^-$ and shared a similar MS/MS fragmentation pattern with compound 24, tentatively assigned as dehydro-SA B. Compound 24 has been previously identified by Liu *et al.* (2007) by the extensive use of MS and MS/MS spectra. It shows a pseudo molecular ion at *m/z* 715.1324 $[M-H]^-$ and prominent MS/MS fragment ions at *m/z* 339, 295, and 185, confirming the tetrameric C_6-C_3 configuration as well as ions at *m/z* 161, 135, 121, 109, and 73 derived from further cleavage of the single C_6-C_3 units ($C_9H_{10}O_5$). Indeed, the MS/MS spectra of compound 24 show ions at *m/z* 339, resulting from the neutral loss of a dehydroxy-danshensu ($C_9H_{10}O_4$) and of a hydroxy-caffeic acid ($C_9H_8O_5$), while the fragment ions at *m/z* 295 and 185 emerged from a further loss of a CO_2 and of a benzendiol (-109 Da) unit, respectively. This clearly suggested the presence of a hydroxybenzofuran ring in the structure (**Table 6**). A similar fragmentation pattern has been found for compound 26. However, the mass difference of 30 Da with respect to compound 24 was assigned, based on the MS/MS data, to the presence of an additional methyl ($-CH_3$) and of a hydroxy group (-OH) at positions 9" and 8, respectively. In particular, the diagnostic MS/MS fragments at *m/z* 467, 193, and 151, not present in the MS/MS spectra of compound 24, suggested the methyl-caffeic unit (CH_3 at position O-9") and the addition of the -OH group at C-8 (Liu *et al.*, 2007) (**Table 6**). According to these findings, compound 26 was tentatively identified as 8-hydroxy-9"methyl-dehydro-SA B and annotated with a chemical formula of $C_{37}H_{30}O_{17}$. Similarly, compound 27 was tentatively assigned as an SA B derivative. It showed a pseudomolecular ion at *m/z* 747.1588 $[M-H]^-$ with a chemical formula of $C_{37}H_{32}O_{17}$ corresponding to that of compounds 26 with the absence of a double bond at position 7". Therefore, the structure was tentatively assigned as 8-hydroxy-9"methyl-SA B. Among the induced ions, dimeric C_6-C_3 forms were identified. Compound 29 presented a pseudomolecular ion at *m/z* 387.0731 $[M-H]^-$ with a prominent MS/MS fragment at *m/z* 135 $[M-H]^-$, suggesting the presence of another dimeric form of caffeic acid units. Interestingly, its pseudomolecular ion corresponded to one of the MS/MS fragments, resulting from the cleavage of compound 25. Thus, a common part between those two molecules was deduced. Our suggestion was further confirmed by the presence of the diagnostic MS/MS fragments at *m/z* 207, 179, 135, and 109, corresponding to

cleavage of the methyl-caffeoyl and hydroxy caffeoyl units as shown in **Table 6**. Therefore, compound 29 was tentatively assigned as 8-hydroxyl-9'-methyl dehydro RA with a chemical formula of $C_{19}H_{16}O_9$. On the other hand, compound 16 represents the only downregulated SM in M plants in both shoot and root tissues, respectively. It showed a pseudomolecular $[M-H]^-$ ion at *m/z* 537.1050 and MS/MS ion fragments at *m/z* 339 and 295, as well as major ions fragments at *m/z* 179, 161, 135, and 109, corresponding to the characteristic cleavage of the three C_6-C_3 units of lithospermic acid ($C_{27}H_{22}O_{12}$). In addition, compound 16 showed a mass difference of -14 Da with respect to compound 23, whose structure was assigned as the methylated derivative of lithospermic acid at position 9".

Arbuscular mycorrhizal fungi symbiosis affected the expression of four glycosylated triterpernoids. In our analysis, compounds 17, 32, 33, and 34 were annotated as saponins and showed a strong accumulation in shoots of M plants. In addition, compound 17 shows a molecular ion at *m/z* 828.4502 $[M-H]^-$, tentatively assigned to the oleanolic acid glycoside Anchusoside-9 through the two characteristic MS/MS fragments at *m/z* 665 and 503. This resulted from the consecutive neutral loss of two hexose units from the structure (-162 and -324 Da) (Romussi *et al.*, 1984a). Compounds 32-34 shared a common fragment ion at *m/z* 455, corresponding to the aglycone part of the structure (oleanolic acid), confirming their structural similitudes. Specifically, compounds 32 and 33 were tentatively characterized as tri- and di-glycosidic esters of oleanolic acid, respectively. They both shared a prominent characteristic MS/MS ion at *m/z* 617, corresponding to a common glucopyranosyl oleanolate unit. Moreover, compound 32 presents additional fragment ions at *m/z* 808 $[M-H-133]^-$, resulting from the neutral loss of one pentose and at *m/z* 323, corresponding to the cleavage of a disaccharide unit that contained the abovementioned pentose and a glucuronic acid methyl ester moiety. Based on these findings and according to the pseudomolecular ion $[M-H]^-$ at *m/z* 939.3993, compound 31 was tentatively assigned as a tri-glycosylated oleanolic acid methyl ester derivative, detected for the first time in *A. officinalis*. Conversely, compound 33, with a molecular ion at *m/z* 779.4612 and the abovementioned characteristic MS/MS fragment, was tentatively assigned as the di-hexoside oleanolic acid derivative Anchusoside-1, commonly found in *A. officinalis*. Compound 34 showed a pseudomolecular ion at *m/z* 941.5106 $[M-H]^-$ and was tentatively assigned as the trihexoside oleanolic acid ester

Anchusoside-2. Based on the main MS/MS fragment at *m/z* 455, corresponding to oleanolic acid, we assumed the presence of a trihexoside unit in the structure. This was further confirmed by the MS/MS fragments at *m/z* 779 and 617, corresponding to the successive loss of three glucosyl moieties (-162, -324, and -486 Da).

Regarding the nutrient solutions, two accumulated compounds were detected in the M plants of Exp. 2 (T4). A potential chemical formula of $C_{11}H_{10}O_4$ and $C_{17}H_{18}O_7$ was determined according to the $[M-H]^-$ pseudomolecular ion at *m/z* 205.0497 and *m/z* 333.0976, respectively, leading to the tentative identification, according to their MS/MS fragmentation pattern, of the coumarin scoparone and of the furanocoumarin byakangelicin. Scoparone showed characteristic MS/MS ion fragments at *m/z* 161 and 133, related to the successive loss of $-CO_2$ from the lactone ring and of $-OCH_3$, respectively, while the ion fragment at *m/z* 119 corresponded to the loss of a further methyl radical (Concannon *et al.*, 2000; Wang *et al.*, 2007). Byakangelicin presented MS/MS ion fragments at *m/z* 303 $(C_{16}H_{15}O_6)^-$ and at *m/z* 290 $(C_{16}H_{18}O_5)^-$ emerged from the loss of $-OCH_3$ and $-CO_2$, respectively, of the lactone ring. Further rearrangements of the structure, for the formation of a more stable ion, gave the fragment ions at *m/z* 203 related to the loss of the side chain and of a carbonyl, while fragments at *m/z* 147 and 131, generated from the consecutive loss of $-CO_2$ and of other carbonyl units, further confirmed the structure of compound 36 (Zhang *et al.*, 2009a)

Table 5. Up and downregulated **(a)** PMs and **(b)** SMs in shoots and roots of *A. officinalis* plants associated with *R. irregularis* MUCL 41833 after 1 week of growth in the S-H cultivation system (Exp. 1). Upregulated SMs (exudates) in nutrients solutions (NS) of M plant after 4 weeks (T4) of growth in the S-H cultivation system (Exp. 2).

		Peak	Proposed phytochemicals	RT (min)	Precursor Ion - $[M-H]^-$	*m/z* calcd.	*Δ*m (ppm)	MS/MS Fragment ions (*m/z*)	Chemical formula	Distribution[1]	Reference
S and R metabolites content[2]	**(a)** Primary metabolism	1	Asparagine	1.44	131.0453	132.0529	-7.3	131, 115, 88, 71	$C_4H_8N_2O_3$	S (5.19), R (6.56) ↑	Zengin *et al.*, 2018
		2	L-Aspartic acid	1.46	132.0294	133.0370	-6.6	132, 115, 88, 71	$C_4H_7NO_4$	S (2.19), R (6.29) ↑	Brieudes *et al.*, 2016
		3	Glutamic acid	1.44	146.0451	147.0526	-5.3	146, 128, 102	$C_5H_8NO_4$	S (5.31), R (6.54) ↑	Brieudes *et al.*, 2016
		4	Gluconic acid	1.49	195.0505	196.0578	-2.6	177, 160, 129, 87, 75	$C_6H_{12}O_7$	S (1.96) ↑	Brieudes *et al.*, 2016
		5	L-Threonic acid	1.54	135.0290	136.0366	-6.8	135, 117, 89, 75, 61	$C_4H_8O_5$	S (6.61), R (3.77) ↑	Brieudes *et al.*, 2016
		6	DL-Malic acid	1.59	133.0134	134.0210	-6.6	133, 115, 89, 72, 71	$C_4H_6O_5$	S (8.17), R (7.79) ↑	Li *et al.*, 2004
		7	DL-pyroglutamic acid	1.65	128.0344	129.0420	-7.1	128, 82, 62	$C_5H_7NO_3$	S (9.24), R (8.39) ↑	Shi *et al.*, 2020
		8	N-Acetylalanine	2.14	130.0501	131.0577	-6.7	130, 88	$C_5H_9NO_3$	R (4.25) ↑	-
		9	Methylpyroglutamate	2.23	142.0502	143.0577	-5.5	142, 100, 98, 58	$C_6H_9NO_3$	R (7.11) ↑	-
		10	Phenylacetic acid	3.65	135.0443	136.0519	-6.2	93, 72	$C_8H_8O_2$	R (5.28) ↑	Lee *et al.*, 2017

Continue in the next page…

		Peak	Proposed phytochemicals	RT (min)	Precursor Ion - [M-H]$^-$	*m/z* calcd.	*Δ*m (ppm)	MS/MS Fragment ions (*m/z*)	Chemical formula	Distribution[1]	Reference
S and R metabolites content[2]	**(b)** Secondary metabolism	11	Syringic acid	3.71	197.0453	198.0523	-1.3	179, 151, 135, 123, 72	$C_9H_{10}O_5$	R (4.55) ↑	Taamalli *et al.*, 2015
		12	*p*-Hydroxybenzoic acid	5.03	137.0236	138.0311	-6.3	135, 93, 65	$C_7H_6O_3$	R (6.90) ↑	Gómez-García *et al.*, 2021
		13	Chorismic acid	5.24	225.0404	226.0472	-0.9	207, 179, 137, 109, 61	$C_{10}H_{10}O_6$	R (2.70) ↑	Khera *et al.*, 2017
		14	Caffeic acid	5.39	179.0344	180.0417	-3.3	135, 109, 89, 73	$C_9H_8O_4$	S (2.11) ↑	Gómez-García *et al.*, 2021
		15	Methyl syringinoside	5.25	547.2039	548.2099	1.3	191, 176, 161, 121, 93, 71	$C_{24}H_{36}O_{14}$	R (1.54) ↑	
		16	Lithospermic acid	5.81	537.1050	538.1106	2.11	339, 295, 269, 197, 179, 161, 135, 109, 73	$C_{27}H_{22}O_{12}$	S (2.28), R (3.07) ↓	Liu *et al.*, 2007
		17	Anchusoside-9	6.07	827.4449	828.4502	1.8	665, 503, 161, 113, 85, 71	$C_{42}H_{68}O_{16}$	S (2.25) ↑	Romussi *et al.*, 1984b
		18	Methyl syringin	6.40	385.1510	386.1571	1.5	223, 191, 176, 161, 121, 93, 71	$C_{18}H_{26}O_9$	R (1.52) ↑	Park *et al.*, 2017
		19	Rosmarinic acid (RA)	6.55	359.0777	360.0840	1.1	197, 179, 161, 135, 123, 73, 62	$C_{18}H_{16}O_8$	R (2.11) ↑	Krzyżanowska-Kowalczyk *et al.*, 2018
		20	Salvianolic acid C	6.86	491.0992	492.1051	1.6	311, 267, 197, 185, 179, 135, 109, 73	$C_{26}H_{20}O_{10}$	S (5.71) ↑	Finimundy *et al.*, 2020
		21	Syringin	6.89	371.1353	372.1415	1.3	176, 161, 121	$C_{17}H_{24}O_9$	S (2.04) ↑	Filipek *et al.*, 2019
		22	Ferulic acid	7.04	193.0502	194.0574	-2.2	179, 161, 133	$C_{10}H_{10}O_4$	S (3.33), R (2.22) ↑	Gómez-García *et al.*, 2021

	23	Methyl lithospermic acid	7.11	551.1202	552.1262	1.5	339, 321, 293, 231, 185, 179, 161, 135, 109, 73	$C_{28}H_{24}O_{12}$	R (2.79) ↑	Liu *et al.*, 2007
	24	Dehydro SA B	7.12	715.1324	716.1372	2.7	357, 339, 295, 185, 135, 109, 72	$C_{36}H_{28}O_{16}$	S (4.31), R (4.47) ↑	Li *et al.*, 2018
	25	Methyl rosmarinic acid	7.17	373.0934	374.0996	1.5	197, 179, 160, 135, 123, 73	$C_{19}H_{18}O_8$	S (1.99) ↑	Krzyżanowska-Kowalczyk *et al.*, 2018
	26	8-hydroxy-9’’-methyl dehydro SA B	7.24	745.1430	746.1478	2.7	467, 387, 339, 295, 193, 185, 151, 133, 109, 73	$C_{37}H_{30}O_{17}$	R (7.17) ↑	Liu *et al.*, 2007
	27	8-hydroxy-9’’-methyl SA B	7.34	747.1588	748.1634	2.6	467, 389, 339, 295, 195, 185, 151, 135, 109, 73	$C_{37}H_{32}O_{17}$	R (3.41) ↑	Liu *et al.*, 2007
	28	Salvianolic acid B (SA B)	7.47	717.1479	718.1528	2.2	357, 339, 321, 295, 265, 197, 185, 161, 135, 109, 73	$C_{36}H_{30}O_{16}$	R (3.72) ↑	Wu *et al.*, 2006
	29	8-hydroxy-9’-methyl dehydroRA	7.50	387.0731	388.0789	2.4	207, 179, 135, 121, 109	$C_{19}H_{16}O_9$	R (4.54) ↑	Grzegorczyk-Karolak *et al.*, 2019
	30	Isobavachalcone hexoside	7.92	485.1827	486.1884	2.0	177, 163, 145, 117	$C_{26}H_{30}O_9$	R (5.58) ↑	Cioffi *et al.*, 2003

Continue in the next page…

		Peak	Proposed phytochemicals	RT (min)	Precursor Ion - [M-H]$^-$	*m/z* calcd.	*Δ*m (ppm)	MS/MS Fragment ions (*m/z*)	Chemical formula	Distribution[1]	Reference
		31	Salvianolic acid F	7.93	313.0723	314.0793	1.6	203, 179, 161, 133, 123	$C_{17}H_{14}O_6$	S (2.48) ↑	Grzegorczyk-Karolak *et al.*, 2019
		32	Oleanolic acid triglycoside	8.06	939.3993	940.5026	3.6	808, 617, 455, 159, 129, 111, 87, 71	$C_{48}H_{78}O_{18}$	S (2.26) ↑	-
		33	Anchusoside-1	8.44	779.4612	780.4654	3.1	617, 455, 141, 112, 71	$C_{43}H_{70}O_{15}$	S (1.73) ↑	Romussi *et al.*, 1979
		34	Anchusoside-2	9.25	941.5106	942.5183	-0.9	779, 617, 455, 161, 113, 85, 71	$C_{48}H_{78}O_{18}$	S (1.91) ↑	Romussi *et al.*, 1979
NS[3]		35	Scoparone	6.25	205.0497	206.0574	-4.4	177, 161, 143, 133, 119	$C_{11}H_{10}O_4$	NS (3.21) ↑	Wang *et al.*, 2007b
		36	Byakangelicin	10.89	333.0976	334.1047	-1.0	303, 249, 202, 147, 131, 125	$C_{17}H_{18}O_7$	NS (9.5) ↑	Zhang *et al.*, 2009b

[1]Numbers with parenthesis represent the fold change of each compound in "M vs. NM" plants and corresponding nutrient solutions. Green arrows indicate up-regulation while red arrows indicate the down-regulation in shoots (S), roots (R) and/or nutrient solutions (NS) of M plants.
[2]PMs and SMs affected by the AMF-plant symbiosis in shoot and root parts of the S-H cultivation system at T1 of experiment.
[3]SMs affected by the AMF-plant symbiosis in nutrient solutions (exudates) of the S-H cultivation system at T4 of experiment.
RT = Retention Time; *Δ*m = mass errors; [M-H]$^-$ = *m/z* of the pseudomolecular ion in negative ionisation mode; *m/z* calcd = theoretical *m/z* value.

Table 6. Chemical structures and fragmentation pattern of compounds 19, 23, and 25 – 28 identified by ESI-HRMS and MS/MS analysis.

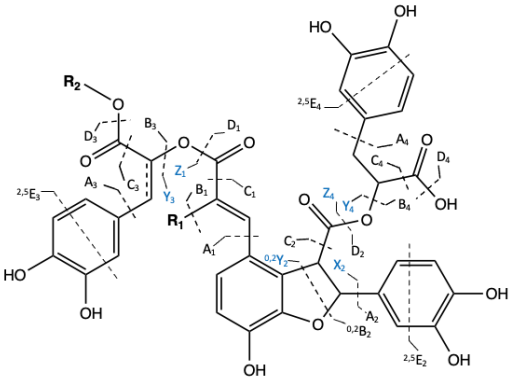

	R_1	R_2
23	-H	-H
25*	-OH	$-CH_3$
26	-H	-H
27*	-OH	$-CH_3$

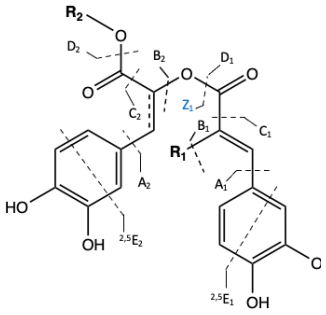

	R_1	R_2
18	-H	-H
28*	-OH	$-CH_3$

Comp.	$[M-H]^-$	MS/MS (*m/z*)
19	359.0777	197 (D_1), 179 (B_1), 161(B_1/D_2), 135 (B_1/C_2), 123, 73 ($^{2,5}E$)
23	715.1324	357 ($^{0,2}Y_2$ or Y_3/Y_4), 339(D_1/Y_4), 321(D_1/D_2), 295(D_1/C_2), 197 (Z_4), 185 ($D_1/X_2/C_2$), 161(B/D), 133(B_1/C_1 or B_3/C_3), 135 ($^{0,2}B_2/C_2$ or B_4/C_4), 109 (A), ($^{2,5}E$)
25	745.1430	467 (A_1), 387 (Y_2), 339 (D_1/D_2), 295 ($B_1/D_1/C_2$), 197 (Z_4), 193 (B_3 or $^{0,2}Y_2$ /Y_3), 185 ($B_1/D_1/C_2/A_2$), 151 ($C_1/^{0,2}Y_2$), 133(B_1/C_1 or B_3/C_3), 135 ($^{0,2}B_2/C_2$ or B_4/C_4), 109 (A), ($^{2,5}E$)
26	747.1588	467 (A_1), 389 ($^{0,2}Y_2$), 339 (D_1/D_2), 295 ($B_1/D_1/C_2$), 197 (A), 195 (Z_4), 185 ($B_1/D_1/C_2/A_2$), 151 ($C_1/^{0,2}Y_2$), 133(B_1/C_1 or B_3/C_3), 135 ($^{0,2}B_2/C_2$ or B_4/C_4), 109 (A), ($^{2,5}E$)
27	717.1479	357 (Y_3/Y_4), 339(D_1/Y_4), 321(D_1/D_2), 295(D_1/C_2), 197 (Z_1 or Z_4), 185 ($D_1/X_2/C_2$), 161(B/D), 135 ($^{0,2}B_2/C_2$ or B_3/C_3 or B_4/C_4), 109 (A), 73 ($^{2,5}E$)
28	387.0731	207 (Z_1), 179 (D_2), 161 (B_1/D_1), 135 (B_1/C_1 or $^{0,2}B_2/C_2$), 109 (A)

* Compounds possessing a double bond at C7' or C7''.

Discussion

Plants interact with a complex community of beneficial microorganisms developing in seeds, leaves, and roots, providing nutritional assistance, stimulating growth, and inducing resistance against pest and diseases as well as against abiotic stresses. Colonization of plant tissues often induces quantitative and qualitative changes in PMs and SMs; some of which may be of commercial interest. Thus, a targeted approach with selected microbial inoculants applied under highly controlled conditions may be of interest to increase or stimulate the production of specific high-value metabolites. Arbuscular mycorrhiza fungi are among those microorganisms improving plant nutrition and growth, stimulating defence mechanisms (Chen *et al.*, 2018), securing plant development under abiotic stress conditions (Plouznikoff *et al.*, 2016), and impacting the up and downregulation of specific PMs (Pedone-Bonfim *et al.*, 2015) and SMs (Zeng *et al.*, 2013) in plants.

Here, two successive experiments were conducted under a S-H cultivation system to investigate the role of AMF in PMs and SMs production in shoots, roots, and exudates of the medicinal plant *A. officinalis*. An untargeted UHPLC-HRMS metabolomics approach combined with multivariate data analysis enabled to provide a broad picture of the *A. officinalis* metabolic profile changes as a result of AMF colonization.

Adequacy of the S-H cultivation system for PMs and SMs analysis in AMF-colonized plants

To evaluate the adequacy of the S-H cultivation system, plant and AMF parameters were assessed. *Anchusa officinalis* growth was clearly observed in both experiments, in the presence and absence of AMF. This was evidenced by an increase in TFW between the start and the end of both experiments and by depletion of Pi and NO^{-3} in the nutrient solutions (monitored in Exp. 2). However, significant differences in TFW were noticed between M and NM plants only in Exp. 1, with higher values recorded in the AMF colonized plants. This could be attributed to the higher TFW of M plants at transfer from pots to the S-H system. Moreover, the plants transfer may have caused an initial stress, which was probably better supported by the M plants, due to the presence of its fungal associate. However, no differences in TFW were

noticed between the two treatments in Exp. 2. The plants were most probably adapted to the longer period of growth in the S-H system, and the initial stress, noticed in Exp.1, was no longer present at the end of this experiment (as reported below for AMF colonization assessment). Besides, each plant received strictly the same amount of nutrients flowing on the root system during several weeks, and similar minerals depletion was reported in the presence and in the absence of AMF, resulting in no visible impact on plant growth. Similar trends have been reported in other studies, using the S-H cultivation system (Garcés-Ruiz *et al.*, 2017; Calonne-Salmon *et al.*, 2018).

Root colonization in both experiments was high, even if significant decreases were noticed between the start and the end of experiments. This was particularly marked in Exp. 1 for TC% and AC%, while it was less noticeable in Exp. 2 with only TC%, showing a significant decrease. The decrease was possibly related to stress conditions occurring between transfer from pot to S-H system and final harvest, with extraradical mycelium partially damaged at plant transfer to the S-H system, requiring more time for the fungus to recover and extend in the root system. The differences were less noticeable in Exp. 2, in which the final observations were done 30 days after transfer in the S-H cultivation system, with a probable better recovery of the AMF. Numerous arbuscules were observed in both experiments with AC% close to 20 and above 20% at the end of Exp. 1 and 2, respectively, suggesting that the symbiosis was functional throughout the duration of experiments.

Impact of AMF on PMs and SMs in shoots, roots, and exudates of *A. officinalis* grown in the S-H cultivation system

Besides the phenotypic trait changes between M and NM plants, primary and secondary metabolism was significantly impacted in the presence of AMF. The untargeted metabolomics approach performed in Exp.1, after 9 days in the S-H cultivation system, showed an upregulation of in total 34 compounds between PMs and SMs, with fold change values ranking from 1.52 to 9.50, and a downregulation of one single SM with a fold change decrement of 2.28 and 3.07 in shoot and root tissues of M plants. Conversely, in Exp. 2, while no significant differences in PMs and SMs were assessed between M and NM plants,

an upregulation of two compounds was reported in the exudates of M plants at T4, with fold change values of about 3.21 and 9.5.

Shoots and Roots

Impact on Primary Metabolism

Regarding the primary metabolism, 10 PMs were significantly upregulated in both shoot and root parts of the plants. An increased accumulation of specific amino acids, such as asparagine, glutamic, and pyroglutamic acids, and organic acids, such as DL-malic, was observed in M plants with a fold change increment varying from 6.29 to 8.39 in the roots and 2.19 to 9.24 in the shoots. Primary metabolic reprogramming was particularly observed in root tissues at Exp. 1, after 9 days in the S-H cultivation system, while no significant differences were assessed between M and NM plants in Exp. 2 after 30 days. In more details, Volcano-plots evidenced pyroglutamic acid as the most upregulated compound, showing a fold change of 8.39 and 9.24 in shoots and roots, respectively. Pyroglutamic acid (PG), also known as 5-oxoproline, is a natural amino acid derivative in which the free amino group of glutamic acid cyclizes to form a lactam (Schliemann *et al.*, 2008; Jiménez-Arias *et al.*, 2019). This PM is an important reservoir and analogue of glutamate (Kumar and Bachhwat, 2011; Jiménez-Arias *et al.*, 2019), which was also increased in M plants (**Table 5a**). Glutamate is considered as the precursor amino acid of glutamine, histidine, arginine, and proline (**Figure 28**). Therefore, the accumulation of glutamate and PG could reflect the intense metabolic activity occurring during the growth and development of M plants. Interestingly, high accumulations of glutamate in M plants have been reported as a significant nitrogen pool, reflecting the ability of AMF to enhance N assimilation in plants (Bucking *et al.*, 2012; Zeng *et al.*, 2013; Rivero *et al.*, 2015). Nitrogen movement in AMF symbiosis includes the uptake of N by the fungal extraradical mycelium, arginine synthesis in the extraradical mycelium, and transport to the intraradical mycelium, where it is broken down to release N for transfer to the host plant (Zhu *et al.*, 2016). Moreover, AMF are capable of accessing organic nitrogen containing compounds directly from the soils, resulting in an improved plant uptake of multiple amino acids: phenylalanine, lysine, asparagine, arginine, histidine, methionine, tryptophan, and cysteine (Whiteside *et al.*, 2012). Zhu *et al.* (2016) reported that AMF symbiosis increased the amino acid concentrations and altered the amino acid profile of maize plants under low

temperature stress, but, still, the mechanism behind the AMF mediated changes in amino acid profile is unknown and merits further studies. More recently, Jiménez-Arias *et al.* (2019) have reported a stress-tolerant effect of PG in crops grown under environmental stress conditions, suggesting that the excessive upregulation of this PM in our S-H cultivation system could also result from an adaptation of the plant-AMF associates to the specific environmental conditions encountered during the short-term experiment. As reported for the changes of the phenotypic traits, the initial stress encountered in Exp. 1 could have played a role in the boosting of metabolism of M plants. Malic acid levels also significantly increased in the M plants, with a fold change increment of 8.17 and 7.79 in shoots and roots, respectively. This organic acid is one of the main intermediates of TCA cycle and precursor of aspartic acid (**Figure 28**), which was also increased in the M plants. The latter is an important intermediate precursor of other amino acids, such as asparagine, threonine, lysine, isoleucine, and methionine, and is mainly present in the early development stage of the plant, while its decrease is a consequence of the relative increase of derived amino acids as the plant matures (Wang and Larkins, 2001). Similar to PG, glutamate, and malic acid, all identified amino acids showed a higher accumulation in M plants (**Table 5a**). These aspects are in accordance with our phenotypic traits observations and indicate that the primary metabolism is strongly affected by the AMF symbiosis (Rivero *et al.*, 2015). However, in Exp. 2, the well-established AMF symbiosis occurred at day 30 of the S-H cultivation system did not affect PMs concentration and neither the TFW of M plants. In all cases, we found that no phenotypic differences between plants lead to a common PM content, reflecting the importance of the growth stage in the production of specific PMs. In our analysis, we hypothesized that the significant effect of the AMF symbiosis, mainly occurring at the early growth stage in the S-H system, was related to the stress conditions of plant establishment in pots and at the transfer to the S-H cultivation system. However, further investigations are needed to fully understand the impact in later growth stages.

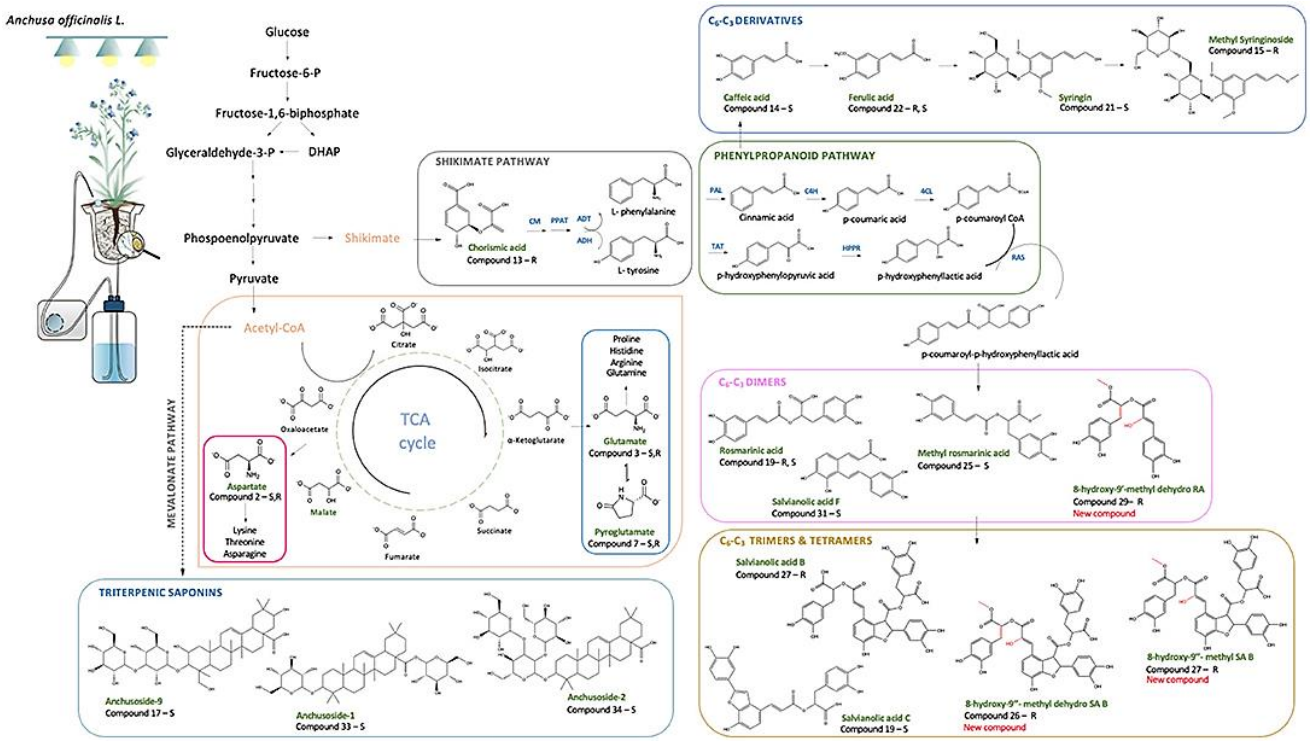

Figure 28. Schematic representation of the main PMs and SMs influenced by the AMF-plant symbiosis in relation to different biosynthetic pathways. Upregulated compounds are reported in green accompanied by the letters R and/or S, indicating whether they were found upregulated in roots and/or shoots, respectively (CM, chorismate mutase; PPAT, prephenate aminotransferase; ADT, arogenate dehydratase; ADH, arogenate dehydrogenase; PAL, phenylalanine ammonia-lyase; TAT, tyrosine aminotransferase; C4H, cinnamic acid 4-hydroxylase; HPPR, hydroxyphenylpyruvate reductase; 4CL, 4-coumaric acid coenzyme A-ligase; RAS, rosmarinic acid synthase; HXL, hydroxylase).

Besides the aforementioned amino acids and organic acids widely present in living organisms, a natural auxin, phenylacetic acid, was found significantly upregulated in the roots of M plants at the end of Exp. 1 (fold change of 5.28). With a less restricted meaning of PMs, the natural auxin phenylacetic acid plays a key role in plant-growth promotion (Hammad *et al.*, 2003). It has been reported as more effective than indole-3-acetic acid (IAA) in the induction of lateral root growth and for carrying cellular growth (Cook, 2019). Auxins are also particularly essential at early growth stages in host-roots (Fusconi, 2014) to ensure successful colonization by AMF since the root architecture is subject to continuous changes by increasing branching and development of lateral roots (Fusconi, 2014; Cook, 2019). This may contribute to phenylacetic acid accumulation in the roots of M plants in Exp. 1. However, as the plants adapt to the S-H system, no statistical difference in phenylacetic acid content was observed between M and NM plants at the end of Exp. 2.

Impact on secondary metabolism

Regarding the secondary metabolism, 24 different SMs were significantly up and downregulated in shoots and roots of AMF colonized plants, with a fold change varying from 1.52 to 6.90. As reported for PMs, SMs were essentially upregulated in the root system of M plants in Exp. 1 after 9 days of growth in the S-H system. In particular, 12 compounds were exclusively accumulated in roots, 9 in shoots, while 3 were identified in both parts of the M plants. Although the increment involved mainly phenolic compounds, colonization by AMF also impacted the production of glycosylated triterpenoids in M shoots. In total 15 phenylpropanoids, among which 10 have been tentatively identified as di-, tri-, or tetramers of C_6- C_3 compounds (e.g., rosmarinic acid, salvionolic acid C, and salvianolic acid B), were significantly upregulated in M plants. Eight of them were upregulated exclusively in the roots, 5 in the shoots, while 2 in both parts. The structures of the aforementioned compounds were assigned according to their pseudomolecular ions and MS/MS spectra. Interestingly, most phenylpropanoids shared common MS/MS ions at *m/z* 179 and at *m/z* 135, corresponding to the typical fragments of the caffeoyl moiety (**Table 5b**). This may also explain their simultaneous upregulation in M plants. Therefore, C_6-C_3 compounds and their di-, tri-, and tetrameric derivatives are affected by the AMF symbiosis, mainly in M roots, presenting a fold change, ranking from 1.99 to 7.17. An increased

production of chorismic acid was also noticed in the roots of M plants. This compound is considered a precursor of hydroxycinnamic acids (C_6-C_3 skeleton) (**Figure 28**) and thus of the ester derivatives of caffeic acid detected in this study (**Table 5b**). In support of this increment, previous studies have reported increasing levels of transcripts encoding for the biosynthetic enzyme phenylalanine ammonia lyase (PAL) in mycorrhized plants. This may further confirm our findings since PAL is involved in the formation and accumulation of phenolic acids *via* the phenylpropanoid biosynthetic pathway (Rivero *et al.*, 2015). Indeed, AMF symbiosis elicited signalling cascades, which cause the activation of specific biosynthetic defence pathways, resulting in the release of specific compounds such as polyphenolic derivatives (Bulgakov *et al.*, 2012; Srivastava *et al.*, 2016).

Special attention was given to compound 26 due to its high accumulation in the roots of M plants (fold change increment of 7.17). Interestingly, this compound represents a previously undescribed natural product tentatively identified as 8-hydroxy- 9”methyl-dehydro-SA B. Similarly, compound 27 was assigned as a new C_6-C_3 tetramer (fold change increment of 3.4) tentatively characterized as 8-hydroxy-9”methyl-SA B. In our analysis, we also identified several dimeric C_6-C_3 forms, including the commonly known rosmarinic acid [*m/z* 359.0777 $(M-H)^-$, compound 19], widely distributed in *Anchusa* species (Kuruuzum-Uz *et al.*, 2012; Dresler *et al.*, 2017; Boskovic *et al.*, 2018) and its new derivative 8-hydroxy-9’-methyl dehydro RA (compound 29). Structures of compounds 26, 27, and 29 are in line with Liu *et al.* (2007) and with Grzegorczyk-Karolak *et al.* (2019), showing a common position of unsaturation at carbons C-7” and C-7’ for compounds 26 and 29, respectively. Moreover, they exhibit a common methylation at C-9’ for compound 29 and at C-9” for compounds 26 and 27, and hydroxylation at C-8 for compounds 29 and at C-8’ for compounds 26 and 27.

According to **Table 5b**, compound 16 represents the only downregulated SM in M plants, showing a fold change decrement of 2.28 and 3.07 in both shoot and root tissues, respectively. Based on HRMS data, compound 16 was structurally annotated as lithospermic acid. Interestingly, and as opposed to lithospermic acid, compound 23, identified as the methylated derivative of lithospermic acid at position 9”, showed significant upregulation in the roots of M plants (fold change of 2.79). During our analysis, we identified a total of 15 C_6-C_3 SMs showing significant upregulation in M plants; among which 7 were

tentatively assigned as methyl derivatives. This could suggest that AMF symbiosis induced changes in host plant metabolism (Lohse *et al.*, 2005). In line with our results, previous studies of *R. irregularis* genome has underlined the expression of different methyltransferases (Sun *et al.*, 2019) involved in the methylation of specific compounds, such as phospholipids (Wewer *et al.*, 2014; Feng *et al.*, 2020) in AMF-colonized roots. However, to the best knowledge of the authors, this is the first time that the impact of AMF on SM methylation was reported.

In addition, p-Hydroxybenzoic acid (HBA) and syringic acid were highly accumulated in M roots (fold change increment of 6.90 and 4.55, respectively) (**Table 5b**). These two are aromatic compounds with a C_6-C_1 skeleton synthesized *via* the shikimate pathway involving different C_6-C_3 intermediates, the main category of accumulated molecules found in our study (**Figure 29**) (Widhalm and Dudareva, 2015; Srinivasulu *et al.*, 2018). Both HBA and SA are crucial precursors of a wide variety of essential molecules (e.g., folic acids and ubiquinone) playing a key role in plant fitness (Widhalm and Dudareva, 2015). Their production is often related as a reaction to biotic/abiotic stresses (Widhalm and Dudareva, 2015; Zubek *et al.*, 2015). The accumulation of these compounds in the roots of M plants grown in the S-H cultivation system is in line with the studies of Kara *et al.* (2015) and Zubek *et al.* (2015), showing higher abundance of benzoic acids and, especially, of HBA in AMF-colonized plants.

Besides the increment in phenolic compounds, AMF symbiosis also impacted the production of glycosylated triterpenoids, such as the oleanane-type saponins. Saponins are essentially found in cell membranes of dicotyledonous plants, and they are mainly involved in plant protection mechanisms (Xie *et al.*, 2018). Wide diversity of chemical structures is reported in the plant kingdom on the basis of aglycone structure and the nature of glycosylation (Mugford and Osbourn, 2012). Their content is influenced by various biotic stimuli, such as herbivory and pest attack or related to plant-microorganism symbiosis (Hussain *et al.*, 2017). Interestingly, the ability to produce these compounds has been already reported for *Anchusa* species, specifically oleanane-type glycosidic derivatives mainly present in the foliar part of the plants (Chen *et al.*, 2017). In our analysis, and in opposition to phenolic compounds, saponins 17, 32, 33, and 34 showed maximum accumulation in M shoots, with a fold change increment ranking from 1.73 to 2.26. Their structures were assigned on the basis of their pseudomolecular ions under a negative ionisation mode and by

their specific MS/MS fragmentation pattern. Anchusoside-2, as well as Anchusoside-1 and Anchusoside-9, is widely reported for *A. officinalis*. However, this is the first report showing that oleanane-type saponins can be upregulated in shoots of M plants.

Despite the pronounced metabolic variations of Exp. 1, no significant differences were observed at the end of Exp. 2. For instance, after 30 days, neither the SMs shoots and roots content of M plants nor their phenotypic traits showed any significant variation when compared with the NM plants. It is worth mentioning that AMF symbiosis remains active at the end of Exp. 2 through the presence of numerous arbuscules. Nevertheless, no benefits from the symbiosis were noticed for M plants from the phenotypic and the metabolic point of view. Taking into consideration this observation, we can suggest that the AMF impact is considered particularly important in the early growth stage of the plants in the pots and S-H system and, apparently, less effective as it grows older. However, the effect of the growth environment offered by the S-H cultivation system should be carefully considered. Indeed, the limited space could exert an inhibitory effect on growth, which gradually increased in relation to the plant development. Finally, the decrease in the content of the minerals (Exp. 2, T4) could have diminished/limited the AMF-plants nutrient requirements. Arbuscular mycorrhizal fungi might have tried to allocate energy mostly on the arbuscules formation in order to optimize the uptake of the remaining nutrients (Le Pioufle *et al.*, 2019).

Interestingly, several of the upregulated secondary metabolites found during our analysis, as a result of the *A. officinalis*-AMF symbiosis, have shown important biological proprieties. For instance, phenylpropanoids and their derivatives, which represent the class of SMs more affected by the AMF symbiosis, have gained attention due to their low toxicity and a wide array of beneficial effects on human health and disease management. Salvianolic acids showed an important impact on cancer treatment and alleviation of fibrosis disease as well as a good therapeutic effect on cardiovascular and neural protection (Ma *et al.*, 2019). Furthermore, other major affected compounds, such as rosmarinic acid, ferulic acid, caffeic acids, and derivatives, present several health-related properties, such as antioxidant, anti-inflammatory, and antimicrobial activities (Boskovic *et al.*, 2018; Luo *et al.*, 2020). In addition to phenolic compounds, saponins present antibacterial, antifungal, and antiviral properties and are extensively used beyond pharmaceuticals for their surfactant properties (Mugford

and Osbourn, 2012). Therefore, AMF symbiosis increases *A. officinalis* performance in the production of several bioactive compounds and lays the foundation for further exploitation of these root symbionts in the manipulation of medicinal plants.

Plant exudates

Despite the fact that AMF symbiosis has been proven to affect different metabolic and physiological processes in plants, the literature related to the impact of AMF on plant exudation is still scarce. It is well-known that plants exude large diversity of compounds, especially SMs, that contribute to the plant fitness by interacting with the surrounding soil microbiota or by playing a role in nutrient acquisition by boosting soil nutrient bioavailability (Voges *et al.*, 2019).

In this study, we took advantage of the controlled environment offered by the S-H cultivation system to investigate any possible differences among plant exudates of M and NM plants. During our analysis, the same Hoagland solution dil100X percolated through M and NM plants for several weeks, without renewing, in order to compare the plant exudation at 9 and 30 days of the experiment. Unlike our previously reported findings showing a pronounced metabolic variation between M and NM plants at T1 (Exp. 1), data resulting from the PCA analysis of plant exudates at the same time period showed no differences between M and NM plants. Conversely, upregulation of two mass signals attributed to the coumarin scoparone (compound 35) and the furanocoumarin byakangelicin (compound 36) were identified in the exudates of M plants at T4 of Exp. 2 with a fold change increment of 3.21 and 9.50. Coumarins are plant-derived natural products synthesized *via* the phenylpropanoid pathway and are widely reported as exuded substances involved in defence mechanisms against pathogens (Harbort *et al.*, 2020). Recently, however, these compounds have been also described for their ability to mobilize iron from deprived soil. For instance, their exudation from roots was induced under Fe limitations, aiming for more efficient iron acquisition (Chutia *et al.*, 2019). In addition, similar studies reported that AMF symbiosis could induce the accumulation of coumarins in the radical part of mycorrhized plants for their secretion in the rhizosphere under Pi limitation (Stringlis *et al.*, 2019). This hypothesis could explain our findings on plant exudates since at T4 clear depletion of Pi and NO^{-3} was observed.

Conclusion

In conclusion, the AMF colonization influenced specific plant's biosynthetic pathways resulting in a qualitative and quantitative modification of different metabolites production. Colonization by the AMF was followed by an enhanced production of PMs, including organic acids (involved in the energy pathways of the eukaryotic cell) and key amino acids, with the potential to act as precursors of other amino acids and as building blocks for the production of macromolecules. Furthermore, SMs production was significantly affected, especially the phenolic compounds and the oleanane-types glycosidic derived from the phenylpropanoid and mevalonate pathways, respectively. In total, 16 C_6-C_3 caffeic acid derivatives were induced mainly in the roots of M plants while 4 oleanane-types saponins were accumulated in the shoot parts. Besides the well-documented C_6-C_3 phenolics herein we noticed, for the first time, the production of two new derivatives of SA and one new derivative of RA, all presenting a common substitution pattern (methylation and hydroxylation) in the roots of M plants. Interestingly, upregulation of methylated compounds was underlined in AMF colonized plants, suggesting that these fungi have the potential to alter the plant biosynthetic pathways and to induce the production of different compounds. It will be of great interest to understand the molecular mechanisms behind the accumulation of specific compounds in the presence of AMF and how this could potentially be translated in increasing the production of specific compounds, which were valuable for human purposes.

Acknowledgments

The authors are thankful to Rebecca Marion from the Statistical Methodology and Computing Service/Louvain Institute of Data Analysis and Modelling in Economics and Statistics (SMCS/LIDAM, UCLouvain) for statistical support.

Chapter II

The metabolic profile of *Anchusa officinalis* L. differs according to its associated arbuscular mycorrhizal fungi

Adapted from the research article published in:

***Metabolites*, 12, 573 (2022)**

doi: 10.3390/metabo12070573

Evangelia Tsiokanos, Annalisa Cartabia, Nikolaos Tsafantakis, Ismahen Lalaymia, Aikaterini Termentzi, Maria Miguel, Stéphane Declerck and Nikolas Fokialakis

Preface

In Chapter I, the effects of a single AMF strain (i.e., *R. irregularis* MUCL 41833) on the metabolism of *A. officinalis* plants were investigated. Up and downregulated PMs and SMs were detected. Specifically, an enhanced production of PMs, including organic acids and amino acids, and SMs, in particular phenolic compounds and oleanane-types glycosidic derived from the phenylpropanoid and mevalonate pathways, respectively, were described. Additionally, two new salvianolic acid B derivatives and one new rosmarinic acid derivative were identified in mycorrhized roots.

However, a number of studies on other medicinal plants and crops have reported that plant-microbe interaction outcomes (e.g., PMs and SMs regulation) are highly dependent on the identity of the applied AMF symbiont. Therefore, the objective of Chapter II was to evaluate the effects of different AMF strains on the production of PMs and SMs in *A. officinalis* shoot and root tissues. Four species of AMF, belonging to the genus *Rhizophagus* (*R. irregularis* MUCL 41833, *R. intraradices* MUCL 49410, *R. clarus* MUCL 46238, *R. aggregatus* MUCL 49408) were considered and the same controlled conditions (i.e., semi-hydroponic cultivation system) and untargeted metabolomics analysis, as in Chapter I, were applied.

Abstract

Anchusa officinalis (L.) interacts with various microorganisms including arbuscular mycorrhizal fungi (AMF). Recently, the AMF *Rhizophagus irregularis* MUCL 41833 has been shown to modulate the metabolome of *A. officinalis*. However, little information is available on the impact that different AMF species may have on primary and secondary plant metabolites. In this study, four AMF species belonging to the genus *Rhizophagus* (*R. irregularis* MUCL 41833, *R. intraradices* MUCL 49410, *R. clarus* MUCL 46238, *R. aggregatus* MUCL 49408), were evaluated for their potential to modulate *A. officinalis* metabolome under controlled semi-hydroponic cultivation conditions. An untargeted metabolomic analysis was performed using UHPLC-HRMS followed by a multivariate data analysis. Forty-two compounds were reported to be highly modulated in relation to the different AMF associations. Among them, six new secondary metabolites were tentatively identified including two acetyl- and four malonyl-phenylpropanoid and saponin derivatives, all presenting a common substitution at position C-6 of the glycosidic moiety. In addition, an enhanced accumulation of primary and secondary metabolites was observed for *R. irregularis* and *R. intraradices*, showing a stronger effect on *A. officinalis* metabolome compared to *R. clarus* and *R. aggregatus*. Therefore, our data suggest that different AMF species may specifically modulate *A. officinalis* metabolite production.

Keywords

Arbuscular mycorrhizal fungi; *Anchusa officinalis* (L.); circulatory semi-hydroponic cultivation system; metabolomics; primary and secondary metabolites

Introduction

The interactions between plants and beneficial microorganisms improve not only growth and health, but also modify the metabolome considerably (Kilam *et al.*, 2017; Kaur and Suseela, 2020). Among these microorganisms, arbuscular mycorrhizal fungi (AMF) are known for their intimate symbiotic relationship with circa 72% of land plants (Brundrett and Tedersoo, 2018). They facilitate phosphorus and nitrogen uptake in exchange for carbohydrates and lipids (Smith *et al.*, 2011; Chen *et al.*, 2018), offer enhanced resistance to pests and diseases, drought and salinity, and are involved in the heavy metal detoxification process (Begum *et al.*, 2019).

An increasing number of studies [reviewed extensively by Zeng *et al.* (2013) and by Kaur and Suseela (2020)] have reported the impact of AMF on the production of primary and secondary metabolites in different plant species, including crops. For instance, a higher accumulation of amino acids, fatty acids, isoflavonoids and phenylpropanoid derivatives was reported in roots of *M. truncatula* colonized by *Rhizophagus irregularis* (Schliemann *et al.*, 2008). Similarly, a significant upregulation of SMs belonging mainly to blumenol derivates and pyrrolizidine alkaloids, was detected in the roots of *Senecio jacobaea* associated with *R. irregularis* (Hill *et al.*, 2018). Not necessarily all plant-AMF associations result in increased metabolite production. The productivity of the host plant - i.e., the outcome of the plant-microbe interaction - is highly dependent on the identity of the AMF symbiont Kaur and Suseela (2020). Indeed, different AMF species can differently affect the production of specific phytochemicals on a specific plant species. For instance, Rivero *et al.* (2015) reported that, although the metabolic pathways of *S. lycopersicum* altered by mycorrhizal symbiosis were common for both *Funneliformis mosseae* and *R. irregularis*, the compound's biosynthesis was altered depending on the particular AMF species involved. Jasmonic acid (JA), methyl-JA and JA-Isoleucine conjugates were accumulated in significantly higher amounts only in the plants associated with *F. mosseae*. This suggests that specific AMFs have a fine-tuned regulation role in biosynthetic pathways.

Besides the increasing interest in plant-AMF associations, those studies applying a metabolomic approach were limited to only two AMF species, *R. irregularis* (formerly *Glomus intraradices*) and *F. mosseae* (formerly *Glomus mosseae*) (Schwiger *et al.*, 2014; Rivero *et*

al., 2015; Hill *et al.*, 2018; Bernardo *et al.*, 2019). In Chapter I (Cartabia *et al.*, 2021), the effects of *R. irregularis* MUCL 41833 on shoots and roots of *A. officinalis*, growing under a semi-hydroponic cultivation system for a period of 9 days, were described. The untargeted metabolomic approach showed an upregulation of 36 PMs and SMs (e.g., organic acids, phenolic compounds, oleanane-types glycosides) in mycorrhized plants as compared to the non-mycorrhized ones.

Interestingly, *A. officinalis* is always found associated with AMF in the wild (Zubek *et al.*, 2011). Thus, considering non-mycorrhized plants as control does not truly reflect the natural conditions. Therefore, in the present study, a metabolomic analysis of roots and shoots of *A. officinalis* associated with four different AMF species belonging to the same genus (*R. irregularis* MUCL 41833, *R. intraradices* MUCL 49410, *R. clarus* MUCL 46238 and *R. aggregatus* MUCL 49408) was conducted to test the hypothesis that different AMF strains impact the plant metabolome differently. *Rhizophagus irregularis* MUCL 41833 was chosen as the reference strain since it is considered as a model organism in AMF research and the most used AMF strain in commercial inoculants (Rivero *et al.*, 2015; Giovannini *et al.*, 2020). It is a generalist colonizer, present in almost all soils and climatic zones (Giovannini *et al.*, 2020), readily grown *in vitro* on root organs (Declerck *et al.*, 2005), and its whole genome sequence has been published recently (Tisserant *et al.*, 2013; Zhang *et al.*, 2017). Moreover, its effects on the metabolome of *A. officinalis* were recently published and described as reported in Chapter I.

To test our hypothesis, the plants were grown for 9 days in the semi-hydroponic cultivation system described above and a similar ultrahigh-performance liquid chromatography high-resolution mass spectrometry (UHPLC-HRMS) analysis was performed. An untargeted metabolomics approach was further conducted to shed light on the overall effects of the different AMF species on *A. officinalis* root and shoot parts.

Material and methods

Chemicals

Same chemicals applied in Chapter I.

Biological material

Same methods for the germination and growth of *A. officinalis* plants were adopted as described in Chapter I.

The four AMF species were similarly supplied by the GINCO. Apart from *R. irregularis*, *Rhizophagus intraradices* (N.C. Schenck & G.S. Sm.) C. Walker & Schuessler) MUCL 49410, *Rhizophagus clarus* (T.H. Nicolson & N.C. Schenck) C. Walker & A. Schüßler) MUCL 46238 and *Rhizophagus aggregatus* (N.C. Schenck & G.S. Sm.) C. Walker MUCL 49408 were applied in this study and proliferated on plants of *Zea mays* as described in the thesis' Material and Methods.

Anchusa officinalis colonization

Similar approach as in Chapter I was applied for the colonization of *A. officinalis* plants. Briefly, two-week-old plants were transferred in 10 L pots containing a sterilized (121°C for 15 min) mix of lava and perlite (w/w, 2:1). The substrate was then half mixed with the AMF-inoculum substrate (final-ratio lava:perlite w/w, 5:1).

Experimental setup

Two-month-old plants (7 replicates per AMF treatment) were gently removed from the 10 L pots above and their root systems were rinsed with deionized water to eliminate lava and perlite debris. They were subsequently transferred to the S-H cultivation system as previously detailed (**Figure 29**). The containers were maintained in the greenhouse set at the same conditions as described in Chapter I. After the acclimatization and initial flushing phases, regular circulation was initiated and maintained at 7.5 mL min^{-1} for 42 h (T1).

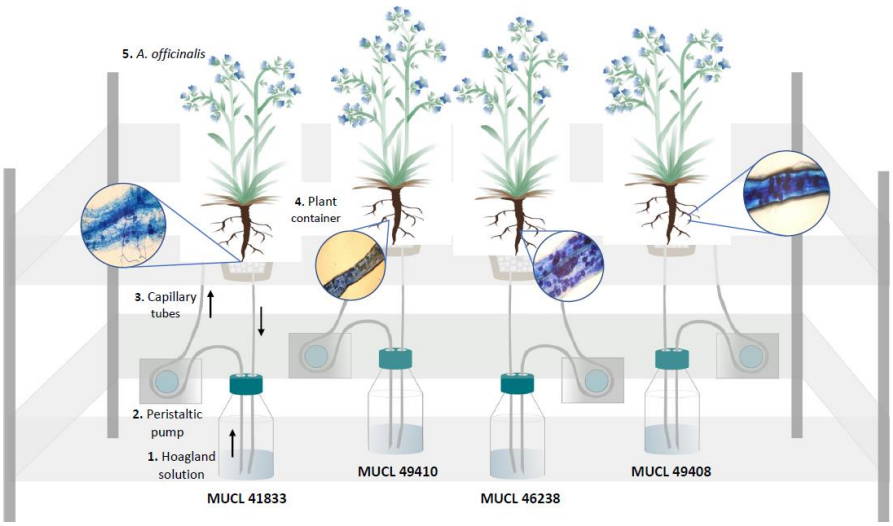

Figure 29. Schematic representation of the circulatory S-H cultivation system. The Hoagland solution circulated through the containers supporting *A. officinalis* plants associated with four different AMF species (*R. irregularis* MUCL 41833; *R. intraradices* MUCL 49410; *R. clarus* MUCL 46238; *R. aggregatus* MUCL 49408). The nutrient solution in the glass bottle **(1)** is pumped using a peristaltic pump **(2)** *via* silicon tubes **(3)** to the upper part of the plant container **(4)** containing *A. officinalis* plants **(5)**. The solution percolates through the plant container back into the glass bottle. The black arrows indicate the flow direction of the nutrient solution in the tubing. The roots-stained images represent the plant-AMF colonization of the four different AMF species applied in this study.

Plant harvest and AMF roots colonization

Total fresh weight (TFW), as well as root colonization, were assessed on the same 7 replicates per AMF treatment at the start (T0) and end of the experiment (T1). The root colonization was evaluated by McGonigle *et al.* (1990) on one-third of the root system (i.e., 1/6 of the root system at T0 and 1/6 at T1), as previously described.

At the end of the circulation above (T1), the plants were harvested to proceed with PMs and SMs analysis on the other two-thirds of the root system.

Analysis of PMs and SMs in roots and shoots of *A. officinalis*

Samples preparation

The remaining two-thirds of the root systems, as well as the shoot parts of each plant, were prepared for UHPLC-HRMS analysis as described in Chapter I (Cartabia *et al.*, 2021).

UHPLC-HRMS analysis and untargeted metabolomics data processing

UHPLC-HRMS analysis and MS/MS data processing of root and shoot samples of the plants associated with *R. irregularis* MUCL 41833, *R. intraradices* MUCL 49410, *R. clarus* MUCL 46238 and *R. aggregatus* MUCL 49408 were processed as explained in Chapter I, with some minor modifications. The data acquisition was performed on the HRMS/MS Orbitrap Q-Exactive platform in the full scan ion mode with a mass range of 100-1,200 Da. The HRMS data were collected in positive and negative ESI ionisation modes applying a resolution of 70,000 on a centroid mode. The conditions for the HRMS ionisation modes were the same as the one described in Chapter I. The HRMS/MS spectra were recorded for the three most intense ion peaks with a threshold of a 10-s dynamic exclusion at a resolution of 35,000. The stepped normalized collision energy was set at 40, 60, and 100. A Hypersil Gold UPLC C18 (2.1x100 mm, 1.9 μm) reverse phase column was used for the separations and the mobile phase consisted of solvents: A ultra-pure H_2O 0.1% (v/v) FA and B ACN. A 16 min gradient method for the elution of compounds was set up as follows: T = 0 min, 5% B; T = 1, 5% B; T = 11 min, 95% B; T = 14 min, 95% B (column cleaning); T: 14.1 min, 4% B; T = 14.6 min, 5% B; T = 16 min, 5% B (column equilibration). The flow rate applied for the analyses was 0.260 mL min^{-1} and the injection volume 5 μ. The column temperature was kept at 40°C while the sample tray temperature was set at 10°C.

In the following steps, an untargeted metabolomics workflow, including the normalization of the dataset (deconvolution, deisotoping, RT alignment and gap-filling procedures), was developed for the detection of known and unknown compounds. All the raw data obtained from the high-resolution metabolomic profiling were uploaded in Compound Discoverer 3.2.0.421 software. Briefly, the peak alignment of the selected spectra was performed from 1 to 12 min with a mass tolerance of 5 ppm and a maximum shift of 2 min. The spectrum properties applied for the peak picking and detection of compounds were the following: S/N > 3, min. peak intensity of 7.5 x 10^5 and MT < 5 ppm, and the integration of selected adducts ions for ESI^- ionisation ($[2M+FA-H]^{-1}$; $[2M-H]^{-1}$, $[M+FA-H]^{-1}$, $[M-H]^{-1}$; $[M-H_2O]^{-1}$). Finally, the grouping of compounds was performed with an MT < 5 ppm and an RT tolerance of 0.5 min.

The structural elucidation of the metabolites of interest was performed by comparison of the chromatographic and spectrometric

features of each respective peak with data from the literature. The high resolving power for both full scan experiments and the MS/MS fragments of the Q-Exactive Orbitrap analyser in correlation to the accurate mass measurements assured the identification of the very important variables (VIP) compounds with high confidence. The suggested EC (Elemental Composition) for molecular ions and MS/MS fragments, as well as the respective RDBeq (Ring Double Bond Equivalents) further assisted the safe identification process. More prediction of compounds was performed by comparing data with in-house and online libraries, and fragment ions were correlated with spectra online databases. The pre-processed data of ESI^- ionisation were exported as a .csv file to a Microsoft Excel spreadsheet and manipulated accordingly for the data filtering and the multivariate statistical analysis followed.

Statistical analysis

Arbuscular mycorrhizal fungi colonization parameters (TC% and AC%) were subjected to a mixed model for repeated measurements fit by restricted maximum likelihood estimation. The normal distribution of residuals was checked for each dependent variable. The model took into account the heterogeneity of the variance (only for TC%) modelling the within-group errors variance structure with the "varIdent" matrix and assuming the different AMF treatments as a stratification variable (Pinheiro and Bates, 2000). Moreover, the repeated measurements (i.e., two sampling times conducted on the same replicates) were modelled through an autoregressive correlation structure of order 1 ("corAR1") for all the dependent variables (TC% and AC%). An analysis of variance (ANOVA) test of the model was provided and the interaction between "time" (T0 and T1) and "treatments" (*R. irregularis*, *R. intraradices*, *R. clarus* and *R. aggregatus*) was checked as well as the significance of every single factor separately. A pairwise multiple comparison test (with the Bonferroni correction) was computed to separate means ($p < 0.05$). Similarly, the total fresh weight of the plants was subjected (as a dependent variable) to the same mixed model as described above. Normal distribution of residuals and homogeneity of variance was checked. The model took into account the repeated measurements (i.e., two sampling times conducted on the same replicates) through an

autoregressive correlation structure of order 1 ("corAR1"). Data analyses were performed by R using the "nlme" package.

Multivariate analyses of HRMS data were carried out using SIMCA 14.1 software (Soft Independent Modelling of Class Analogy) to assign the discriminant metabolic changes between the different AMF treatments after 9 days of the experiment. The interpretation of imported data was performed through PCA and PLS-DA according to Pareto correlation. In addition, a permutation test with n = 100 was performed to exclude any overfitting of the aforementioned PLS-DA models (**Supplementary Figures 1-4**, Annex II). Volcano-plot analyses were carried out using Compound Discoverer 3.2.0.421 on the basis of filtering criteria such as $p < 0.05$ and fold change > 1.5, while the graphical representation (bar charts) of discriminant variables (targeted compounds) were generated with GraphPad Prism 7 (GraphPad Software, San Diego, CA, USA). One-way ANOVA and Tukey's test were provided in order to reveal significant differences ($p < 0.05$) in the discriminant metabolites between the four AMF treatments. Data analyses were performed by R (R Core Team, 2018) using "ggplots 2" and "agricolae" packages. Finally, the identification and matching of discriminant variables were performed by comparing the MS and MS/MS spectra with bibliographic data as well as with commercial and in-house libraries.

Results

Root colonization by AMF and plant total fresh weight

Intraradical AMF structures were assessed in *A. officinalis* plants treated with four different AMF species (*R. irregularis*, *R. intraradices*, *R. aggregatus* and *R. clarus*) both at the plants' transfer in the containers (T0) and at the end of the experiment (i.e., after 9 days of growth in the system-T1). The overall data for AMF colonization and the total fresh weight (TFW, e.g., the sum of roots and shoots) at the two sampling times are reported in **Supplementary Table 1**, Annex II. To correctly analyse the data, a mixed model for repeated measurements was conducted. For the AMF total colonization (TC%), no significant interaction ($p = 0.0853$) was found between "treatments" and "time", while a significant effect ($p < 0.001$) was noticed for both single factors. The pairwise multiple comparison test revealed a general significant decrease in TC% (i.e., averaged of the four AMF treatments)

between T0 and T1 (data not shown). A significantly lower TC % (i.e., average of the two sampling times for each AMF treatment) was also observed in plants associated with *R. irregularis* as compared to *R. intraradices*, while the plants associated with *R. clarus* and *R. aggregatus* had intermediate values (**Table 7**). Similarly, for the percentage of arbuscules (AC%), no significant interaction ($p = 0.7479$) was found between "treatments" and "time", while a significant effect ($p < 0.001$) was noticed only for the single factor "time". The pairwise multiple comparison test revealed a general decrease in AC% (i.e., average of the four AMF treatments) between T0 and T1 (data not shown).

The total fresh weight was measured on the same plants associated with the four AMF species at T0 and T1. No significant effect ($p = 0.5699$) was reported between "treatments" and "time", or for the single factors ($p = 0.3570$ and $p = 0.0897$, respectively) (**Table 7**).

Table 7. AMF-root colonization (TC% and AC%) and total fresh weight (TFW) averaged between the two-time samplings (T0 and T1) of *A. officinalis* associated with each AMF species (*R. irregularis*, *R. intraradices*, *R. clarus* and *R. aggregatus*) and growing for 9 days in the S-H cultivation system.

AMF treatments	AMF-root colonization (%)		Total Fresh Weight (g)
	TC	AC	TFW
R. irregularis (MUCL 41833)	70 ± 2 a	10 ± 3 a	5.68 ± 1.5 a
R. intraradices (MUCL 49410)	81 ± 2 b	17 ± 3 a	8.22 ± 1.5 a
R. clarus (MUCL 46238)	74 ± 2 ab	12 ± 3 a	5.13 ± 1.5 a
R. aggregatus (MUCL 49408)	77 ± 2 ab	14 ± 3 a	8.06 ± 1.5 a

The parameters measured are expressed as mean ± standard errors (SE) of 14 replicates per each AMF treatment. The AMF treatment means followed by the same lowercase letters are not significantly different according to Bonferroni post-hoc test ($p < 0.05$).

Metabolic profiles and metabolomic analysis of *A. officinalis* plants

Metabolic profiles of root and shoot samples of plants associated with four different AMF species were analysed using multivariate analyses. The results of the unsupervised principal component analyses (PCA) highlighted the presence of two major and distinguished clusters (*R. irregularis*/*R. intraradices* on one side and *R. clarus*/*R. aggregatus* on the other side) in both the root and shoot samples (**Figure 30 a-b**). Shoot samples showed a higher proximity of individuals in cluster 2 (*R. clarus*/*R. aggregatus*) as compared to the corresponding root samples,

which were more widespread in the model. Both root and shoot parts of the plants showed an outlier in cluster 1, in *R. irregularis* and *R. intraradices* treatments, respectively, and were subsequently removed from the analysis.

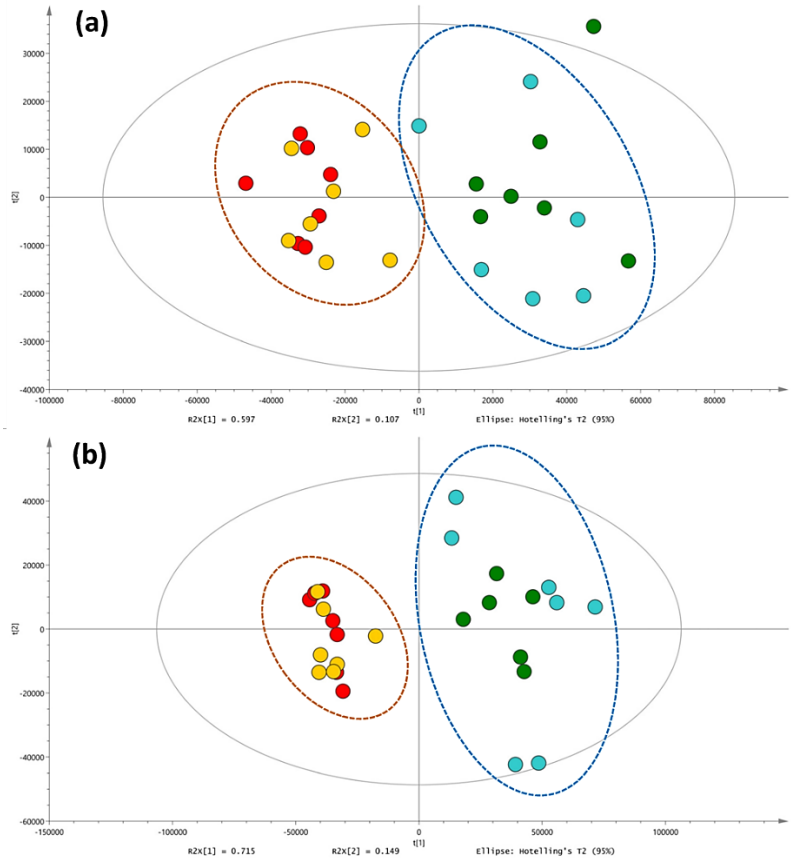

Figure 30. Principal component analysis (PCA) - Comparison of UHPLC-HRMS metabolic profiles from *A. officinalis* root (**a**) and shoot (**b**) samples associated with *R. irregularis*, *R. intraradices*, *R. clarus* and *R. aggregatus*, after 9 days of growth in the S-H cultivation system (*R. irregularis* MUCL 41833: blue dots; *R. intraradices* MUCL 49410: green dots; *R. clarus* MUCL 46238: red dots; *R. aggregatus* MUCL 49408: yellow dots).

The UHPLC-HRMS metabolic analysis of root and shoot samples associated with the four AMF species gave, in total, 201 and 265 different mass signals, respectively, during the peak picking process. Based on the Volcano-plot analysis performed, only 96 and 101 compounds passed the defined criteria ($p < 0.05$ and fold change > 1.5) in all the possible AMF combinations tested (**Figures 31-32**). No

differentiation was observed in treated root and shoot samples belonging to the same PCA cluster. However, significant up and downregulation of mass signals were highlighted when comparing *R. irregularis* and *R. intraradices* treatments, from cluster 1 to *R. clarus* and *R. aggregatus* treatments from cluster 2 (**Figures 31-32**). Among root and shoot samples, 22 and 35 mass signals, respectively, showed significant differences in all possible AMF-plants combinations between the two generated clusters. Thus, special attention was given and a detailed dereplication process was followed.

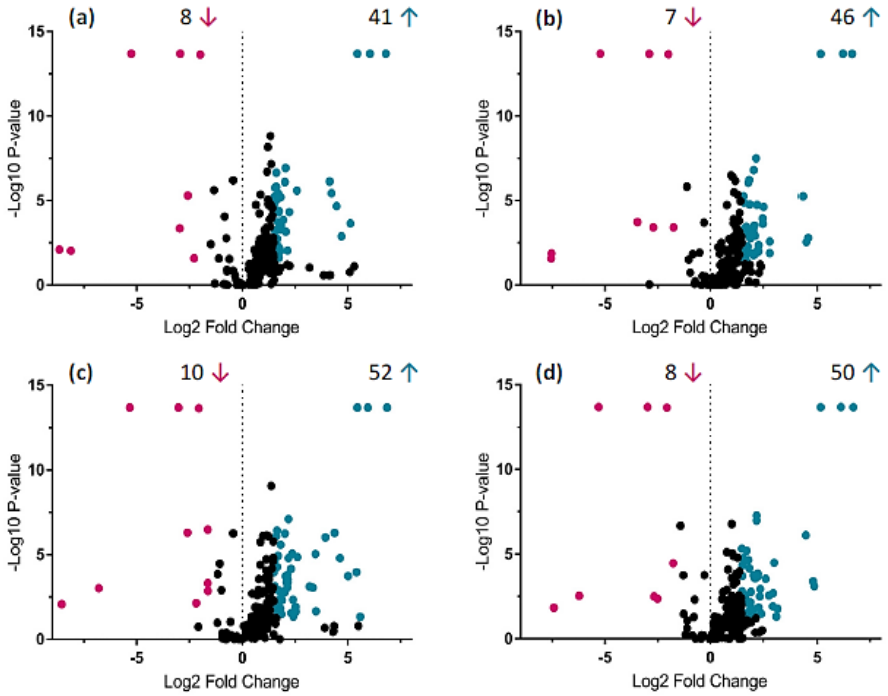

Figure 31. Volcano-plot analysis - Identification of up and downregulated compounds ($p < 0.05$ and fold change > 1.5) between *A. officinalis* root samples associated with the four AMF species (*R. irregularis* MUCL 41883, *R. intraradices* MUCL 49410, *R. clarus* MUCL 46238 and *R. aggregatus* MUCL 49408) after 9 days of growth in the S-H cultivation system. Comparison of metabolic profiles from root samples associated with **(a)** *R. irregularis* MUCL 41833 and *R. clarus* MUCL 46238; **(b)** *R. irregularis* MUCL 41833 and *R. aggregatus* MUCL 49408; **(c)** *R. intraradices* MUCL 49410 and *R. clarus* MUCL 46238; **(d)** *R. intraradices* MUCL 49410 and *R. aggregatus* MUCL 49408. Significant upregulated compounds are represented in blue (right side of the plots) and downregulated in magenta (left side of the plots). Blue and magenta arrows represent the amount of up and downregulated compounds, respectively, in specific AMF-plants treatment.

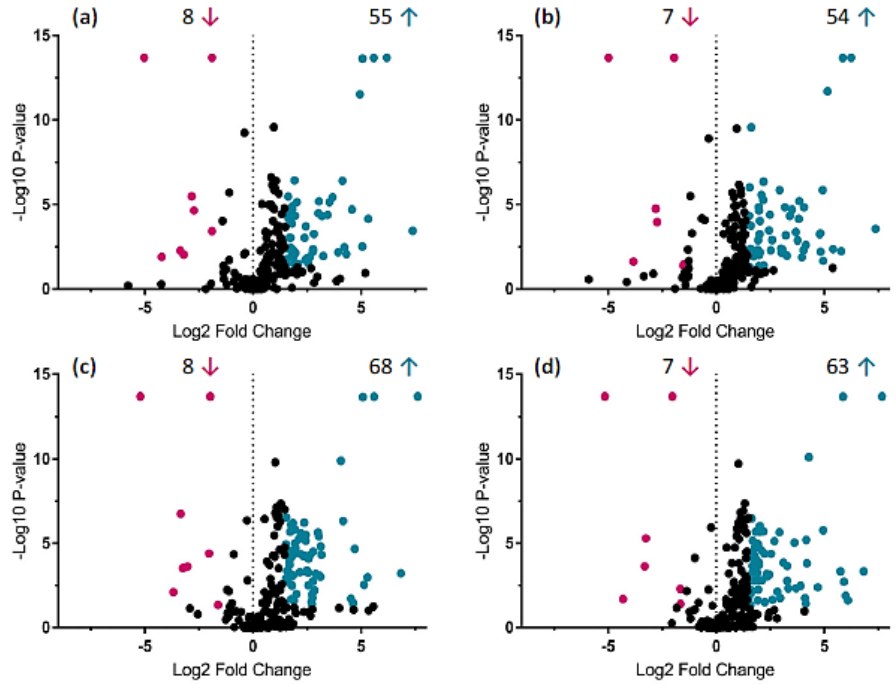

Figure 32. Volcano-plot analysis - Identification of up and downregulated compounds ($p < 0.05$ and fold change > 1.5) between *A. officinalis* shoot samples associated with the four AMF species (*R. irregularis* MUCL 41883, *R. intraradices* MUCL 49410, *R. clarus* MUCL 46238 and *R. aggregatus* MUCL 49408) after 9 days of growth in the S-H system. Comparison of metabolic profiles from shoot samples associated with **(a)** *R. irregularis* MUCL 41833 and *R. clarus* MUCL 46238; **(b)** *R. irregularis* MUCL 41833 and *R. aggregatus* MUCL 49408; **(c)** *R. intraradices* MUCL 49410 and *R. clarus* MUCL 46238; **(d)** *R. intraradices* MUCL 49410 and *R. aggregatus* MUCL 49408. Significant upregulated compounds are represented in blue (right side of the plots) and downregulated in magenta (left side of the plots). Blue and magenta arrows represent the amount of up and downregulated compounds, respectively, in specific AMF-plants treatment.

Identification of PMs and SMs affected by AMF

The dereplication process of root and shoot extracts obtained from *A. officinalis* plants associated with the four different AMF species highlighted 42 differently modulated PMs and SMs, strictly related to the specific AMF association. These modulated compounds were showed only in negative ESI ionisation mode, thus compounds from the positive mode were not reported.

As shown in **Table 8a**, six compounds were characterized as primary metabolites. Among them, compounds 1, 2, 3, 6 were tentatively identified as amino acids, while compounds 4 and 5 as organic acids. Compounds 3 and 4 (glutamic and threonic acids, respectively) were overall increased in the shoots of the AMF-treated plants. Indeed, in the *R. intraradices* treatment, a significant induction of compound 3 was noticed and, together with *R. irregularis* treatment, of compound 4 in the shoots. Similarly, compound 1 (glutamine) was upregulated in the roots associated with *R. irregularis* and *R. intraradices*. Among the common compounds, which were affected in both parts of the plant and felt within our selection criteria ($p < 0.05$ and fold change > 1.5), compounds 5 and 6 showed the highest increment in plants associated with *R. irregularis*. In particular, compound 6 showed a maximum fold change of 8.66x and 7.37x in roots and shoots, respectively, while regarding compound 5, the increment was slightly higher in the shoots (7.67x) as compared to the roots (6.85x). Conversely, compound 2 showed a 6.22x fold change in roots and a 5.87x fold change in shoots of *A. officinalis* associated with *R. intraradices*. Regarding the increment of compounds 1, 3 and 4, only those related to the roots, for compound 1 (1.7x fold change), and to the shoots, for compounds 3 and 4 (1.58x and 5.85x fold change, respectively) of the plants associated with *R. intraradices*, felt within our selection criteria ($p < 0.05$ and fold change > 1.5) (**Figure 33**).

The colonization of *A. officinalis* plants by the four different AMF species also impacted the secondary metabolites production in both parts of the plants (**Figures 33-34**) (**Table 8b**). Overall, thirty-six SMs were characterized, belonging to different chemical classes of natural products. The majority of the identified compounds were assigned to phenylpropanoid derivatives (20) and to glycosidic triterpenes (9, saponins), while a less pronounced impact was observed in other chemical classes such as benzoic acids (1), secoiridoids (1), coumarins (2) and imidazolidines (1) (compounds 7, 14, 18, 36, 41, 42).

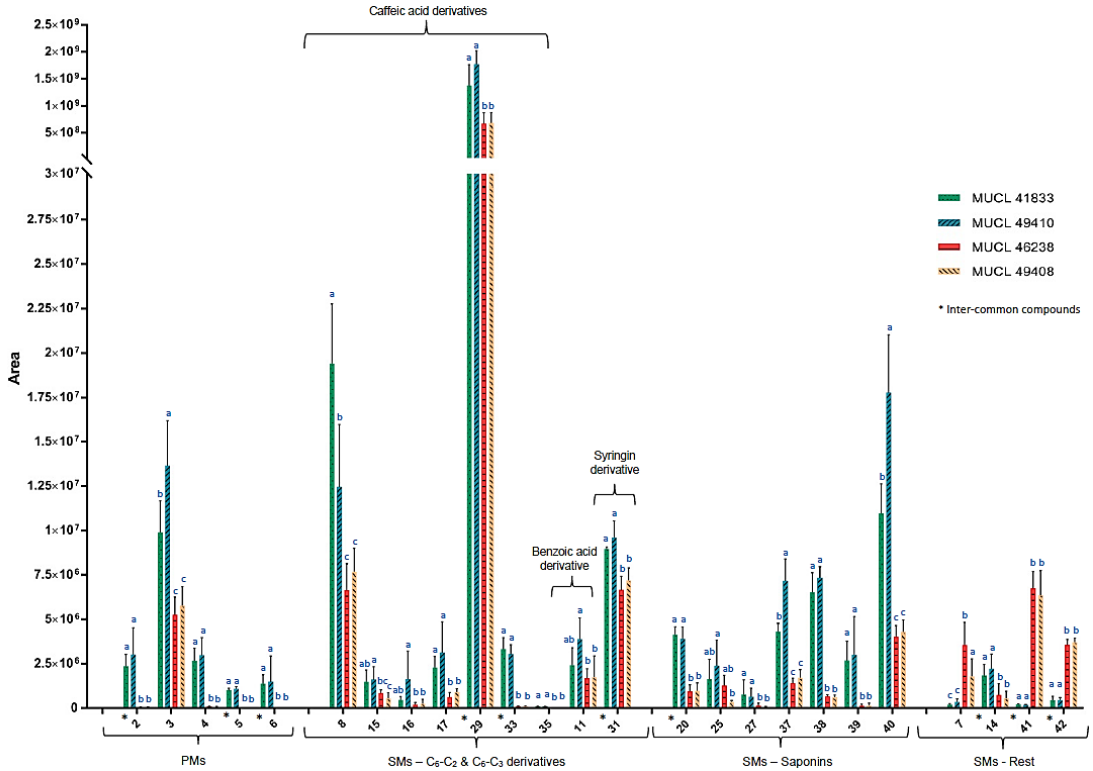

Figure 33. Graphical representation of metabolome profile variations in shoots of *A. officinalis* associated with four different AMF species (*R. irregularis* MUCL 41883, *R. intraradices* MUCL 49410, *R. clarus* MUCL 46238 and *R. aggregatus* MUCL 49408). The AMF treatment means followed by the same lowercase letters are not significantly different according to HSD Tukey's test ($p < 0.05$).

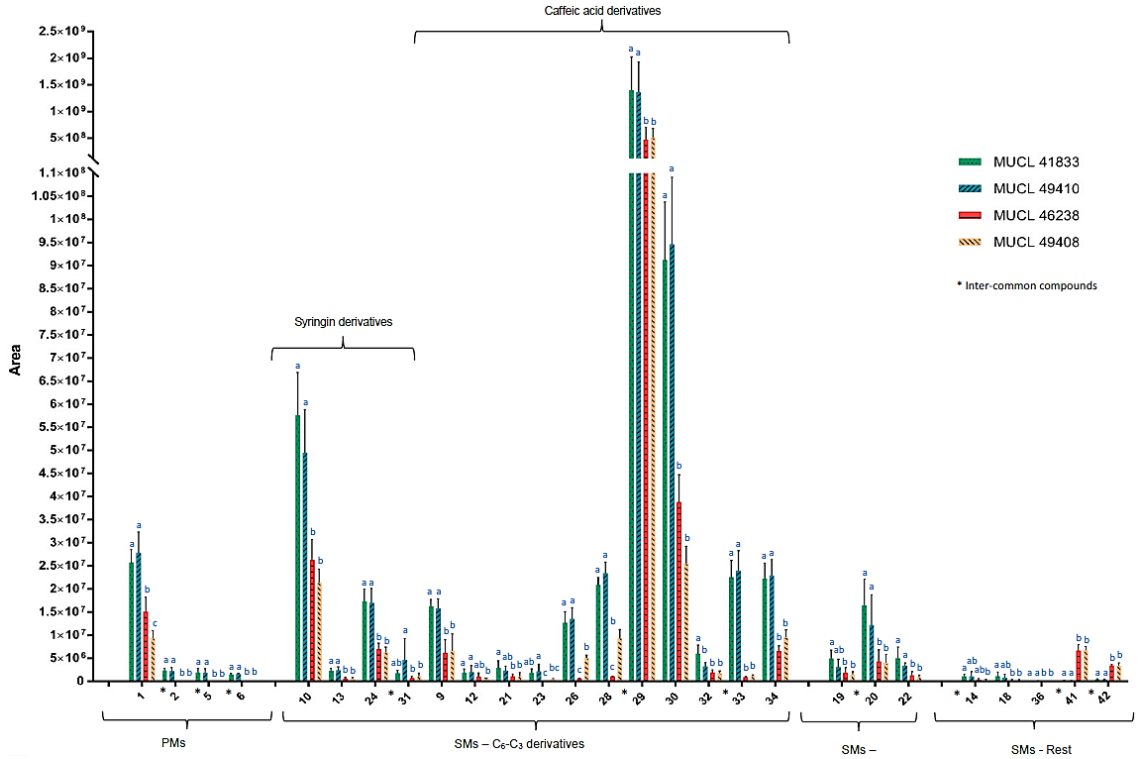

Figure 34. Graphical representation of metabolome profile variations in roots of *A. officinalis* associated with four different AMF species (*R. irregularis* MUCL 41883, *R. intraradices* MUCL 49410, *R. clarus* MUCL 46238 and *R. aggregatus* MUCL 49408). The AMF treatment means followed by the same lowercase letters are not significantly different according to HSD Tukey's test ($p < 0.05$).

Table 8. Affected primary **(a)** and secondary **(b)** metabolism in root and shoot samples of *A. officinalis* associated with *R. irregularis* MUCL 41833, *R. intraradices* MUCL 49410, *R. clarus* MUCL 46238 and *R. aggregatus* MUCL 49408 and growing for 9 days in the S-H cultivation system.

	Peak	Proposed phytochemicals	RT (min)	Precursor Ion - $[M-H]^-$	*m/z* calcd.	*Δ*m (ppm)	MS/MS Fragment ions (*m/z*)	Chemical formula	Affected in	Reference
(a) Primary metabolism	1	D-Glutamine	1.43	145.0620	146.0686	1.13	146, 128, 102	$C_5H_{10}N_2O_3$	R	Brieudes *et al.*, 2016
	2	L-Aspartic acid	1.44	132.0303	133.0370	0.67	132, 115, 88, 71	$C_4H_7NO_4$	S, R	Brieudes *et al.*, 2016
	3	L-Glutamic acid	1.46	146.0660	147.0530	0.75	146, 128, 102	$C_5H_9NO_4$	S	Brieudes *et al.*, 2016
	4	L-Threonic acid	1.51	135.0300	136.0366	1.06	135, 117, 89, 75, 61	$C_4H_8O_5$	S	Brieudes *et al.*, 2016
	5	DL-Malic acid	1.59	133.0144	134.0210	0.93	133, 115, 89, 72, 71	$C_4H_6O_5$	S, R	Li *et al.*, 2004
	6	DL-pyroglutamic acid	1.65	128.0355	129.0420	1.28	128, 82, 62	$C_5H_7NO_3$	S, R	Shi *et al.*, 2020
(b) Secondary metabolism	7	Allantoin	1.49	157.0359	158.0434	-1.56	114, 97, 71, 59	$C_4H_6N_4O_3$	S	Dresler *et al.*, 2017
	8	Danshensu	3.53	197.0451	198.0523	0.64	179, 153, 135, 121, 73	$C_9H_{10}O_5$	S	Liu *et al.*, 2007
	9	Glomeratose A	4.50	561.1837	562.1892	2.19	342, 240, 191, 163, 121, 59	$C_{24}H_{34}O_{15}$	R	Zhang *et al.*, 1998
	10	Methyl dihydrosinapic acid glucoside	4.90	401.1458	402.1520	1.15	208, 193, 175, 163, 121, 93, 71	$C_{18}H_{26}O_{10}$	R	Nomoto *et al.*, 2013
	11	Salicylic acid glucoside	4.94	299.0776	300.0840	1.50	137, 93	$C_{13}H_{16}O_8$	S	Abu-Reidah *et al.*, 2013

Continue in the next page…

Peak	Proposed phytochemicals	RT (min)	Precursor Ion - $[M-H]^-$	*m/z* calcd.	*Δ*m (ppm)	MS/MS Fragment ions (*m/z*)	Chemical formula	Affected in	Reference
12	Acetyl feruloylsucrose	5.05	559.1679	560.1736	2.16	193, 179, 161, 133	$C_{24}H_{32}O_{15}$	R	Cho *et al.*, 2015
13	Methyl syringinoside	5.22	547.2039	548.2100	1.26	219, 191, 176, 161, 121, 93, 71	$C_{24}H_{36}O_{14}$	R	Cartabia *et al.*, 2021
14	Barlerin	5.37	447.1514	448.1575	1.97	269, 161, 113, 101, 71	$C_{19}H_{28}O_{12}$	S, R	-
15	Dihydroferulic acid 4-*O*-glucuronide	5.78	371.0990	372.1051	1.67	179, 163, 121, 73	$C_{16}H_{20}O_{10}$	S	Pereira-Caro *et al.*, 2016
16	Yunnaneic acid D	5.79	539.1206	540.1262	1.82	297, 271, 197, 179, 161, 135, 109, 73	$C_{27}H_{24}O_{12}$	S	Abu-Reidah *et al.*, 2019
17	Lithospermic acid	5.81	537.1050	538.1106	2.11	339, 295, 269, 197, 179, 161, 135, 109, 73	$C_{27}H_{22}O_{12}$	S	Liu *et al.*, 2007
18	Isofraxidin	5.98	221.0457	222.0523	1.30	177, 161, 145, 133, 123, 108, 95, 85, 67	$C_{11}H_{10}O_5$	R	-
19	Anchusoside-9	6.07	827.4449	828.4502	1.8	665, 503, 161, 113, 85, 71	$C_{42}H_{68}O_{16}$	R	Romussi *et al.*, 1984
20	Bayogenin triglycoside	6.09	1001.4954	1002.5030	0.17	942, 797, 635	$C_{49}H_{78}O_{21}$	R	-
21	Rosmarinic acid glucoside	6.14	521.1311	522.1368	2.13	359, 197, 179, 161, 135, 123, 73	$C_{24}H_{26}O_{13}$	R	Barros *et al.*, 2013

(b) Secondary metabolism	22	Acetylanchusoside-9	6.22	869.4543	870.4608	0.33	707, 503, 161, 113, 85, 71	$C_{44}H_{70}O_{17}$	R	Romussi *et al.*, 1984
	23	SA derivative I	6.33	537.1049	538.1106	2.73	285, 185, 135, 109, 121	$C_{27}H_{22}O_{12}$	R	-
	24	Methyl syringin	6.40	385.1509	386.1571	1.57	207, 191, 176, 161, 121, 93, 71	$C_{18}H_{26}O_{9}$	S, R	Cartabia *et al.*, 2021
	25	Bayogenin diglycoside	6.42	839.4435	840.4502	1.00	633, 423, 161, 113, 85, 71	$C_{43}H_{68}O_{16}$	S	Bandara *et al.*, 1989
	26	Salvianolic acid (SA) A	6.48	493.1150	494.1207	2.11	295, 267, 197, 185, 169, 135, 109, 73	$C_{26}H_{22}O_{10}$	R	Sharma *et al.*, 2020
	27	Dihydroxybyogenin diglycoside	6.49	843.4406	844.4451	2.58	621, 459, 161, 113, 101, 71	$C_{42}H_{68}O_{17}$	S	Fu *et al.*, 2006
	28	SA derivative II	6.51	537.1046	538.1106	3.01	295, 185, 135, 109, 121	$C_{27}H_{22}O_{12}$	R	-
	29	Rosmarinic acid (RA)	6.53	359. 0779	360.0840	1.95	197, 179, 161, 135, 123, 73, 62	$C_{18}H_{16}O_{8}$	S, R	Kowalczyk *et al.*, 2018
	30	Salvianolic acid (SA) E	6.70	717.1478	718.1528	1.72	339, 321, 295, 185, 161, 135, 109, 73	$C_{36}H_{30}O_{16}$	R	Liu *et al.*, 2007
	31	Acetyl methyl syringin	6.75	427.1616	428.1677	0.59	384, 219, 208, 191, 176, 161, 121, 93, 73	$C_{20}H_{28}O_{10}$	R	-
	32	Clinopodic acid A	6.98	343.0829	344.0891	0.59	197, 179, 145, 135, 123, 117, 89, 73	$C_{18}H_{16}O_{7}$	R	-
	33	Dehydro SA B	7.10	715.1324	716.1372	2.70	339, 295, 185, 135, 109, 72	$C_{36}H_{28}O_{16}$	R	Liu *et al.*, 2007
	34	Dehydro RA	7.00	357.0622	358.0683	0.70	197, 179, 161, 133, 123, 73	$C_{18}H_{14}O_{8}$	R	Cartabia *et al.*, 2021
	35	Methyl RA	7.06	373.0935	374.0996	0.65	197, 179, 161, 135, 123, 73	$C_{19}H_{18}O_{8}$	S	Kowalczyk *et al.*, 2018
	36	Citrinin	7.75	249.0771	250.0836	0.22	205, 157, 143, 122, 104	$C_{13}H_{14}O_{5}$	R	Shi *et al.*, 2020

Continue in the next page…

Peak	Proposed phytochemicals	RT (min)	Precursor Ion - $[M-H]^-$	*m/z* calcd.	*Δ*m (ppm)	MS/MS Fragment ions (*m/z*)	Chemical formula	Affected in	Reference
37	Malonylanchusoside-2	8.15	1027.5135	1028.5187	1.38	779, 659, 617, 599, 455, 159, 129, 113, 101, 87	$C_{51}H_{80}O_{21}$	S	Lehbili *et al.*, 2017
38	Hydroxy Malonylanchusoside-7	8.30	1043.5081	1044.5136	2.21	795, 659, 617, 471, 159, 129, 113, 101, 87	$C_{51}H_{80}O_{22}$	S	-
39	Hydroxy dimalonylanchusoside 2/7	8.43	1129.5087	1130.5140	2.24	659, 471, 455, 159, 111, 101, 87	$C_{54}H_{82}O_{25}$	S	-
40	Malonylanchusoside-7	9.26	1027.5138	1028.5187	1.86	779, 659, 617, 599, 455, 161, 113, 101, 89	$C_{51}H_{80}O_{21}$	S	Romussi *et al.*, 1979
41	Gingerol	9.54	293.1662	294.1826	1.39	236, 221, 148, 127, 97, 72	$C_{17}H_{26}O_4$	S, R	Shi *et al.*, 2020
42	Embellin	10.07	293.1766	294.1826	2.51	249, 193, 177, 136, 97, 79	$C_{17}H_{26}O_4$	S, R	-

RT = Retention Time; *Δ*m= mass errors; $[M-H]^-$ = *m/z* of the pseudomolecular ion in negative ionisation mode respectively; *m/z* calcd= theoretical *m/z* value; R = roots; S = shoots

The phenolic C_6-C_3 derivatives represented the chemical group with the most important variation. In total, twenty phenylpropanoid derivatives were annotated. Fifteen of them were significantly increased in roots, nine in shoots, while three were affected in both roots and shoots (compounds 29, 31 and 33) (**Figures 33-34**). Compound 29 was equally affected in both parts, while compounds 31 and 33 showed a stronger accumulation in shoots and roots, respectively. In all cases, a higher impact was observed in the *R. irregularis* and *R. intraradices* treatments (**Figures 33-34**).

Among the C_6-C_3 derivatives, sixteen compounds were identified as mono-, di-, tri and tetrameric derivatives of caffeic acid (compounds 8, 9, 12, 15-17, 21, 23, 26, 28-30, 32-35) and four of them were found in the corresponding glycosidic form (compounds 9, 12, 15, 21). Besides the hydroxycinnamates, compounds 13, 24 and 31 were identified as derivatives of syringin and showed characteristic fragment ions at *m/z* 191, resulting from the cleavage of the glucose moiety, and fragment ions at *m/z* 176, 161, and 121 from the fragmentation of the remaining sinapyl alcohol (Cartabia *et al.*, 2021). In particular, compounds 13 and 24 were identified as the methyl derivatives of syringin and of syringinoside, already described in *A. officinalis* (Cartabia *et al.*, 2021). This was evident by the mass difference of 14 Da in their $[M-H]^-$ pseudomolecular ions and by their MS/MS fragmentation ions at *m/z* 208 and 219, suggesting the presence of an additional methyl group ($-CH_3$). Compound 31 showed a mass difference of 42 Da when compared to compound 24. Both compounds shared similar MS/MS fragment ions (208, 191, 176, 121) suggesting their structural similarities to syringin. An additional diagnostic fragment ion at *m/z* 384 suggested the presence of an additional acetyl group (CH_3CO) in the structure, which was assigned to the position C-6 of glucose moiety (**Table 9**). This leads to the identification of compound 31 as the acetyl derivative of compound 24 which represents a previously undescribed molecule in the literature. Compound 10 showed a mass difference of 30 Da with respect to syringin (sinapyl alcohol glucoside). The presence of an additional fragment at *m/z* 208, characteristic to a methyl ester group in the structure, and of the ion at *m/z* 193 allowed us to hypothesize the presence of a dihydrosinapic acid glucoside moiety. Further investigation of the MS/MS data and by comparison with bibliographic references (Nomoto *et al.*, 2013), compound 10 was identified as a glycosylated methyl ester derivative of dihydrosinapic acid.

Table 9. Chemical structure and fragmentation pattern of compound 19 and potential new compounds 22, 31, 37, 40 identified by ESI-HRMS and MS/MS analysis.

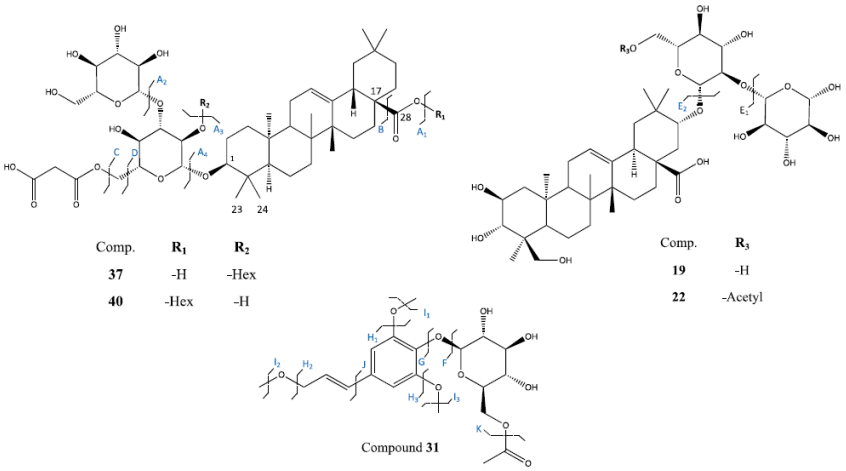

Comp	$[M-H]^-$	MS/MS (*m/z*)
19	827.4449	665 (E_1), 503 (E_2), 161, 113, 85, 71
22	869.4543	707 (E_1), 503 (E_2), 161, 113, 85, 71
31	427.1616	384 (K), 219 (F), 208 (G), 191(G/I), 176 (G/H), 161 (G/H/I), 121(G/I/J), 93, 73
37	1027.5135	779 (A/C), 659 (B/A_1/A_2), 617 (A_1/A_2/C), 599 (A_1/A_2/D), 455 (A_4), 159, 129, 113, 101, 87
40	1027.5138	779 (A/C), 659 (B/A_2/A_3), 617 (A_2/A_3/C), 599 (A_2/A_3/D), 455 (A_4), 159, 129, 113, 101, 87

Regarding the glycosidic saponins, the four AMF species associated with *A. officinalis* modulated the expression of four di-glycosides (compounds 19, 22, 25 and 27) and five tri-glycosides (compounds 20, 37-40) of oleanolic acid, mainly in the shoot of the plants (**Figure 33**). Indeed, six compounds were exclusively increased in the shoots (compounds 25, 27, 37, 38, 39, 40), while one was increased in both parts of the plants (compound 20). This accumulation was noticed in plants associated with *R. irregularis* and *R. intraradices*.

Saponins 19 and 22 showed a molecular ion at *m/z* 828.4502 and at *m/z* 870.4608, respectively. Compound 19 was already reported as the oleanolic acid diglycoside anchusoside-9 presenting the two characteristic MS/MS fragments at *m/z* 665 and 503 resulting from the

consecutive neutral loss of two glucose units (-162 Da and -324 Da). Further analysis of the MS/MS fragmentation pattern of compounds 19 and 22 showed common ions at *m/z* 503, 161, 113, 85, 71 corresponding to the aglycone hydroxybayogenin. Compound 22 presented the additional MS/MS fragment at *m/z* 707 resulting from the neutral loss of a hexose unit (-162 Da) and by the presence of an acetylated hexose unit esterified at the C-21 of hydroxybayogenin aglycone. These data lead to the tentative identification of compound 22 as the acetyl derivative of anchusoside-9 ($C_{44}H_{69}O_{17}$) (**Table 8b**). Compound 22 represents a previously undescribed molecule in the literature.

Compound 25 showed a pseudomolecular ion *m/z* 839.4435 $[M-H]^-$ and was tentatively annotated as a diglycoside derivative of bayogenin (Bandara *et al.*, 1989), while compound 20 showed a molecular ion at *m/z* 1001.4954 corresponding to the presence of an additional glycosidic unit in the structure (+162 Da) (**Table 8b**). The analysis of the MS/MS fragmentation pattern of both compounds showed a common fragment at *m/z* 633 corresponding to the cleavage of a glucuronic acid methyl ester, for compound 25, and of a disaccharide moiety, containing a glucuronic acid methyl ester moiety and of an additional hexose unit, regarding compound 20. Further, MS/MS fragments at *m/z* 797 and at *m/z* 633 for compounds 20 and 25, respectively, derived from the neutral loss of the esterified sugar moiety at C-17, confirmed this hypothesis.

The MS/MS spectra of compound 27 (*m/z* 843.4406 $[M-H]^-$) showed two major fragment ions at *m/z* 621 and 459 corresponding to the consecutive loss of a carboxyl unit at C-17 and of a glycosidic unit and a hydroxyl group (-222 Da) following a further cleavage of the second hexose (-162 Da). The above-mentioned fragments suggested the presence of two additional hydroxyl groups in the aglycone with respect to bayogenin and leads to the tentative identification of compound 27 as a diglycosidic derivative of dihydroxybayogenin (Fu *et al.*, 2006).

An increased production of compounds 37 to 40 was also noticed in shoots of *A. officinalis* associated with *R. irregularis* and *R. intraradices*. Both compounds, 37 and 40, showed a common molecular ion at *m/z* 1028.5187 and a common MS/MS fragmentation pattern, suggesting their structural similarity. Indeed, they both shared fragments at 779, 659, 617 and 455 (**Table 9**), characteristic of a tri-glycosylated configuration in both structures. In more detail, fragment

ion at *m/z* 779 was obtained from the neutral loss of a hexoside unit and of a malonyl at C-6′ position, while the diagnostic fragment MS/MS ions at *m/z* 617 corresponded to the cleavage of an additional hexose unit. Further loss of the third sugar moiety at position C-3 offered the MS/MS ion at *m/z* 455 corresponding to the aglycone oleanolic acid. The position of the malonyl unit was established based on the diagnostic MS/MS fragment at *m/z* 659, corresponding to the loss of two hexoses (-324 Da) and of a carboxyl unit at C-17 (-46 Da) (**Table 9**). Based on the above-mentioned HRMS/MS data and by comparison with previously reported data (Cartabia *et al.*, 2021; Romussi *et al.*, 1979), compounds 37 and 40 were tentatively assigned as isomers of anchusoside-2 and anchusoside-7. Compounds 37 and 40 presented a retention time of 8.15 and 9.26 min. Based on their calculated ClogP values of 5.15 and 4.67 for compounds 37 and 40, respectively, the peak at 8.15 min was tentatively identified as the malonyl derivative of anchusoside-2 (compound 37) (Jiang *et al.*, 2020), while the peak at 9.26 min as the malonyl derivative of anchusoside-7 (compound 40). Both malonyl saponins represent previously undescribed molecules in the literature.

Compound 38 presented a molecular ion at *m/z* 1043.5081 and a chemical formula of $C_{51}H_{80}O_{22}$. The HRMS/MS fragmentation pattern showed prominent characteristic ions at *m/z* 795, 659, 617 and 471, suggesting the similarity with compounds 37 and 40. The mass difference of 17 Da with respect to compounds 37 and 40 suggested the presence of a hydroxylated oleanolic type aglycone in the structure, which was confirmed by the presence of the fragment ion *m/z* at 471 as well as of the fragment at *m/z* 795 generated by cleavage of one malonyl unit and of one hexoside. Accordingly, compound 38 was assigned as the hydroxyl malonyl derivative of anchusoside-7. Compound 39 showed a pseudomolecular ion at *m/z* 1129.5087 $[M\text{-}H]^-$ and the diagnostic MS/MS fragments at *m/z* 659, 471 and 455. The mass difference of 86 Da with respect to compound 38 was attributed to the presence of an additional malonyl moiety leading to its tentative identification as the hydroxy di-malonyl derivative of anchusoside-2/7. Both compounds 38 and 39 represent previously undescribed molecules in the literature.

Discussion

The association between plants and arbuscular mycorrhizal fungi (AMF) is one of the most widespread symbioses (Chen *et al.*, 2018). These fungi provide numerous benefits to the host plants, especially in terms of nutritional assistance and resistance to a/biotic stresses (Chen *et al.*, 2018; Basiru *et al.*, 2020). A growing body of studies has reported the beneficial effects of these root symbionts on the modulation of specific biosynthetic pathways increasing/modifying the production of PMs and SMs (Schlieman *et al.*, 2008; Hill *et al.*, 2018; Kaur and Suseela, 2020; Cartabia *et al.*, 2021).

Herein, an untargeted metabolomic study on several AMF species belonging to the same genus was conducted under the highly-controlled S-H cultivation system developed by Cartabia *et al.* (2021), to evaluate the effects of four different AMF species (*R. irregularis*, *R. intraradices*, *R. clarus* and *R. aggregatus*) on the metabolome of *A. officinalis*.

During the experimental period, the root colonization was high for the four AMF species, even if a general significant decrease was noticed after 9 days of growth in the S-H cultivation system (i.e., total colonization means value varying between 85% at T0 to 66% at T1, and the percentage of arbuscules above 10% and close to 10% at T0 and T1, respectively).

Impact of AMF species on PMs and SMs in roots and shoots of *A. officinalis*

The major impact of AMF on *A. officinalis* metabolome was detected in the primary metabolism, mainly in the amino acid and organic acid content (compounds 1-6), but also in some specific secondary metabolites, derived from the phenylpropanoid (compounds 8-10, 12, 13, 15-17, 19, 21, 23, 24, 26, 28, 29-35) and the mevalonate (compounds 19, 20, 22, 25, 27, 37-40) pathways. The untargeted metabolomic approach performed on root and shoot tissues of *A. officinalis* evidenced forty-two compounds that fulfilled the defined threshold ($p < 0.05$ and fold change > 1.5) applied in the Volcano-plot analysis in at least one of the associations between the AMF species and *A. officinalis*.

Impact on primary metabolism

Six primary metabolites (compounds 1-6) were significantly affected in root and shoot samples in relation to the four AMF species. While compound 1 (glutamine) was produced in significantly higher amounts in the roots, compounds 2-6 were mainly accumulated in the shoots. All compounds (1-6) showed a similar accumulation increment in plants associated with *R. irregularis* and *R. intraradices* (cluster 1). *Rhizophagus irregularis* and, especially, *R. intraradices* are strong elicitors of amino acids, such as aspartic (compound 2), glutamic acid (compound 3), glutamine (compound 1) and its derivative, pyroglutamic acid (compound 6), as well as of organic acids, such as threonic acid (compound 4) and malic acid (compound 5), as compared to *R. clarus* and *R. aggregatus*. Based on these results, *R. clarus* and *R. aggregatus*, belonging to cluster 2, affect the primary metabolism less than the two other AMF strains belonging to cluster 1 (**Figure 30**).

Among the PMs, compounds 2 and 3 have been reported as N precursors and donors, reflecting the AMF's ability to enhance ammonium assimilation in mycorrhized plants by the GS/GOGAT enzymatic pathway (Xie *et al.*, 2021). Together with compound 5, they are also important intermediate of the TCA, and they act as precursors for the synthesis of key amino acids, such as asparagine, threonine, lysine, isoleucine and glutamine (compound 1), which are building blocks for the production of macromolecules (Cartabia *et al.*, 2021; Xie *et al.*, 2021). Pyroglutamic acid (compound 6), reported as the lactam of glutamic acid, is considered an important reservoir of glutamate (Jiménez-Arias *et al.*, 2019), while compound 4 (threonic acid) is linked to ascorbic acid metabolism and catabolism involved in anti-oxidant activities and correlated to the well-maintaining of plant fitness (Canellas *et al.*, 2019). Threonic acid was already mentioned in previous studies as a naturally occurring constituent of shoots (Helsper and Loewus, 1982; Sun *et al.*, 2021), and its modulation in AMF-plant symbiosis was mentioned by Schweiger *et al.* (2014). These results are in accordance with the ones reported in Chapter I, where an important accumulation of the above-mentioned compounds in *A. officinalis* plants associated with *R. irregularis* was shown.

Impact on secondary metabolism

Thirty-six secondary metabolites emerged from the Volcano-plot analysis of root and shoot samples, as the most affected compounds by the colonization of *A. officinalis* with the four different AMF species. The annotated compounds were divided into four major categories: (1) twenty C_6-C_3 derivatives, from which four were classified as syringin derivatives and sixteen as caffeic acid derivatives; (2) one C_6-C_2 derivative; (3) nine glycosylated triterpenoids; (4) six compounds belonging to other chemical classes, such as secoiridoids, coumarins, and imidazolidines. Among them, eight compounds were affected both in roots and shoots of the AMF-colonized plants in one, at least, symbiotic association (compounds 14, 20, 29, 31, 33, 34, 41, 42).

Phenylpropanoids were the most impacted SMs class by the AMF treatments. They were characterized as mono, di, tri or tetrameric derivatives of caffeic acid and of syringin according to their characteristic MS and MS/MS fragments as previously reported. Monomers and dimers of caffeic acid derivatives share characteristic fragment ions at *m/z* 179, 161, 135, 121, deriving from the cleavage of a single C_6-C_3 unit, while the tri- and tetrameric forms show additional ions at *m/z* 339, 295 and 185 derived from the cleavage of multiple units. Our results are in line with reported data suggesting a discernible enhancement of phenylpropanoid pathway in the roots of mycorrhized plants (Rivero *et al.*, 2015; Kaur and Suseela, 2020; Cartabia *et al.*, 2021). In addition, these compounds were already reported in *A. officinalis* (Boskovic *et al.*, 2018).

All the identified C_6-C_3 and C_6-C_2 compounds were found in significantly higher amounts in plants associated with *R. irregularis* and *R. intraradices* (cluster 1) as compared to those associated with *R. clarus* and *R. aggregatus* (cluster 2). This suggests that the first two AMF could influence *A. officinalis* metabolome in a similar way by activating common biosynthetic pathways. However, in a few cases, such as compounds 11 and 16 in shoots, their amount was exclusively affected ($p < 0.05$) in plants associated with *R. intraradices*. Besides the close response on metabolite productions by *R. irregularis* and *R. intraradices* species, minor differences can be observed in triggering specific compounds. In fact, AMF species belonging to the same cluster in the PCA affected *A. officinalis* plants in a similar way, however, not strictly identical. On the other hand, AMF-plant associations, which are differently clustered and present major differences in affecting *A.*

officinalis metabolome, could equally affect the accumulation of specific SMs. This is the case of compounds 12, 23, 31 and 32 in roots, and compounds 11, 15 and 16 in shoots, which did not show a significant accumulation ($p < 0.05$) among the AMF species belonging to different clusters.

The AMF species also affect the production of oleanane-type saponins. In this study, and in contrast to the phenylpropanoids derivatives, these compounds were essentially affected/modulated in the shoots of *A. officinalis*. Saponins are involved in plant defence mechanisms against biotic constraints, such as pest or herbivores attack, and their content is strongly influenced by plant-AMF symbiosis (Mugford and Osbourn, 2012; Hussain *et al.*, 2017; Xie *et al.*, 2018). Nine significantly modulated compounds from the different AMF treatments were tentatively identified. Our analysis led to the identification of four oleanane-type derivatives, which possessed two glycosidic units in their configuration (compounds 19, 22, 25 and 27) and five tri-glycosylated derivatives of bayogenin (compound 20) and of oleanolic acid (compounds 37-40). The tri-glycosylated compounds 20 and 25 presented a similar glycosylation, with the presence of a glucuronic methyl ester group, observed for the first time Chapter I (Cartabia *et al.*, 2021). The ability of *A. officinalis* to produce saponins was already reported in previous studies (Romussi *et al.*, 1979; Romussi *et al.*, 1984; Chen *et al.*, 2017) and their strong accumulation in shoot parts of mycorrhized *A. officinalis* is in line with Chapter I.

Seven compounds (20, 25, 27, 37-40) were essentially modulated in the shoots of plants associated with *R. irregularis* and *R. intraradices* (cluster 1) as compared to the plants associated with *R. clarus* and *R. aggregatus* (cluster 2), from which six are exclusively identified in the shoots. On the other hand, Volcano-plot analysis of root parts showed the accumulation of two saponins (compounds 19 and 22). Similarly, to the phenylpropanoid derivatives, triterpenoids are mainly affected during the association of *A. officinalis* with *R. irregularis* and *R. intraradices* (cluster 1). However, within cluster 1, compounds 37 and 40 appeared to be more affected in the shoots of plants associated with *R. intraradices* (fold change of 1.68 and 1.60, respectively). When compared to the AMF of cluster 2, *R. irregularis* failed to exert any significant upregulation of compound 25 in the shoots, while *R. intraradices* failed to induce any significant effect of compound 19 in the roots. In all the other cases, AMF belonging to cluster 1 significantly affected triterpenoids accumulation.

Special attention was given to compounds 37-40, which represent the most affected saponins of plants associated with *R. irregularis* and *R. intraradices* (fold change ranking from 1.34x to 4.55x). They are all undescribed molecules in the literature, characterized by a conjugated malonyl-sugar moiety and they represent derivatives of anchusoside-7 and anchusoside-2 (Romussi *et al.*, 1979; Romussi *et al.*, 1984; Cartabia *et al.*, 2021). Our results are in line with similar conjugated structures identified from the association of different plants with *R. irregularis* (Hill *et al.*, 2018; Kaur and Suseela, 2020). Kobayashi *et al.* (2018) reported the presence of FAS II gene, responsible for the synthesis of lipoic acid through the mitochondrial pathway in bacteria, in both *R. irregularis* and *R. clarus* from which some subunits are encoding for enzymes such as malonyl-CoA ACP transacylase. This could explain the potential ability of AMF to upregulate and synthesize malonyl conjugated compounds.

The four AMF species also promoted, differently, the accumulation of acetylated compounds. This is the case of compound 19, characterized as the acetyl derivative of anchusoside-9 (compound 22), already reported in *A. officinalis* (Cartabia *et al.*, 2021). The mass difference between those two compounds, equal to the presence of an additional acetyl group, as well as to the presence of the diagnostic MS/MS fragment ions at *m/z* 707, deduced an acetylated hexose unit at the C-21 of the structure (Cho *et al.*, 2015). Compound 19 represents a previously undescribed molecule in the literature. Besides saponins, two additional compounds from the phenylpropanoid pathway, both induced in plants associated with *R. irregularis* and *R. intraradices* (compounds 12 and 31) presented a similar acetyl-sugar conjugation. Compound 31 was tentatively identified as a new acetylated derivative of methylsyringin, while compound 12 was the 3-feruloyl-6′-acetyl sucrose (Cho *et al.*, 2015). To the best of our knowledge, these results pointed out, for the first time, the ability of specific AMF species to enhance the production of acetylated secondary metabolites.

The accumulation of methylated compounds was also reported in our analysis, essentially in the root parts of *A. officinalis* associated with *R. irregularis* and *R. intraradices*. Indeed, a significant increment of methylated syringin derivatives (compounds 13, 24, 31) and of the methylated phenylpropanoids, methyl dihydrosinapic acid glucoside (compound 10) and methylrosmarinic acid (compound 35), was observed. This result is consistent with the ones reported in Chapter I, pointing out the methylation potential of AMF *R. irregularis*.

Despite the widely accepted fact that different AMF genera could affect plant metabolome differently (Maeda *et al.*, 2018), one of the main observations of the present study is that AMF species belonging to the same genus may induce similar, but not strictly identical, metabolomic responses in *A. officinalis* plants, without being strongly related phylogenetically. Indeed, the latest updates regarding the phylogenetic classification of under-investigated AMF strains showed that *R. irregularis* is phylogenetically more closely related to *R. clarus* than to *R. intraradices* (Walker *et al.*, 2021b). Therefore, the outcome of the association in terms of, e.g., plant growth promotion and metabolites enhancement, is highly specific to the identity of the AMF symbiont (Yang *et al.*, 2017; Kaur and Suseela, 2020; Luthfiana *et al.*, 2021).

Conclusion

In conclusion, the association between *A. officinalis* and different AMF species belonging to the same genus resulted in a different modulation of several metabolites. Based on our data, PMs and SMs production was significantly affected especially in the plants associated with *R. irregularis* and *R. intraradices*. Indeed, a higher accumulation of phenolic compounds and of saponins was detected in roots and shoots of *A. officinalis* plants associated with these two AMF species. Additionally, an increased production of malonyl, acetyl and methyl derivatives of phenylpropanoids (e.g., 3-feruloyl-6′acetyl sucrose, methylsyringinoside, methylsyringin, 6″-acetylmethylsyringin) and of oleanane-type saponins (e.g., acetylanchusoside-9, malonylanchusoside-2, malonylanchusoside-7) was observed. Among them, six compounds (acetylanchusoside-9, 6″-acetylmethylsyringin, malonylanchusoside-2, hydroxy-malonylanchusoside-7, hydroxy-dimalonylanchusoside2/7 and malonylanchusoside-7) were tentatively characterized as new SMs. Within this study, evidence leads to the AMF species-specific metabolic response of *A. officinalis*. However, some AMF may be more closely related to each other in modulating the plant metabolome of their host. These observations may open the door to the selection of the most adequate AMF species and/or strains for the production of desirable active compounds.

Acknowledgements

The authors are thankful to Rebecca Marion from the Statistical Methodology and Computing Service/Louvain Institute of Data Analysis and Modelling in Economics and Statistics (SMCS/LIDAM, UCLouvain) for statistical support.

PART 2

ALKANNA TINCTORIA STUDIES

Chapter III

In vitro propagation of *Alkanna tinctoria* Tausch.: a medicinal plant of the Boraginaceae family with high pharmaceutical value

Adapted from the research article published in:

Industrial Crops & Products (2022):182, 114860

doi: 10.1016/j.indcrop.2022.114860

Annalisa Cartabia, Virginia Sarropoulou, Katerina Grigoriadou, Eleni Maloupa and Stéphane Declerck

Preface

The second part of this Ph.D. focuses on *Alkanna tinctoria* Tausch. This important medicinal plant belongs to the Boraginaceae family and is characterized by the production of therapeutic metabolites, among which naphthoquinone enantiomers (A/S). These metabolites are most known and studied due to their application in the pharmaceutical and industrial sectors.

The distribution of Boraginaceae plants across the world is not uniform, and furthermore, they are widely collected from their natural environment. In addition, their cultivation following conventional agriculture practices is difficult due to several constraints, which are poor seeds germination, low availability of planting material, time needed (three to four years) for noticeable production of A/Sd, and high harvesting costs. The extensive exploitation of these plants has required the need for their preservation and cultivation (e.g., mass production) trough different techniques.

These drawbacks are particularly valid for *A. tinctoria*, which has been placed by the IUCN on the red list of endangered species in several European regions.

Therefore, in Chapter III, the objective was to develop a protocol for the *in vitro* mass production of *A. tinctoria* plants using shoot-tip explants, and for their adequate acclimatization to *ex vitro* conditions.

Abstract

Alkanna tinctoria Tausch. (Boraginaceae), commonly known as alkanet or dyers' bugloss/alkanet, is a perennial plant rich in naphthoquinone enantiomers, such as alkannin and shikonin (A/S), which possess a wide range of pharmaceutical properties and are used as cosmetics, food additives, and natural dyes. This plant is mostly exploited from the wild, increasing the risk of its extinction as reported for other A/S producing plants extracted from their natural environment. Its cultivation under controlled conditions remains difficult and the need for alternative production systems both for preserving this endangered species and for increasing the production of A/S at a marketable level, has become a necessity. In the present study, a protocol for the *in vitro* production of *A. tinctoria* plants using shoot-tip explants was developed. Several culture media, concentrations of hormones, sugar, and gelling agents were tested to improve proliferation, rooting, and acclimatization of micropropagated shoot-tip explants from plants collected in the wild. Surface disinfection was optimal after immersion of shoot-tips and/or nodal explants in Signum® fungicide (30 min), ethanol 70% (1 min), and sodium hypochlorite 3% (10 min). Shoot proliferation was the highest on Murashige-Skoog basal medium enriched with 1.1 µM 6-benzyladenine, 0.15 µM α-naphthalene acetic acid, and 0.3 µM gibberellic acid with a proliferation rate of 3.9 every two weeks. For rooting, the Root Culture 1 (RC1) modified medium free of ammonium nitrate and enriched with 2.85 µM indole-3-acetic acid was the more adequate with 80% of roots formation after 30 days. Finally, acclimatization was optimal (100% survival rate) following transfer of the rooted explants in pots containing a peat moss:perlite (1:1, w/w) mixture, kept under a 90% relative humidity fog system for 10 days, followed by a decrease in relative humidity of 5% every day until 40% and a gradual increase in light intensity. The protocol developed allowed the production under *in vitro* culture conditions of a sufficient number of *A. tinctoria* plants with high levels of *ex vitro* survival, opening the door to industrial exploitation of its secondary metabolites and to the conservation of this important medicinal plants.

Keywords

Alkanet, micropropagation, acclimatization, alkannin, shikonin

Graphical abstract

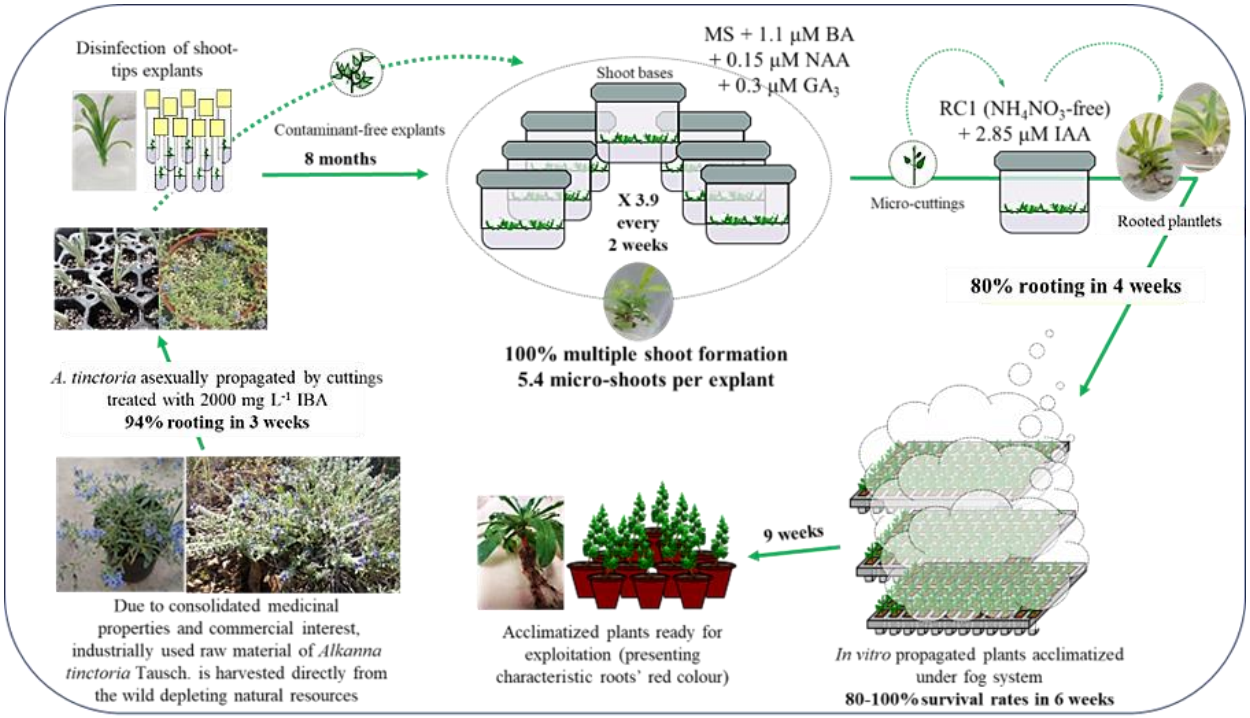

Introduction

Alkanna tinctoria Tausch. (family Boraginaceae) is a perennial herbaceous plant with a central distribution in the Mediterranean region (Valdés, 2011). It has a long history of medicinal uses characterized by its major active compounds, the naphthoquinone enantiomers alkannin and shikonin (A/S) (Papageorgiou *et al.*, 1999). These compounds and their derivatives (A/Sd) possess a wide range of medicinal properties (e.g., wound healing, antioxidant, antimicrobial, anti-inflammatory, and anti-cancer) and are used as well as cosmetics, food additives or dyes (Assimopoulou *et al.*, 2004; Papageorgiou *et al.*, 2008; Malik *et al.*, 2016).

Several efforts have been made to produce A/Sd from plants grown under controlled conditions. Cell tissues and root cultures of *A. tinctoria* as well as cell suspensions of *Arnebia* species in stirred-tank and air-lift bioreactors have been attempted, but the level of production remained insufficient (Urbanek *et al.*, 1996; Gerardi *et al.*, 1998; Gupta *et al.*, 2014). The only successful example of shikonin scaling up from cell cultures was with *L. erythrorhizon*. (Yazaki, 2017). Yet, A/Sd remains mostly extracted from roots of plant grown in nature, such as *A. tinctoria*, resulting in an unconsidered exploitation and risk of extinction for this important medicinal plant.

The cultivation of Boraginaceae following conventional agriculture practices is not feasible due to poor seed germination, low availability of planting material, extensive time needed for noticeable A/Sd production, and high harvesting costs (Malik *et al.*, 2016). For these reasons, direct plant regeneration and micropropagation are options that have been considered in the recent years for several Boraginaceae, such as *Arnebia hispidissima* (Lehm). DC. (Pal and Chaudhury, 2010), *Sericostoma pauciflorum* Stocks ex Wight (Satish *et al.*, 2014), and *Mertensia maritima* L. (Park *et al.*, 2019). These methods are useful for the conservation and propagation of plants, and for fulfilling the demands of pharmaceutical industries. For instance, the total content of shikonin from 1 g of induced *A. hispidissima* root tissue was 0.50 mg after 50 days of *in vitro* culture (Pal and Chaudhury, 2010).

The *in vitro* cultivation of *A. tinctoria* may represent a viable and innovative method to maintain and produce sufficient number of plants, further opening the doors to pharmaceutical exploitation. However, no improvement in the cultivation or either in the development of an

exhaustive *in vitro* propagation protocol have been made so far. Therefore, the objective of this Chapter is to report a successful protocol for the *in vitro* production of *A. tinctoria* plants using shoot-tip explants, and their full acclimatization to *ex vitro* conditions. The method and growth conditions are detailed and potential for mass production discussed.

Material and methods

Collection of plant material

One botanical expedition to collect wild-growing *A. tinctoria* plants was conducted on the 19 July 2017, in a suburban pine forest, altitude 50 m of Northern Greece (Evaggelistria, Seih Sou, Thessaloniki). A special collection permit, obtained by the Institute of Plant Breeding and Genetic Resources, Hellenic Agricultural Organization Demeter (IPBGR, HAO Demeter), which is issued annually by the Greek Ministry of Environment and Energy, was used. The habitat collection of the plant material was described as a rocky opening in a pine forest, temperate and sub-Mediterranean grassland, xeric Mediterranean Phrygana and grassland. The wild plants collected were taxonomically identified and were given the International Plant Exchange Network (IPEN) accession number GR-1-BBGK-17,5975 for their long-term *ex situ* conservation (including also sexual, asexual – vegetative, and *in vitro* propagation trials) at the premises of IPBGR, HAO-Demeter.

A. tinctoria ex situ conservation

Alkanna tinctoria was propagated asexually by cuttings. Six rooting trials were conducted during summer – autumn 2017. In total, 451 softwood top cuttings (3-4 cm long) were treated by immersion of their base in a 2,000 mg L^{-1} indole-3-butyric acid (IBA) solution for 10 s. The cuttings were then transferred in 76 mL pots (4.15×4.05×7 cm) containing a peat moss (Terrahum, Klasmann-Deilmann Gmbh, Germany) and perlite (Geoflor, Perlite Hellas S.A., Greece) (1:3, w/w) mixture. After 20 days of growth in the heated mist of the greenhouse [18-21°C soil, 25-30°C/18-25°C day/night air temperature, and 65-80 % relative humidity (RH)], plants' rooting was checked (**Figures 35 a-b**). Then, the plants were maintained, for further experimentation, in 0.33 L square plastic pots (7x7x8 cm) containing a peat moss (TS2 basic substrate medium, Klasmann-Deilmann Gmbh, Germany) and perlite

(3:1, w/w) mixture under unheated-greenhouse conditions (**Figures 35 c-d**). Soil and air temperature, and RH were different due to seasonal variability of the IPBGR, HAO-Demeter greenhouse (i.e., during summer: 18-22°C soil, 25-35°C air, and 60-70% RH; during autumn: 18-20°C, 15-25°C air, and 70-85% RH; during winter: 17-19°C soil, 5-15°C air, and 85-99% RH).

Figure 35. *Ex situ* conservation of *A. tinctoria* plants: (**a, b**) asexual propagation by cuttings from wild-growing plants collected on mid-summer (July 2017); (**c, d**) vegetative growth and blooming of mother plants inside the greenhouse in following spring (March 2018).

Disinfection and initial establishment *in vitro* of plant material

Nine disinfection protocols were compared, during autumn-winter 2017 and late spring-early summer 2018, for the establishment of *in vitro* contaminant-free plant material. Shoot-tips or shoot intermediate nodes (1-1.5 cm) were detached with scalpels from the mother plants above to proceed with the disinfection as follows: soaked in Signum® fungicide 26.7/6.7 WG (0.070g/100 mL ddH_2O, BASF Agricultural solutions, The Netherlands) for 30 min, then bathed or not in 70% ethanol for 1 min and in sodium hypochlorite (NaOCl) solutions at different concentrations (1, 2, 3%) and duration of immersion (3, 10, 15 min) under continuous agitation. The explants were finally rinsed 4-5 times with sterilized deionized water and placed individually in borosilicate glass test tubes (100x25 mm) containing Murashige-Skoog (MS) medium (Murashige and Skoog, 1962) supplemented with 20 g L^{-1} sucrose (Duchefa, The Netherlands) and 6 g L^{-1} Plant Agar (Duchefa, The Netherlands). The successfully established contaminant-free explants were sub-cultured every 3-4 weeks. Eight to 10 successive subcultures were done during 8 months until a sufficient number of plants was produced for further experimentation. The cultures were maintained in a growth chamber under 16 h/8 h light/dark photoperiod, temperature of 22 ± 1°C (day/night), 80% RH, and cool white fluorescent light (PHILIPS, 36 W/830 G13 1214 mm) intensity of about 40 μmol $m^{-2}s^{-1}$. The percentage of contaminant-free and microbial-contaminated explants were recorded after 20 days of culture.

In vitro shoot proliferation

Three proliferation experiments were conducted using shoot-tip explants derived from the *in vitro* cultures above. The explants were transferred into Magenta™ vessels (Baby food jars, 62.4 ×95.8 mm, size: 200 mL, Sigma-Aldrich, Merck KGaA, Germany), cover by Magenta™ B-caps, and containing 35 mL of the culture media described below. The cultures were maintained in a growth chamber under the same conditions as described above. In the first experiment, three different culture media were tested, MS, Woody Plant Medium (WPM) (Lloyd and McCown, 1980) and Gamborg B5 (GB5) (Gamborg *et al.*, 1968) , all enriched with 1.1 µM 6-benzyladenine (BA), 0.15 µM α-naphthalene acetic acid (NAA), and 0.3 µM gibberellic acid (GA_3) (**Figure 36 a-b**). Chemical composition of the basal culture media is presented in **Supplementary Table 1**, Annex III. In the second experiment, two different gelling agents [6 g L^{-1} Plant Agar and 3 g L^{-1} Gelrite (Duchefa, The Netherlands)] in combination with MS and WPM culture media enriched with 1.1 µM BA, 0.15 µM NAA, and 0.3 µM GA_3 were tested (**Figures 36 c-d**). In the third experiment, MS culture medium PGR's-free supplemented with two sucrose and Plant Agar concentrations (20/30 g L^{-1} and 6/7 g L^{-1}, respectively) was tested. After 15 days of culture for the first and 20 days for the second and third proliferation experiment, the following measurements were recorded: shoot formation percentage, number of new shoots per explant, shoot length, proliferation rate (i.e., the mean number of new non-hyperhydric shoots of at least 1 cm height per inoculated shoot-tip explant, expressed as the ratio between non-hyperhydric-proliferated and total number of initial explants), and hyperhydricity percentage. In the first and second experiment, 20 explants distributed in 4 vessels (each containing 5 explants) were considered per treatment, while in the third experiment, 18 explants distributed in 3 vessels (each containing 6 explants) were considered per treatment.

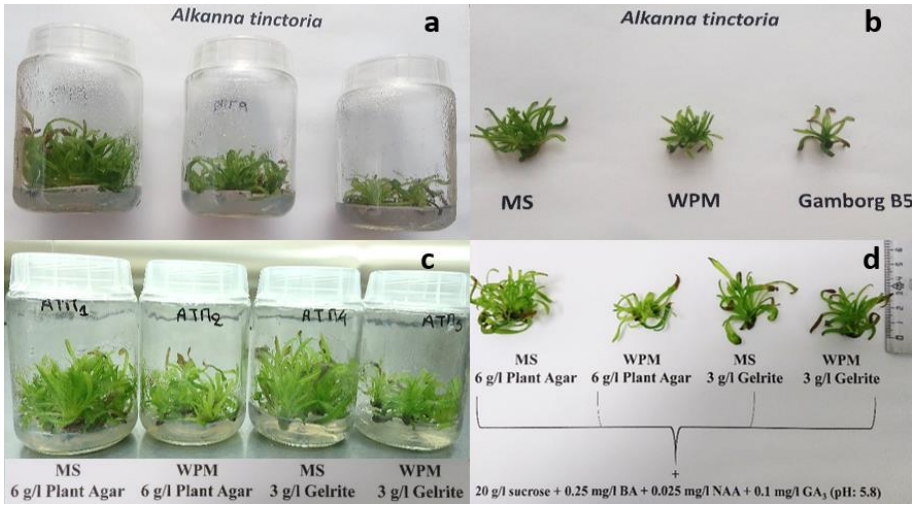

Figure 36. *In vitro* proliferation of *Alkanna tinctoria* explants: **(a, b)** MS, WPM, and GB5 culture media enriched with 1.1 µM BA, 0.15 µM NAA, 0.3 µM GA_3; **(c, d)** MS and WPM culture media solidified with different gelling agents (Plant Agar and Gelrite), and enriched with 1.1 µM BA, 0.15 µM NAA, 0.3 µM GA_3.

In vitro rooting

Three rooting experiments were conducted using shoot-tip explants derived from the *in vitro* shoot proliferation above. The explants were transferred into Magenta™ vessels and maintained in a growth chamber under the same conditions as described previously. In the first experiment, full-strength MS and ½ MS in macro and micro-nutrients and ethylenediaminetetraacetate ferric sodium (FeNaEDTA) were tested in combination with three different IBA concentrations (0, 2.5, 5 µM). In the second experiment, MS basal medium was enriched with two different NAA concentrations (2.69 and 5.4 µM) and combined with three different IBA concentrations (0, 2.5, 5 µM). In the third experiment, MS and RC1 ammonium nitrate (NH_4NO_3)-free culture media (Shimomura *et al.*, 1991), both supplemented with IAA at four concentrations (0, 2.85, 5.71, 11.42 µM), were tested (**Figures 37 a-d**). Chemical composition of RC1 and ½ MS is presented in **Supplementary Table 1**, Annex III.

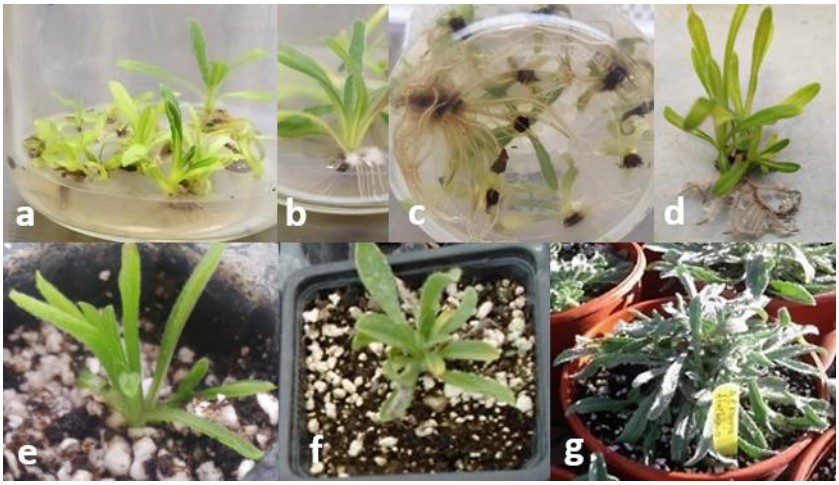

Figure 37. *In vitro* rooting and *ex vitro* acclimatization of *Alkanna tinctoria* explants: (**a-c**) rooted explants in RC1 with 2.85 µM IAA medium; (**d-f**) vegetative growth of acclimatized plants after 5 and 40 days, respectively, in trays in the fog system; (**g**) *A. tinctoria* transplanted in 0.33 L pots inside the greenhouse.

After 20 days of culture for the first and second, and 30 days for the third rooting experiment, the following parameters were recorded: root numbers per rooted explant, root length, rooting and hyperhydricity percentages. In the first and third experiment, 20 explants distributed in 4 vessels (each containing 5 explants) were considered per treatment, while in the second experiment, 15 explants distributed in 3 vessels (each containing 5 explants) were considered per treatment.

Ex vitro acclimatization

Ex vitro acclimatization was conducted using rooted explants from the *in vitro* rooting experiments above, after being rinsed with tap water to remove the adhering medium (**Figures 37 e-g**). The rooted explants (10 replicates per culture media) were subsequently planted in 76 mL pots (4.15×4.05×7 cm) filled with a peat moss (Terrahum):perlite (1:1, w/w) mixture. The pots were placed in greenhouse under a 90% RH fog system, 25-30°C/18-25°C day/night air temperature, and 50% shading for 10 days. For the following 10 days, RH was reduced by 5% every day until 40%, while the light intensity was gradually increased to 250 µmol $m^{-2}s^{-1}$. The number of successfully acclimatized explants was recorded 40 days after transplanting in the greenhouse and was expressed as survival percentage. The plants were then transferred into 0.33 L pots for 20 days and then into 2.5 L pots containing a white peat moss (TS2, Klasmann):perlite (3:1, w/w) mixture. The pots were

transferred to the greenhouse (summer conditions: 25-30°C/18-25°C day/night air temperature, approximately 16 h light duration of about 250 μmol $m^{-2}s^{-1}$ intensity, and 45-55% RH) and the plants were watered by sprinkling. After 60 days, the plants were transferred outside the greenhouse nursery to the external environment (28-35°C/20-28°C day/night air temperature and 50-55% RH, under a 50 % shading net), where their *ex vitro* acclimatization was completed.

Statistical analysis

For all the experiments presented, vessels were randomized, and plant growth parameters analysed by one-way ANOVA followed by Duncan's multiple range test ($p < 0.05$) in order to discriminate among the means between the treatments. For all parameters, normal distribution of residuals variance and normality were checked before analyses. If the assumptions were not verified, the non-parametric Kruskal-Wallis test (K independent samples) was adopted. Data analyses were performed by SPSS Statistics for Windows, version 17 (SPSS Inc., Illinois, New York, USA).

Results and discussion

Different types of explants and tissue culture techniques have been used for growing and maintaining Boraginaceae species *in vitro*: callus cultures for *A. tinctoria* (Urbanek *et al.*, 1996) and *Onosma bulbotrichom* DC. (Bagheri *et al.*, 2018), root and suspension cultures for *L. erythrorhizon* (Tatsumi *et al.*, 2016), suspension cultures for *Echium italicum* L. (Zare *et al.*, 2010) , callus and suspension cultures for *A. hispidissima* (Singh and Sharma, 2014). Although plant cell cultures have shown great potential to produce an array of valuable products, limited success has been achieved at the industrial scale. Yet, as mentioned before, A/Sd remains mostly extracted from roots of plant grown in nature, leading to the over-exploitation of important medicinal plants (Papageorgiou *et al.*, 2008). Based on the literature available, *A. tinctoria in vitro* plants production using shoot-tip explants has never been attempted so far and may thus represents a promising and potentially easy approach for large-scale production of *in vitro*/*ex vitro* plants. In this Chapter, a protocol for the *in vitro* production and *ex vitro* acclimatization of *A. tinctoria* was developed, aimed at solving the problem of plants availability, and possibly helping in the development

of innovative approaches for the production of A/Sd, which are important pharmacological compounds.

The more suitable protocol can be summarized as follows (**Figure 38**): (1) disinfection of shoot-tip explants by a combination of Signum® fungicide (30 min), ethanol 70% (1 min), and NaOCl 3% (10 min). (2) Proliferation of the surface-disinfected explants on MS medium enriched with 1.1 µM BA, 0.15 µM NAA, and 0.3 µM GA_3, supplemented with 20 g L^{-1} sucrose and solidified with 6 g L^{-1} Plant Agar. The explants are sub-cultured every 2 weeks, with a proliferation rate of about 3.9. (3) Rooting of the explants for a period of 4 weeks on RC1 medium (NH_4NO_3-free) supplemented with 2.85 µM IAA. (4) Transfer of the rooted explants in pots filled with a peat moss:perlite (1:1, w/w) mixture, kept under a 90% RH fog system for 10 days, followed by a decrease in RH of 5% every day until 40% and a gradual increase in light intensity. After 9 weeks, the explants are transferred into 2.5 L pots containing a white peat moss:perlite (3:1, w/w) mixture. Starting from 20 *A. tinctoria* contaminant-free explants sub-cultured 2 times in MS medium (4 weeks), rooted in RC1 (4 weeks) and acclimatized *ex vitro* (9 weeks), around 244 plants can be obtained fully adapted to the external environment.

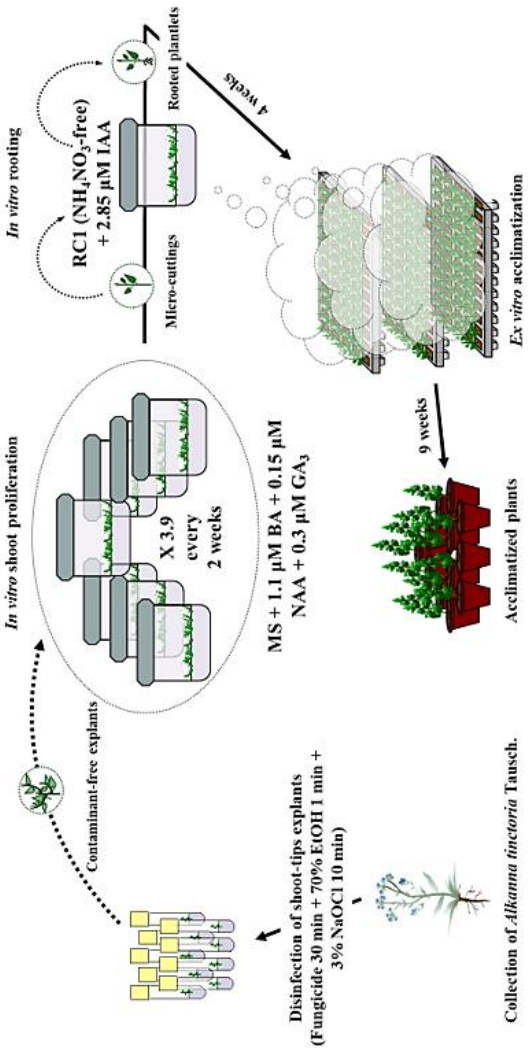

Figure 38. Outline schema of the *in vitro* cultivation and *ex vitro* acclimatization protocol of *Alkanna tinctoria* explants.

The disinfection protocol reported above yielded the best percentage of successfully disinfected starting explant material close to 50% (**Table 10**). Regarding the *in vitro* shoot proliferation, the best result was obtained in MS medium (**Table 11.I**). Indeed, shoot formation was noticed in 100% of the explants with a proliferation rate of 3.9. This could be related to the higher macronutrients content, especially nitrogen (KNO_3 and NH_4NO_3), as compared with the two other culture media tested, WPM and GB5 (Arab *et al.*, 2014). Moreover, the result obtained is consistent with the study of Yaman *et*

al. (2019) on *Alkanna orientalis* (L.) Boiss. and *Alkanna sieheana* Rech. Fil., which reported a high percentage of shoot formation (30-66.6%), number, and length of shoots on MS medium containing 5.72 μM IAA. Improved shoot proliferation using different explant types (e.g., nodal segments, callus, leaf lamina, petioles) proliferated in MS medium supplemented with different plant growth regulators – PGRs (e.g., 1 N6-benzylaminopurine – BAP, IBA, kinetin, NAA) concentrations was also reported for other Boraginaceae plant species: *Rotula aquatica* Lour. (Martin, 2003), *Cordia verbenacea* DC. (Lameira and Pinto, 2006), *A. hispidissima* (Phulwaria and Shekhawat, 2013), *Echium orientale* L. (Turker *et al.,* 2018). Several studies have described that the combination of cytokinins and auxins improve shoot proliferation in Boraginaceae plants (Pal and Chaudhury, 2010; Mahesh and Jeyachandran, 2013). Although 6-benzyladenine (BA) has often been considered as the prior cytokinin type used, because it is readily metabolized in plant tissues and can lead to the production of natural hormones (zeatin) (Rai *et al.*, 2009), its use can lead to hyperhydricity symptoms (Ivanova and Van Staden, 2011) a phenomenon noticed as well in this Chapter. In order to improve the quality of the explants, two different gelling agents (Plant Agar and Gelrite) in combination with MS and WPM media were tested (**Table 11.II**). The percentage of shoot formation and number of new shoots per explant was significantly lower in WPM+ Plant Agar treatment, while shoot length was significantly higher in MS+ Plant Agar medium. Moreover, the highest proliferation rate was confirmed in MS medium, characterized as well by a lower, but not significant, hyperhydricity percentage as compared with WPM medium and Gelrite gelling agent applied. Indeed, the symptoms remained quite evident in all the treatments tested at this stage. The slightly lower intensity of hyperhydric *A. tinctoria* explants on medium solidified with Plant Agar could be explained by the presence of a sulphated galactan (Nairn *et al.*, 1995) , which is involved in the control of hyperhydricity (Ivanova and Van Staden, 2011). Moreover, Gelrite has been reported to increase hyperhydricity symptoms in various plant species due to its physical structure, which allows a better absorption of cytokinins, NH_4^+, and water, suspected to be responsible of hyperhydricity (Ivanova and Van Staden, 2011). To investigate further and obtain a higher shoot proliferation rate, different sucrose and Plant Agar concentrations (20/30 g L^{-1} and 6/7 g L^{-1}, respectively) were tested (**Supplementary Table 2,** Annex III). However, both parameters did not have a significant impact on the proliferation rate and hyperhydric shoots' percentage. Regarding the

sucrose concentration, this result contradicts the study conducted on another Boraginaceae plant, *Rindera umbellata* (Waldst. & Kit.) Bunge, which reported that the highest percentage of explants with developed buds was achieved with a sucrose concentration of 0.06 M (± 20 g L^{-1}) as compared with 0.1 M (± 30 g L^{-1}) (Perić *et al.*, 2012). Sucrose concentrations, higher than the optimum for shoot proliferation, could delay the development of cultured cells, leading to a decrease in the nutrient's uptake (Wu *et al.*, 2006), lowering the water potential of the medium (Shim *et al.*, 2003), and inducing osmotic stress (Shohael *et al.*, 2006). In this Chapter, higher sucrose concentration (30 g L^{-1} instead of 20 g L^{-1}) did not inhibit explants proliferation, indicating that both sucrose concentrations were not supra-optimal and that they were perceived by cells as chemical signals, but without acting as stress agents (Silva, 2004).

Table 10. Disinfection protocols tested on *Alkanna tinctoria* explants.

Type of explant	Season	Disinfection protocols			Number of explants	Disinfection success (%)
		Fungicide[1]	Ethanol[2]	NaOCl[3]		
Shoot-tip	Spring	+	-	1 (3 min)	75	22
Shoot-tip	Summer	+	+	2 (10 min)	25	25
Shoot-tip	Early-autumn	+	+	3 (10 min)	76	12
Shoot-tip	Late-autumn	+	+	3 (10 min)	25	47
Shoot-tip	Autumn	+	+	3 (15 min)	23	0
Nodes	Spring	+	+	-	51	0
Nodes	Spring	+	+	3 (15 min)	138	4

[1]Signum® fungicide at 0.07 g/100 mL ddH_2O for 30 min immersion.
[2]Immersion in ethanol for 1 min.
[3]NaOCl solutions at different concentrations (1, 2, 3 %).

Table 11. Effects of Murashige and Skoog-MS, Woody Plant Medium-WPM, and Gamborg B5-GB5 culture media enriched with 1.1 μM BA, 0.15 μM NAA, 0.3 μM GA_3, and solidified with two gelling agents (6 g L^{-1} Plant Agar or 3 g L^{-1} Gelrite), on proliferation parameters of *Alkanna tinctoria* explants measured after 15 and 20 days of culture in the first (**I**) and second (**II**) experiment, respectively.

Exp.	Treatments	Shoot formation (%)	N. of new shoot/explant	Shoot length (cm)	Prolif. rate	Hyperhydricity (%)
I	MS + Plant Agar	100 ± 0 a	5.4 ± 0.4 a	1.4 ± 0.1 a	3.9 ± 0.4 a	15 ± 9.2 a
	WPM + Plant Agar	95 ± 5.0 a	3.5 ± 0.3 b	1.3 ± 0.1 a	2.7 ± 0.3 b	30 ± 5.8 a
	GB5 + Plant Agar	95 ± 5.0 a	3.4 ± 0.3 b	1.3 ± 0.1 a	2.4 ± 0.2 b	15 ± 9.6 a
II	MS + Plant Agar	100 ± 0 a	4.7 ± 0.5 a	1.8 ± 0.1 a	4.2 ± 0.3 a	20 ± 8.2 a
	WPM + Plant Agar	75 ± 5.0 b	3.5 ± 0.4 b	1.4 ± 0.1 b	2.8 ± 0.3 c	20 ± 8.2 a
	MS + Gelrite	100 ± 0 a	4.7 ± 0.4 a	1.5 ± 0.1 b	3.8 ± 0.3 ab	20 ± 14.1 a
	WPM + Gelrite	95 ± 5.0 a	4.6 ± 0.3 ab	1.4 ± 0.1 b	3.3 ± 0.2 bc	25 ± 12.6 a

Data for number of new shoots per explant, shoot length, and proliferation rate are means ± SE of 20 replicates, while data for shoot formation and hyperhydricity are means ± SE of 4 replicates (i.e., the vessels, each containing 5 explants). For both experiments separately (I and II) means followed by different letters within the same column differed significantly (Duncan's multiple range test, $p < 0.05$).

For several Boraginaceae, the MS medium full or half-strength, proved to be effective for the *in vitro* rooting once enriched with different PGRs, such as IBA for *M. maritima* (Park *et al.*, 2017), NAA for *R. aquatica* (Martin, 2003), and IBA + NAA + kinetin for *Arnebia pulchra* (Willd. ex Roem. & Schult.) Edm. (Ezati *et al.*, 2015). In the current study, neither the individual application of IBA, NAA, and IAA nor the combination of IBA + NAA in MS medium gave satisfactory rooting results for *A. tinctoria* explants. Indeed, no roots were produced in MS + IAA treatments. The highest rooting (50%) and root number (3.2 roots per rooted explant) was obtained in MS + 5 μM IBA (**Table 12.I**), while higher root length (1.2 cm) was evident in MS + 2.69 μM NAA + 5 μM IBA (**Table 12.II**). Indole-3-butyric acid is characterized by higher stability than IAA, because it has longer side chain, slower rate of oxidation and metabolism within plant tissues, and can be converted to IAA (Strader and Bartel, 2011). Besides, NAA concentrations higher than the optimum stimulate ethylene biosynthesis affecting adversely rooting (Tesfa and Admassu, 2016), thus enabling IBA to maintain the auxin activity in the medium for a longer period

and promoting rooting better than NAA. Indeed, these three auxin types have different receptors, uptake rates, transport, and metabolism (De Klerk et al., 1997) depending also on the concentration of the mineral elements presented in the medium (Shohael *et al.*, 2013). Hyperhydricity was noticed in almost all treatments and in higher extent (46.7 %) in *A. tinctoria* explants growing in MS + 5.4 μM NAA + 5 μM IBA (**Table 12.I** and **II**).

Table 12. Effect of Murashige and Skoog-MS and ½ MS supplemented with three IBA concentrations, of MS with six NAA+IBA combinations, and of Root Culture 1-RC1 with four IAA concentrations, on rooting parameters of *Alkanna tinctoria* explants measured after 20 days of culture in the first (**I**) and second (**II**) experiments, and after 30 days in the third (**III**) experiment.

Exp.	Culture media	Treatments (µM)	Rooting (%)	Root number/ rooted explant	Root length (cm)	Hyperhydricity (%)
I	MS	0 IBA	0 ± 0	0 ± 0	0 ± 0	20 ± 8.2 a
	MS	2.5 IBA	30 ± 5.8 a	3.3 ± 1.2 a	0.9 ± 0.1 a	10 ± 5.8 a
	MS	5 IBA	50 ± 17.3 a	3.2 ± 0.9 a	0.9 ± 0.1 a	15 ± 9.6 a
	½ MS	0 IBA	0 ± 0	0 ± 0	0 ± 0	10 ± 10 a
	½ MS	2.5 IBA	45 ± 15 a	1.8 ± 0.4 a	0.6 ± 0.1 a	0 ± 0
	½ MS	5 IBA	25 ± 12.6 a	2.8 ± 1.1 a	0.7 ± 0.1 a	0 ± 0
II	MS	2.69 NAA + 0 IBA	6.7 ± 6.7 a	1 ± 0 d	0.5 ± 0 c	6.7 ± 6.7 b
	MS	5.4 NAA + 0 IBA	0 ± 0	0 ± 0	0 ± 0	13.3 ± 6.7 ab
	MS	2.69 NAA + 2.5 IBA	6.7 ± 6.7 a	3 ± 0 a	0.3 ± 0 d	13.3 ± 6.7 ab
	MS	5.4 NAA + 2.5 IBA	13.3 ± 6.7 a	1.5 ± 0 b	1.0 ± 0.1 b	13.3 ± 6.7 ab
	MS	2.69 NAA + 5 IBA	26.7 ± 17.6 a	1 ± 0 d	1.2 ± 0.1 a	13.3 ± 13.3 ab
	MS	5.4 NAA + 5 IBA	20 ± 0 a	1.3 ± 0.1 c	0.5 ± 0 c	46.7 ± 17.6 a
III	RC1	0 IAA	30 ± 5.8 b	5.1 ± 0.2 b	2.1 ± 0.3 b	0 ± 0
	RC1	2.85 IAA	80 ± 8.2 a	6 ± 0.8 a	3.4 ± 0.8 a	0 ± 0
	RC1	5.71 IAA	10 ± 5.8 c	1 ± 0.3 c	0.7 ± 0.2 c	0 ± 0
	RC1	11.42 IAA	0 ± 0	0 ± 0	0 ± 0	0 ± 0

Data for root number per rooted explant and root length are means ± SE of 20 replicates for IBA and IAA treatments, and 15 for NAA+IBA combinations, while data for rooting and hyperhydricity are means ± SE of 4 replicates for IBA and IAA treatments, and 3 for NAA+IBA combinations (i.e., the vessels, each containing 5 explants). For the experiments separately (I, II, and III), means followed by different letters within the same column differed significantly (Duncan's multiple range test, $p < 0.05$). Values in columns with means ± SE of 0 were not considered in the statistical analysis.

Interestingly, rooting percentage, root number, and root length were significantly higher in RC1 medium enriched with 2.85 μM IAA as compared with the other RC1 treatments (**Table 12.III**). Moreover, hyperhydricity symptoms were completely reversed after a 30-days culture period. According to Hartmann and Hartmann (2002), IAA is the naturally occurring auxin produced in leaves and buds, and transported basipetally from the top towards the lower part of the plant (i.e., base of the cut), thus promoting rooting through interactions with other endogenous substances that lead to its raised endogenous level. Hyperhydricity is reported to decline or totally reverse when using culture media with reduced or null concentrations of NH_4NO_3 (Liu *et al.*, 2003), while NH_4NO_3 stimulated rejuvenation and height of *Paeonia lactiflora* Pall. hyperhydric explants (Wu *et al.*, 2011). The irreversible loss of regenerative ability of tissues and the poor *ex vitro* survival rate of hyperhydric shoots limit the potential for *in vitro* mass propagation (Ivanova and van Staden, 2008).

The use of IAA and the elimination of NH_4NO_3 for *in vitro* rooting of *A. tinctoria* led to a successful rooting and further acclimatization protocol. In fact, the best *ex vitro* plant survival (100%) was obtained once applying explants rooted in RC1 + 2.85 μM IAA medium (**Supplementary Table 3,** Annex III). Phulwaria and Shekhawat (2013), described a lower survival rate (60%) of *in vitro* rooted *A. hispidissima*, another important alkannin yielding plant, while a higher rate (75%) of plants developed from *ex vitro* rooting. Moreover, this technique reduces the steps of micropropagation, saving cost, labour, and resources. In the present study, the asexual propagation by softwood cuttings gave a rooting percentage around 92%. This alternative, characterized by a direct *ex vitro* cultivation, could be taken into account in case no contaminant-free explants are needed in further applications, but it will not fulfil the need for a large-scale production of *A. tinctoria*. Nevertheless, the probable reason of higher survival percentages of *A. tinctoria* plants developed from *in vitro* rooting in the current study may be due to the fully developed root system (i.e., more and longer lateral roots), enabling better adaptation to the acclimatization process. Similar results with high greenhouse survival rates were reported for *R. umbellate* (70-100%) (Perić *et al.*, 2012) and *C. verbenacea* (90-95%) (Lameira and Pinto, 2006).

Conclusion

An efficient protocol for the micropropagation and *in vitro* rooting of an important medicinal plant, *A. tinctoria,* has been developed. High amounts of *in vitro* produced plants with high levels of survival during *ex vitro* acclimatization have been obtained. This could presumably reduce the pressure on the natural population of this plant and at the same time open the door for mass production of *in vitro* or acclimatized plants useful for the production of SMs. Plant tissue culture represents thus a useful tool for the conservation and propagation of this important medicinal plant, potentially appropriate for the large-scale production of A/Sd *via* root induction either *in vitro* and/or growth under *ex vitro* conditions.

Funding

Part of the research done at the Institute of Plant Breeding and Genetic Resources, Hellenic Agricultural Organization - DEMETER (Greece) has been co-financed by the European Union and Greek national funds through the Operational Program Competitiveness, Entrepreneurship and Innovation, under the call RESEARCH - CREATE – INNOVATE (project code: BIOREACT T2EDK-02927).

Acknowledgements

The authors would like to thank Dr. Nikos Krigas, researcher of the IPB&GR, for the collection and botanical identification of *Alkanna tinctoria* plants, Alicia Varela Alonso for valuable suggestions regarding the plants' rooting protocol and YanYan Zhao for the precious help in maintaining the *A. tinctoria* plants *in vitro*.

Chapter IV

Arbuscular mycorrhizal fungi impact the production of alkannin/shikonin and their derivatives in *Alkanna tinctoria* Tausch. grown in semi-hydroponic and pot cultivation systems

Adapted from the research article submitted in:

Frontiers in Microbiology section Microbe and Virus Interactions with Plants (2023)

Yanyan Zhao, Annalisa Cartabia, Sergio Ortiz, Mónica Garcés-Ruiz, Marie-France Herent, Joëlle Quetin-Leclercq, Stéphane Declerck, Ismahen Lalaymia

Preface

After developing an optimal protocol for the mass production of *ex vitro Alkanna tinctoria* plants (Chapter III), the general aim of Chapter IV was to assess the effects of AMF on the production of naphthoquinones alkannin/shikonin and their derivatives (A/Sd) in the roots of this important medicinal plant. As reported for *A. officinalis*, no studies, to our knowledge, could be found in the literature.

Moreover, specific AMF were shown to induce the production of metabolites in *A. officinalis* plants (Chapter II). In more details, two separated groups of AMF were reported. An increased accumulation of PMs and SMs was obtained from the association of *A. officinalis* with *R. irregularis* MUCL 41833 and *R. intraradices* MUCL 49410 as compared to *R. clarus* MUCL 46238 and *R. aggregatus* MUCL 49408. Forty-two compounds were reported to be highly modulated in relation to the different AMF associations. Among them, six new SMs were tentatively identified, including two acetyl- and four malonyl-phenylpropanoid and saponin derivatives.

Therefore, in Chapter IV, two major objectives were addressed. First, assessing the effects of the AMF GINCO strain *Rhizophagus irregularis* MUCL 41833 on A/Sd production and relative genes expression in *A. tinctoria* roots. Second, assessing the effects of two AMF GINCO strains previously characterized by a higher and lower impact (*R. irregularis* MUCL 41833 and *R. aggregatus* MUCL 49408, respectively) and two AMF isolated from roots of wild-growing *A. tinctoria* (*Rhizophagus irregularis* and *Septoglomus viscosum*) on A/Sd production in roots and correspondent relative genes expression. The study was conducted under two different growing systems: the S-H cultivation system (as in Chapters I and II), and a conventional pot cultivation system in the greenhouse. The quantification of A/Sd and their identification were carried out by HPLC-PDA and HPLC-HRMS/MS, respectively. In addition, target genes modulating A/Sd biosynthesis were evaluated through RT-qPCR analysis.

Abstract

Alkanna tinctoria is a medicinal plant, producing alkannin/shikonin and derivatives (A/Sd). It associates with arbuscular mycorrhizal fungi (AMF), which are known to modulate the plant secondary metabolites (SMs) biosynthesis. However, to the best of our knowledge, no study on the effects of AMF strains on the growth and production of A/Sd in *A. tinctoria* has been reported in the literature. Here, three experiments were conducted. In Exp. 1, plants were associated with the GINCO strain *R. irregularis* MUCL 41833 and in Exp. 2, with two strains of GINCO (*R. irregularis* MUCL 41833 or *R. aggregatus* MUCL 49408) and two native strains (*R. irregularis* and *S. viscosum*) in a semi-hydroponic (S-H) cultivation system. Plants were harvested after 9 and 37 days in Exp. 1 and 9 days in Exp. 2. In Exp. 3, plants were associated with the two native AMF strains and with *R. irregularis* MUCL 41833 and were grown for 85 days in pots under greenhouse conditions. Quantification and identification of A/Sd were performed by HPLC-PDA and by HPLC-HRMS/MS, respectively. *LePGT1*, *LePGT2* and *GHQH* genes involved in the A/Sd biosynthesis were analysed through RT-qPCR. In Exp. 1, no significant differences were noticed in the production of A/Sd, while in Exp. 2 and 3, plants associated with native AMF *R. irregularis* had the highest content of total A/Sd expressed as shikonin equivalent. In Exp. 1, a significantly higher relative expression of both *LePGT1* and *LePGT2* was observed in plants inoculated with *R. irregularis* MUCL 41833 compared with control plants after 37 days in the S-H system. Similarly, a significantly higher relative expression of *LePGT2* in plants inoculated with *R. irregularis* MUCL 41833 was noticed after 9 days versus 37 days in the S-H cultivation system. In Exp. 2, a significant lower relative expression of *LePGT2* was observed in native AMF *R. irregularis* inoculated plants compared to the control. Overall, our study showed that the native *R. irregularis* strain increased A/Sd production in *A. tinctoria* regardless of the system used, further suggesting that the inoculation of native/best performing AMF is a promising method to improve the production of important SMs.

Keywords

Arbuscular mycorrhizal fungi; *Alkanna tinctoria*; semi-hydroponic cultivation system; *Rhizophagus irregularis*; Alkannin/Shikonin derivatives; gene expression

Introduction

The hydroxynaphthoquinones (HNQs) of natural origin, and in particular the isohexenylnaphthazarins (IHNs), such as the chiral pair alkannin and shikonin (A/S), are lipophilic red pigments characterized by a wide spectrum of wound healing, antibacterial, anti-inflammatory, anticancer, and antithrombotic activities (Papageorgiou *et al.*, 1999; Tappeiner *et al.*, 2014). Monomeric A/S derivatives, mainly esters of the side chain hydroxyl group, have been found in the root periderm of several plants of the Boraginaceae family, including *Alkanna tinctoria* Tausch. This important medicinal plant, commonly known as alkanet or dyers' bugloss/alkanet, is found across southern Europe, northern Africa, and southwestern Asia, with a central distribution in the Mediterranean region (Valdés, 2011). Preparations made with *A. tinctoria* roots are commonly used in traditional medicine to treat wounds, burns, and ulcers, while extracted A/S are employed as active ingredients in different marketed pharmaceutical formulations (e.g., Histoplastin Red®, HELIXDERM®) as strong wound healing medicines. Root extracts are also used as cosmetics, food additives or natural dyes for staining silk (Papageorgiou *et al.*, 2008; Malik *et al.*, 2016).

Today, nature remains the main source of commercial A/S and their derivatives (A/Sd), despite significant efforts to synthesize these compounds over the years (Papageorgiou *et al.*, 2008). The only successful example of shikonin scaling up from cell cultures was with *Lithospermum erythrorhizon* Siebold & Zucc. (Boraginaceae) by Mitsui Petrochemical Industries Ltd. (now Mitsui Chemicals Inc., Tokyo, Japan) in 1984 (Yazaki, 2017). Few more attempts have been made with cell suspension cultures of *Arnebia* spp. (Boraginaceae) in stirred-tank (New Brunswick Scientific Company Inc., Edison, NJ) and in air-lift bioreactors, but no further commercial successes have been reported (Gupta *et al.*, 2014; Malik *et al.*, 2016). For *A. tinctoria*, cell tissues and root cultures have been used, but the level of A/S production remained insufficient for commercial use (Urbanek *et al.*, 1996; Gerardi *et al.*, 1998). Yet, these important compounds remain mostly extracted from plants grown in the wild, with a risk of extinction as already documented for other Boraginaceae spp. (e.g., *L. erythrorhizon* in Japan, *Alkanna sieheana* Rech. Fil. and *Alkanna orientalis* L. Boiss. in Turkey). Indeed, *A. tinctoria* is considered as very rare in some European countries, such as Slovakia, Bulgaria, and Hungary (Yazaki,

2017; Yaman *et al.*, 2019; Ahmad *et al.*, 2021). Moreover, this plant is characterized by a very low seed germination rate and its cultivation under conventional agriculture practices is hampered by several constraints (e.g., time needed for A/S production, high costs of harvesting, exposure to biotic/abiotic stresses) (Malik *et al.*, 2016). For these reasons, *in vitro* and *ex vitro* cultivation protocols have been developed for the propagation and preservation of this plant (Cartabia *et al.*, 2022, Chapter III). In addition, hydroponic cultivation of medicinal plants has attracted the attention of the scientific community and industrial sector, as it can effectively meet the nutrients needs of the plants under controlled/stable environmental conditions (Gontier *et al.*, 2002; Sgherri *et al.*, 2010).

Interestingly, these cultivation systems are adapted to the growth of microorganisms such as arbuscular mycorrhizal fungi (AMF) (IJdo *et al.*, 2011; Garcés-Ruiz *et al.*, 2017; Cartabia *et al.*, 2021). These obligate plant symbionts, belonging to the Glomeromycota Phylum, provide their hosts with nutrients (especially N and P) in exchange for carbon and lipids (Smith and Read, 2008; Chen *et al.*, 2018). A number of studies have reported their impact on the production of secondary metabolites (SMs) in leaves, roots or fruits/tubers of different crops used as food or for medicinal purposes (Zeng *et al.*, 2013; Pandey *et al.*, 2018; Avio *et al.*, 2018; Kaur and Suseela, 2020; Zhao *et al.*, 2022). For instance, artemisinin in leaves of *Artemisia annua* L. (Chaudhary *et al.*, 2008), caffeic acid and rosmarinic acid in shoots of *Ocimum basilicum* L. (Toussaint *et al.*, 2007), and triterpenes and phenolics in *Dioscorea* spp. (Lu *et al.*, 2015) were increased in AMF-colonized plants. In addition, the AMF *Rhizophagus irregularis* MUCL 41833 was shown to modulate the primary and secondary metabolites (PMs and SMs, respectively) production of *Anchusa officinalis* L. (i.e., shoot and root tissues as well as exudates in the nutrient solution), another important Boraginaceae plant, under a semi-hydroponic (S-H) cultivation system (Cartabia *et al.*, 2021, Chapter I). A similar study, conducted with *A. officinalis* associated with different AMF species (*R. irregularis* MUCL 41833, *R. intraradices* MUCL 49410, *R. clarus* MUCL 46238, *R. aggregatus* MUCL 49408), demonstrated that specific symbiotic associations can affect the production of bioactive compounds differently in the same host (Tsiokanos *et al.*, 2022, Chapter II).

Biosynthesis of A/Sd involves two pathways, the phenylpropanoid and mevalonate pathways (Song *et al.*, 2020). Several genes, responsible for encoding enzymes involved in the biosynthesis of

shikonin, have been identified in Boraginaceae plant species (Wang *et al.*, 2014; Wu *et al.*, 2017; Takanashi *et al.*, 2019). The *p*-hydroxybenzoate geranyltransferase (*PGT*) gene plays a key role in coding the enzyme catalysing the coupling of *p*-hydroxybenzoic acid and geranyl diphosphate to produce *m*-geranyl-*p*-hydroxybenzoic acid, which is the first step in the formation of the basic carbon skeleton leading to A/Sd, and it has been cloned and characterized in *L. erythrorhizon* and *Arnebia euchroma* (Royle) Johnston cell cultures (Yazaki *et al.*, 2002; Singh *et al.*, 2010). In addition, geranylhydroquinone 3''-hydroxylase (*GHQH*), an enzyme hydroxylating the isoprenoid side chain of geranylhydroquinone (GHQ), a well-known precursor of shikonin, has also been identified in *L. erythrorhizon* cell suspension cultures (Yamamoto *et al.*, 2000). However, to our knowledge, no study has investigated the gene regulation of the biosynthesis of A/Sd in *A. tinctoria*, in particular in the presence of AMF.

In this Chapter, the main objectives were to determine whether (1) standard strains of AMF could enhance the production of A/Sd and whether this effect is more/less significant compared to AMF isolated from *A. tinctoria* grown in the wild; (2) AMF can modulate the expression of genes involved in the A/Sd biosynthetic pathway; (3) the production of A/Sd is affected similarly under semi-hydroponic and pot cultivation systems. To address these objectives, the quantification of A/Sd was performed through High-Performance Liquid Chromatography coupled with Photodiode Array detection (HPLC-PDA) and the related genes expression through Real-Time Quantitative Reverse Transcription PCR (RT-qPCR). Moreover, putative identification of the main A/Sd was performed using HPLC coupled with High-Resolution Mass Spectrometry detection (HPLC-HRMS/MS).

Material and Methods

Chemicals

All used organic solvents (i.e., n-hexane 97%, methanol, trifluoroacetic acid (TFA), and acetonitrile (ACN) (VWR INTERNATIONAL, Leuven, Belgium) were HPLC/LC-MS grade. Water was purified and demineralized with a Milli-Q system manufactured by Millipore (Bedford, MA, USA). Shikonin (purity >

98%) was purchased from Cayman Chemical Company (Biomol GmbH, Hamburg, Germany) and used as internal standard. Discovery® DSC-C18 Supelco Solid-Phase Extraction (SPE) cartridges of 500 mg bedweight and 3 mL tubes were purchased from Sigma-Aldrich (Taufkirchen, Germany).

For gene expression analysis (i.e., RNA extraction) all non-disposable materials (e.g., glass materials, mortars, pestles) were first treated with RNase AWAY™ Surface Decontaminant (ThermoFisher Scientific™, Belgium) and 0.1% diethylpyrocarbonate (DEPC)-treated sterile water. All the reagents were prepared with sterilized (121°C for 15 min) DEPC-treated water. Reagents used in RNA extraction are as follows: extraction buffer [100 mM Tris-HCl (pH 8.0), 20 mM EDTA, 1.4 M NaCl, 2% CTAB (w/v) and 2% PVP (w/v)], 2% β-mercaptoethanol (v/v), 5 M NaCl, 1.2 M NaCl, 0.38 M trisodium citrate dihydrate, chloroform, isopropanol and 70% ethanol (stored at -20°C).

Biological Materials

Rhizophagus irregularis MUCL 41833 and *Rhizophagus aggregatus* MUCL 49408 were supplied by the GINCO, and mass produced as previously described. Two other AMF (*R. irregularis* and *Septoglomus viscosum*) were isolated from *A. tinctoria* growing in a suburban pine forest, altitude 50 m of Northern Greece (Evaggelistria, Seih Sou, Thessaloniki, special collection permit obtained by the Institute of Plant Breeding and Genetic Resources, Hellenic Agricultural Organization Demeter - IPBGR, HAO Demeter). They were first trapped on *Plantago lanceolata* L. (Ecosem, Belgium) and *Medicago truncatula* Gaertn. (SARDI, Australia) to stimulate the production of numerous spores and then grown as monospores on *P. lanceolata* at the GINCO premises to obtain single species cultures (**Isolation and purification of AMF**, **Supplementary Figures 1-4** and **Supplementary Table 1**, Annex IV)**.** Two identified AMF species (*R. irregularis* and *S. viscosum*) were finally mass-produced as for the GINCO strains above. The four AMF strains were grown under greenhouse conditions at 25°C/18°C (day/night), a relative humidity (RH) of 38%, a photoperiod of 16 h day^{-1} and a photosynthetic photon flux (PPF) of 120 µmol m^{-2} s^{-1}.

Alkanna tinctoria unrooted *in vitro* explants (International Plant Exchange Network -IPEN- accession number GR-1-BBGK-17,5975)

were provide by IPBGR, HAO Demeter (Thessaloniki, Greece). The plants were proliferated on Murashige-Skoog (MS) basal medium enriched with plant growth regulators (PGRs) and rooted on Root Culture 1 (RC1) modified medium free of ammonium nitrate (Cartabia *et al.*, 2022, Chapter III). The rooted *A. tinctoria* plants were further acclimatized following different steps resulting in an optimal plant survival rate (***Alkanna tinctoria* acclimatization protocol, Supplementary Figure 5,** Annex IV). The acclimatization protocol was applied for all the experiments in order to have plants of the same age and established under identical growth conditions (first acclimatization from 2nd November 2020 to 7th December 2020 and second from 1st February 2021 to 10th March 2021).

Colonization of *A. tinctoria*

After the acclimatization phase, the plants were carefully removed from the substrate, gently washed under a stream of demineralized water, and transplanted into 1 L pots (11x11x12 cm) containing a sterilized (121°C for 15 min) substrate mixture (2 peatmoss/2 compost/1 perlite/1 quartz 0.4-0.8 mm/1 quartz 1-2 mm) (**Supplementary Figure 5**, Annex IV). Total fresh weight (TFW) of the plants was evaluated before AMF inoculation. In each experiment, plants were associated [i.e., the mycorrhizal (M) treatments] or not [i.e., the non-mycorrhizal (NM) treatments] with AMF. For the M plants, the substrate was half mixed with the AMF-inoculum substrate above, whereas for the NM treatments, the substrate was half mixed with the same AMF-inoculum substrate above but sterilized (121°C for 15 min). The plants were grown in the substrates for two months under greenhouse conditions set at 24°C/22°C (day/night), RH of 50%, photoperiod of 16 h day^{-1} and LED light (lumigrow) intensity of about 220 μmol m^{-2}s^{-1}.

Exp. 1: A/Sd production and genes expression of *A. tinctoria* associated with *R. irregularis* before and after 9 and 37 days in an S-H cultivation system

In Exp. 1, the objective was to evaluate the production of A/Sd and the expression of genes involved in the biosynthetic pathways of A/Sd in *A. tinctoria* roots colonized (later abbreviated for fluency as M^{irr}) or not (NM) with *R. irregularis* MUCL 41833, before (T0) and after 9 (T1) and 37 days (T2) of growth in the S-H cultivation system.

Two-month-old M^{irr} and NM plants were gently removed from the pots above and their roots cleaned with demineralized water to eliminate substrate debris (**Supplementary Figure 5**, Annex IV). Six plants belonging to the M^{irr} and NM treatments were randomly harvested, and AMF root colonization assessed before (T0) transfer to the S-H cultivation system. Twenty-four additional plants from the M^{irr} and NM treatments were transferred to the S-H cultivation system as previously detailed. The containers were covered with a superficial layer of black lava rock (1-3 mm) and wrapped in aluminium foil to avoid algae development as well as inhibition of shikonin production (as shikonin is sensitive to light) (Yazaki, 2017). The containers were maintained in the greenhouse set at the same conditions as described above. The same 90% P-impoverished modified Hoagland solution (**Supplementary Figure 1, Annex I**) was applied in this study, but lacking ammonium nitrate (NH_4NO_3) [as NH_4^+ is an inhibitor of shikonin production (Yazaki, 2017)]. 4.6 mm diameter black supply pipe (GARDENA®, Micro-Drip System, Ulm, Germany) were applied in this Chapter during the circulatory system to avoid shikonin production inhibition. After the acclimatization and initial flushing phases, four successive circulations were performed at a velocity of 7.5 mL min^{-1} for different durations: 42 h at day 9 (T1), 8 h at day 17, 24 and 31, and finally 42 h at day 37 (T2).

Exp. 2: A/Sd production and genes expression of *A. tinctoria* associated with different AMF strains after 9 days in an S-H cultivation system

In Exp. 2, the objective was to evaluate the production of A/Sd and the expression of genes involved in the biosynthetic pathways of A/Sd in *A. tinctoria* roots colonized (later abbreviated for fluency as M^{irr}, M^{aggreg}, M^{Rhiz}, M^{Sept}) or not (NM) with *R. irregularis* MUCL 41833, *R. aggregatus* MUCL 49408, the native *R. irregularis* and *S. viscosum* and growing for 9 days in the S-H cultivation system. The same procedure as in Exp.1 was applied. Briefly, after cleaning the roots system, two-month-old plants (6 per treatment) were transferred in the S-H cultivation system. After the acclimatization and initial flushing phases, a regular circulation was initiated and maintained at 7.5 mL min^{-1} for 42 h.

Exp. 3: A/Sd production and genes expression of *A. tinctoria* associated with different AMF strains in an 85 days pot-experiment in the greenhouse

In Exp. 3, the objective was to evaluate the production of A/Sd and the expression of genes involved in the biosynthetic pathways of A/Sd in *A. tinctoria* roots colonized (M^{irr}, M^{Rhiz}, and M^{Sept}) or not (NM) with *R. irregularis* MUCL 41833, the native *R. irregularis* and *S. viscosum* and growing for 85 days in pots under greenhouse conditions. In this experiment, *R. aggregatus* MUCL 49408 was not considered due to inoculum limitation.

The plants were gently removed from the 1 L pots above and transplanted in 3 L pots (3x18.5x17 cm) containing a sterilized (2x 121ºC for 15 min) substrate mixture (2 peatmoss/2 compost/1 perlite/1 quartz 0.4-0.8 mm/1 quartz 1-2 mm). They received 200-ml $Hoagland^{dil200X}$ solution and were randomly moved every week until harvest 45 days later. The plants were grown under the same conditions as for the S-H cultivation system in Exp. 1 and 2.

Plants biomass and AMF root colonization

For the three experiments, plants were harvested and biomass as well as AMF root colonization evaluated. In Experiment 1, plants were harvested before starting the S-H cultivation system (T0) and after 9 (T1) and 37 days (T2) corresponding to 57 and 94 days after AMF inoculation of the plants, respectively. In Exp. 2, they were harvested after 9 days (i.e., 79 days after AMF inoculation of the plants), and in Exp. 3, 85 days after AMF inoculation of the plants. The nutrient solutions at the end of Exp. 1 were kept in the bottles at 4°C in the dark before proceeding with the exudates content analysis.

Whatever the experiment, shoots were separated from roots (cleaned under demineralized water and gently dried). Shoot fresh weigh (SFW) and roots fresh weight (RFW) were then measured. Root colonization was further evaluated by McGonigle *et al.* (1990) as previously described. Roots (an approximate of 2 g fresh material) were previously cut into circa 1 cm length pieces and placed in 50 mL Falcon tubes. Around 200 root intersections were observed for each plant in Exp. 1 and 2, and around 300 intersections for the plants in Exp. 3. The total colonization percentage (TC%) of roots (e.g., hyphae, arbuscules, and vesicles/spores), and arbuscules colonization percentage (AC%) was further calculated as previously described.

The remaining root system of each replicate was divided in two parts of around 5 g each for metabolites and gene expression analysis. Regarding the metabolites analysis, roots were freeze-dried during 72 h and kept at -80°C before proceeding with A/Sd extraction. For gene expression analysis, roots were transferred within 5-10 min after sampling into liquid nitrogen and then kept at -80°C before proceeding with the RNA extraction.

Quantitative and qualitative analysis of A/Sd in *A. tinctoria* roots

Standards stock solutions, calibration curves and validation parameters

The standard stock solution of shikonin was serially diluted in HPLC-grade methanol to obtain a range of concentrations from 0.05 to 0.8 mg mL^{-1} (i.e., stock solution of 1 mg mL^{-1} of shikonin was prepared and diluted in HPLC-grade methanol to obtain the calibration solutions of 0.8, 0.6, 0.4, 0.2, 0.1 and 0.05 mg mL^{-1}). The calibration curve was made by plotting the average peak areas of three independent experiments vs the concentration of each analyte. The method was validated with three independent series of experiments based on total error and tolerance intervals (Hubert *et al.*, 2003). Specificity was evaluated by analysis of an extract sample by HPLC-HRMS and comparison of MS^1 signals of blank, shikonin standard, and *A. tinctoria* extract at 0.8 µg mL^{-1}, respectively. Linear regression equation, response function, linearity (R^2), precision, trueness, accuracy, limit of detection (LOD), limit of quantification (LOQ), and stability were provided (**HPLC quantification: methodology validation**, **Supplementary Figures 6-7** and **Supplementary Table 2**, Annex IV).

Samples Preparation

For the three experiments, primary and secondary roots of *A. tinctoria* plants were freeze-dried separately and reduced into powder using liquid nitrogen, mortar and pestle. Fifty mg of each root type was then mixed in glass test tube (labbox 10 mL neutral glass, TU04-160-100) closed with a plastic cap. Then, the total 100 mg of root material was subjected to a 20-min ultrasound-assisted extraction (two cycles), using *n*-hexane 97% (2 mL) at room temperature. The samples were finally centrifuged at 1,500 rpm for 10 min at 4°C and the supernatants

of each cycle were combined and evaporated at room temperature. The extraction protocol was adapted from Bossard *et al.* (2022). In parallel, four randomly chosen nutrient solutions from M^{irr} and NM plants sampled after 37 days (T2) in Exp. 1 were prepared for analysis as follows: 100 mL of each nutrient solution was subjected to SPE process using a C18 cartridge (500 mg/3 mL) previously preconditioned with 6 mL of MeOH, followed by an equilibration step with 6 mL of Milli-Q water. The SPE cartridges were loaded with the nutrient solutions, washed with Milli-Q water, and dried under a slight vacuum. Finally, the elution was performed, using 30 mL of methanol, and the resulting solutions were dried under a nitrogen stream. Prior to analysis, the plant extracts residues were weighed and solubilised in methanol and were filtered through a 45-µm PTFE membrane (Whatman™, Maidstone, UK). Each sample was adjusted to the final concentration of 2 mg mL^{-1}, using methanol LCMS-grade.

HPLC-PDA and HPLC-HRMS/MS analysis

For the three experiments, the quantification of HNQ enantiomers (A/Sd) in their free form (not linked to sugars) was performed following the protocol of Bossard *et al.* (2022). For HPLC-PDA analysis, the system consists in an Accela HPLC system (Thermo Fischer Scientific™, Bremen, Germany) coupled with a photodiode array (PDA) detector, an autosampler equipped with a conventional sample tray compartment with its cooler (set at 4°C), an injection system with a sample loop of 20 µL, and a quaternary pump, all piloted by ChronQuest software. The column used was an Alltech ALLTIME C8 250x4.6 mm, packed with 5 µm particles. Twenty µL of sample was injected in full loop injection mode by the autosampler. The column was eluted at constant flow rate of 1 mL min^{-1} using a binary solvent system: solvent A, MilliQ water 0.1% TFA and solvent B, ACN, isocratic mode (25% A: 75% B). Quantification analyses were conducted at a wavelength of 510 nm corresponding to the maximum absorption of A/Sd and their content was calculated according to the shikonin standard curve. The total shikonin equivalent production was calculated as the sum of peaks corresponding to A/Sd free forms (i.e., by integration of the different peaks identified as A/Sd-type compounds by their UV spectra) contained in the root powder, reported as mg g^{-1} root powder using the same shikonin standard curve (so not corresponding to an absolute quantification of each compound). Peaks

were identified by comparing their retention times (RT) and UV spectra with the standard chromatogram of shikonin. The chromatographic profiles are in agreement with the chemical profile reported by Bossard *et al.* (2022), for A/Sd obtained from *A. tinctoria* roots. In total, 18 M and 18 NM root samples (6 NM and 6 M^{irr} plants for each time harvest-T0, T1 and T2) were considered in Exp. 1, 30 root samples (6 M^{irr}, 6 M^{aggreg}, 6 M^{Rhiz}, 6 M^{Sept}, and 6 NM) in Exp. 2, and 24 root samples (6 M^{irr}, 6 M^{Rhiz}, 6 M^{Sept}, and 6 NM) in Exp. 3. All samples were analysed in duplicates.

The HPLC-HRMS/MS analysis was performed at the end of Exp. 2 and 3 on an HPLC-PDA-HRMS system consisting of an Accela pump and PDA detector (ThermoFisher Scientific™, Bremen, Germany) connected with a LTQ orbitrap XL mass spectrometer (ThermoFisher Scientific™, Bremen, Germany). The instrument was controlled using a ThermoFisher Scientific™ Xcalibur X software. The LC separation was done as reported above except for the solvent A: MilliQ water 0.1% formic acid (FA). The chromatograms were recorded between 200 and 600 nm. HRMS analyses were realised in ESI positive and negative modes with the following inlet conditions for the positive mode: capillary temperature 250°C; sheath gas flow 10 a.u.; auxiliary gas flow 5 a.u. and sweep gas flow 5 a.u.; ionisation spray voltage 3 kV; capillary voltage of 15 V; tube lens voltage of 90 V. For negative mode, the only differences from the positive mode were the capillary voltage (-10 V) and tube lens voltage (-125 V). The data-dependent MS/MS events were performed on the three most intense ions detected in full scans MS. Peaks were tentatively identified by comparing their HRMS and MS/MS spectra with the literature data of A/Sd.

MS data treatment, organization and dereplication

All HRMS run data (.RAW) files were treated using MZmine software suite version 2.5.3 (Pluskal *et al.*, 2010). For mass detection at MS^1 level, the noise level was set to $1.5x10^4$ for positive mode and to $8.5x10^3$ for negative mode. For MS^2 detection, the noise level was set to 1. The ADAP chromatogram builder was used and set to a minimum group size of scans of 4, a minimum group intensity of $1.0x10^4$, a minimum highest intensity of $1.0x10^4$, and *m/z* tolerance of 8 ppm. The ADAP algorithm (wavelets) was used for chromatogram deconvolution. The intensity window signal to noise (S/N) was used as

a S/N estimator with S/N ratio set at 10, a minimum feature height of $1.0x10^4$, a coefficient area threshold at 25, a peak duration ranging from 0.02 to 0.8 min, and the RT wavelet range from 0.02 to 0.2 min. Isotopes were detected using the isotope peak grouper with a *m/z* tolerance of 8 ppm, a RT tolerance of 0.02 min (absolute), the maximum charge set at 1, and the representative isotope used was the most intense. Then, the aligned list peak was gap-filled with RT range of 0.05 min and *m/z* tolerance of 8 ppm. The resulting list was filtered using the peak list rows filter option to remove all the duplicates and all the features without MS^2 spectrum associated.

A molecular network was constructed from the .mgf file exported from MZmine, using the online workflow on the GNPS website (Wang *et al.*, 2016). The precursor ion mass tolerance was set to 0.02 Da with a MS/MS fragment ion tolerance of 0.02 Da. A network was then created where edges were filtered to have a cosine of 0.7 and more than 3 matched peaks. The spectra in the network were then searched against GNPS's spectral libraries filtered under the same conditions as before. Putative identification was carried out comparing available MS/MS fragmentation patterns from the literature. Data visualization was achieved using Cytoscape 3.8.0 (Shannon *et al.*, 2003). Peak area data from the .csv file obtained from MZmine was added to the network. Size nodes were set proportionally to the total area of each peak detected in both analysed extracts.

Analysis of A/Sd target genes expression in *A. tinctoria* roots

Total RNA extraction

Frozen roots of each replicate were ground in liquid nitrogen (-196°C) with a pestle and mortar. Total RNA extraction was done on 0.2 g root material using the protocol from Xu *et al.* (2010) slightly modified as previously described. Further, the total RNA was treated with TURBO DNA-free™ Kit (Thermo Fisher Scientific™, Belgium), according to the manufacturer protocol. The RNA of all samples was loaded on 1.5% agarose gel, electrophoresed to separate RNA, stained with GelRed® (Biotium, United States), and visualised under UV light to assess the integrity of ribosomal bands. Moreover, concentration of each RNA sample was measured using NanoDrop® -ND 1000 UV-vis Spectrophotometer (NanoDrop Technologies, United States) and RNA purity estimated from the A260/A280 and A260/A230 absorbance ratios. Finally, a 1 µg aliquot of total RNA was used for the first-strand cDNA synthesis according to the protocol of the Transcriptor High

Fidelity cDNA Synthesis Kit (Roche, Montreal, QC, Canada). For each RNA sample, a reaction without Transcriptor High Fidelity Reverse Transcriptase (Hifi RT) enzyme was performed as a control for contamination by genomic DNA.

Five biological replicates (i.e., means of relative genes expression) for M and NM treatments at each time harvest (T0, T1, and T2) were considered in Exp. 1, six biological replicates for each treatment (M^{irr}, M^{aggreg}, M^{Rhiz}, M^{Sept}, and NM) in Exp. 2, and six biological replicates for each treatment (M^{irr}, M^{Rhiz}, and NM) and five for M^{Sept} in Exp. 3. For all the experiments, tissue samples for A/Sd and molecular determinations were simultaneously collected at the same period of the day, between 9:00 and 11:00 a.m.

Real-Time quantitative PCR (RT-qPCR)

For RT-qPCR, the expression of three target genes: *LePGT1*, *LePGT2* and *GHQH* involved in the shikonin (A/Sd) biosynthesis was analysed as previously described. Since no published genomic resources are available for *A. tinctoria*, a previously published primer for amplification of *LePGT1* in *Onosma paniculatum* Bur. *et* Franch was used, while for *PGT2* and *GHQH* new primer pairs were designed. Sequences of each gene (*LePGT2* or *GHQH*) from two phylogenetically distant Boraginaceae species (*L. erythrorhizon* and *A. euchroma*) were obtained from NCBI, aligned, and primers generated from conserved regions (**Supplementary Figure 8, Alignments used to design primers,** Annex IV). The glyceraldehyde-3-phosphate dehydrogenase gene (*GAPDH*) was used as internal reference control. RT-qPCR was performed using a LightCycler® FastStart Essential DNA Green Master (Roche) in 10 µL volume of reaction formed as follows: 5 µL Master mix (or Mix SYBR 2x), 0.5 µL of each primer from the pair (10 µM), and 4 µL cDNA (dil 5x). The reaction was carried out in a Roche LightCycler® 96 System using the following parameters: 10 min at 95°C, followed by 40 (for housekeeping gene) and 50 (for target genes) cycles of denaturation (95°C, 10 s)/annealing (60°C housekeeping gene/56°C target genes, 15 s)/extension (72°C, 10 s), and finalized by a standard melting curve analysis (95°C). Reactions were performed in three replicates. Normalization was achieved for each experiment separately using the reference gene (i.e., *GAPDH*) and the "Pfaffl" method as previously described (Pfaffl, 2001).

Statistical Analysis

For all the experiments, a one-way ANOVA followed by HSD Tukey post-hoc test ($p < 0.05$) was applied to discriminate between means of growth parameters (i.e., SFW, RFW, and TFW), AMF colonization (i.e., TC% and AC%), A/Sd content, and relative genes expression at different time points (Exp. 1) or different AMF treatments (Exp. 2 and 3). Moreover, in Exp. 1, differences between M and NM treatments were highlighted by pairwise comparison with Bonferroni correction ($p < 0.05$) at each harvesting time (T0, T1, and T2). For all parameters, normal distribution of residuals variance and normality was checked before analyses. Non-normal data were normalized by log10 transformation before analysis. Data analyses were performed by IBM SPSS Statistics for Windows, version 28 (IBM Corp., Armonk, N.Y., USA).

Results

Exp. 1: A/Sd production of *A. tinctoria* associated with *R. irregularis* before and after 9 and 37 days in an S-H cultivation system

Plants biomass and root colonization by AMF

Biomass (i.e., SFW, RFW and TFW) and AMF root colonization (i.e., TC% and AC%) of *A. tinctoria* plants in M^{irr} and NM treatments were assessed before their transfer to the containers (T0), and after 9 (T1) and 37 (T2) days of growth in the S-H cultivation system (**Table 13**). No significant differences between harvesting times were noticed in the SFW, RFW and TFW of plants in the M^{irr} treatment and the SFW of plants in the NM treatment. Conversely, a significantly greater RFW was noticed at T1 and T2 as compared to T0, and greater TFW at T2 compared to T0 for plants in the NM treatment. Irrespective of the harvest time, no significant difference was reported between the SFW of plants in the M^{irr} and NM treatments, while at T2, the RFW and TFW in the NM treatment was significantly higher than that in the M^{irr} treatment. In the M^{irr} treatment, a significant decrease in TC% was observed at T2 compared to T0 and T1 and in AC% at T1 and T2 compared to T0. No root colonization was observed in NM plants.

A/Sd content

The content of A/Sd in the roots of *A. tinctoria* plants in the M^{irr} and NM treatments was evaluated before their transfer to the containers (T0), and after 9 (T1) and 37 (T2) days of growth in the S-H cultivation system (**Table 13**). Whatever the harvesting time (T0, T1 or T2) or treatment (M^{irr} or NM) no significant differences in content of A/Sd were noticed. Moreover, in the nutrient solution, only few small peaks lower than the limit of detection (LOD) were observed at the corresponding retention times of A/Sd, indicating their quasi absence in the exudates.

A/Sd target genes expression

The relative expression of the three target genes (*LePGT1*, *LePGT2* and *GHQH*) involved in the biosynthesis of A/Sd in the roots of *A. tinctoria* plants in the M^{irr} and NM treatments was evaluated before their transfer to the containers (T0) and after 9 (T1) and 37 (T2) days of growth in the S-H cultivation system (**Table 14**). Whatever the time of evaluation (T0, T1 or T2) or treatment (M^{irr} or NM) no significant differences were noticed in gene expression of *GHQH*. Similarly, no significant differences between harvesting times were observed in expression of *LePGT1* gene of the plants in the M^{irr} treatment and expression of *LePGT1* and *LePGT2* genes of the plants in the NM treatment. Conversely, a significantly higher expression of *LePGT2* gene was observed at T2 compared to T1 for the plants in the M^{irr} treatment, while an intermediate gene expression was noticed at T0. A significant higher relative expression of both *LePGT1* and *LePGT2* genes was observed in the plants of the M^{irr} treatment compared to that of the NM treatment at T2.

Exp. 2: A/Sd production and genes expression of *A. tinctoria* associated with different AMF strains after 9 days in an S-H cultivation system

Plants biomass and root colonization by AMF

Biomass (i.e., SFW, RFW and TFW) and AMF root colonization (i.e., TC% and AC%) of *A. tinctoria* plants in M^{irr}, M^{aggreg}, M^{Rhiz}, M^{Sept} and NM treatments were assessed after 9 days of growth in the S-H cultivation system (**Table 13**). No significant differences were observed in the biomass and TC% between the different treatments. Conversely, a significant higher AC% was observed for the plants in

the M^{Rhiz} treatment compared to those in the M^{aggreg} treatment, while intermediate values were noticed in the plants of the M^{Sept} and M^{irr} treatments. No root colonization was observed in NM plants.

A/Sd content

The content of A/Sd in the roots of *A. tinctoria* plants in the M^{irr}, M^{aggreg}, M^{Rhiz}, M^{Sept}, and NM treatments was evaluated after 9 days of growth in the S-H cultivation system (**Table 13**). A significant higher content of total A/Sd expressed as shikonin equivalent was observed in the plants of the M^{Rhiz} treatment compared to those in the M^{irr}, M^{agreeg} and NM treatments, while an intermediate value was observed for the plants of the M^{Sept} treatment.

A/Sd target genes expression

The relative expression of the three target genes (*LePGT1*, *LePGT2* and *GHQH*) involved in the biosynthesis of A/Sd in the roots of *A. tinctoria* plants in the M^{irr}, M^{aggreg}, M^{Rhiz}, M^{Sept} and NM treatments was evaluated after 9 days of growth in the S-H cultivation system (**Table 14**). Whatever the treatment, no significant differences were observed in expression of *GHQH* and *LePGT1* genes. A significant lower relative expression of *LePGT2* was observed in the plants of the M^{Rhiz} treatment compared with the other treatments that did not differ among them.

Table 13. Shoot, root and total fresh weights (SFW, RFW, TFW, respectively), total colonization percentage (TC%), arbuscules colonization percentage (AC%), and total A/Sd expressed as shikonin equivalent content of *A. tinctoria* plants inoculated (M^{irr}) or not (NM) with *R. irregularis* MUCL 41833 before (T0) and after 9 (T1) and 37 (T2) days in the S-H cultivation system (Exp. 1), and of *A. tinctoria* plants inoculated (M^{irr}, M^{aggreg}, M^{Rhiz}, M^{Sept}) or not (NM) with different AMF strains (two from GINCO - *R. irregularis* MUCL 41833 and *R. aggregatus* MUCL 49408, and two isolated from wild *A. tinctoria* – *R. irregularis* and *S. viscosum*) after 9 days in the S-H cultivation system (Exp. 2).

Exp. 1

Treatments	Time	SFW (g)	RFW (g)	TFW (g)	TC%	AC%	Total shikonin equivalent mg g^{-1} root powder
M^{irr}	T0	14 ± 2.3	10 ± 1.6	24 ± 2.4	61 ± 7 **a**	34 ± 4 **a**	3.3 ± 1.5
	T1	13 ± 2.7	10.8 ± 2.2	23.7 ± 3.6	53 ± 7 **a**	17 ± 5 **b**	1.9 ± 1.5
	T2	13 ± 1.2	12.4 ± 1.1*****	25.7 ± 2*****	29 ± 4 **b**	12 ± 3 **b**	2.1 ± 1
NM	T0	13.5 ± 2	7.9 ± 2.3 **b**	21.4 ± 3.8 **b**	-	-	2.5 ± 1
	T1	14.2 ± 2	11 ± 2.4 **a**	25.2 ± 3.7 **ab**	-	-	2.6 ± 1.1
	T2	13.6 ± 0.6	14 ± 1 **a***	28 ± 1 **a***	-	-	2.3 ± 0.7

Exp. 2						
Treatments	**SFW (g)**	**RFW (g)**	**TFW (g)**	**TC%**	**AC%**	**Total shikonin equivalent mg g^{-1} root powder**
M^{Rhiz}	9.8 ± 1	11.3 ± 1	21 ± 1.8	44 ± 7	21 ± 5 **a**	8.7 ± 1.3 **a**
M^{Sept}	11.1 ± 2	13.1 ± 2.6	24.2 ± 1	39 ± 9	17 ± 7 **ab**	6.8 ± 2.2 **ab**
M^{irr}	11.2 ± 1	12.8 ± 1.7	24.2 ± 2.4	42 ± 6	16 ± 2 **ab**	4.3 ± 2.1 **b**
M^{aggreg}	10.3 ± 5	11 ± 3.3	20 ± 5	43 ± 9	12 ± 4 **b**	5 ± 0.6 **b**
NM	10.3 ± 2	11 ± 2.1	21.5 ± 3.3	-	-	4.9 ± 1.9 **b**

The parameters measured are expressed as mean ± standard deviation (SD) of five replicates per treatment (M^{irr} and NM) and harvesting time (T0, T1, and T2) in Exp. 1, and 6 replicates per treatment (M^{irr}, M^{aggreg}, M^{Rhiz}, M^{Sept} and NM) in Exp. 2. Means followed by different lowercase letters within the same column are significantly different according to HSD Tukey post-hoc test ($p < 0.05$) (Exp. 1 and 2). Means followed by * within the same column are significantly different according to pairwise comparison with Bonferroni correction ($p < 0.05$) (Exp. 1).

Table 14. RT-qPCR relative genes expression analysis of *GHQH*, *LePGT1*, and *LePGT2* in *A. tinctoria* roots inoculated (M^{irr}) or not (NM) with *R. irregularis* MUCL 41833 before (T0) and after 9 (T1) and 37 (T2) days in the S-H cultivation system (Exp. 1), and in *A. tinctoria* roots inoculated (M^{irr}, M^{aggreg}, M^{Rhiz}, M^{Sept}) or not (NM) with different AMF strains (two from GINCO - *R. irregularis* MUCL 41833 and *R. aggregatus* MUCL 49408, and two isolated from wild *A. tinctoria* – *R. irregularis* and *S. viscosum*) after 9 days in the S-H cultivation system (Exp. 2).

Exp. 1

Treatments	Time	*GHQH*	*LePGT1*	*LePGT2*
M^{irr}	T0	2.7 ± 3.5	3 ± 5	2.5 ± 3.8 **ab**
	T1	0.8 ± 0.2	1 ± 0.7	0.9 ± 0.5 **b**
	T2	1.9 ± 1.4	5.5 ± 4*****	5.2 ± 3.6 **a***
NM	T0	1.1 ± 0.6	1.2 ± 0.7	1.2 ± 0.7
	T1	1.2 ± 0.7	1.1 ± 0.6	1.1 ± 0.6
	T2	1 ± 0.2	1 ± 0.4*****	1.1 ± 0.4*****

Exp. 2

Treatments	*GHQH*	*LePGT1*	*LePGT2*
M^{Rhiz}	1.4 ± 0.3	1.6 ± 1.2	0.05 ± 0.02 **b**
M^{Sept}	1.5 ± 0.4	0.9 ± 0.6	0.7 ± 0.4 **a**
M^{irr}	1.1 ± 0.2	0.9 ± 0.8	0.7 ± 0.6 **a**
M^{aggreg}	1.4 ± 0.3	0.9 ± 0.8	0.7 ± 0.6 **a**
NM	1.0 ± 0.4	1.8 ± 1.6	1.4 ± 1.6 **a**

The parameters measured are expressed as mean ± standard deviation (SD) of five replicates per treatment (M^{irr} and NM) at each harvesting time (T0, T1, and T2) in Exp. 1 and of 6 replicates per treatment (M^{irr}, M^{aggreg}, M^{Rhiz}, M^{Sept} and NM) in Exp. 2. Means followed by different lowercase letters within the same column are significantly different according to HSD Tukey post-hoc test ($p < 0.05$) (Exp. 1 and 2). Means followed by * within the same column are significantly different according to pairwise comparison with Bonferroni correction ($p < 0.05$) (Exp. 1).

Exp. 3: A/Sd production and genes expression of *A. tinctoria* associated with different AMF strains in a 85 days pot-experiment in greenhouse

Plants biomass and root colonization by AMF

Biomass (i.e., SFW and RFW) and AMF root colonization (i.e., TC% and AC%) of *A. tinctoria* plants in M^{irr}, M^{Rhiz}, M^{Sept} and NM treatments were assessed after 85 days of growth in pots (**Table 15**). No significant differences were observed in SFW and RFW between the different treatments. Similarly, no significant differences were observed for TC% between the different treatments, while a significantly higher AC% was observed for the plants in the M^{Sept} treatment compared to those of the M^{irr} treatment. Plants in the M^{Rhiz} treatment had intermediate value. No root colonization was observed for NM plants.

A/Sd content

The content of A/Sd in the roots of *A. tinctoria* plants in the M^{irr}, M^{Rhiz}, M^{Sept}, and NM treatments was evaluated after 85 days of growth in pots (**Table 15**). A significantly higher content of shikonin, whose values were nevertheless below the limit of quantification (LOQ, **Supplementary Table 2,** Annex IV), and in total A/Sd expressed as shikonin equivalent, was reported in the roots of the plants in the M^{Rhiz} treatment compared to the other treatments.

A/Sd target genes expression

The relative expression of the two target genes (*GHQH* and *LePGT1*) involved in the biosynthesis of A/Sd in the roots of *A. tinctoria* plants of the M^{irr}, M^{Rhiz}, M^{Sept}, and NM treatments was evaluated after 85 days of growth in pots. In this experiment, *LePGT2* target gene was not considered due to contamination by the primer dimer. Whatever the treatment, no significant differences were observed in expression of *GHQH* and *LePGT1* genes (data not presented).

Table 15. Shoot and root fresh weights (SFW, RFW, respectively), total colonization percentage (TC%), arbuscules colonization percentage (AC%), shikonin and total A/Sd expressed as shikonin equivalent of *A. tinctoria* inoculated (M^{irr}, M^{Rhiz}, M^{Sept}) or not (NM) with different AMF strains (one from GINCO - *R. irregularis* MUCL 41833, and two isolated from wild *A. tinctoria* – *R. irregularis* and *S. viscosum*) and growing for 85 days in pots under greenhouse conditions.

Treatments	**SFW (g)**	**RFW (g)**	**TC%**	**AC%**	**mg shikonin g^{-1} root powder**	**Total shikonin equivalent mg g^{-1} root powder**
M^{irr}	15.8 ± 2	13.3 ± 2.6	25 ± 6.6	4 ± 2 **b**	0.04 ± 0.01 **b**	7.2 ± 1 **b**
M^{Rhiz}	17.7 ± 0.6	14 ± 2.1	23 ± 16	8 ± 10 **ab**	0.12 ± 0.07 **a**	9.6 ± 0.7 **a**
M^{Sept}	16.3 ± 2.3	12.8 ± 1.7	25 ± 13	22 ± 11 **a**	0.06 ± 0.02 **b**	7.8 ± 1 **b**
NM	16.1 ± 1.3	14.4 ± 0.6	-	-	0.04 ± 0.01 **b**	8 ± 1 **b**

The parameters measured are expressed as mean ± standard deviation (SD) of 6 replicates per treatment (M^{irr}, M^{Rhiz}, M^{Sept} and NM). Means followed by different lowercase letters within the same column are significantly different according to HSD Tukey post-hoc test ($p < 0.05$).

HPLC-HRMS/MS analysis

To better recognise the metabolites produced in *A. tinctoria* roots, the main chemical compounds were tentatively identified in Exp. 2 and 3 by performing a dereplication strategy based on HPLC-HRMS/MS analysis (**Figure 39, Tables 16-17**) and molecular network organization (**Figures 40-42**). These analyses were not performed in Exp. 1 since no significant differences were reported in the production of A/Sd.

In Exp. 2, the HPLC-HRMS/MS analysis was performed in positive and negative modes. However, shikonin was not detected in any root samples analysed. Dereplication analyses of shikonin derivatives were done on positive mode to compare our results with published data available in the literature (Bossard *et al.*, 2022). The major detected compounds were organized in two distinctive clusters: A/Sd naphthoquinones (cluster A, **Figure 40A, Table 16**) and lipid amides derivatives (cluster B, **Figure 40B, Table 16**). In cluster A, the first eluted derivative was putatively identified as a methylshikonin isomer (**1**) which gave a protonated molecular ion $[M+H]^+$ at *m*/*z* 303 and fragmented to *m*/*z* 285, 243 and 233, corresponding to the loss of a H_2O molecule, a $C_2H_4O_2$ and a C_5H_{10} fragment from the alkyl chain. Similar fragmentation pattern was observed for compound **4** with a protonated dehydrated molecular ion $[M+H-H_2O]^+$, putatively identified as a second methylshikonin derivative. Similar loss was observed for compounds **3** and **6**, putatively corresponding to methyl-1'-deoxyshikonin and anhydro alkannin at *m*/*z* of 287 and 271, respectively. Data also indicated that the major shikonin derivative produced by the plant under these conditions was anhydroalkanin (**6**) (Kyogoku *et al.*, 1973; Bai and Jin, 1994). Moreover, a group of lipid amides were also putatively detected from the *A. tinctoria* roots samples and represented in cluster B. These amides derivatives were tentatively identified as palmitoleamide (**7**), linoleamide (**8**), oleamide (**9**) and stearamide (**10**) with protonated molecular ions $[M+H]^+$ at *m*/*z* 254, 280, 282 and 284, presenting a loss of a fragment of *m*/*z* 17, corresponding to the loss of an ammoniac molecule (Divito *et al.*, 2012). Other isomeric compounds were also detected by HPLC-HRMS/MS, but the absence of their fragmentation patterns, putative identities are not proposed. No significant differences were noticed in the metabolites' production profile of *A. tinctoria* roots associated or not with different AMF strains (**Figure 41**).

In Exp. 3, shikonin was detected only in negative mode and this result was corroborated by co-injection with shikonin standard solution (**Table 17**). Due to the important differences in the fragmentation spectra in positive mode of A/Sd, clusters of these compounds were not formed (**Figure 42**). In addition, the abovementioned shikonin derivatives isomers (**1** and **6**) were also observed as deprotonated molecular ion $[M-H]^-$ at *m*/*z* 301 with fragmentation signals at *m*/*z* 286 and 232 corresponding to the loss of a CH_3 and C_5H_9 groups, for **1**, and at *m*/*z* 269 with fragment loss at *m*/*z* 251 and 241, corresponding to the loss of a H_2O and CO molecules, for **6**. The deprotonated molecular ion $[M-H]^-$ of shikonin (**11**) was observed at *m*/*z* 287 with fragmentation signals at *m*/*z* 218 and 190, corresponding to the loss of C_5H_9 and the subsequent loss of a CO group (Liao *et al.*, 2015). Moreover, an additional shikonin derivative was observed with a deprotonated molecular ion $[M-H]^-$ at *m*/*z* 329, putatively identified as acetylshikonin (**13**), with fragmentation loss at *m*/*z* 269, 251 and 241 corresponding to a McLafferty rearrangement (i.e., neutral loss of acetic acid), and the subsequent loss of a H_2O and CO molecules (Liao *et al.*, 2015). Three others unidentified compounds (**12**, **14** and **15**) were detected under negative mode ionisation with deprotonated molecular ion $[M-H]^-$ at *m*/*z* 797, 1111 and 1147. However, no clusters were observed between compounds **1**, **6**, **11** and **13** (shikonin derivatives) and for **12**, **14** and **15** (unknow compounds) because they show a low degree of similarities in their fragmentation spectra (in positive ionisation mode).

Slightly differences in metabolites production were observed between Exp. 2 and 3, when samples were analysed in the same ionisation mode. Nevertheless, the most important difference between the two experiments was the detection of shikonin only in Exp. 3. Analyses performed in negative mode for root samples of Exp. 2 did not show the presence of shikonin. Similarly, in Exp. 3, no significant differences were observed in the metabolites' production profile of *A. tinctoria* roots associated or not with different AMF strains, thus producing similar chromatographic profiles.

Table 16. Putative identification of major chemical constituents in *A. tinctoria* extracts from Exp. 2 (positive mode ESI).

	Code	Retention time [min]	UV	[*m/z*]	MS Major Ion(s)	Molecular Formula	Δppm	ΔmDa	MS/MS Fragments [*m/z*]	Putative Identification
Cluster A	**1**	4.60	513, 272	303.1224	$[M+H]^+$	$C_{17}H_{18}O_5$	-2.80	-0.85	285.1119 243.1013 233.0442	methylshikonin isomer I
	2	5.41	n.d.	220.1119	$[M+H]^+$	$C_{16}H_{13}N$	-3.29	-0.72	205.0883 142.0648 128.0618	*N*-phenyl-naphthylamine
	3	5.66	515, 272, 489	287.1267	$[M+H]^+$	$C_{17}H_{18}O_4$	-5.69	-1.63	219.0649 269.1168 231.0648 245.0804	*O*-methyl-1'-deoxyshikonin
	4	6.74	415, 258	285.1125 303.1228	$[M+H-H_2O]^+$ $[M+H]^+$	$C_{17}H_{18}O_5$	-0.65	-0.18	267.1012 243.0649 233.0443	methylshikonin isomer II
	5	7.16	n.d.	403.2317	$[M+H]^+$	$C_{20}H_{34}O_8$	-3.70	-1.49	361.2221 329.1594 273.0968 213.0757	not identified

Continue in the next page…

	Code	Retention time [min]	UV	[*m/z*]	MS Major Ion(s)	Molecular Formula	Δppm	ΔmDa	MS/MS Fragments [*m/z*]	Putative Identification
	6	8.00	517, 484, 281	271.0955 541.1843	$[M+H]^+$ $[2M+H]^+$	$C_{16}H_{14}O_4$	-5.66	-1.53	229.0493 253.0855 165.0181 191.0338 179.0338 243.1014	anhydroalkannin
Cluster B	**7**	8.76	n.d.	254.2475	$[M+H]^+$	$C_{16}H_{31}NO$	-3.50	-0.89	237.2209 219.2104	palmitoleamide
	8	9.52	n.d.	280.2627 559.5198	$[M+H]^+$ $[2M+H]^+$	$C_{18}H_{33}NO$	-4.78	-1.34	263.2365 245.2260	linoleamide
	9	12.33	n.d.	282.2793 563.2793	$[M+H]^+$ [2M+H]+	$C_{18}H_{35}NO$	-1.38	-0.39	265.2522 247.2417	oleamide
	10	17.87	n.d.	284.2943	[M+H]+	$C_{18}H_{37}NO$	-3.66	-1.04	267.2267	stearamide

Δm = mass errors; $[M-H]^+$ = *m/z* of the protonated molecular ion in positive ionisation mode; *m/z* = mass to charge ratio.

Table 17. Putative identification of major chemical constituents in *A. tinctoria* extracts (Exp. 3, negative mode, ESI).

Code	Retention time [min]	UV	[*m/z*]	MS Major Ion(s)	Molecular Formula	Δppm	ΔmDa	MS/MS Fragments [*m/z*]	Putative Identification
1	4.60	513, 272.	301.1086	$[M-H]^-$	$C_{17}H_{18}O_5$	3.30	1.00	286.0847 232.0375	methylshikonin isomer I
11	4.78	515, 274, 490	287.0934	$[M-H]^-$	$C_{16}H_{16}O_5$	5.06	1.45	218.0227 190.0273	shikonin
12	5.26	n.d.	797.2762	$[M-H]^-$	$C_{33}H_{50}O_{22}$	5.83	4.65	527.1894	not identified
13	5.85	516, 274, 490	329.1030	$[M-H]^-$	$C_{18}H_{18}O_6$	1.48	0.49	269.0829 251.0709 241.0865	acetylshikonin
14	7.62	n.d.	1111.3696	$[M-H]^-$	$C_{47}H_{68}O_{30}$	-1.90	-2.12	841.2741 571.1847 1023.3120	not identified

Continue in the next page…

Code	Retention time [min]	UV	[*m/z*]	MS Major Ion(s)	Molecular Formula	Δppm	ΔmDa	MS/MS Fragments [*m/z*]	Putative Identification
15	7.98	n.d.	1147.3676	$[M-H]^-$	$C_{50}H_{68}O_{30}$	-3.59	-4.12	877.2743 607.1854 1047.3101	not identified
6	8.00	517, 484, 281	269.0829	$[M-H]^-$	$C_{16}H_{14}O_4$	5.63	1.52	251.0712 241.0868	anhydroalkannin

Δm = mass errors; $[M-H]^-$ = *m/z* of the deprotonated molecular in negative ionisation mode; *m/z* = mass to charge ratio.

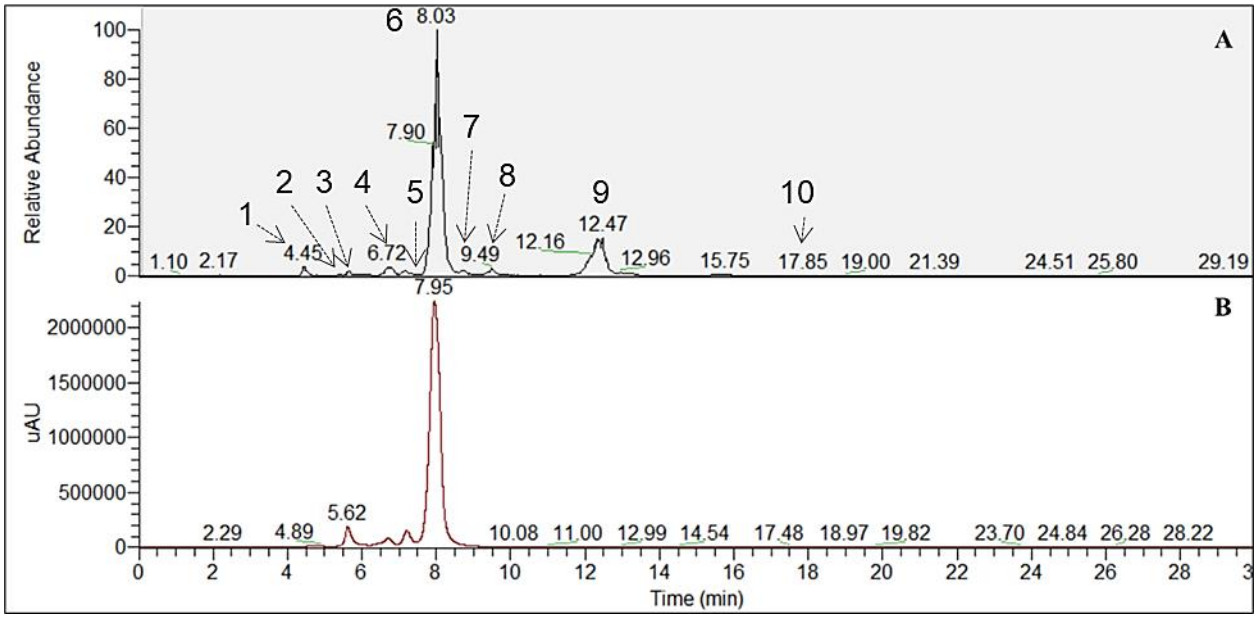

Figure 39. Chromatographic profile of *A. tinctoria* root samples associated with *Septoglomus viscosum* detected under **(A)** HPLC-MS (BP+) and **(B)** HPLC-PDA (510 nm). Each peak defined by a number referred to a tentative identified compound, which has been described in Table 16.

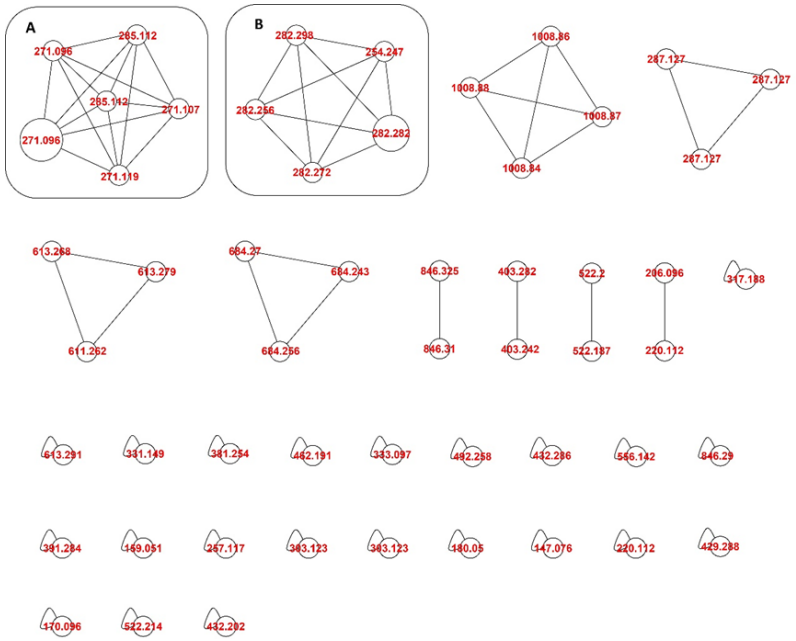

Figure 40. Molecular network of *A. tinctoria root* extracts obtained in Exp. 2 in positive mode. **(A)** HNQ naphthoquinone's enantiomers (A/Sd); **(B)** lipide amides. Clusters were built with a cosine of 0.7 with a minimum of 3 common ions. Size nodes are proportional to corresponding peak area.

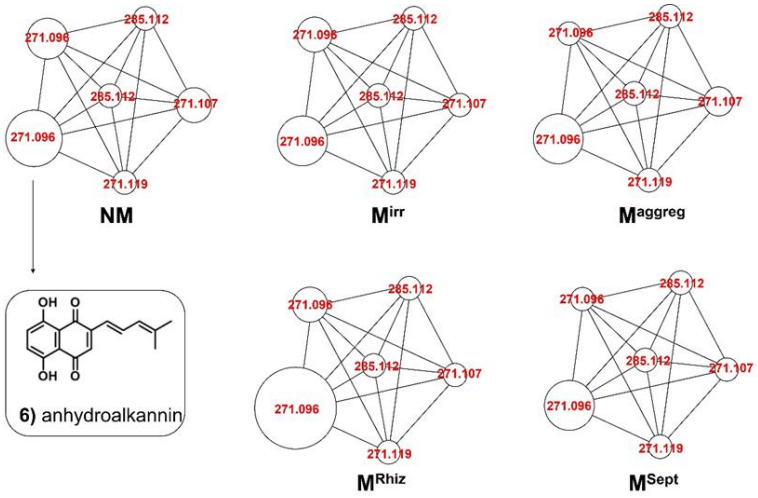

Figure 41. Comparative molecular networking of shikonin derivatives cluster (different nodes) between *A. tinctoria* roots inoculated or not (control) with different AMF strains (two from GINCO - *R. irregularis* MUCL 41833 and *R. aggregatus* MUCL 49408, and two isolated from wild *A. tinctoria* – *R. irregularis* and *S. viscosum*) and growing for 9 days in the S-H cultivation system (Exp. 2).

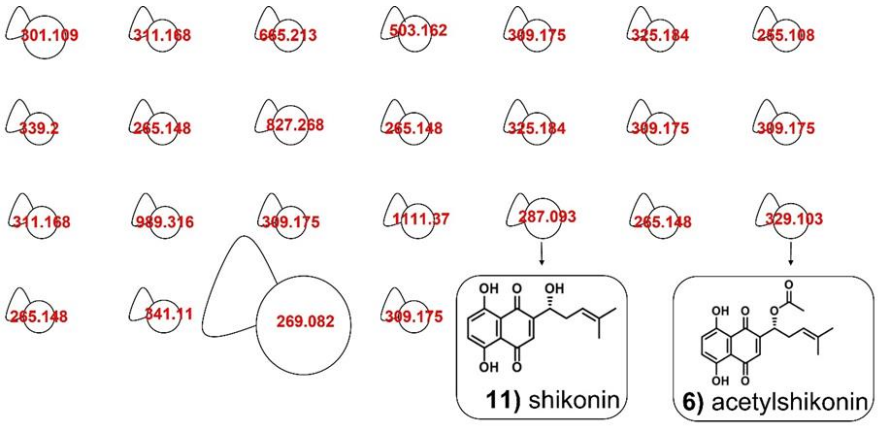

Figure 42. Molecular network if *A. tinctoria* root extracts obtained in Exp. 3 in negative mode. Size nodes are proportional to corresponding peak area.

Discussion

In the present Chapter, two native AMF strains isolated from *A. tinctoria* roots and two strains from GINCO were tested and compared on the production of A/Sd and on the expression of genes involved in A/Sd biosynthesis in *A. tinctoria* plants grown either in a semi-hydroponic or in a pot cultivation system. In Exp. 1, conducted only with the GINCO strain *R. irregularis* MUCL 41833, no effect was observed on the production of A/Sd, while a significantly higher relative expression of LePGT2 was observed after 37 days compared to 9 days of growth in the S-H cultivation system. Furthermore, the relative expression of *LePGT1* and *LePGT2* genes were significantly higher in the plants colonized with this AMF compared to the non-mycorrhized plants. In Exp. 2, four AMF strains (two from GINCO: *R. irregularis* MUCL 41833 and *R. aggregatus* MUCL 49408 and two isolated from *A. tinctoria*: *R. irregularis* and *S. viscosum*) were associated to *A. tinctoria* in the S-H cultivation system. The native strain *R. irregularis* significantly increased the production of A/Sd in the roots of *A. tinctoria*, although this was not accompanied by an increased expression of genes involved in the A/Sd biosynthesis pathway. In Exp. 3, the two native strains (*R. irregularis* and *S. viscosum*) and the GINCO one (*R. irregularis* MUCL 41833) were associated to *A. tinctoria* in pots. The native strain *R. irregularis* was confirmed to significantly enhance the content of shikonin and total

A/Sd in *A. tinctoria* roots. However, no significant increase in relative genes expression was observed.

The S-H and pot cultivation systems are adequate for growth and AMF colonization of *A. tinctoria*

Whatever the growth system (S-H or pot), an increase in biomass of *A. tinctoria* was observed in the presence as well as absence of AMF. No significant difference was observed in SFW between the M and NM treatments after 9 days in the S-H cultivation system (Exp. 1 and 2) or after 85 days in the pots cultivation system (Exp. 3). However, a significantly lower RFW and TFW were reported in the M plants compared to the NM after 37 days in the S-H cultivation system (Exp. 1), unlike the results obtained with *A. officinalis* colonized by *R. irregularis* MUCL 41833 in the same S-H cultivation system (Cartabia *et al.*, 2021, Chapter I). These results are not surprising as it has often been reported that plant growth response to AMF inoculation can vary among AMF species and that the direction (e.g., increase or decrease in plant biomass) and magnitude of the response strongly depends on the combination of plant and AMF taxa (Klironomos, 2003).

Root colonization was observed in each AMF-inoculated plant. However, colonization measured at transfer and after 9 and 37 days in the S-H cultivation system (Exp. 1), decreased steadily, probably because of damages caused to the extraradical mycelium at transfer to the S-H cultivation system with no full recovery and development within the roots throughout the experiment. It is not excluded that this is also a rationale for the lower plant biomass reported at the end of Exp. 1 compared to the control, due to an imbalance between the carbon resources transported from the plant to the fungus in exchange for nutrients transported from fungus to the plants. Interestingly, in both Exp. 2 and 3, the total root colonization was almost similar among the AMF strains, while the percentages of arbuscules were higher in presence of the native *R. irregularis* and *S. viscosum* strains, suggesting that they were better adapted to *A. tinctoria* than the GINCO strains. This has often been reported by comparing commercial strains with local strains; the latter being more prone to rapid and effective colonization (Chenchouni *et al.*, 2020; Wu *et al.*, 2021). Unfortunately, this was not translated into higher plant biomass, probably because of the same rationale explained above.

AMF isolated from wild *A. tinctoria* impact the production of A/Sd

The production of A/Sd was not impacted by the GINCO strain *R. irregularis* MUCL 41833 (Exp. 1), whereas a significant increase in production was observed with the native *R. irregularis* strain (Exp. 2 and 3), and an intermediate production between this strain and the GINCO strains with the other native strain *S. viscosum* (Exp. 2). Similarly, no significant effect was observed with the GINCO strains *R. irregularis* MUCL 41833 and *R. aggregatus* MUCL 49408 (Exp. 2 and 3). It cannot be ruled out that these results are related to the fungal genotypes, with native ones being more prone to stimulate the production of A/Sd than GINCO ones. The difference between the two native strains further suggests some degree of functional specialization. This is supported by recent studies revealing that various species/strains of AMF can induce different changes in the production of metabolites in the same plant species (Copetta *et al.*, 2006; Kapoor *et al.*, 2002a, b; Khaosaad *et al.*, 2006; Larose *et al.*, 2002; Toussaint *et al.*, 2007; Zubek *et al.*, 2010, 2012b). For example, Toussaint *et al.* (2007) showed that *Glomus caledonium* increased rosmarinic acid and caffeic acid production in *O. basilicum*, whereas *F. mosseae* only increased caffeic acid production. In another study, Jurkiewicz *et al.* (2010) showed that total phenolic acids accumulation was significantly higher in the roots of *Arnica montana* L. associated with AMF collected from particular plant's natural stands (in Kurpie or in Karkonosze), while intermediate increase was observed with AMF isolated from other regions (i.e., *R. intraradices*[7] UNIJAG PL24-1 and *R. intraradices* BEG 140 or a mixture composed of the above and of *Glomus geosporum* UNIJAG PL 12-2, *Glomus constrictum* 265-5 Walker and *F. mosseae* BEG 12). Finally, Frew (2021) reported that the inoculation with a mixture of four commercial species of AMF (*C. etunicatum*, *Funneliformis coronatum*, *F. mosseae*, and *R. irregularis*) had a greater effect on phenolic concentrations in *Hordeum vulgare* L. cv. "Hindmarsh" as compared to a single commercial inoculant (*R. irregularis*). Interestingly, the author also demonstrated that the effects of the commercial mixture were not different from the results obtained with a native multi-species AMF inoculant extracted from field soil. This suggested that a commercial AMF mixture provided little to no additional benefits (Frew, 2021). Conversely, several specialized

[7] It is to be noticed that the species names of AMF follow the nomenclature of today not the one at the time of publication.

compounds produced by plants may be synthesised as a chemical defence against the presence of AMF in the roots (Copetta *et al.*, 2006). However, this defence mechanism would be likely to occur with AMF strains that have never been associated to the plant. Our native strains isolated from the wild *A. tinctoria* in their natural habitat are more adapted to the plant and are likely to have evolved as good associates. Natives *R. irregularis* and *S. viscosum* could be better adapted to the presence of A/Sd, which are characterized by different biological activities and by various effects on soil microorganisms (e.g., antifungal activities), and thus better interact with their host plants to regulate and enhance the production of these important therapeutic metabolites (Yan *et al.*, 2019). As reported above, a significant higher AC% was observed with M^{Rhiz} and M^{Sept} treatments in Exp. 2 and 3, respectively. An increase in nutrients uptake *via* the arbuscules can lead to an enhanced production of precursor compounds, such as NADPH, ATP, acetyl-CoA (mevalonic acid pathway), and pyruvate glyceraldehyde and phosphate (methylerythritol-4-phosphate pathway) that are required for the biosynthesis of various SMs (e.g., terpenoids, phenolic, alkaloids) (Kapoor *et al.*, 2017). In this study, a higher AC% could have led to an increase in the precursor compounds essential to produce A/Sd. However, this was not confirmed in Exp. 3, where the higher AC% in M^{Sept} treatment was not accompanied by a higher production of A/Sd.

AMF modulate the expression of genes involved in the A/Sd biosynthetic pathway in *A. tinctoria* roots

At the end of Exp. 1, a significantly higher relative expression of *LePGT1* and *LePGT2* genes was observed in *A. tinctoria* associated with *R. irregularis* MUCL 41833 compared to the NM treatment. In addition, a significantly higher relative expression of *LePGT2* was observed in the AMF-colonized plants at day 37 compared to day 9. However, these increases were not accompanied by an enhanced production of A/Sd. Conversely, in Exp. 2, a significant lower relative expression of *LePGT2* was observed in plants associated with the native *R. irregularis* strain, compared with the other AMF and NM treatments, whereas a significantly higher production of A/Sd was observed with this strain. In both experiments, no differences were reported for *GHQH*. In Exp. 3, no significant differences between the treatments were noted for all the genes tested (data not presented).

Although these results may seem surprising, similar outcomes were reported in the literature. For example, Wang *et al.* (2014) demonstrated that the application of methyl jasmonate (MeJA) on shikonin-deficient *A. euchroma* cell lines rapidly led to the overexpression of several genes involved in the biosynthesis of A/Sd, including *PGT*, but was not accompanied by a significant higher production of A/Sd. In another study, Ahmad *et al.* (2022a), showed a significantly higher expression of *LePGT1*, *LePGT2*, and *LeGHQH1* in *Lithospermum officinale* L. roots treated with MeJA, but no higher accumulation of total A/Sd, after eight weeks. Conversely, the same authors in a subsequent study demonstrated that the bacterium *Chitinophaga* sp. strain R-73072 significantly upregulated *LePGT1* and *LePGT2*, and a cytochrome P450-*LeCYP76B101* genes, resulting in a significant enhanced production of total A/Sd in *L. erythrorhizon* roots, after 2-3 weeks (Ahmad *et al.*, 2022b).

In the current study, a few hypotheses can be advanced to explain why upregulation of *PGT*s was not followed by higher production of A/Sd and, conversely, why downregulation was followed by higher production of A/Sd. Firstly, it is not excluded that the duration of Exp. 1 (37 days) was too short to result in a significant increased production of A/Sd, or that the timing of plant harvesting in our experiments was not optimal (i.e., gene expression behavioural oscillations due to the plant circadian cycle) (Merrow *et al.*, 2005). The *PGT*s regulate the first biosynthetic steps forming the basic carbon skeleton that leads to A/Sd, and therefore, it is possible that the resulting modulation of A/Sd production took longer after the upregulation of the relative expression of target *PGT*s gene, as supported by Ahmad *et al.* (2022b), or that the genes oscillations were not timely targeted during our harvest times, as suggested by Wang *et al.* (2014) (**Figure 7**). Secondly, in a study by Andrade *et al.* (2013), a mismatch between alkaloid levels, another important SM group, and gene expression was reported in different *Catharanthus roseus* (L.) G. Don tissues. The authors reported that AMF *Claroideoglomus etunicatum* had a greater influence (i.e., alkaloids production) in roots than in shoots, and a higher gene expression was reported in the older leaves of M plants as well as in the youngest leaves of NM plants (leaves were harvested at the same time) (Andrade *et al.*, 2013). These results suggest a very precise phenological and spatial regulation process during alkaloid biosynthesis (Mahroug *et al.*, 2007). Moreover, the reported influence of AMF on idioblast and laticifer density in *C. roseus* plants might have

enhanced the expression of enzymes specifically located in these cells (St-Pierre *et al.*, 1999). An increase in glandular trichome density upon mycorrhization was also linked with an enhanced concentration of another group of SMs, the terpenoids (Zhao *et al.*, 2022). This is an interesting aspect that needs to be further verified. In fact, A/Sd compounds are sequestered as granules in the phospholipid layer and are accumulated in the apoplastic spaces, and they can be found in the cork layer of mature roots (Brigham *et al.*, 1999; Singh *et al.*, 2010; Tatsumi *et al.*, 2016). A difference in A/Sd accumulation might have occurred (i.e., higher content in the primary roots as compared to the secondary) upon AMF colonization and might have not been fully displayed across *A. tinctoria* root samples used for our RT-qPCR analysis (i.e., no homogenous samples analysed with mostly secondary roots utilized). Thirdly, the regulation and accumulation of SMs in plants is usually controlled by a complex network characterised by transcription factors (TFs), which promote or inhibit the expression of multiple genes involved in one or more biosynthetic pathways (Yang *et al.*, 2012; Wu *et al.*, 2021). Transcription factors can act alone or in combination with other TFs to modulate the expression of target genes, and also one TF can regulate the expression of multiple genes participating in one or more biosynthetic pathways (Pinson *et al.*, 2009; Goossens *et al.*, 2016; Hassani *et al.*, 2020). In the current study, different TFs might have regulated the target genes (*PGT*s and *GHQH*), yet the full landscape of the A/Sd biosynthesis pathway is not entirely understood, with co-expressed genes still to be identified (Suttiyut *et al.*, 2022). Finally, even after a gene has been transcribed, its expression could still be regulated at various stages. Post transcriptional modifications changes might occur to a newly transcribed primary RNA transcript after transcription has occurred and prior to its translation into a protein.

<u>Chemical profile of *A. tinctoria* does not markedly differ between semi-hydroponic and pot cultivation systems and in presence of different AMF</u>

A similar chemical composition was reported in *A. tinctoria* roots associated with the different AMF and non-colonized control plants in Exp. 2 (S-H cultivation system) and 3 (pot cultivation system) (**Figures 41** and **42**) except for the detection of shikonin in Exp. 3 (**Tables 16** and **17**). The major compound detected in both experiments was

putatively identified as anhydroalkannin (**6**). This compound is also a main product of shikonin biotransformation by several human intestinal bacteria in aerobic conditions and it was found to be less cytotoxic against a series of human tumour cell lines *in vitro*, in comparison with shikonin (Meselhy *et al.*, 1994; Min *et al.*, 2000). Methoxy A/Sd isomers, as detected in our samples, were also identified from *Lithospermum*, *Alkanna*, and *Onosma* species. 1'-methyl shikonin was isolated and characterized from roots of *L. erythrorhizon*, exerting moderate antioxidant activity (Han *et al.*, 2008). To the best of our knowledge, 5- or 8- methoxyshikonin derivatives have not yet been identified from natural sources. To better clarify the chemical composition of our samples, putative methylshikonin derivatives (**1** and **4**) must be purified and the methoxyl position elucidated in the structure of these isomers. In addition, in both experiments, four main lipid amides were tentatively identified as palmitoleamide (**7**), linoleamide (**8**), oleamide (**9**), and stearamide (**10**). Fatty acids amides are a group of nitrogen-containing, lipid-soluble fatty acid derivatives, which act against a variety of diseases such as cancer, bacterial infections, parasitic infection, inflammations, diabetes, and obesity (Kim *et al.*, 2010; Tanvir *et al.*, 2018). Further, it has been reported that fatty acid amides as oleamide from plant root exudates can participate in strong plant-microbe interactions, stimulating nitrogen metabolism in rhizospheric bacteria (Sun *et al.*, 2016).

The data of chemical composition obtained from *A. tinctoria* growing in our cultivation systems cannot be accurately compared with data from literature (i.e., from nature, commercial samples, and/or from cell plant suspension). Indeed, the proportion and quantity of A/Sd varies depending on the level of stress and microorganisms present in the rhizosphere (Brighman *et al.*, 1999). The influence of the cultivation systems on the production of these methoxy and anhydro A/Sd must be deeply studied to better understand their significance. Secondary metabolites' production and compositional changes have a strong correlation and association with the environment, and thus synthesized only under specific growth conditions (Peñuelas and Llusià, 1997). Variations in an environmental factor, such as light, temperature, soil water, soil fertility, and salinity, may alter the plant metabolites content (Yang *et al.*, 2018). Indeed, many chemical and physical factors have been found to inhibit shikonin production, such as NH_4^+, 2,4-dichlorophenoxyacetic acid (a synthetic auxin), low pH, temperature higher than 28°C, and light, especially blue light (Tatsumi *et al.*, 2016). Skoneczny *et al.* (2017), using a metabolomic approach profiling

HNQs and pyrrolizidine alkaloids (PAs), demonstrated the influence of high temperature and water withholding on the accumulation of A/Sd in *Echium plantagineum* L. Abundance of HNQs, especially deoxyshikonin, shikonin, and dimethylacrylshikonin, rapidly increased in roots exposed to elevated temperatures. Water withholding initially increased NQ abundance, but prolonged drought resulted in reduced total PAs and HNQs (Skoneczny *et al.*, 2017). In the current study, *A. tinctoria* growing in the S-H cultivation system were kept in perlite, while a mixture of peatmoss, perlite, and quartz was used in the pots experiment. Perlite is a growing medium frequently used in hydroponic cultivation system since it has a high-water retention and provide the plants' roots with strong anchor points for stability and strength. Moreover, in this system, plants received minerals by the circulating nutrient solution flowing directly through the plants' container, while in the pots it was added at constant intervals and left to be completely absorbed by the plants. Therefore, it is possible that the temperature and the water/nutrient solution retention was higher in the conventional pots than in the S-H system's plant containers. Moreover, shikonin and A/Sd might have better accumulated in the pots, while leached out in the S-H system. Finally, plant developmental stage qualitatively and quantitatively influences primary and secondary metabolism. A recent study by Csorba *et al.* (2022) reported this aspect as the most important driver influencing *A. tinctoria* metabolite content, revealing a peak content of A/Sd at the fruiting stage. In the current study, plants were harvested during the vegetative growth (around five months old), and thus, might have played a role in the chemical profile reported.

Conclusion

For the first time, to the best of our knowledge, AMF isolated from wild-growing *A. tinctoria* were identified and applied under the cultivation systems described in this study. Native *R. irregularis* significantly increased A/Sd production in *A. tinctoria* roots, whatever the system used (S-H or pots), thus opening new perspectives towards the application of AMF in the production of these valuable therapeutic compounds in medicinal plants. A better adaptation of this indigenous strain towards its host was demonstrated, with higher arbuscules formation and production of A/Sd reported in *A. tinctoria* roots. This result suggests that the selection of the most effective AMF species (native or not; single or combinations of different AMF strains) remains

a key point in studying the modulation/increase of SMs. However, the mechanisms behind AM symbiosis and their impact on the A/Sd biosynthetic pathways still need to be further clarified. Additionally, the condition characterizing the conventional pots system seemed to be the optimal one in term of shikonin detection. Therefore, the application of the best growing conditions should be further investigated as well. Since shikonin was reported only in the pots system, the recovery of SMs can yet be conducted only in a destructive way (i.e., using the roots of *A. tinctoria*). For this reason, further studies applying the S-H system/innovative systems are required, especially for testing non-destructive ways of trapping of the metabolites exudates by the roots in the circulating nutrient solution.

Funding

Yanyan Zhao and Annalisa Cartabia were financially supported by the Special Research Funds (FSR) of the Université catholique de Louvain (Belgium).

Acknowledgments

The authors would like to thank the Université catholique de Louvain (Belgium) for financial support via the Special Research Funds (FSR), to Yanyan Zhao and Annalisa Cartabia. The authors would also like to thank Dr. Muhammad Ahmad and Dr. rer. nat. Eva Maria Molin from the Center for Health & Bioresources, AIT Austrian Institute of Technology GmbH (Tulln, Austria), for the design of the primers applied in the RT-qPCR analysis; the Institute of Plant Breeding and Genetic Resources, Hellenic Agricultural Organization Demeter (IPBGR, HAO Demeter), in particular Dr. Virginia Sarropoulou and Dr. Katerina Grigoriadou, for the supply of the *A. tinctoria in vitro* explants, and Dr. Nikos Krigas for the collection and botanical identification of *A. tinctoria* plants. Moreover, we thank Stéphanie Huret and Céline Bivort (Technician at UCLouvain Earth and Life Institute - Applied Microbiology - Laboratory of Mycology) for the help in the RNA extraction and genes expression analysis and molecular identification of AMF, respectively, and Catherine Rasse (Statistical Methodology and Computing Service/Louvain Institute of Data Analysis and Modelling in Economics and Statistics, SMCS/LIDAM, UCLouvain) for the statistical support. Finally, MS data were obtained at the MASSMET platform of UCLouvain.

GENERAL DISCUSSION

Medicinal plants have been used worldwide for thousands of years and today the growing demand for their products (i.e., therapeutic metabolites) has spurred the development of artificial cultivation systems (Zeng *et al*., 2013). Indeed, these therapeutic metabolites can be produced from plant cells, tissues or organs cultivated on ***synthetic growth media in Petri plates or bioreactors***. However, these cultivation systems present some limitations, which are their high costs, slow growth and limited metabolites excretion from cells or tissues, and lack of reproducibility due to plants genetic variability and differences in growing conditions (Gontier *et al.*, 2002; Malik *et al.*, 2016; Naik and Al-Khayri, 2016). The quality and quantity of therapeutic metabolites produced greatly depends on the physiological and developmental stage of the plants (Halder *et al.*, 2019). For these reasons, direct ***plant regeneration and micropropagation*** are methods that have been considered in the recent years for the conservation and propagation of medicinal plants, and for fulfilling the demands of the pharmaceutical sector. This also explains the importance of developing efficient protocols to produce sufficient numbers of plants, particularly those which are difficult to cultivate and /or are overexploited from the wild, in *in vitro* culture conditions with high levels of survival when transferred to *ex vitro* conditions (Cartabia *et al.*, 2022). ***Hydroponic cultivation*** of medicinal plants is another strategy that has attracted the attention of the scientific community and industrial sector in the recent decades, as it can effectively meet the nutrients needs of the plants under controlled/stable environmental conditions (Gontier *et al.*, 2002; Sgherri *et al.*, 2010). Interestingly, in this system, the addition of microorganisms (e.g., endophytic, or symbiotic bacteria or fungi) or the application of abiotic elicitors (e.g., drought, salinity, osmotic stress, thermal stress, hormones, etc.) are possible to stimulate the production of selected metabolites (Dayani and Sabzalian, 2017).

Growing evidence suggests that plant-associated microorganisms have a marked impact on the biochemical composition of their hosts, affecting their fitness through direct or indirect effects on functional traits (e.g., nutrient provision, changes in photosynthesis efficiency, alteration of plant development and increased stress tolerance) (Goh *et al.*, 2013; Mitter *et al.*, 2013). Among these microorganisms are the ***arbuscular mycorrhizal fungi (AMF)***. These obligate root symbionts

have repeatedly been shown to affect the metabolism of plants, often resulting in the overproduction of important metabolites, thus influencing the quality of herbal medicines (Zeng *et al.*, 2013). In nature most plants are associated to AMF (Zubek *et al.*, 2011), but to our knowledge, no information is available on the effects of these fungi on the metabolome of *Anchusa officinalis* and *Alkanna tinctoria*, two major medicinal plants from the Boraginaceae family.

To comprehensively examine the impact of AMF on the metabolites produced by *A. officinalis* tissues, an ***untargeted metabolomics*** approach was performed, allowing the separation and detection of a wide range of metabolites, and therefore providing a global fingerprint of the quantitative and qualitative changes in the metabolism of the plant in presence/absence of AMF. In the vast majority of studies, a targeted analysis was applied to investigate specific chemical groups, without detecting the full range of induced chemical responses to AMF (Rivero *et al.*, 2015; Hill *et al.*, 2018). This targeted approach was used as well in this study, only for *A. tinctoria*, considering the well-known reported therapeutic effects of the hydroxynaphthoquinone enantiomers (HNQs), alkannin/shikonin and their derivatives (A/Sd).

To meet the global demand for plant-derived medicines, the use of a semi-hydroponic cultivation system, as developed by Garcés-Ruiz *et al.* (2017), may represent a sustainable approach to exploit the mutualistic symbiosis established between *A. officinalis* or *A. tinctoria* and AMF towards the modification and enhancement of primary and secondary metabolites (PMs and SMs, respectively). This system was applied in this Ph.D. study to address the general hypothesis that a single or different AMF strains may modify or induce the production of specific therapeutic metabolites in these important medicinal plants.

The most important results of this Ph.D. are discussed below.

Rhizophagus irregularis MUCL 41833 effects on the metabolites production of *A. officinalis* and *A. tinctoria* medicinal plants

In a first approach, *R. irregularis* MUCL 41833, a strain belonging to the worldwide commercially used species *R. irregularis*, was shown to increase the production of several metabolites in shoot and roots of *A. officinalis* after 9 days of growth in a semi-hydroponic (S-H) cultivation system. Higher contents in PMs, including organic acids

involved in the energy pathways of eukaryotic cells and key amino acids, with the potential to act as precursors of other amino acids and as building blocks for the production of macromolecules, were observed. Among the significantly increased amino acids observed in this study was pyroglutamic acid. This PM is an important reservoir and analogue of glutamate, which was also increased in mycorrhized plants, and has a well know stress-tolerant effect in crops grown under environmental stress conditions (Kumar and Bachhawat, 2011; Jiménez-Arias *et al.*, 2019). High accumulations of both PMs in mycorrhized plants represent a significant nitrogen pool, reflecting the ability of AMF to enhance N assimilation in plants (Bücking *et al.*, 2012; Zeng *et al.*, 2013; Rivero *et al.*, 2015; Jiménez-Arias *et al.*, 2019). Among the significantly increased organic acids were malic and aspartic acids. The latter is an important intermediate precursor of amino acids, such as asparagine, threonine, lysine, isoleucine, and methionine (Wang and Larkins, 2001). The therapeutic use of amino acids (i.e., branched-chain amino acids leucine, isoleucine, valine and glutamine) presents also a viable and important option for natural medicine (Tamanna and Mahmood, 2014). Phenylacetic acid, an auxin, was also significantly upregulated in mycorrhized plants. This metabolite plays a key role in plant-growth promotion and in the induction of lateral root growth (Hammad *et al.*, 2003; Cook, 2019).

Phenylpropanoids and derivatives were the class of SMs most affected by the association between *R. irregularis* MUCL 41833 and *A. officinalis*. These metabolites are characterized by a low toxicity and a wide array of beneficial effects on human health and disease management. Among the significantly increased phenylpropanoids observed in this study were salvianolic acids. These SMs were reported to have important impacts on cancer treatment and alleviation of fibrosis disease as well as a good therapeutic effect on cardiovascular and neural protection (Ma *et al.*, 2019). Rosmarinic acid was confirmed as the predominant metabolite produced by *A. officinalis* and its content was significantly increased in presence of the AMF, together with ferulic and caffeic acids, and their derivatives. These metabolites present several health-related properties, such as antioxidant, anti-inflammatory, and antimicrobial activities (Boskovic *et al.*, 2018; Luo *et al.*, 2020). Finally, saponins content was upregulated in AMF-colonized *A. officinalis* plants. Theses SMs present antibacterial, antifungal, and antiviral properties and are extensively used beyond pharmaceuticals for their surfactant properties (Mugford and Osbourn,

2013). Interestingly, for the first time, the production of two new derivatives of salicylic acid and one new derivative of rosmarinic acid, all presenting a common substitution pattern (methylation and hydroxylation), as well as SMs methylation and oleanane-type saponins upregulation, were described in mycorrhized *A. officinalis*. The fact that these compounds were not found in the literature, and therefore, not yet identified, suggests that they might have been produced by *A. officinalis* when associated with *R. irregularis* MUCL 41833.

Our results are in line with the physiological changes noticed in mycorrhizal plants, including the increased number of mitochondria and plastids and increased photosynthesis activity and jasmonic acid level (Lohse *et al.*, 2005; Gaude *et al.*, 2015; French, 2017). Moreover, similar metabolite upregulations were reported in earlier studies. For instance, the amino acids glutamate, pyroglutamate, aspartate in tomato plants (Rivero *et al.*, 2015), threonine, glycine, lysine, histidine, and arginine in maize plants (Zhu *et al*., 2016). Studies have also reported an increase in PAL synthesis and consequent formation, and accumulation of phenolic acids (e.g., rosmarinic acid) *via* the phenylpropanoid biosynthetic pathway in tomato and basil plants (Rivero *et al.*, 2015; Srivastava *et al.*, 2016), in p-Hydroxybenzoic and syringic acids in olive and wild pansy plants (Kara *et al.*, 2015; Zubek *et al.*, 2015), and in saponins in *Passiflora alata* Curtis and *Wedilia chinensis* (Osbeck) Merril. (Muniz *et al.*, 2021; Nisha, 2010). The AMF *Funneliformis geosporum* was also reported to strongly increase the production of tanshinones (important therapeutic compounds that exert anti-oxidation, anti-inflammation, antitumor, neuroprotection, etc. activities) in *S. miltiorrhiza* (Wang *et al.*, 2020).

In our study, only the SM lithospermic acid was downregulated in colonized *A. officinalis*. Other studies reported similar result, for instance, *F. geosporum* significantly inhibited the production of salvianolic acid in *S. miltiorrhiza*, while caffeic and chlorogenic acids were downregulated in *S. lycopersicum* roots colonized by *R. intraradices* and *F. mosseae* (López-Ráez *et al.*, 2010; Wu *et al.*, 2021).

Despite the pronounced metabolic variations noticed after 9 days of plants growth in the S-H cultivation system, no significant differences were observed after 30 days of experiment. The AMF symbiosis remains active during all the experiment duration through the presence of numerous arbuscules. Nevertheless, no increased growth or modification in metabolites production were noticed for M plants. We

suggested that the AMF impact is considered particularly important in the early stage of plants growth in the pots and S-H cultivation system and, apparently, less effective as it grows older. However, the growth environment in the S-H cultivation system should be carefully considered, as reported in the following section. The decrease in the content of minerals could have diminished/limited the AMF-plants nutrient requirements. Arbuscular mycorrhizal fungi might have tried to allocate energy mostly on the formation of arbuscules in order to optimize the uptake of the remaining nutrients (Le Pioufle *et al.*, 2019), instead of enhancing the production of the plants' metabolites and growth. Future perspectives are provided in the following section.

Despite no up/downregulated PMs and SMs in shoots and roots of mycorrhized *A. officinalis* were reported after 30 days of growth in the S-H cultivation system, an increased concentration of coumarin scoparone and furanocoumarin byakangelicin was noticed in the nutrient solutions collected from AMF-colonized plants. This was the first successful attempt to trap root exudates directly from the circulating nutrient solution. Coumarins are synthesized *via* the phenylpropanoid pathway and are widely reported as substances involved in defense mechanisms against pathogens (Harbort *et al.*, 2020). Moreover, it has been reported that their exudation from roots into the rhizosphere was induced under Fe and Pi limitations, improving the efficiency of plant nutrients acquisition (Chutia *et al.*, 2019; Stringlis *et al.*, 2019). Indeed, it is well-known that plants exude a wide diversity of compounds, especially SMs, contributing to plant fitness by interacting with surrounding soil microbiota or by playing a role in nutrient acquisition increasing the bioavailability of soil nutrients (Voges *et al.*, 2019).

In a second approach, a target analysis was applied to detect and quantify hydroxynaphthoquinones, the isohexenylnaphthazarins chiral pair A/Sd, in the roots of *A. tinctoria* associated with *R. irregularis* MUCL 41833 growing for 9 and 37 days in the S-H cultivation system. No increased production of A/Sd was noticed in the roots of the AMF-colonized plants, suggesting an absence of effect of the fungus on the biosynthesis of these compounds. A molecular analysis was conducted to confirm this result. The relative expression of *PGT* (p-hydroxybenzoate geranyltransferase) and *GHQH* (geranylhydroquinone 3"-hydroxylase), two genes involved in the biosynthetic pathway of A/Sd, was assessed. The *PGT*s gene code for *LePGT1* and *LePGT2*, two enzymes catalyzing the reaction of

geranylpyrophosphate with p-hydroxybenzoic acid to form geranylhydroxybenzoic acid, a direct precursor of A/Sd, while *GHQH* is an enzyme hydroxylating the isoprenoid side chain of geranylhydroquinone (GHQ), also a well-known precursor of A/Sd (Tang *et al.*, 2020; Yamamoto *et al.*, 2000). Although a significant upregulation of *PGT*s gene was detected in the roots of AMF-colonized plants, it was not accompanied by an increase in A/Sd production. Other genes from the two different biosynthetic pathways leading to the shikonin formation (shikimic acid and MVA pathways) were tested in this study (i.e., 3-hydroxy-3-methylglutaryl-CoA reductase – *HMGR* – and phenylalanine ammonia lyase – *PAL*). However, no amplifications were detected and thus these results were not reported in this study.

Few hypotheses can be advanced on why the upregulation of *PGT*s in our study was not followed by a higher production of A/Sd. Firstly, it is not excluded that the duration of the experiment (37 days) was too short to result in a significantly increased production of A/Sd, or that the timing of plant harvesting was not optimal (i.e., gene expression behavioural oscillations due to the plant circadian cycle) (Merrow *et al.*, 2005). The *PGT*s regulate the first biosynthetic steps forming the basic carbon skeleton that leads to A/Sd, and therefore, it is possible that the resulting modulation of A/Sd production took longer after the upregulation of the relative expression of target *PGT* genes or that the genes oscillations were not timely targeted during our harvest times. Secondly, a difference in A/Sd accumulation might have occurred (i.e., higher content in the primary roots as compared to the secondary) upon AMF colonization and might have not been fully displayed across *A. tinctoria* root samples used for our RT-qPCR analysis (i.e., no homogenous samples analysed with mostly secondary roots utilized). Thirdly, different transcription factors might have regulated the target genes analysed in this study, yet the full landscape of the A/Sd biosynthesis pathway is not entirely understood, with co-expressed genes still to be identified (Suttiyut *et al.*, 2022). Indeed, no similar studies with *A. tinctoria* or other Boraginaceae plants have been reported in the literature, to our knowledge. Most studies so far were focused on *L. erythrorhizon* cell cultures, which allowed for the identification of gene coding enzymes in catalysing the steps toward the formation of A/Sd (Yazaki *et al.*, 2002; Singh *et al.*, 2010; Oshikiri *et al.*, 2020). In a recent study by Varela Alonso *et al.* (2022), the bacteria *Chitinophaga* sp. R-73072 was shown to upregulate *PGT* genes, resulting in an enhanced production of A/S esters in *L. erythrorhizon*.

However, in another study conducted with *Arnebia euchroma* cells, Wang *et al.* (2014) demonstrated that the application of MeJA on shikonin-deficient cell lines led to the overexpression of several genes involved in the biosynthesis of A/Sd, including *PGT*, without resulting in the actual increased production of A/Sd. These results suggest that *PGT* genes alone are not sufficient to ensure the production of these compounds and that the production of A/Sd seems likely to result from the co-expression of several genes (Varela Alonso *et al*., 2022).

Results from the literature and our study suggest that different AMF species may impact differently the quantitative and qualitative production of metabolites in *A. officinalis* and *A. tinctoria*. For this reason, the effects of different AMF species (i.e., from international collection and/or newly isolated and identified) were further tested.

Metabolites production in *A. officinalis* differs with AMF species

Four GINCO-AMF strains (*R. irregularis* MUCL 41833, *R. intraradices* MUCL 49410, *R. clarus* MUCL 46238, and *R. aggregatus* MUCL 49408) were associated with *A. officinalis* in the S-H cultivation system and metabolites production assessed. Through an untargeted metabolomic analysis, *R. irregularis* and *R. intraradices* were demonstrated to exert a stronger effect on *A. officinalis* metabolome compared to *R. clarus* and *R. aggregatus*. In fact, although the same plant species can be colonized by different AMF genera/species/isolates (i.e., low specificity of association), the overall response of the plant is dependent on the identity of the associated AMF (i.e., high specificity of the outcome) (Kaur *et al.*, 2022).

The two best performing AMF strains (*R. irregularis* and *R. intraradices*) mainly affected the amino acids (aspartic, glutamic acid, glutamine and its derivative, and pyroglutamic acid) and organic acids (threonic and malic acids) production, as well as some specific SMs derived principally from the phenylpropanoid and mevalonate pathways (e.g., mono, di, tri or tetrameric derivatives of caffeic acid and of syring acid, and methylated compounds). In addition, both strains induced the accumulation of oleanane-type saponins, which are involved in plant defence mechanisms against biotic constraints, and the acetylation-methylation of various compounds (e.g., acetyl derivative of anchusoside-9, methylated syringin derivatives, methyl dihydrosinapic acid glucoside and methylrosmarinic acid). These

results are in line with those reported above with *A. officinalis* associated to *R. irregularis* MUCL 41833 and those reported in other studies suggesting a discernible increase of PMs and SMs in the roots of mycorrhized plants. For instance, in Rivero *et al.* (2015), bioactive forms of JA, Me-JA and JA-Ile conjugates were accumulated in significantly higher amounts only in *S. lycopersicum* roots associated with *F. mosseae* as compared to *R. irregularis*.

Six metabolites (acetylanchusoside-9, 6”-acetylmethylsyringin, malonylanchusoside-2, hydroxy-malonylanchusoside-7, hydroxy-dimalonylanchusoside2/7 and malonylanchusoside-7) were tentatively characterized as new SMs and were more accumulated in the tissues of *A. officinalis* formerly associated with the most efficient AMF (*R. irregularis* and *R. intraradices*).

Moreover, in this Ph.D., AMF strains belonging to the same genus were demonstrated to induce similar metabolomic responses in *A. officinalis* plants, without being strongly related phylogenetically. Indeed, the latest updates regarding the phylogenetic classification of AMF strains showed that *R. irregularis* is phylogenetically more closely related to *R. clarus* than to *R. intraradices* (Walker *et al.*, 2021). It has been extensively reported that the outcome of the association in terms of e.g., plant growth promotion and metabolites enhancement, is highly specific to the identity of the AMF symbiont (Luthfiana *et al.*, 2021; Yang *et al.*, 2017). This aspect is further highlighted in the next paragraph comparing two GINCO-AMF strains (*R. irregularis* MUCL 41833 and *R. aggregatus* MUCL 49408) with two isolated from roots of wild-growing *A. tinctoria* plants (*R. irregularis* and *S. viscosum*).

AMF isolated from wild-growing *A. tinctoria* exert a stronger impact on A/Sd production than AMF-GINCO strains

Rhizophagus irregularis MUCL 41833 has been widely used as a model AMF for studying changes in plant metabolism. However, no significant effect in the production of A/Sd was reported following association with *A. tinctoria* roots. Similar results were obtained with *R. aggregatus* MUCL 49408. Conversely, the native AMF *R. irregularis* significantly increased the production of these important therapeutic metabolites, while an intermediate effect was noticed with the native AMF *S. viscosum*. A better co-adaptation between AMF and their host has been reported once the applied symbiotic microorganism

is isolated from the same location of its host (Chen *et al.*, 2018). For instance, Jurkiewicz *et al.* (2010) showed that total phenolic acid accumulation was increased in roots and leaves of *Arnica montana* L. associated with AMF isolated from one of the plant's natural locations. Similar results were obtained by Wu *et al.* (2021), with native AMF species inoculated to *S. miltiorrhiza* promoting roots growth and increased SMs production (e.g., phenolic acids). In the current study, a significant lower relative expression of *LePGT2* target gene was observed in plants associated with the native *R. irregularis* strain. As mentioned above, the interpretation of these results is quite challenging since no similar studies are available in the literature. We hypothesize that native AMF were able to induce *LePGT2* expression prior to plant harvest and, therefore, at the time of metabolites analysis, higher production of A/Sd was observed. However, this effect was not confirmed by the results obtained with the two other target genes (*GHQH* and *LePGT1*). Moreover, other AMF, including the native *S. viscosum*, exerted similar genes regulation, also compared to non-mycorrhized (i.e., control) plants. Future perspectives are reported in the following section.

Interestingly, the significant higher production of A/Sd in *A. tinctoria* roots associated with the native *R. irregularis* was confirmed in a subsequent experiment. Here the plants were grown in a conventional pots system under greenhouse conditions, and, only in this experiment, shikonin was detected in *A. tinctoria* roots. Yet, total shikonin equivalent content was confirmed to be higher in roots associated with the native *R. irregularis* strain, as earlier reported for the plants growing in the S-H cultivation system. However, in this experiment, *S. viscosum* did not exert an intermediate effect on the production of A/Sd. On the contrary, the A/Sd were produced similarly as in non-mycorrhized and *R. irregularis* MUCL 41833 associated plants. This result suggested that a degree of functional specialization in AMF interactions with host plant has occurred. As widely reported in literature, various fungal strains/species can induce the production of metabolites differently in the same plant species (Copetta *et al.*, 2006; Zubek *et al.*, 2010; Zhao *et al.*, 2022). In addition, different factors, such as light, temperature, humidity, soil fertility, and cultivation techniques, can influence the production of metabolites by medicinal plants (Zhao *et al.*, 2022). Controlling the growth parameters (i.e., substrate, pH, nutrient content, light, temperature) is thus essential for the optimal production of plant metabolites. Finally, A/Sd exert different biological

activities and may have various impacts on soil microorganisms, such as antifungal effect (Yan *et al.*, 2019). Arbuscular mycorrhizal fungi have been found to induce the transcript levels of two pivotal enzymes of the MEP pathway, 1-deoxy-D-xylulose 5-phosphate synthase (DXS), and 1-deoxy-D-xylulose 5-phosphate reductoisomerase (DXR) in wheat roots (Zhao *et al.*, 2022). These enzymes are linked to the biosynthesis of isoprenoids, catalysing the initial step of the MEP pathway, which is linked to the production of A/Sd. Furthermore, the increased uptake of phosphorus by AMF-colonized plants has been reported to enhance terpenoid biosynthesis by increasing the concentration of pyrophosphate compounds, such as isopentenyl pyrophosphate (IPP) and dimethylallyl pyrophosphate (DMAPP), which yet again are linked with the production of A/Sd (Zhao *et al.*, 2022). The native *R. irregularis* isolated from wild *A. tinctoria* applied in this study might be better adapted to the presence of A/Sd, compared to the standard AMF strains, and it might better interact with its host plant to regulate and improve production of these important therapeutic metabolites.

A combination of Plant Growth Regulators and nutrients under adequate culture conditions allows the mass-production of healthy *in vitro* and *ex vitro A. tinctoria* plants

Studying the effects of AMF on the production of medicinal plant metabolites is central and will open doors to future applications. However, this production is linked to the development of protocols allowing the mass production of plants. The intensive utilization of plants and plant based natural products creates an enormous discrepancy between their demand and availability, which is now evident for the *Alkanna* plant species as reported in Chapter IV (Marchev *et al.*, 2020). Indeed, even if *A. tinctoria* is a well-known species producing A/Sd, its cultivation remains difficult and is particularly hampered by poor germination and low availability of planting material. Furthermore, extensive time is needed to reach acceptable A/Sd contents for economically viable exploitation (Malik *et al.*, 2016). To overcome these challenges, several studies have focused on increasing the production of A/Sd through chemical synthesis or plant tissue culture technologies. Cell cultures in suspension have the advantage of growing rapidly, and the metabolites produced can be extracted more easily than from intact plants (Varela

Alonso *et al.*, 2022). However, SMs are usually produced by specialised cells and some of them might not be produced in undifferentiated cell suspensions. These undifferentiated cell cultures make these systems also limited in terms of studying the biosynthesis of plant metabolites. Therefore, whole plant culture systems are preferable for understanding the metabolic interactions of the plant with its environment and associated microorganisms.

As part of this Ph.D., a successful protocol for the *in vitro* production of *A. tinctoria* plants using shoot-tip explants, and their complete acclimatization to *ex vitro* conditions was developed. This protocol overcomes major problems, such as symptoms of hyperhydricity, low percentage of roots formation and survival to *ex vitro* acclimation. First, various culture media (MS, WPM, and GB5) were tested characterized by different concentrations of PGRs (e.g., 1 N6-benzylaminopurine – BAP, IBA, kinetin, NAA), gelling agents and sucrose. The highest proliferation rate was obtained in MS medium solidified with Plant Agar. Indeed, the presence of sulphated galactan in this gelling agent has been reported to reduce symptoms of hyperhydricity (Ivanova and Van Staden, 2011). However, only when the rooting medium (RC1) enriched with IAA and lacking NH_4NO_3 was applied, the hyperhydricity symptoms were annihilated and a successful rooting of *A. tinctoria in vitro* and optimal survival percentage of *ex vitro* plants was reached. The decrease or totally reversed hyperhydricity has already been reported when using culture media with reduced or no concentration of NH_4NO_3 (Liu *et al.*, 2003). This leads to a successful *ex vitro* survival rate since hyperhydricity limits the regenerative ability of plant tissues and, therefore, increases the potential of *in vitro* and *ex vitro* mass propagation (Ivanova and van Staden, 2008).

CONCLUSION AND PERSPECTIVES

The main objective of this Ph.D. was to assess whether AMF could influence the biosynthesis of PMs and SMs in two major Boraginaceae plant species with recognized medicinal properties. The effect of a single strain of AMF on *A. officinalis* and *A. tinctoria* was first evaluated before comparison of several strains belonging to GINCO and finally the comparison between strains from GINCO and strains isolated in nature on *A. tinctoria*. The experiments were mainly conducted in a semi-hydroponic or greenhouse cultivation systems and, among other assessments, the metabolome of the plants was analyzed.

All reported results may represent possible innovative ways to increase/modify the production of metabolites with potential therapeutic value. The results are summarized below in response to the questions addressed in this Ph.D.

1- *Does the AMF R. irregularis MUCL 41833 modulate the production of metabolites in shoot and root tissues as well as in the nutrient solution of A. officinalis plants grown in a semi-hydroponic cultivation system? What specific biosynthetic pathways are up or down regulated as compared to uncolonized plants?*

Yes*, specific biosynthetic pathways in the tissues of A. officinalis were influenced by R. irregularis MUCL 41833*, potentially opening the door to manipulation of plant metabolism with the AMF inoculant for possible applications in the pharmaceutical and cosmeceutical industry. The S-H cultivation system was successfully used to grow the plant-AMF associates and for establishing the metabolic profile of *A. officinalis* in presence/absence of the fungal symbiont. However, the significant effects on PMs and SMs observed in AMF-colonized plants occurred primarily at the early stage of plants growth (i.e., after 9 days experiment), suggesting that the stressful conditions during plant establishment in pots and at transfer to the S-H cultivation system might also have had an impact.

Perspectives:

Further research is needed to fully understand the impact of AMF on SMs and PMs production by plants taking also into consideration the different developmental stages of the fungus (e.g., asymbiotic, pre-symbiotic and symbiotic stages of development). For instance, it would

be interesting to evaluate whether the production of SMs and PMs are linked with the presence of arbuscules (i.e., the principal site of C-P exchange between plant and AMF) in the root cortical cells. The elicitation of genes involved in SMs production can be further explored during both early and late stages of AMF development, applying a high-throughput transcriptome study. Transcriptional changes in roots could give an overall insight of different expressed genes in plants associated or not with AMF. This analysis would help assessing the real roles of AMF, and thus clarify whether the induced production of plants' metabolites is predominantly linked to (1) the plants' initial response to the AMF colonization, (2) the stress encountered during the transplant in the S-H cultivation system, or (3) the sole beneficial effects of AMF symbiosis (i.e., enhanced plant photosynthesis, nutrients absorption…).

In addition, a first test on the trapping of root exudates directly from the circulating nutrient solution has been successfully achieved (Chapter I), thanks to the controlled environment offered by the S-H cultivation system, making it possible to study differences between roots exudates of AMF-colonized and non-colonized *A. officinalis* plants.

Perspectives:

This promising observation paves the way for further testing potential innovative extraction methods of secondary metabolites (e.g., new eco-friendly category of solvent, natural deep eutectic solvents as 'extractive' solution, see below), and improve cultivation systems to optimize the extraction. This will make it possible to differentiate the metabolites released/exudates by plants with and without AMF.

2- *Is the metabolome of A. officinalis dependent on AMF species (R. irregularis MUCL 41833, R. intraradices MUCL 49410, R. clarus MUCL 46238, and R. aggregatus MUCL 49408) and are PMs and SMs productions species specific?*

Yes, ***the metabolic response of A. officinalis to AMF is strain-dependent,*** with *R. irregularis* MUCL 41833 and *R. intraradices* MUCL 49410 being the most efficient. This observation opens the door to the selection of AMF species and/or strains particularly suitable for the production of desirable metabolites, and to the question of whether specific AMF are responsible for the production of new undescribed metabolites.

Perspectives:

The combination of multiple AMF strains should be further explored to determine whether synergistic interactions and increased functional complementarities between AMF provide greater benefits to these important Boraginaceae plants. A high degree of genetic and functional diversity of AMF could be sought, theoretically providing complementary services to the host plants, thus contributing to greater plant productivity. This specificity of the outcome in plant-AMF symbiosis was reported in several studies using mixtures of AMF species (Wagg *et al.*, 2011).

Further in-depth investigations should fully exploit the wide physiological and genetic diversity of AMF, testing the highest possible range of diverse species and isolates. As previously discussed, transcriptomic studies would allow the identification of AMF strains differentially expressing genes relevant to the biosynthesis of therapeutic compounds in medicinal plants.

3- What is the best protocol to mass produce healthy ex vitro A. tinctoria plants starting from in vitro shoot-tip explants?

The best protocol for the successful mass production of *A. tinctoria* consists in (1) disinfection of shoot-tip explants by *ad hoc* combination of fungicide, ethanol, and NaOCl, (2) proliferation of the surface-disinfected explants on MS medium enriched with *ad hoc* concentrations of hormones (BA, NAA, and GA_3), (3) rooting of the explants for a period of 4 weeks on RC1 medium (NH_4NO_3-free) supplemented with IAA, (4) transfer of the rooted explants in pots filled with a peat moss:perlite mixture, followed by a specific relative humidity gradual decrease and light intensity increase. With this protocol, a large amount of *in vitro* produced *A. tinctoria* plants, with high levels of survival during *ex vitro* acclimatization, was obtained. It made it possible to carry out our studies on the effects of AMF on *A. tinctoria* production of therapeutic metabolites, and it would contribute to reduce the pressure on the natural population of *A. tinctoria*.

Perspectives:

Medicinal plants cultivation under field condition remains one of the most cost-effective production systems for metabolites of interest (Brinckmann *et al.*, 2022), but can endangered the plants if

overexploited. Therefore, new biotechnology cultivation systems are needed. The protocol developed here opens the door to the mass production of *in vitro* and/or *ex vitro* plants useful to produce important therapeutic metabolites. The approach applied in the present study might be further extended to other overexploited medicinal plants, which are not yet currently protected in their habitat or preserved in culture collections.

The successful production of rooted *in vitro A. officinalis* and *A. tinctoria* plants (i.e., clonal plants) can be further exploited to elucidate the metabolites biosynthetic modification occurring in the plants following their association with beneficial microorganisms. Indeed, the response of clonal plants to AMF (or other inoculants) might be potentially more stable and reproducible. For instance, Varela Alonso *et al.* (2022) investigated the effects of bacteria on the modulation of SMs in the medicinal plant *L. officinale* (Boraginaceae), with a focus on the naphthoquinones A/Sd, using plant clones grown strictly *in vitro*.

This approach can be extended to AMF species (e.g., *R. irregularis* MUCL 41833) to evaluate, under strict controlled conditions, the effects of root colonization by an obligate symbiont on PMs and SMs production.

The *in vitro* plant materials could be used as well to perform an A/Sd antimicrobial activity test to investigate whether some microbial inoculants are more/less prone/adapted to colonize the plants.

4- *Does the AMF R. irregularis MUCL 41833 increase the production of A/Sd and the relative expression of genes in the root tissues of A. tinctoria plants growing in a semi-hydroponic cultivation system?*

No*, R. irregularis MUCL 41833 did not exert a significant effect on the production of A/Sd* in the root tissues of *A. tinctoria*, but ***upregulated specific genes involved in the A/Sd biosynthetic pathway***.

Perspectives:

Further investigations are required to shed light on the link between the optimal time of plants harvest (i.e., plants growth stage with highest A/Sd production) and the impact of the S-H cultivation system. As mentioned above, the different development stages of AMF should be taken into consideration in further high-throughput transcriptome studies.

Today, no published genomic resources are available for *A. tinctoria*. Thus, further studies are required to better understand the effects of AMF on the A/Sd biosynthetic pathways regulation. Indeed, despite the interesting properties of naphthoquinones and especially A/Sd, no studies, to our knowledge, have been performed so far on the stimulation of plant naphthoquinones by AMF.

5- *Does the association of A. tinctoria plants with different AMF strains from GINCO (R. irregularis MUCL 41833, R. aggregatus MUCL 49408) and isolated from wild-growing A. tinctoria (R. irregularis and S. viscosum) results in similar effects on the production of A/Sd and relative genes expression?*

No*, the native strain R. irregularis significantly enhanced the production of A/Sd* in the root tissues of *A. tinctoria*, while ***the native strain S. viscosum exerted an intermediate effect, compared to the GINCO-AMF strains.*** Despite the evident natural variability between the *A. tinctoria* plants used in this study, the beneficial effect of native *R. irregularis* on the production of A/Sd was highly significant both in the S-H cultivation systems and pots. Interestingly, this AMF was characterized by a significantly higher presence of arbuscules (i.e., the principal site of exchange between plant and fungus within the root cells). Hypothesis was advanced on the better adaptation of native fungal associates with this important medicinal plant, and especially with the antimicrobic compounds produced in its roots (A/Sd). However, this hypothesis could not be truly confirmed with the other native strain *S. viscosum*.

Perspectives:

To demonstrate that the native AMF strains are better adapted to their plant associates and thus more prone to stimulate plants to produce SMs of medicinal importance, different molecular tools need to be developed oriented towards the exploration of gene expression within the biosynthetic pathways of the SMs of interest. This would also require conducting the S-H cultivation experiment for a much longer period (i.e., > 6 weeks). Importantly, an antimicrobial activity test applying A/Sd, as mentioned before, should be performed *in vitro* either on micropropagated *A. tinctoria* plants or HRCs to select the best AMF strains.

Finally, it is not excluded that the different growth conditions (i.e., S-H cultivation system and pots) used in our experiments have played a role in the production of plant metabolites. Indeed, the nutrient solution applied in this study was adapted both to allow the AMF symbiosis (low P concentration) and to avoid shikonin production inhibition (lacking NH_4NO_3). The growth parameters were adjusted as well, to simulate the native growth conditions of *A. tinctoria*. However, these systems remain artificial and still require further improvements (i.e., size of the containers, circulation of fresh solution). Thus, the application of different AMF coupled to optimal culture conditions should be further investigated for improving the quality and production of metabolites by plants.

The amount of A/Sd differs in relation to the plants' populations, and this might depend on the plant genotype, soil type, content of soil macro/micronutrients available, environment conditions, physiological status of the plants. Thus, AMF belonging to different locations (i.e., sandy costal habitats instead of pine forest) could induce different effects on the production of metabolites by the plants and thus should be further studied.

As mentioned above, one of the major limitations of this Ph.D. was the lack of scientific background and literature concerning both *A. officinalis* and *A. tinctoria*. Hence, micropropagation protocols, culture media and root-inducing media had to be established and optimized by trial and error to sustain a suitable environment for growth and development of Boraginaceae plant species. Moreover, we provided the first data on the role of AMF in the production of metabolites by two medicinal plants (*A. officinalis* and *A. tinctoria*), allowing to innovatively explore the initial steps towards the improvement of their medicinal metabolites production. Standard and native AMF were demonstrated to positively improve the production of several metabolites. Combinations of AMF should be further explored, together with an improved experimental/scale up arrangement and molecular analysis.

In addition, recovering metabolites from a circulating nutrient solution rather than from the soil or the plant tissues is safer and more practical and should be further investigated using a nutrient film technique hydroponic cultivation system coupled to a non-destructive

extraction method. For instance, a new eco-friendly category of solvent, named natural deep eutectic solvents (NaDESs), was applied as an "extractive" solution and its toxicity was preliminarily assessed. This system might reduce the time required to extract the exudates from the nutrient solution. Moreover, it requires less effort in the setting up since no inert substrate is required compared to the S-H cultivation system. Finally, the NFT is composed by PVC tubes, allowing the roots to grow extensively, and the system to be run for a longer period of time (**Figure 43**). Further studies are required to optimize the application of these solvents in scaled-up hydroponic cultivation systems, as well as the *ad hoc* addition of biotic elicitors in association with the medicinal plants. The Plant Milking® technology could also be taken into consideration to harvest metabolites from the plant roots. Different plant elicitors could be tested (i.e., best performing AMF, MeJA). Finally, a recent patent (WO 2019/003240 A1 by the Energy and Resources Institute, New Dehli) presented the invention of a novel gas-phase (mist) bioreactor for the *in vitro* production of AMF cultivating the fungal spores and roots using transformed plant roots in a limited aseptic space. Since a similar system is used to produce bioactive compounds, as previously reported, further research could investigate the implementation of this bioreactor applying the best AMF strains and transformed hairy roots of Boraginaceae plants. However, as previously mentioned, an antimicrobial test should be performed in order to identify the best performing/adapted AMF species/strains towards the presence of A/Sd or other antimicrobial compounds. Moreover, the costs of the different systems should be taken into consideration.

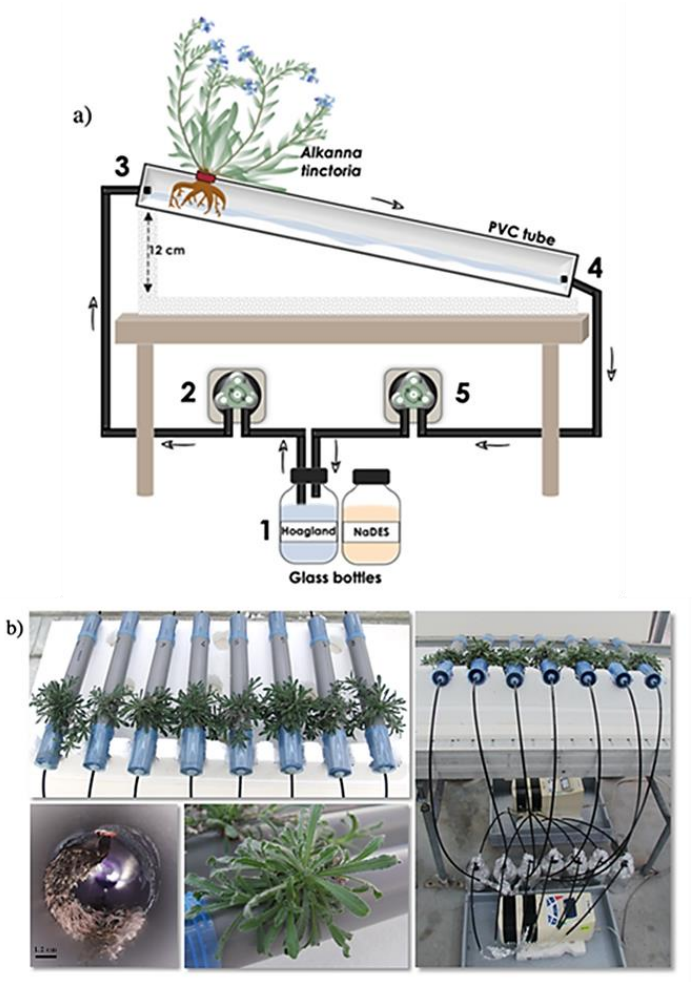

Figure 43. The NFT cultivation system applied for the toxicity assessment of NaDES on *A. tinctoria* plants. (**a**) Schematic representation of the system. The Hoagland solution and/or NaDES is circulated through the grey PVC tube supporting the *A. tinctoria* plant. The nutrient solution (or NaDES) in the glass bottle (**1**) is pumped using a peristaltic pump (**2**) to the upper part of the PVC tube (**3**) via black pipes. The solution percolates through the PVC tube (**4**) and is pumped back to the bottle using a second peristaltic pump (**5**). Gray arrows indicate the flow direction of the nutrient solution (or NaDES) in the tubing. (**b**) Pictures from the experimental setup conducting under greenhouse conditions at UCLouvain.

ANNEXES

Annex I

The Arbuscular Mycorrhizal Fungus *Rhizophagus irregularis* MUCL 41833 modulates metabolites production *of Anchusa officinalis* L. under semi-hydroponic cultivation

Supplementary Table 1. Nutrients composition of the modified Hoagland solution, based on Hoagland and Arnon (1950), used in this study.

Chemical composition	Concentration [mg/L]
Macronutrients	
NH_4NO_3	80
$Ca(NO_3)_2 \cdot 4H_2O$	826
KNO_3	357
KCl	45.1
K_2SO_4	105.4
Micronutrients	
KNO_3	50
KH_2PO_4	27.4
$MgSO_4$	120.4
$MnSO_4 \cdot H_2O$	0.5
H_3BO_3	1.4
$CuSO_4 \cdot 5H_2O$	0.2
$(NH_4)_6Mo_7O_2 \cdot 4H_2O$	0.1
$ZnSO_4 \cdot 7H_2O$	0.6
Iron	
Fe-EDTA	19

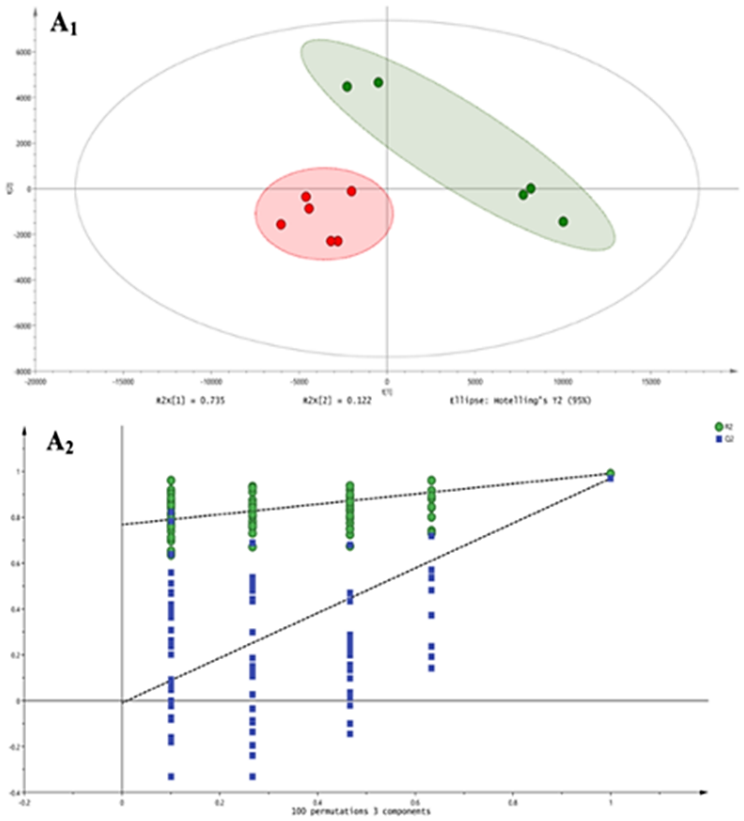

Supplementary Figure 1 (A1-A2). Partial least square analysis – Discriminant analysis (PLS-DA) and permutation test (100 rearrangements) – Comparison of UHPLC-HRMS metabolic profiles from M and NM root samples after 1 week (T1) of growth in the S-H cultivation system (M_T1: green dots; NM_T1: red dots).

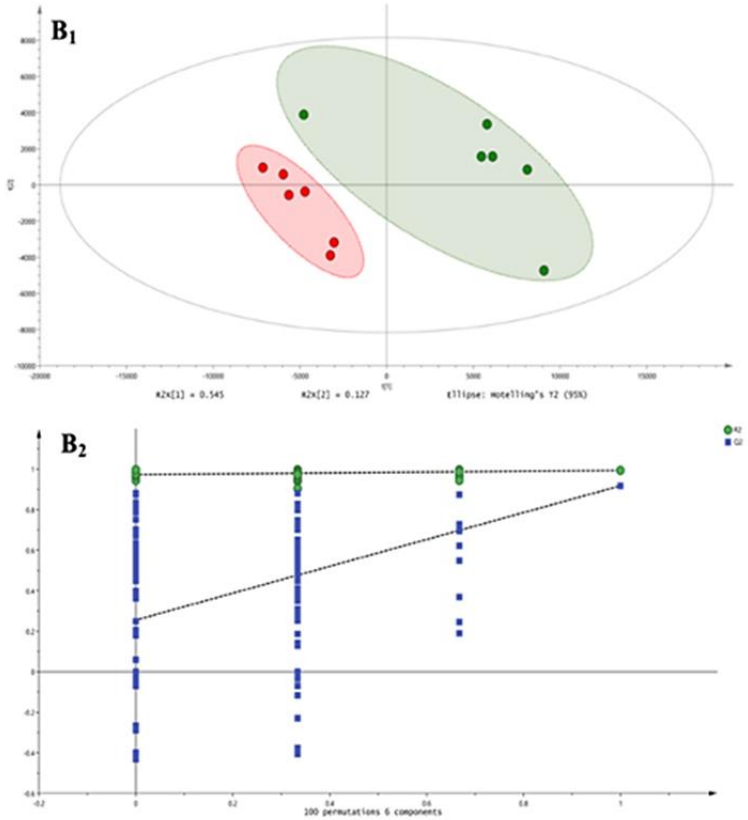

Supplementary Figure 1(B1-B2). Partial least square analysis – Discriminant analysis (PLS-DA) and permutation test (100 rearrangements) – Comparison of UHPLC-HRMS metabolic profiles from M and NM shoot samples after 1 week (T1) of growth in the S-H cultivation system (M_T1: green dots; NM_T1: red dots).

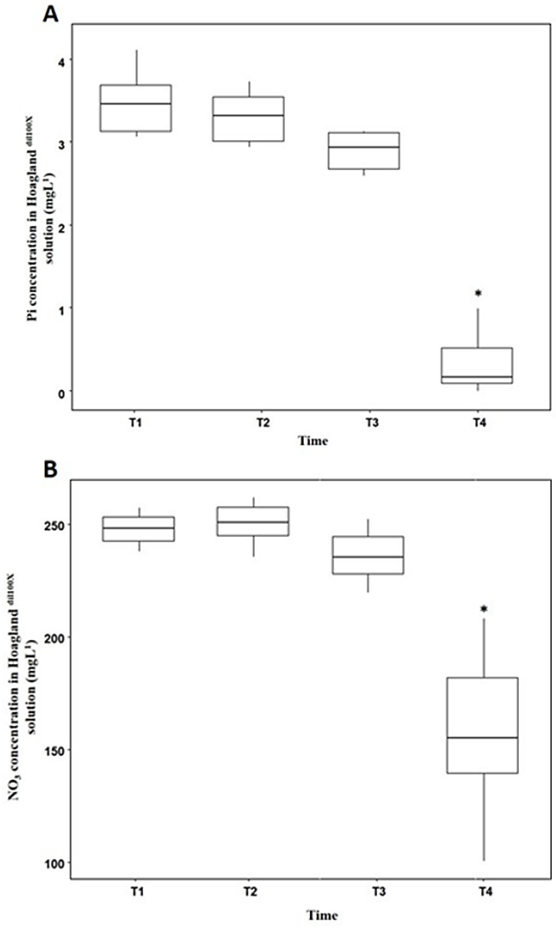

Supplementary Figure 2. Boxplots illustrate the means of Pi (**A**) and NO^{-3} (**B**) concentration in the nutrient solutions of M and NM plants at four different time sampling (day 9 - T1; day 15 - T2; day 22 - T3 and day 30 - T4). The presence of * indicates a significant difference at T4, according to the pairwise comparison test ($p < 0.05$). Means of the single time are averaged between the two treatments (M and NM).

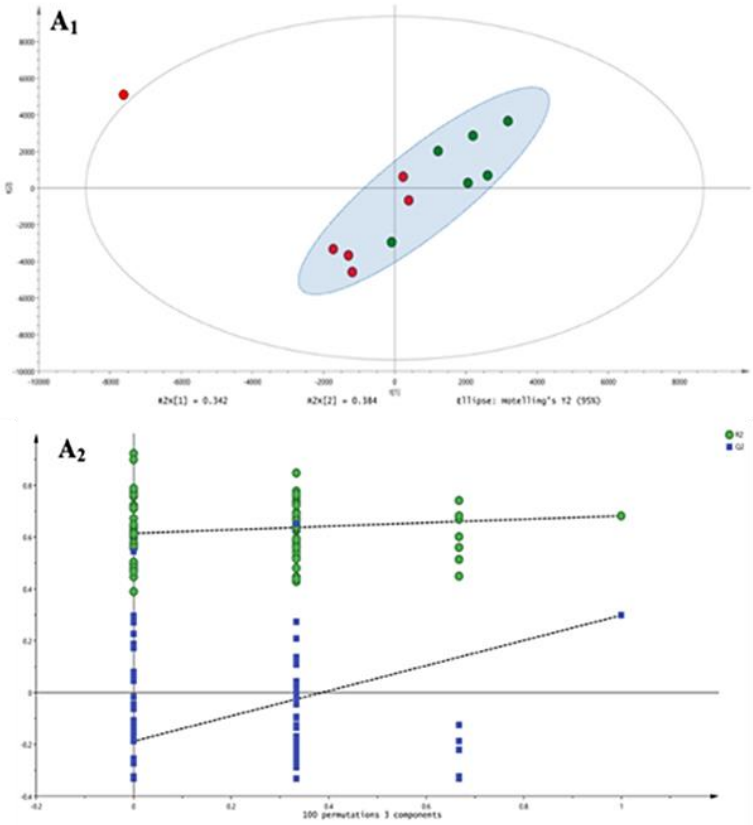

Supplementary Figure 3 (A1-A2). Partial least square analysis – Discriminant analysis (PLS-DA) and permutation test (100 rearrangements) – Comparison of UHPLC-HRMS metabolic profiles from M and NM root samples after 4 weeks (T4) of growth in the S-H cultivation system (M_T1: green dots; NM_T1: red dots).

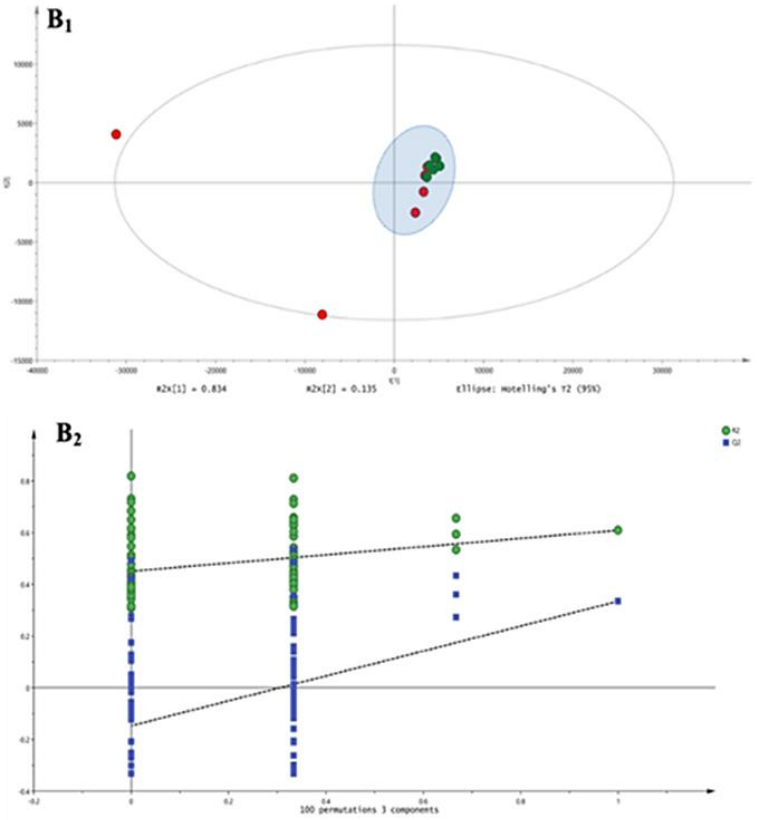

Supplementary Figure 3 (B1-B2). Partial least square analysis – Discriminant analysis (PLS-DA) and permutation test (100 rearrangements) – Comparison of UHPLC-HRMS metabolic profiles from M and NM and shoot samples after 4 weeks (T4) of growth in the S-H cultivation system (M_T1: green dots; NM_T1: red dots).

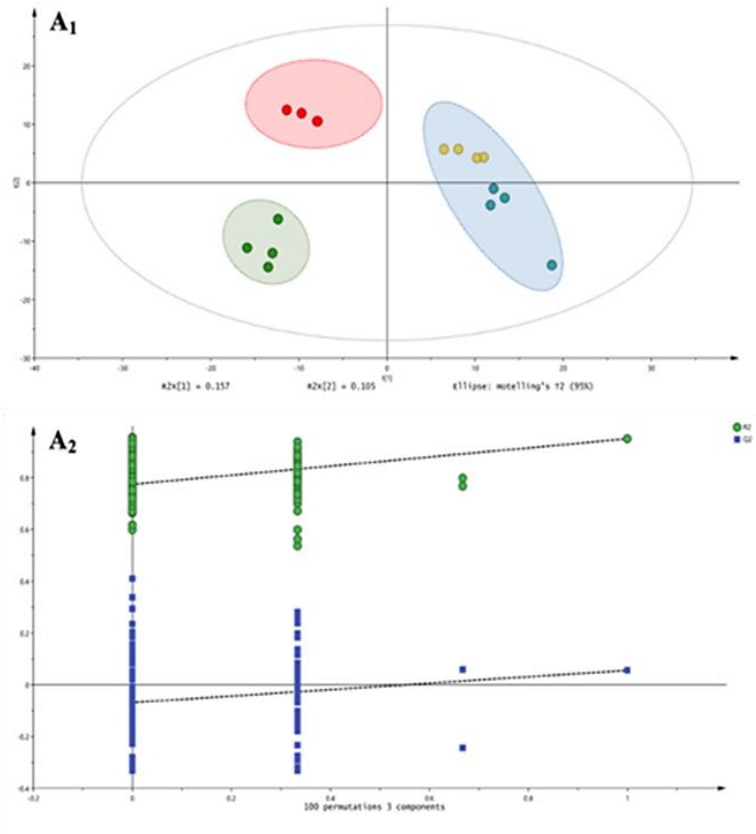

Supplementary Figure 4. Partial least square analysis – Discriminant analysis (PLS-DA) and permutation test (100 rearrangements) – Comparison of UHPLC-HRMS metabolic profiles from M and NM nutrient solution samples after 1 (Exp. 1 - T1) and 4 weeks (Exp. 2 - T4) of growth in the S-H cultivation system (M_T1: blue dots; NM_T1: yellow dots; M_T4: green dots; NM_T4: red dots).

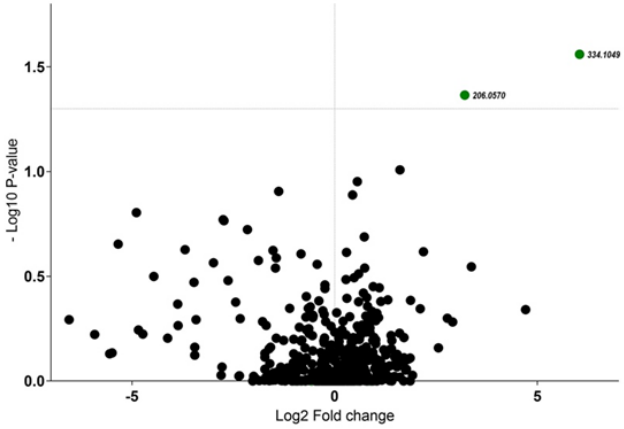

Supplementary Figure 5. Volcano-plot analysis: Up and downregulation of PMs and SMs between M and NM nutrient solutions after 4 weeks (T4) of growth in the S-H system. The statistically significant compounds (p < 0.05 & fold change > 1.5), upregulated in M nutrient solutions, were represented in green in the upper right-side part of the plot.

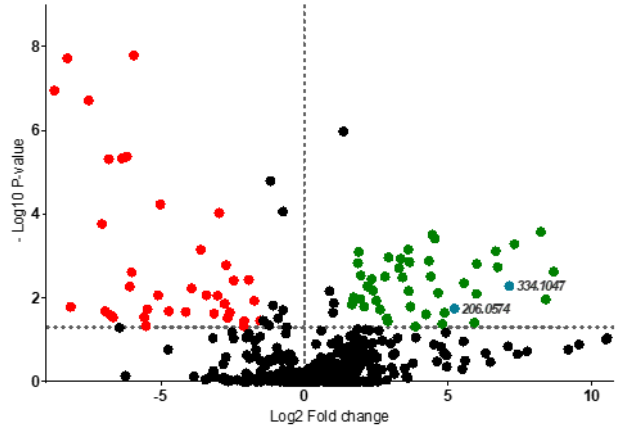

Supplementary Figure 6. Volcano-plot analysis – Up and downregulation of statistically significant compounds (p < 0.05 & fold change > 1.5) between nutrient solutions of M plants after 1 (Exp. 1 - T1) and 4 weeks (Exp. 2 - T4) of S-H cultivation system. Upregulated compounds at T4 of experiment were represented in green in the right side of the plot, while upregulated compounds at T1 of experiment were represented in red in the left side of the plot.

Annex II

The metabolic profile of *Anchusa officinalis* L. differs according to its associated arbuscular mycorrhizal fungi

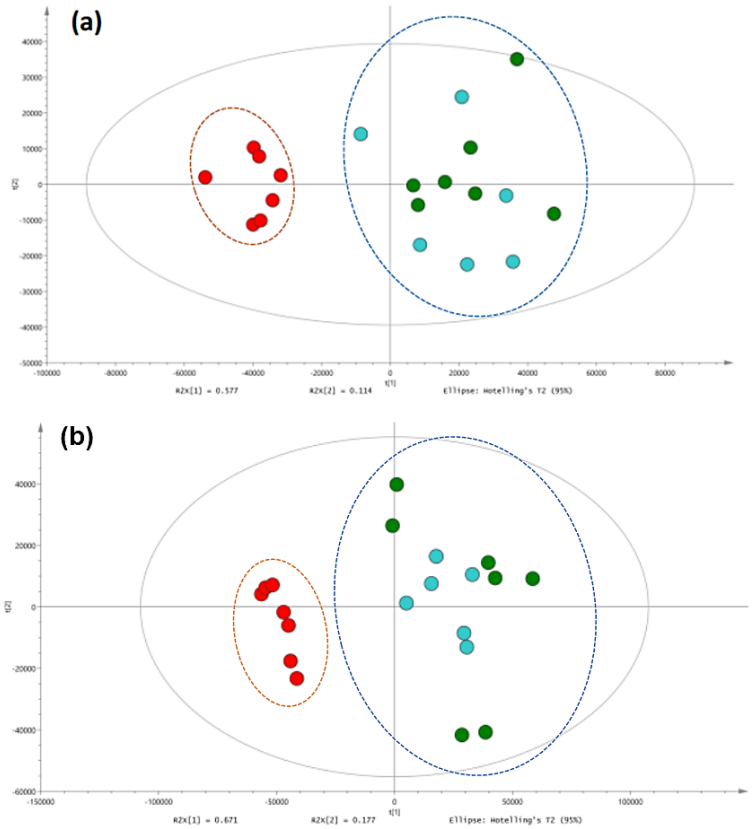

Supplementary Figure 1. Principal component analysis (PCA) – Comparison of UHPLC-HRMS metabolic profiles from *A. officinalis* root (**a**) and shoot (**b**) samples associated with four different AMF species after 9 days of growth in the S-H cultivation system (*R. irregularis* MUCL 41833: blue dots; *R. intraradices* MUCL 49410: green dots; *R. clarus* MUCL 46238: red dots).

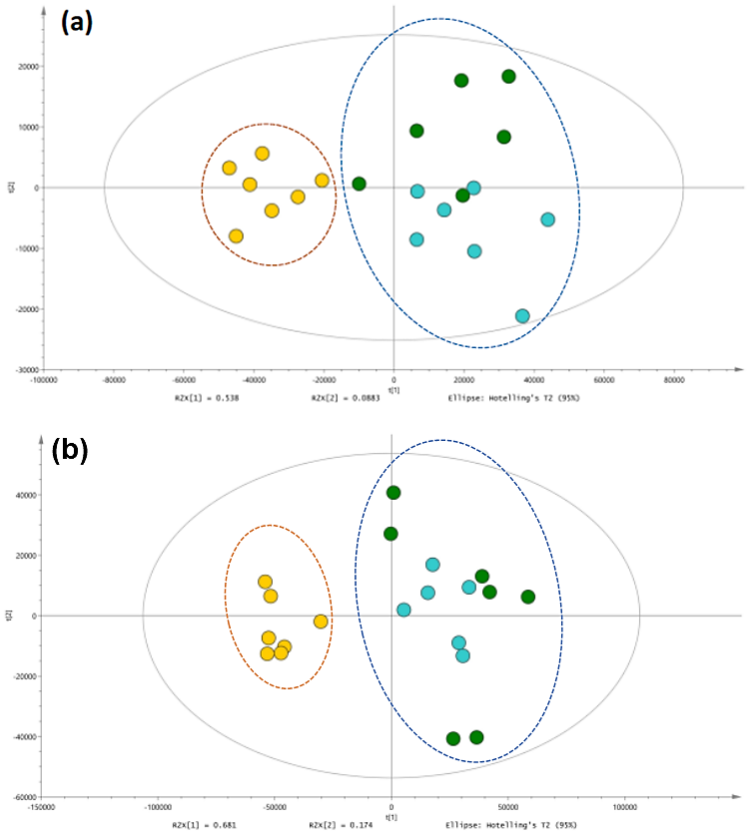

Supplementary Figure 2. Principal component analysis (PCA) – Comparison of UHPLC-HRMS metabolic profiles from *A. officinalis* root (**a**) and shoot (**b**) samples associated with four different AMF species after 9 days of growth in the S-H cultivation system (*R. irregularis* MUCL 41833: blue dots; *R. intraradices* MUCL 49410: green dots; *R. aggregatus* MUCL 49408: yellow dots).

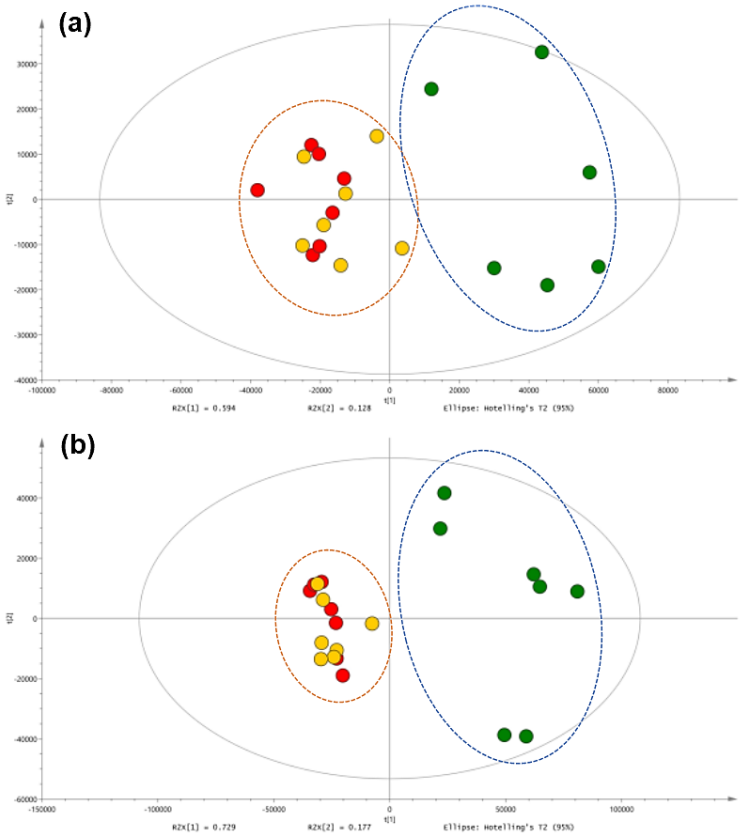

Supplementary Figure 3. Principal component analysis (PCA) – Comparison of UHPLC-HRMS metabolic profiles from *A. officinalis* root (**a**) and shoot (**b**) samples associated with four different AMF species after 9 days of growth in the S-H cultivation system (*R. intraradices* MUCL 49410: green dots; *R. clarus* MUCL 46238: red dots; *R. aggregatus* MUCL 49408: yellow dots).

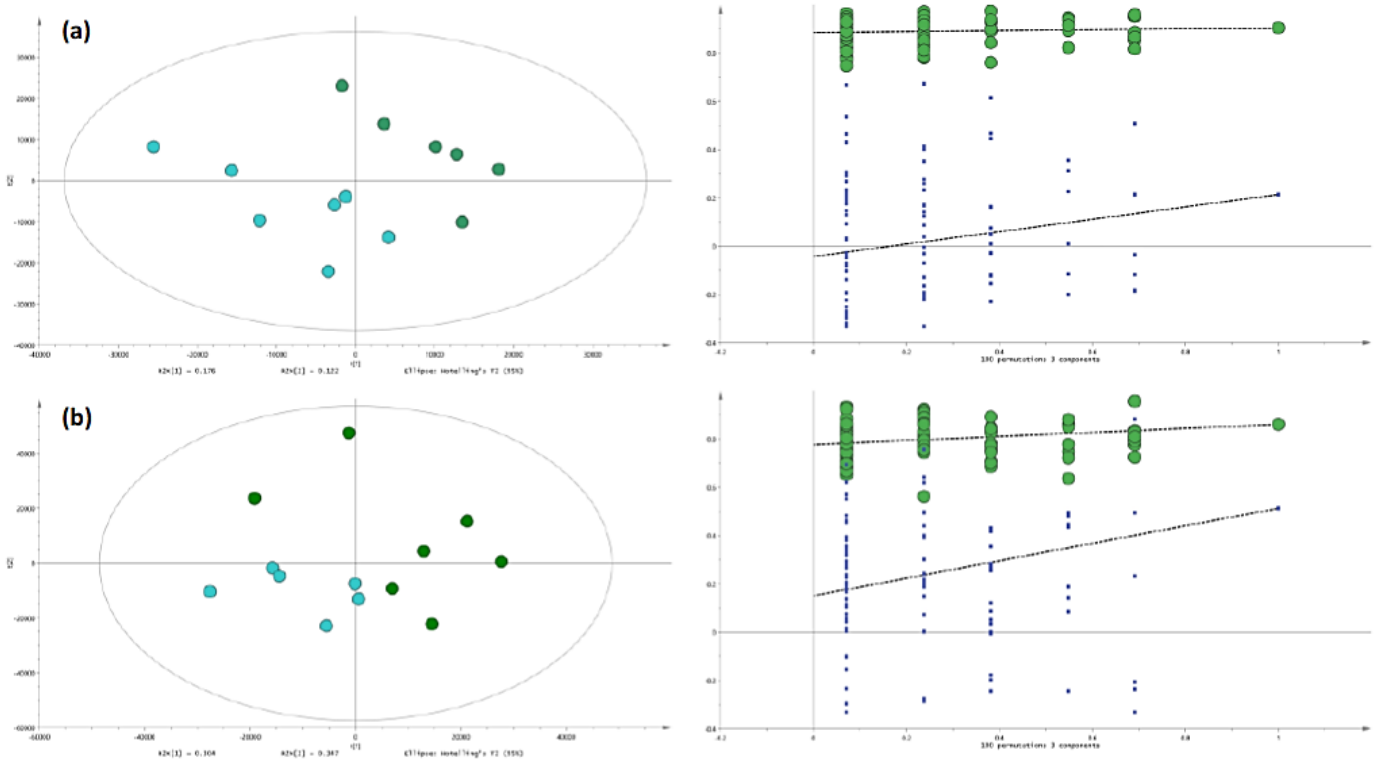

Supplementary Figure 4. Partial least square analysis – Discriminant analysis (PLS-DA) and permutation test (100 rearrangements) – Comparison of UHPLC-HRMS metabolic profiles from *A. officinalis* root (**a**) and shoot (**b**) samples associated with four different AMF species after 9 days of growth in the S-H cultivation system (*R. irregularis* MUCL 41833: blue dots; *R. intraradices* MUCL 49410: green dots).

Supplementary Table 1. Evolution of AMF-root colonization (TC % and AC %) and total fresh weight (TFW) of *A. officinalis* associated to one AMF species (*R. irregularis* MUCL 41833, *R. intraradices* MUCL 49410, *R. clarus* MUCL 46238 and *R. aggregatus* MUCL 49408) before (T0) and after 9 days (T1) of growth in the S-H cultivation system.

		AMF-root colonization (%)		**Fresh weight (g)**
AMF treatments	**Harvest time**	**TC**	**AC**	**TFW**
R. irregularis (MUCL 41833)	T0	76 ± 3	14 ± 3	5.74 ± 1.5
R. intraradices (MUCL 49410)	T0	91 ± 3	22 ± 3	7.78 ± 1.5
R. clarus (MUCL 46238)	T0	86 ± 3	18 ± 3	4.95 ± 1.5
R. aggregatus (MUCL 49408)	T0	85 ± 3	17 ± 3	7.73 ± 1.5
R. irregularis (MUCL 41833)	T1	63 ± 3	6 ± 3	5.63 ± 1.5
R. intraradices (MUCL 49410)	T1	70 ± 3	12 ± 3	8.66 ± 1.5
R. clarus (MUCL 46238)	T1	61 ± 3	6 ± 3	5.31 ± 1.5
R. aggregatus (MUCL 49408)	T1	68 ± 3	10 ± 3	8.39 ± 1.5

The parameters measured are expressed as mean ± standard errors (SE) of 7 (T0) and 7 (T1) replicates per each AMF treatment.

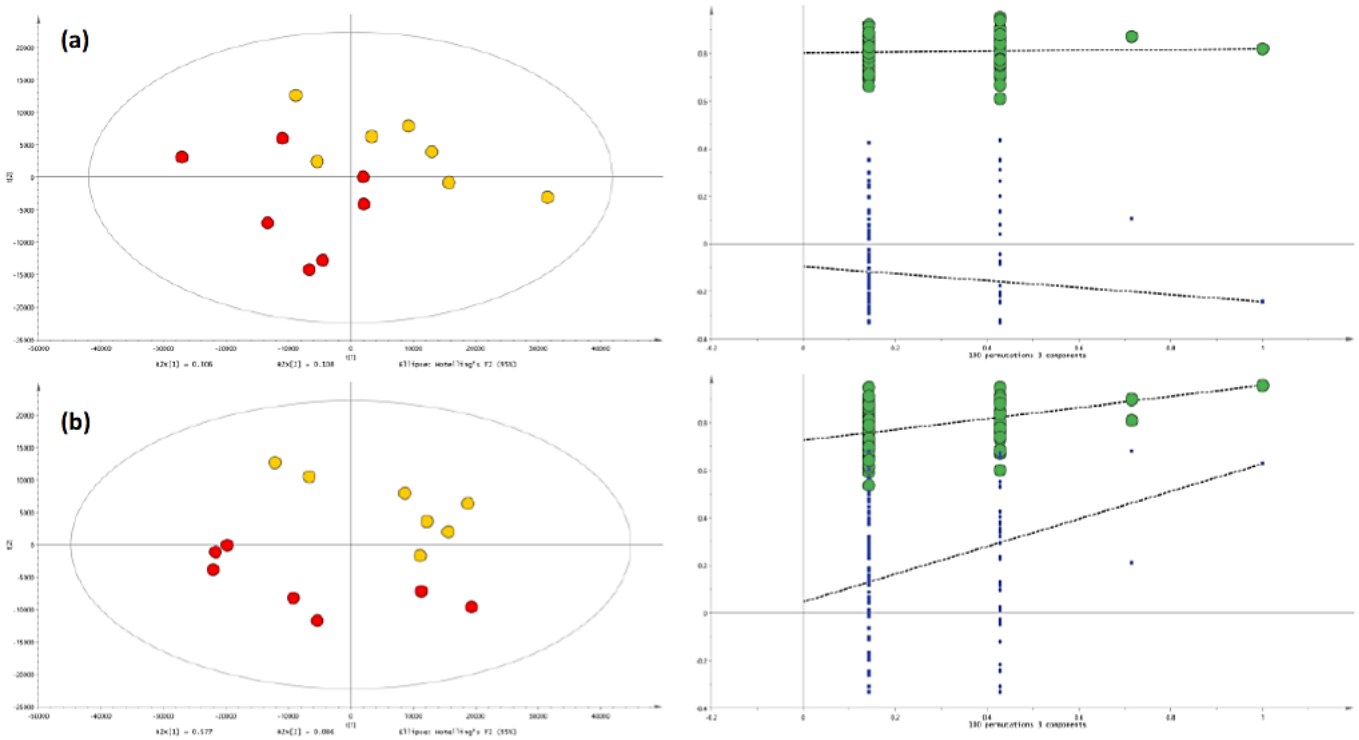

Supplementary Figure 5. Partial least square analysis – Discriminant analysis (PLS-DA) and permutation test (100 rearrangements) – Comparison of UHPLC-HRMS metabolic profiles from *A. officinalis* root (**a**) and shoot (**b**) samples associated with four different AMF species after 9 days of growth in the S-H cultivation system (*R. clarus* MUCL 46238: red dots; *R. aggregatus* MUCL 49408: yellow dots).

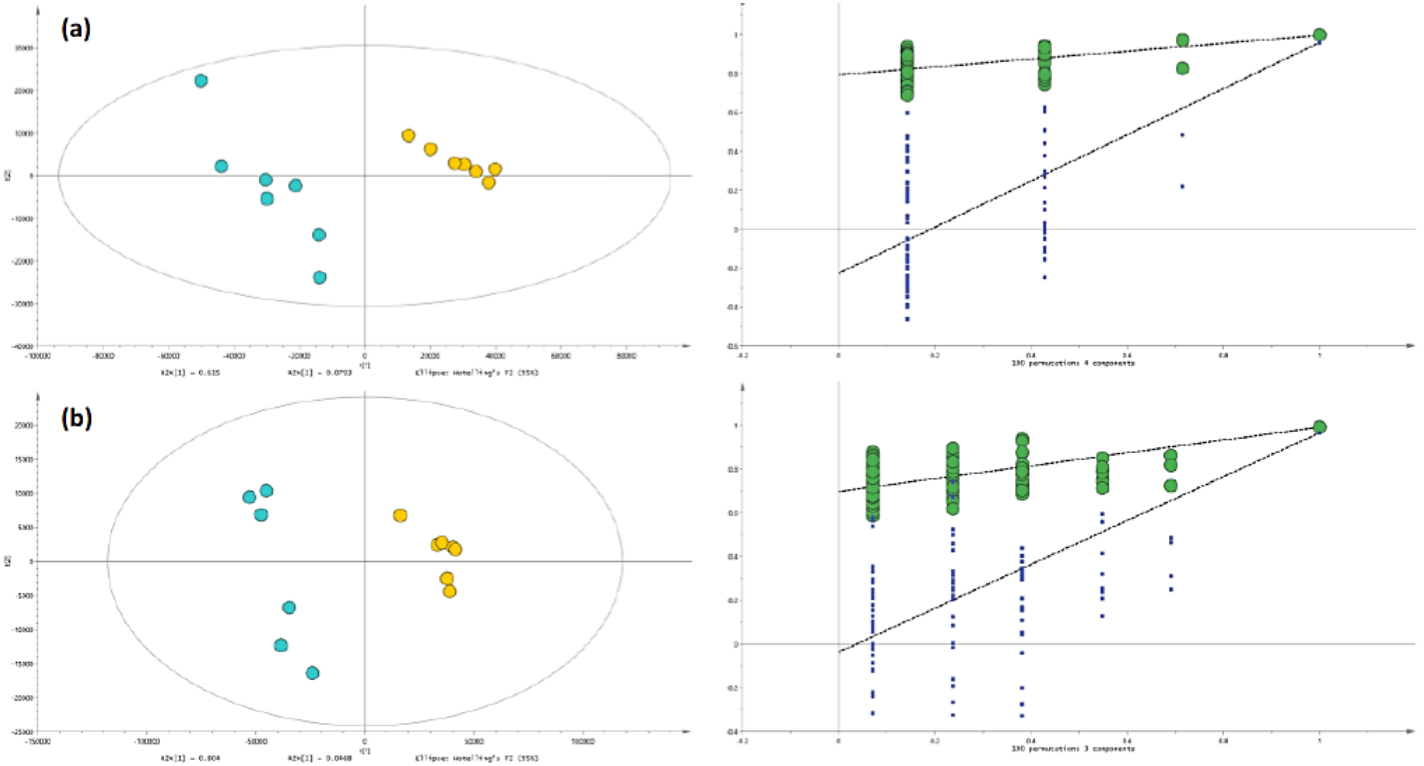

Supplementary Figure 6. Partial least square analysis – Discriminant analysis (PLS-DA) and permutation test (100 rearrangements) – Comparison of UHPLC-HRMS metabolic profiles from *A. officinalis* root (**a**) and shoot (**b**) samples associated with four different AMF species after 9 days of growth in the S-H cultivation system (*R. irregularis* MUCL 41833: blue dots; *R. aggregatus* MUCL 46238: yellow dots).

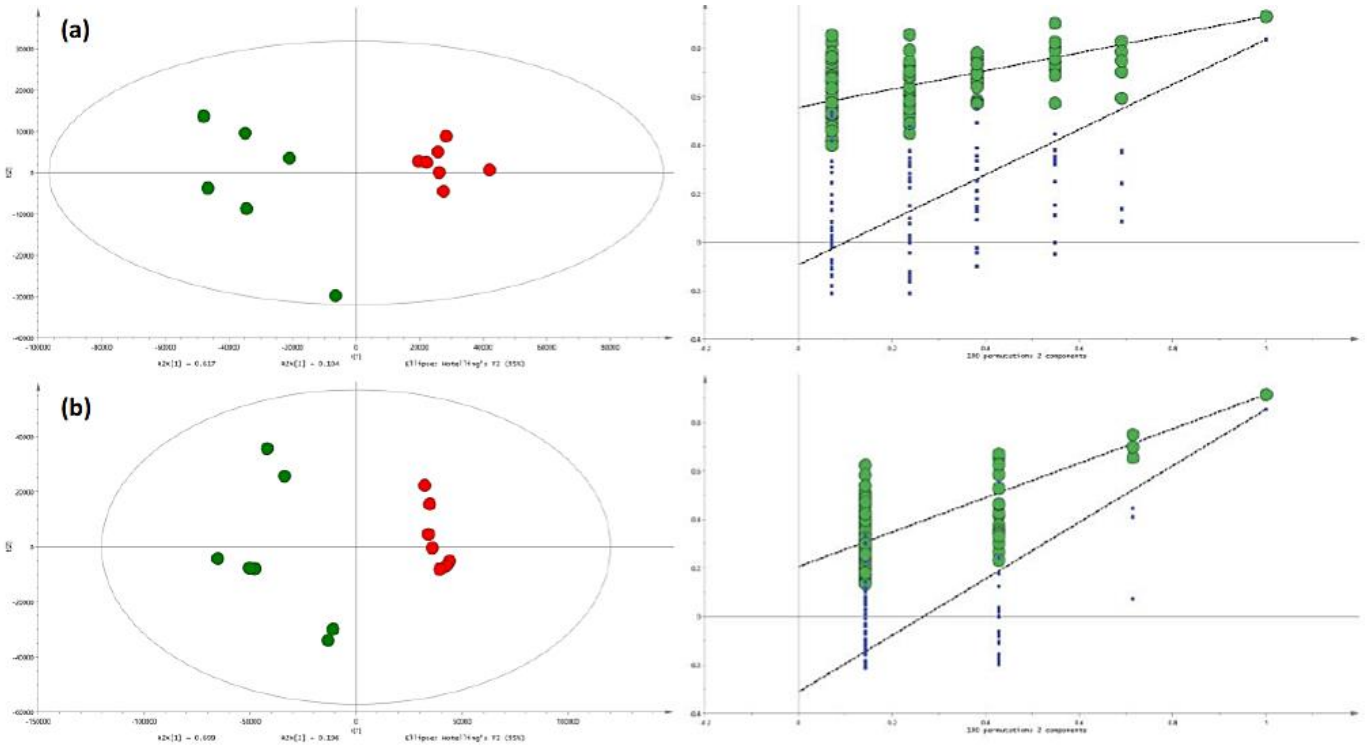

Supplementary Figure 7. Partial least square analysis – Discriminant analysis (PLS-DA) and permutation test (100 rearrangements) – Comparison of UHPLC-HRMS metabolic profiles from *A. officinalis* root (**a**) and shoot (**b**) samples associated with four different AMF species after 9 days of growth in the S-H cultivation system (*R. intraradices* MUCL 49410: green dots; *R. clarus* MUCL 4623: red dots).

Annex III

In vitro propagation of *Alkanna tinctoria* Tausch.: a medicinal plant of the Boraginaceae family with high pharmaceutical value

Supplementary Table 1. Chemical composition of the different culture media tested in the study.

Component (mg L^{-1})	**MS[1]**	**½ MS[2]**	**WPM[3]**	**GB5[4]**	**RC1[5]**
KNO_3	1900	950	-	2500	80
NH_4NO_3	1650	825	400	-	-
$(NH_4)2SO_4$	-	-	-	134	-
K_2SO_4	-	-	990	-	-
$MgSO_4.7H_2O$	370	185	306.54	247.56	370
KH_2PO_4	170	85	170	-	-
$CaCl_2.2H_2O$	440	220	108.5	149.23	-
$Ca(NO_3)_2.4H_2O$	-	-	471.26	-	288
KCl	-	-	-	-	65
$NaH_2PO_4.4H_2O$	-	-	-	202.44	131
NaFeEDTA	36.7	18.35	36.7	36.7	36.7
$MnSO_4.H_2O$	17	8.5	22.3	10	16.9
H_3BO_3	6.2	3.1	6.2	3	1.5
$ZnSO_4.7H_2O$	8.6	4.3	8.6	2	2.65
$Na_2MoO_4.2H_2O$	0.25	0.125	0.25	0.25	0.25
$CuSO_4.5H_2O$	0.025	0.0125	0.25	0.025	0.02
$CoCl_2.6H_2O$	0.025	0.0125	-	0.025	-
KI	0.83	0.415	-	0.75	0.75
Thiamine HCl	0.1	0.1	1	10	0.1
Nicotinic acid	0.5	0.5	0.5	1	0.5
Pyridoxine HCl	0.5	0.5	0.5	1	0.1
Glycine	2	2	2	-	3
myo-Inositol	100	100	100	100	100
Sucrose (g L^{-1})	20-30	20	20	20	30
Plant Agar (g L^{-1})	6	6	6	6	6
pH	5.8	5.8	5.8	5.8	5.8

[1]Murashige-Skoog (MS) (Murashige and Skoog, 1962).
[2]½ MS in macro and micro-nutrients and FeNaEDTA.
[3]Woody Plant Medium (WPM) (Lloyd and McCown, 1980).
[4]Gamborg B5 (GB5) (Gamborg *et al.*, 1968).
[5]Root Culture 1 (RC1) (Shimomura *et al.*, 1991).

Supplementary Table 2. Effects of Murashige and Skoog-MS supplemented with two sucrose and Plant Agar concentrations on different *Alkanna tinctoria* explants parameters after 20 days of culture.

Treatments		**Shoot formation (%)**	**N. of new shoots/ explant**	**Shoot length (cm)**	**Prolif. rate**	**Hyperhydricity (%)**
Sucrose (g L^{-1})	Plant Agar (g L^{-1})					
20	6	83.3 ± 16.7 a	3.6 ± 0.4 a	0.8 ± 0.1 a	3.0 ± 0.4 a	44.4 ± 14.7 a
20	7	88.9 ± 11.1 a	3.8 ± 0.3 a	0.8 ± 0.1 a	3.4 ± 0.3 a	50.0 ± 0 a
30	6	83.3 ± 9.6 a	3.6 ± 0.5 a	0.7 ± 0 a	3.3 ± 0.4 a	61.1 ± 11.1 a
30	7	84.6 ± 7.6 a	3.8 ± 0.4 a	0.9 ± 0 a	3.7 ± 0.4 a	53.9 ± 22.9 a

Data for number of new shoots per explant, shoot length and proliferation rate are means ± SE of 18 replicates, while data for shoot formation and hyperhydricity are means ± SE of 3 replicates (i.e., the vessels, each containing 6 explants). Means followed by different letters within the same column differed significantly (Duncan's multiple range test, $p < 0.05$).

Supplementary Table 3. Effect of Murashige and Skoog-MS full-strength, ½ MS, and Root Culture 1-RC1 supplemented with different auxin types and concentrations on the survival rate of *in vitro Alkanna tinctoria* rooted explants to *ex vitro* greenhouse conditions.

Basal culture medium *in vitro*	**Auxins (µM)**	***Ex vitro* survival of rooted explants (%)**
MS	2.5 IBA	85
MS	5 IBA	90
½ MS	2.5 IBA	75
½ MS	5 IBA	80
MS	2.69 NAA + 0 IBA	70
MS	2.69 NAA + 2.5 IBA	90
MS	5.4 NAA + 2.5 IBA	60
MS	2.69 NAA + 5 IBA	60
MS	5.4 NAA + 5 IBA	50
RC1	0 IAA	90
RC1	2.85 IAA	100
RC1	5.71 IAA	80

Data are means of 10 replicates per treatment.

Annex IV

Arbuscular mycorrhizal fungi impact the production of alkannin/shikonin and their derivatives in *Alkanna tinctoria* Tausch. grown in semi-hydroponic and pot cultivation systems

Isolation and mono-species culture of AMF

Evaluation of the presence of AMF in root/soil samples

Roots of *Alkanna tinctoria* were sampled from the wild in Greece and stained following the protocol of Vierheilig *et al.* (1998), and Walker (2005), to evaluate root colonization (**Supplementary Figure 1A**). In parallel, rhizospheric soils were sampled to collect AMF spores applying a procedure adapted from Cranenbrouck *et al.* (2005) and Walker (2009) (personal communication) (**Supplementary Figure 1B**). Spores were subsequently mounted on slide with polyvinyl alcohol-lacto-glycerol (PVLG) solution (Omar et al., 1978) and checked under stereomicroscope (Olympus BH2–RFCA, Japan) to confirm AMF presence.

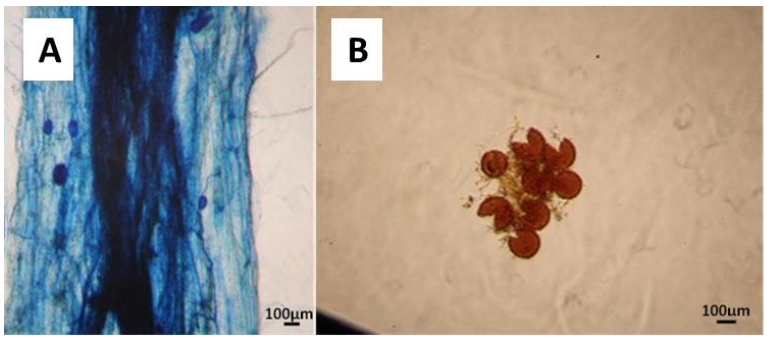

Supplementary Figure 1. (**A**) Stained *A. tinctoria* root and (**B**) spores, collected from the wild in Greece (Photographs taken with Canon EOS 60D, through the lens of a bright field light stereomicroscope, Olympus BH2-RFCA, Japan).

Establishment of AMF trap cultures

Seeds of *Plantago lanceolata* L. (Ecosem, Belgium) and *Medicago truncatula* Gaertn. (SARDI, Australia) were surface sterilized by soaking in 70% of ethanol for 1 min and in sodium hypochlorite (8% active chloride) for 5 min, and subsequently rinsed 3 times with

deionized water. The seeds were then germinated in a 1.3 L pot (15×11.4 cm) filled with a sterilized (121°C for 15 min) substrate that consist of a mixture of calcinated clay (DCM, Belgium), quartz (0.4-0.8 mm), quartz (1-2 mm), 2:2:1 w/w.

A. tinctoria plant rhizospheric soils and roots pieces were used in trap cultures. For roots, thin fragments were placed near the root system of 15-day old seedlings of *M. truncatula* and *P. lanceolate.* Two and 5 seedlings, respectively, were placed in each pot (1.3 L, 15×11.4 cm) filled with the same sterilized substrate mixture as above. For rhizospheric soils, samples were placed in individual pots between two layers of the same sterilized substrate as above, and in contact with 15-day old *M. truncatula* and *P. lanceolate* seedlings. In total 24 trap cultures were established (12 for rhizospheric soils and 12 for root samples).

To maintain the trap cultures, the pots were watered to field capacity and supplemented with slow release NPK beads (four beads per pot) (Osmocote PRO 5-6 months, 17-11-10+2MgO+TE, or Osmocote PRO 16-3-11+3 MgO, Everris, France). The pots were maintained in Sunbags (Sigma-Aldrich, Germany) closed with plastic paper clips (Laurel, Germany). They were watered with deionized water every three weeks and kept under greenhouse condition set at 20°C, 50% RH, photoperiod of 16 h day^{-1} and PPF of 96 µmol $m^{-2}s^{-1}$ (**Supplementary Figure 2**).

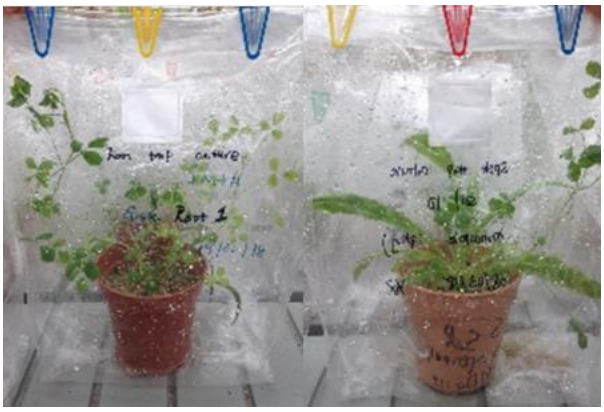

Supplementary Figure 2. Trap cultures of rhizospheric soils with *M. truncatula* and *P. lanceolata* plants, under greenhouse conditions (UCLouvain).

Establishment of AMF mono-species pot cultures

Roots and substrates from the trap cultures above were used to collect new, actively growing, and healthy AMF spores. Roots and substrates were sieved through a sequence of sieves (i.e., 250, 106 and 38 µm, Euromatest Sintco, France) and supernatant cleaned with tap water. Different fractions from the sieves were collected in Petri dishes (50 mm) and observed under stereomicroscope (Olympus, SZ61) to collect healthy-looking spores with tweezer and needles. Single spores or cluster of spores attached by a common mycelium were placed at the intersection between a main root and newly growing secondary root of 15-day old *P. lanceolata* seedlings. Then, the seedlings were placed in 7x7x6 cm pots filled with sterilized substrate mixture as above. Four pots were placed in one closed Sunbag and watered with low-P Hoagland solution (Hoagland and Arnon, 1950) 100x diluted every 20 days. Sunbags were maintained under greenhouse conditions set as above (**Supplementary Figure 3**). In total, around 220 single spores AMF pot cultures were established.

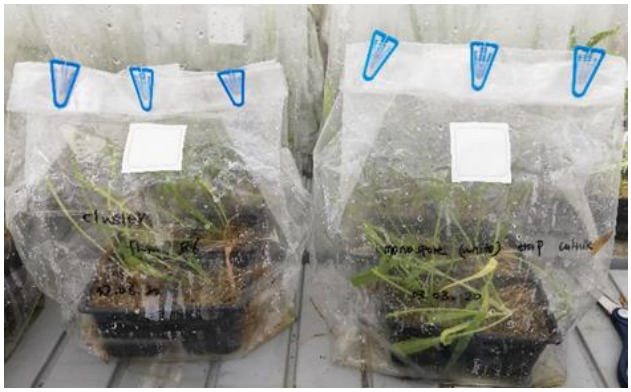

Supplementary Figure 3. Single spores AMF trap cultures with *P. lanceolata* host plants maintained under greenhouse conditions (UCLouvain).

Molecular identification of isolated AMF

In total 44 cultures of AMF were successful. A selection of 9 cultures (with contrasting spores' morphologies) were used for molecular identification. Three to 5 healthy spores were collected in each pot by wet sieving and picked with needle and tweezer (Vomm 113 SA). They were used for DNA extraction trough sterile needle (AGANI™ NEEDLE, 0.45×23 mm, TERUMO) in 0.2 mL PCR tubes (SARSTEDT, Germany) under laminar flow hood. Five µL of PCR

water was added to each sample to crush the spores and obtain the starting 5 µL of template DNA. Two-step PCR applying specific AMF primers amplifying a part of the SSU rRNA gene, the complete ITS region (including the 5.8S rRNA gene) and approx. 800 bp of the LSU rRNA gene, named SSU-ITS-LSU, were used (Krüger et al., 2009). For the first PCR, primer pairs mixtures SSUmAf – LSUmAr were used, and for the nested PCR, primer pairs mixtures SSUmCf – LSUmBr (**Supplementary Table 1**) were used. In both amplifications, the reaction mix contained Phusion High Fidelity PCR Master Mix with HF Buffer (Thermo Fisher Scientific, Lithuania) with 0.5 µM concentration of each primer (Sigma, Germany) and 0.2 µg mL^{-1} BSA (Albumin Bovine, AMRESCO, United States). In the first PCR reaction mix, 5 µL of template DNA (as above), 10 µl of Phusion High-Fidelity PCR Master Mix, 1 µL of SSUmAf and LSUmAr, and 3 µL of ultra clean water (Sigma) were used in 20 µL of final reaction. Thermal cycling was performed in an Eppendorf Master-cycler Gradient (Eppendorf Nexus X2, Germany) using the following parameters for the first PCR: initial denaturation of 5 min at 99°C, followed by 40 cycles of denaturation (10 s at 99°C)/ annealing (30 s at 60°C)/ elongation (1 min at 72°C), and a final elongation of 10 min at 72°C. For the nested PCR, 1 µL of the first PCR product was used as template in the same final reaction volume (20 µL) as above, and the same thermal cycling conditions were set up with slight differences: 30 cycles and annealing temperature of 63°C. The PCR products were visualized on 1.0% agarose gel with 1× TAE buffer (Tris/Acetic Acid/EDTA buffer 50x, Carl Roth) and stained with GelRed® (Biotium, USA).

Supplementary Table 1: Forward and reverse primers sequences used to amplify AMF following Kruger *et al.* (2009).

	Primer	Nucleotide sequence (5´-3´)	Primer mixtures
First PCR	SSUmAf1	TGGGTAATCTTTTGAAACTTYA	SSUmAf: mixSSUmAf1-2 (equimolar)
	SSUmAf2	TGGGTAATCTTRTGAAACTTCA	
	LSUmAr1	GCTCACACTCAAATCTATCAAA	LSUmAr: mixLSUmAr1-4 (equimolar)
	LSUmAr2	GCTCTAACTCAATTCTATCGAT	
	LSUmAr3	TGCTCTTACTCAAATCTATCAAA	
	LSUmAr4	GCTCTTACTCAAACCTATCGA	

Nested PCR	SSUmCf1	TCGCTCTTCAACGAGGAATC	SSUmCf: mixSSUmCf1-3 (equimolar)
	SSUmCf2	TATTGTTCTTCAACGAGGAATC	
	SSUmCf3	TATTGCTCTTNAACGAGGAATC	
	LSUmBr1	DAACACTCGCATATATGTTAGA	LSUmBr: mixLSUmBr1-5 (equimolar)
	LSUmBr2	AACACTCGCACACATGTTAGA	
	LSUmBr3	AACACTCGCATACATGTTAGA	
	LSUmBr4	AAACACTCGCACATATGTTAGA	
	LSUmBr5	AACACTCGCATATATGCTAGA	

Cloning protocol was followed as described by Krüger *et al.* (2009). Briefly, the 1.5 kb fragments from the nested PCR products were cloned with the Zero Blunt TOPO PCR Cloning Kit (Invitrogen, United States) following the manufacturer's protocol. Five colonies of each sample were analysed for correct length of plasmid inserts by colony-PCR using 1x GoTaq DNA Polymerase (Promega, United States) and M13F-M13R primers. Correct clone PCR products were sequenced using M13F-M13R primers at Macrogen Inc. (Korea).

Sequences were assembled and edited with software Sequencher 5.4.6 version (Gene Codes Corporation, USA). Homologous sequences were searched by blastn at the National Center for Biotechnology Information (NCBI). An AMF freely available reference alignment from Krüger *et al.* (2012), was also applied to compare and establish the phylogenetic tree. Assembled sequences, homologous environmental sequences from the NCBI platform and reference alignment were aligned and performed with MAFFT online (Katoh and Standley, 2013) and then manual adjusted at the Phylogenetic Data Editor (PhyDE).

A maximum-likelihood phylogenetic tree was assembled with references using RAxML-HPC2 (Stamatakis, 2014) on XSEDE ver. 8.2.9 on the CIPRES Science Gateway6 with 1000 bootstrap and the GTRGAMMA model (Krüger *et al.*, 2012). Taxonomic annotations followed the classification of Schüßler and Walker (2010). The AMF species selected in the paper were closest to *Rhizophagus irregularis* and *Septoglomus viscosum* (**Supplementary Figure 4**).

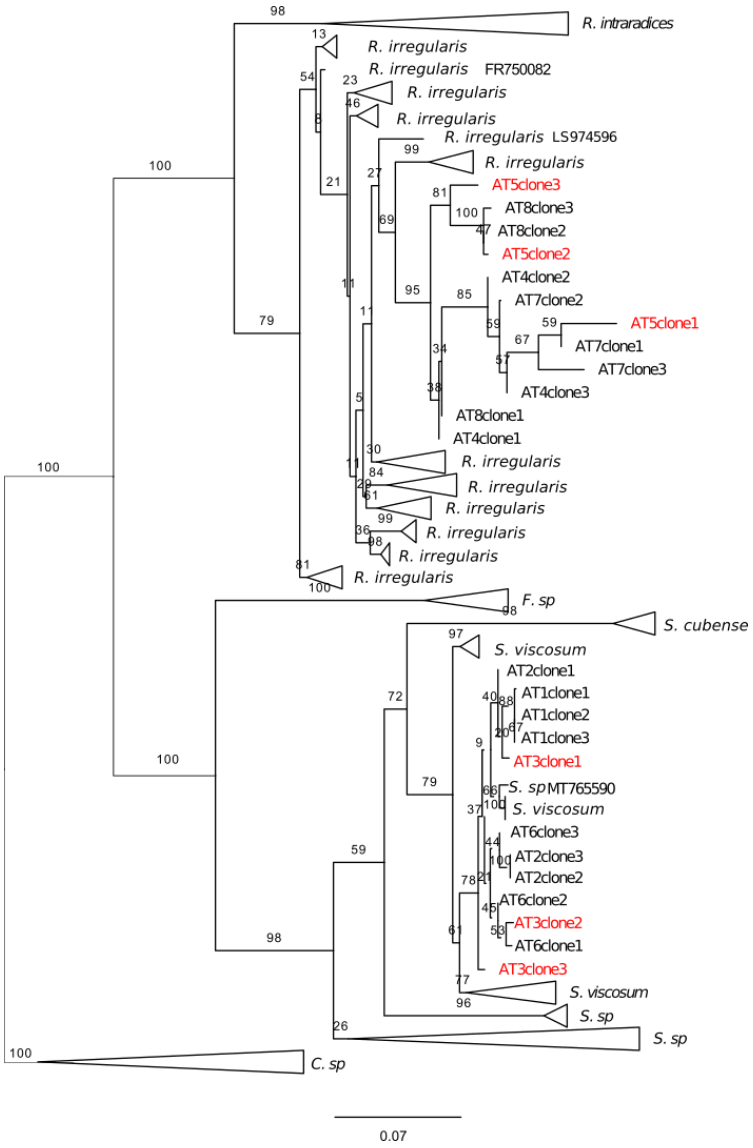

Supplementary Figure 4. Phylogenetic maximum likelihood tree of the isolates AT from *A. tinctoria* and reference AMF species. Characterised *Claroideoglomus* species were used as outgroup. Size of triangles represent the sequence numbers (vertically) and distances (horizontally). Two isolates used in this paper were highlighted with red colour.

Mass production of *Rhizophagus irregularis* and *Septoglomus viscosum*

The two AMF strains selected above (*Septoglomus viscosum* and *Rhizophagus irregularis*) were used to establish mass-production cultures with maize plants. Briefly, bleach soaked, and water washed maize seeds were germinated on sterilized lava substrate (120°C for 15 min) in a 5 L size pot. One-week old maize seedling was inoculated with AMF propagules of the two species (i.e., colonized *P. lanceolata* roots and substrates). Both AMF were used in association with *A. tinctoria* plants growing in the S-H system and in pots under greenhouse conditions (**Exp. 2 and 3, Chapter IV**).

Alkanna tinctoria acclimatization protocol

In vitro produced *Alkanna tinctoria* plants (Cartabia *et al.*, 2022, Chapter III) were acclimatized *ex vitro* as follows: plants were carefully removed from the culture medium (**Supplementary Figure 5A**) and gently washed under running deionized water to remove any medium adhering to the roots. Subsequently, three to four rooted plants were transferred into glass pots (J. Weck GmbH u. Co. KG, Germany, 147x100 mm, size: 580 mL) closed by a cover and a cotton layer and containing a sterile (2x 121ºC for 15 min) substrate mixture [3 peatmoss (DCM, Grobbendonk, Belgium)/2 compost (DCM, Grobbendonk, Belgium)/1 perlite (Perligran Premium, KNAUF GMBH, Dortmund, Germany)/1 quartz 0.4-0.8 mm (no. 4, Euroquartz, Belgium)/1 quartz 1-2 mm (no. 1, Euroquartz, Belgium)] (**Supplementary Figure 5B**). The plants were kept constantly moist in a growth chamber set at 24°C/20°C (day/night), RH of 80%, photoperiod of 16 h day-1 and PPF 130 µmol $m^{-2}s^{-1}$ (white fluorescent light, OSRAM L36 W830 Luminux). After 2 weeks, the glass pots were opened and placed inside a closed Sunbag (Sigma-Aldrich, Taufkirchen, Germany) (**Supplementary Figure 5C**). After 1 week, the plants were transplanted into single pots (7x7x6 cm) containing a sterile substrate mixture (2 peatmoss/2 compost/1 perlite /1 quartz 0.4-0.8 mm /1 quartz 1-2 mm) closed again under the Sunbag (**Supplementary Figure 5D**). After 1 week, the Sunbags were gradually opened (2, 4, 6, 8 h) until the plants were completely adapted (± 15 days) at the conditions in the growth chamber presented above (**Supplementary Figure 5E-G**).

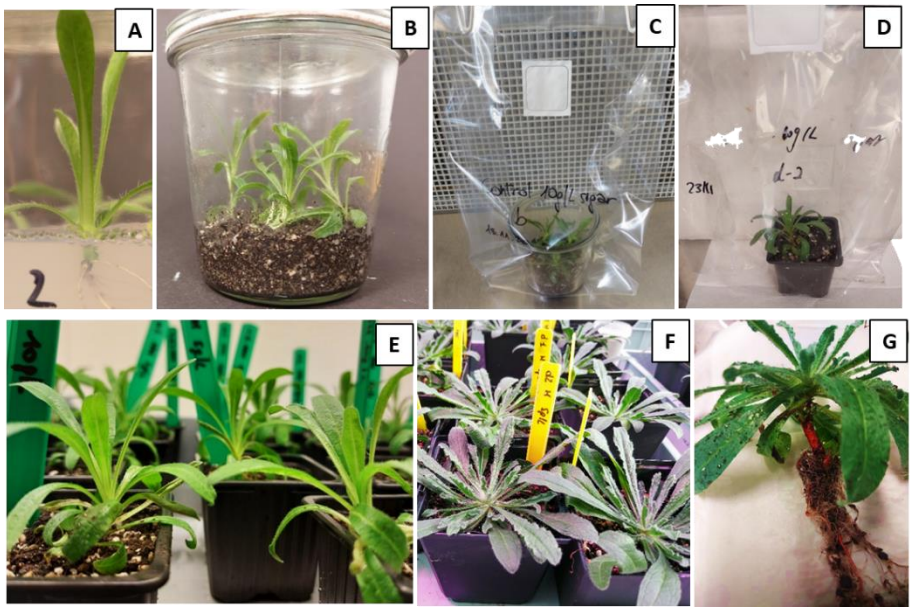

Supplementary Figure 5. *Ex vitro* acclimatization and adaptation of *in vitro* produced plantlets of *A. tinctoria*: (**A**) rooted plantlets growing under *in vitro* conditions; (**B**) plantlets transferred into closed glass pot filled with mixed sterile substrate; (**C**) glass pot opened inside a closed Sunbag; (**D**) plants transplanted into an individual pot in a closed Sunbag; (**E**) plants adapted to the growth chamber conditions; (**F**) plants transplanted in bigger pots for the AMF-colonization and kept under greenhouse conditions (UCLouvain); (**G**) details of the characteristic roots' reddish colour during the plants harvest.

HPLC quantification: methodology validation

Response function

The most adequate linear regression was selected with 95% expectation tolerance intervals included inside the ± 20% acceptance limits for each concentration level of the validation standards except the lowest one (**Supplementary Figure 6**).

Trueness, precision and accuracy

Trueness was calculated at each concentration level of the validation standard and expressed in relative bias (RB). Relative bias was less than 3%, except for the lowest concentration.

Precision was evaluated intra-day (repeatability) and inter-day (intermediate precision) and expressed as relative standard deviations

(RSD). The repeatability and the intermediate precision were less than 1.40% and 3.49%, respectively. All the trueness and precision results are in accordance with EMA guidelines criteria (≤ 15%).

Accuracy profiles, evaluating the sum of systematic and random errors of the test values (total error), are shown in **Supplementary Figure 7**, indicating that the relative upper and lower 95% β-expectation tolerance limits are inside the acceptance limits, set at 20%, except for the lowest concentration. The method can thus be considered as accurate between 0.1 and 0.8 mg mL^{-1}. The accuracy results are presented in **Supplementary Table 2**.

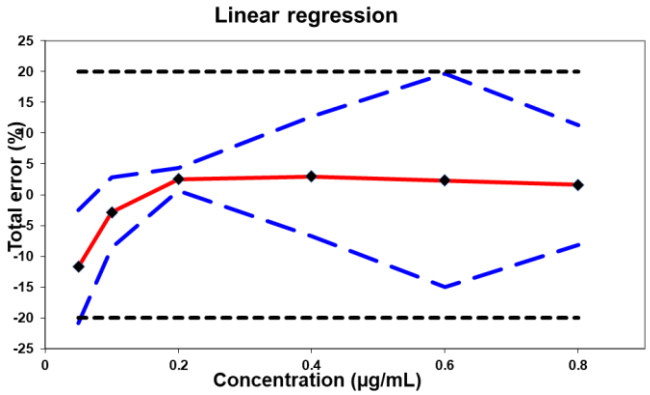

Supplementary Figure 6. Accuracy profile of the mixture of shikonin obtained with linear regression. The plain line is the relative bias, dashed lines are the β-expectation tolerance limits (β = 95%) and dotted lines represent the acceptance limits (± 20%).

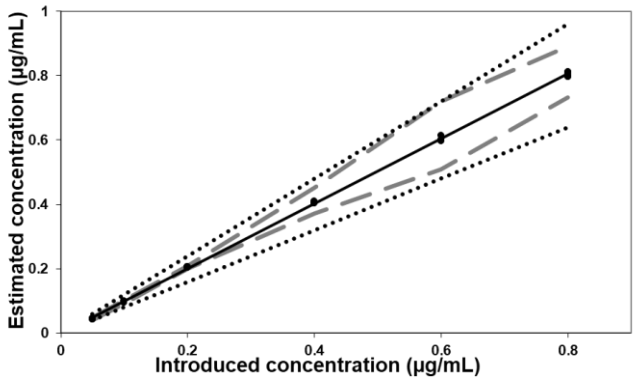

Supplementary Figure 7. Linear profile of shikonin standard. The plain line is identity line (y = x), the dashed lines are the β-expectation tolerance limits (β = 95%) and dotted lines represent the acceptance limits (± 20%).

Supplementary Table 2: Validation results obtained for the quantification of shikonin.

Validation criteria		**Concentration levels (µg mL^{-1})**					
		0.05	0.1	0.2	0.4	0.6	0.8
Response function		Linear regression					
		Calibration range (5 points)					
		0.05-0.8					
Trueness	Relative bias (%)	-11.68	-2.84	2.53	2.98	2.31	1.58
Precision	Repeatability (RSD %)	0.34	0.72	0.31	1.40	0.76	0.53
	Intermediate precision (RSD %)	1.85	1.58	0.51	2.71	3.49	1.97
Accuracy (95 % relative β-expectation lower and upper tolerance limits in %)		-20.85	-8.55	0.71	-6.76	-14.97	-8.15
		-2.52	2.85	4.36	12.71	19.6	11.31
Linearity	Slope	1.0252					
	Intercept	-0.0032					
	R^2	0.9986					
Limit of detection		0.0215					
Limit of quantification		0.0651					

Analysis of A/Sd target genes expression in *A. tinctoria* roots

Supplementary Figure 8. Partial representation of the Boraginaceae Phylogeny tree. Species relevant to this study are indicated by red boxes (adapted from Hilger *et al.*, 2020)

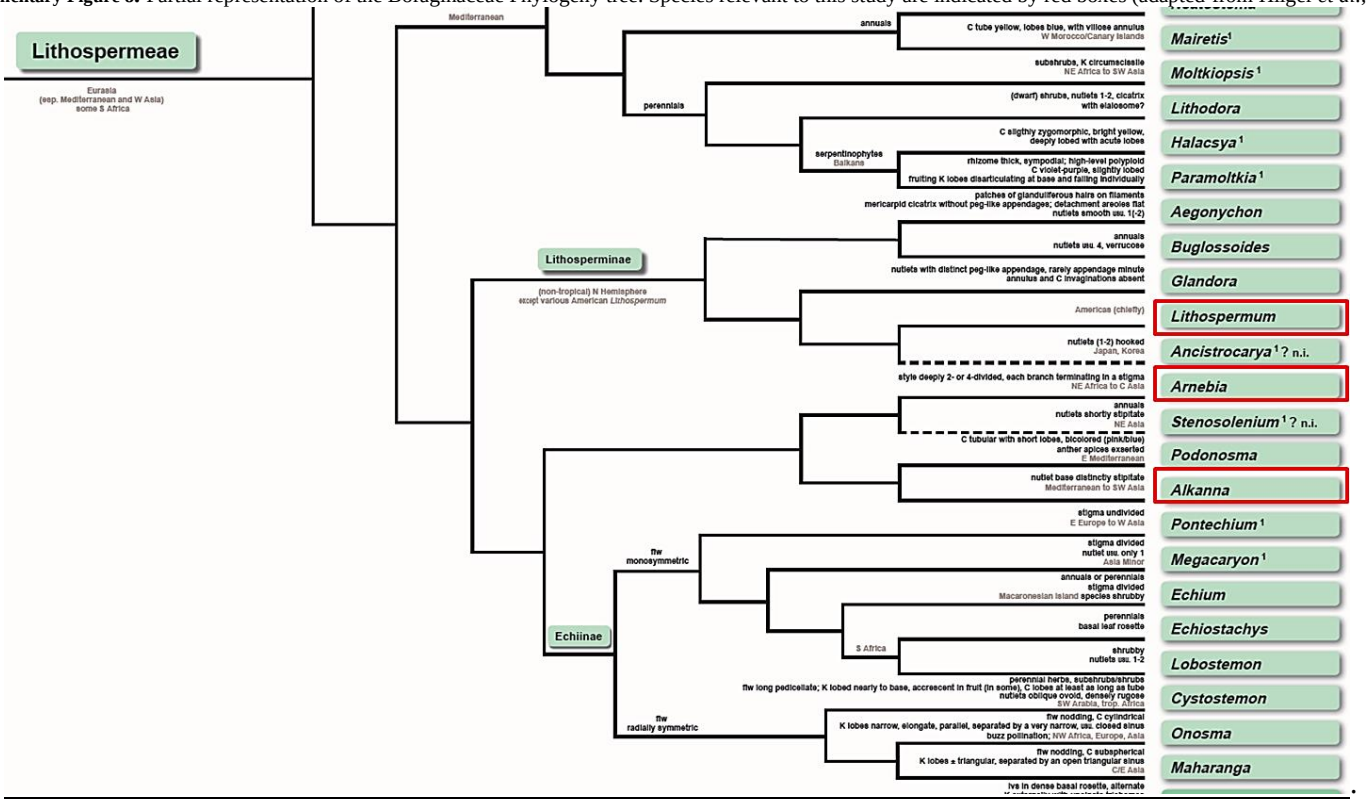

Alignments used to design primers

Aligned GHQH sequences (MH077962 = *Arnebia euchroma*; MN056184 = *Lithospermum erythrorhizon*). Coloured sequences are conserved regions that were used for primer designing.

```
                490       500       510       520       530       540
           ----:----|----:----|----:----|----:----|----:----|----:----|
Consensus GGCGAGGCAGUCGAAAUMGGCCAGGCUGCYUACAGGACWUCCYUSAAYUUGUURUCUAGC
MH077962  GGCGAGGCAGUCGAAAUCGGCCAGGCUGCUUACAGGACUUCCCUCAACUUGUUGUCUAGC
MN056184  GGCGAGGCAGUCGAAAUAGGCCAGGCUGCCUACAGGACAUCCUUGAAUUUGUUAUCUAGC

                550       560       570       580       590       600
           ----:----|----:----|----:----|----:----|----:----|----:----|
Consensus ACAAUMUUUUCCAAGGAYUUGGCGGAYUAYUAUWSUGAGACAGGUGCCCCAMGGGAGUUC
MH077962  ACAAUCUUUUCCAAGGAUUUGGCGGACUACUAUAGUGAGACAGGUGCCCCAAGGGAGUUC
MN056184  ACAAUAUUUUCCAAGGACUUGGCGGAUUAUUAUUCUGAGACAGGUGCCCCACGGGAGUUC

                610       620       630       640       650       660
           ----:----|----:----|----:----|----:----|----:----|----:----|
Consensus AAAGAUGCAAUUUGGAACAUWUUGGUUGAGUCWGUKAAGCCAAAUUUGGCRGAYUUUKUU
MH077962  AAAGAUGCAAUUUGGAACAUUUUGGUUGAGUCAGUUAAGCCAAAUUUGGCAGAUUUUGUU
MN056184  AAAGAUGCAAUUUGGAACAUAUUGGUUGAGUCUGUGAAGCCAAAUUUGGCGGACUUUUUU

                670       680       690       700       710       720
           ----:----|----:----|----:----|----:----|----:----|----:----|
Consensus CCAAUUCUUAGUAUGUUUGAYCUACARGGUAUUAAGCRACGUGCURGURUYCAUUUUGGA
MH077962  CCAAUUCUUAGUAUGUUUGACCUACAAGGUAUUAAGCGACGUGCUGGUAUCCAUUUUGGA
MN056184  CCAAUUCUUAGUAUGUUUGAUCUACAGGGUAUUAAGCAACGUGCUAGUGUUCAUUUUGGA

                730       740       750       760       770       780
           ----:----|----:----|----:----|----:----|----:----|----:----|
Consensus AAGGGSCUCAAGAUUAUGGAARGUCUAGUYAAUGAACGUCUAGARCAYAGGGAARYMCAY
MH077962  AAGGGCCUCAAGAUUAUGGAAGGUCUAGUCAAUGAACGUCUAGAACACAGGGAAACCCAC
MN056184  AAGGGGCUCAAGAUUAUGGAAAGUCUAGUUAAUGAACGUCUAGAGCAUAGGGAAGUACAU

                790       800       810       820       830       840
           ----:----|----:----|----:----|----:----|----:----|----:----|
Consensus GGUGCUACWCAUAAUGAUAUUUUGGAUAUMUUUCUCAAUUAUUGYGAUGAACAUCCSGAW
MH077962  GGUGCUACUCAUAAUGAUAUUUUGGAUAUCUUUCUCAAUUAUUGUGAUGAACAUCCGGAU
MN056184  GGUGCUACACAUAAUGAUAUUUUGGAUAUAUUUCUCAAUUAUUGCGAUGAACAUCCCGAA

                850       860       870       880       890       900
           ----:----|----:----|----:----|----:----|----:----|----:----|
Consensus GAAMUUGAUCGUCACCGYGUYAAGCACACGAUCCUGGAUCUUUUUAUUGCUGGGACUGAU
MH077962  GAACUUGAUCGUCACCGCGUCAAGCACACGAUCCUGGAUCUUUUUAUUGCUGGGACUGAU
MN056184  GAAAUUGAUCGUCACCGUGUUAAGCACACGAUCCUGGAUCUUUUUAUUGCUGGGACUGAU

                910       920       930       940       950       960
           ----:----|----:----|----:----|----:----|----:----|----:----|
Consensus ACAACYUCUAGUGUGACYGAAUGGACMAUGGCAGAAUUAAUCMAGAAYCCMCAMGUSAUG
MH077962  ACAACUUCUAGUGUGACUGAAUGGACCAUGGCAGAAUUAAUCCAGAAUCCACAAGUGAUG
MN056184  ACAACCUCUAGUGUGACCGAAUGGACAAUGGCAGAAUUAAUCAAGAACCCCCACGUCAUG

                970       980       990       1000      1010      1020
           ----:----|----:----|----:----|----:----|----:----|----:----|
Consensus AAAARGGCUAAAGAUGAGCUMKCACAAGUGAUYGGUAAAGGUAAAUSKUUAGAAGAAUCC
MH077962  AAAAGGGCUAAAGAUGAGCUCGCACAAGUGAUUGGUAAAGGUAAAUGUUUAGAAGAAUCC
MN056184  AAAAAGGCUAAAGAUGAGCUAUCACAAGUGAUCGGUAAAGGUAAAUCGUUAGAAGAAUCC

                1030      1040      1050      1060      1070      1080
           ----:----|----:----|----:----|----:----|----:----|----:----|
Consensus GAUGUUGCACGUYUACCUUACCUACGUUGUAUAAUGAAAGAAGCCUUAAGGAAACAUCCW
MH077962  GAUGUUGCACGUUUACCUUACCUACGUUGUAUAAUGAAAGAAGCCUUAAGGAAACAUCCA
MN056184  GAUGUUGCACGUCUACCUUACCUACGUUGUAUAAUGAAAGAAGCCUUAAGGAAACAUCCU

                1090      1100      1110      1120      1130      1140
           ----:----|----:----|----:----|----:----|----:----|----:----|
Consensus CCUGGUCCRUUUUUGUUUCCWCGAMGACCYGAGGAAGAYGUYGAAGUAGCSGGUUACACC
MH077962  CCUGGUCCGUUUUUGUUUCCACGACGACCUGAGGAAGAUGUCGAAGUAGCGGGUUACACC
MN056184  CCUGGUCCAUUUUUGUUUCCUCGAAGACCCGAGGAAGACGUUGAAGUAGCCGGUUACACC
```

Aligned LePGT2 sequences (KT991522 = *Arnebia euchroma*; AB055079.1 = *Lithospermum erythrorhizon*). Coloured sequences are conserved regions that were used for primer designing.

```
                10        20        30        40        50        60
           ----:----|----:----|----:----|----:----|----:----|----:----|
Consensus  AKKWSYWSCAAACAAACMCAGCUMAAGAAAGGCAAGCAACCAUCAUGGAUUGAGAUKUAU
KT991522   AGUUCCAGCAAACAAACCCAGCUCAAGAAAGGCAAGCAACCAUCAUGGAUUGAGAUGUAU
AB055079.1 ATGAGTTCCAAACAAACACAGCTAAAGAAAGGCAAGCAACCATCATGGATTGAGATTTAT

                70        80        90        100       110       120
           ----:----|----:----|----:----|----:----|----:----|----:----|
Consensus  UUGCCYMAAGARGUUCGRCCUUAUGCKCAYCUUGCAAGGYUAGACAAGCCUAUAGGCAGY
KT991522   UUGCCCCAAGAAGUUCGACCUUAUGCUCAUCUUGCAAGGUUAGACAAGCCUAUAGGCAGC
AB055079.1 TTGCCTAAAGAGGTTCGGCCTTATGCGCACCTTGCAAGGCTAGACAAGCCTATAGGCAGT

                130       140       150       160       170       180
           ----:----|----:----|----:----|----:----|----:----|----:----|
Consensus  UGGYURCUMGCUUGGCCMGCSUUYUGGUCCGUYGCAUUGRYUGCUGAUMUUGRMAGUCUA
KT991522   UGGUUGCUAGCUUGGCCAGCCUUCUGGUCCGUCGCAUUGGCUGCUGAUAUUGAAAGUCUA
AB055079.1 TGGCTACTCGCTTGGCCCGCGTTTTGGTCCGTTGCATTGATTGCTGATCTTGGCAGTCTA

                190       200       210       220       230       240
           ----:----|----:----|----:----|----:----|----:----|----:----|
Consensus  CCWAAAAUGKURGCAAUAUUUGGAUGGUGGGCAGUUUGGAUCMGAGGUGCUGGAUGYACC
KT991522   CCUAAAAUGGUAGCAAUAUUUGGAUGGUGGGCAGUUUGGAUCAGAGGUGCUGGAUGCACC
AB055079.1 CCAAAAATGTTGGCAATATTTGGATGGTGGGCAGTTTGGATCCGAGGTGCTGGATGTACC

                250       260       270       280       290       300
           ----:----|----:----|----:----|----:----|----:----|----:----|
Consensus  AUUAAYGAUUACUUCGACCGCGAUUUYGAYAARAARGUGGAACGUACAAAAUCUAGACCW
KT991522   AUUAAUGAUUACUUCGACCGCGAUUUCGACAAGAAGGUGGAACGUACAAAAUCUAGACCU
AB055079.1 ATTAACGATTACTTCGACCGCGATTTTGATAAAAAAGTGGAACGTACAAAATCTAGACCA

                310       320       330       340       350       360
           ----:----|----:----|----:----|----:----|----:----|----:----|
Consensus  CUYGCUAGUGGCGCUGUCUCRCCWKCMMAAGGRYUSUGGUGGCUUGCWUUUCARCURUUY
KT991522   CUUGCUAGUGGCGCUGUCUCACCUUCCCAAGGAUUGUGGUGGCUUGCAUUUCAGCUGUUC
AB055079.1 CTCGCTAGTGGCGCTGTCTCGCCAGCAAAAGGGCTCTGGTGGCTTGCTTTTCAACTATTT

                370       380       390       400       410       420
           ----:----|----:----|----:----|----:----|----:----|----:----|
Consensus  AUUGGMUUGGGUGUUCUUUACCAAUUCAAYAUCUUGACUCUUGCAUURGCUAUYKUGCAU
KT991522   AUUGGCUUGGGUGUUCUUUACCAAUUCAACAUCUUGACUCUUGCAUUGGCUAUCUUGCAU
AB055079.1 ATTGGATTGGGTGTTCTTTACCAATTCAATATCTTGACTCTTGCATTAGCTATTGTGCAT

                430       440       450       460       470       480
           ----:----|----:----|----:----|----:----|----:----|----:----|
Consensus  GUKCCCYUUGUKUUUGCUUAYCCUCUCAUGAAAAGAAUUACMUAUUGGCCUCAAGCKUUU
KT991522   GUUCCCCUUGUUUUUGCUUAUCCUCUCAUGAAAAGAAUUACCUAUUGGCCUCAAGCUUUU
AB055079.1 GTGCCCTTTGTGTTTGCTTACCCTCTCATGAAAAGAATTACATATTGGCCTCAAGCGTTT

                490       500       510       520       530       540
           ----:----|----:----|----:----|----:----|----:----|----:----|
Consensus  CUUGGMGUWAUGAUMAGUUGGGGAGCUCUYUUAGGSUCCUCUGCYCUUAAAGGAAGUGUU
KT991522   CUUGGAGUAAUGAUCAGUUGGGGAGCUCUCUUAGGCUCCUCUGCUCUUAAAGGAAGUGUU
AB055079.1 CTTGGCGTTATGATAAGTTGGGGAGCTCTTTTAGGGTCCTCTGCCCTTAAAGGAAGTGTT

                550       560       570       580       590       600
           ----:----|----:----|----:----|----:----|----:----|----:----|
Consensus  GUYCCAAGYAKYGCCUACCCRCUYUACAUUUCGAGCUUUUUCUGGACUCUUGUUUAUGAU
KT991522   GUUCCAAGUAGCGCCUACCCGCUUUACAUUUCGAGCUUUUUCUGGACUCUUGUUUAUGAU
AB055079.1 GTCCCAAGCATTGCCTACCCACTCTACATTTCGAGCTTTTTCTGGACTCTTGTTTATGAT

                610       620       630       640       650       660
           ----:----|----:----|----:----|----:----|----:----|----:----|
Consensus  ACWAUYUAUGCACAUCAAGAUAAGGUMGACGAYGCAAAAGCWGGRAUUAAAUCCACWGCU
KT991522   ACUAUCUAUGCACAUCAAGAUAAGGUAGACGAUGCAAAAGCAGGGAUUAAAUCCACUGCU
AB055079.1 ACAATTTATGCACATCAAGATAAGGTCGACGACGCAAAAGCTGGAATTAAATCCACAGCT

                670       680       690       700       710       720
           ----:----|----:----|----:----|----:----|----:----|----:----|
Consensus  CUAMGMUUUGGWGAUGCWACMAARAUAUGGAUUASWUGGUUCGGMRUAGGAUGCAUUGSU
KT991522   CUAAGAUUUGGAGAUGCAACCAAGAUAUGGAUUAGUUGGUUCGGAGUAGGAUGCAUUGCU
```

OVERVIEW OF SCIENTIFIC ACHIEVEMENT

Scientific publications

Research articles published

Cartabia, A., Tsiokanos, E., Tsafantakis, N., Lalaymia, I., Termentzi, A., Miguel, M., Fokialakis, N., Declerck, S., 2021. **The Arbuscular Mycorrhizal Fungus *Rhizophagus irregularis* MUCL 41833 Modulates Metabolites Production of *Anchusa officinalis* L. Under Semi-Hydroponic Cultivation.** *Frontiers in Plant Science* 12, 724352. https://doi.org/10.3389/fpls.2021.724352

Cartabia, A., Sarropoulou, V., Grigoriadou, K., Maloupa, E., Declerck, S., 2022. ***In vitro* propagation of *Alkanna tinctoria* Tausch.: a medicinal plant of the Boraginaceae family with high pharmaceutical value.** Ind. Crops Prod. 182, 114860. https://doi.org/10.1016/j.indcrop.2022.114860

Tsiokanos, E., **Cartabia, A**., Tsafantakis, N., Lalaymia, I., Termentzi, A., Miguel, M., Declerck, S., Fokialakis, N., 2022. **The Metabolic Profile of *Anchusa officinalis* L. Differs According to Its Associated Arbuscular Mycorrhizal Fungi**. *Metabolites* 12, 573. https://doi.org/10.3390/metabo12070573

Zhao, Y., **Cartabia, A.**, Lalaymia, I., Declerck, S., 2022. **Arbuscular mycorrhizal fungi and production of secondary metabolites in medicinal plants**. *Mycorrhiza*. 32, 221-256 https://doi.org/10.1007/s00572-022-01079-0

Research article submitted

Zhao Y., **Cartabia A.**, Ortiz S., Garcés-Ruiz M., Herent M., Quetin-Leclercq J., Declerck S., Lalaymia I., 2023. **Arbuscular mycorrhizal fungi impact the production of alkannin/shikonin and their derivatives in *Alkanna tinctoria* Tausch. grown in semi-hydroponic and pot cultivation systems.** *in Microbiology Microbe and Virus Interactions with Plants.*

Conference participation

Cartabia A. (2019). **A semi-hydroponic cultivation system associating Boraginaceae plants with arbuscular mycorrhizal fungi for optimal production of plant secondary metabolites**. Oral presentation at the 24th National Symposium for Applied Biological Sciences (NSABS) at Ghent University, Belgium, February 4, 2019. ISSN 1379-1176.

Cartabia, A., Tsiokanos, E., Tsafantakis, N., Lalaymia, I., Termentzi A., Machera K., Miguel, M., Fokialakis, N., Declerck, S. (2019). **A semi-hydroponic cultivation system associating *Anchusa officinalis* with arbuscular mycorrhizal fungi for optimal production of plant secondary metabolites.** Poster presentation at the International Conference on Mycorrhiza (ICOM 10) in Merida, Mexico, June 30 – July 5, 2019.

Cartabia, A. (2021). **Impact of Arbuscular Mycorrhizal Fungi on primary and secondary metabolites production in medicinal plants.** Oral presentation at the ELI-Day, Louvain-la-Neuve, Belgium, 26-28 May 2021.

Training and students' supervision

- International Training on *in vitro* Culture of Arbuscular Mycorrhizal Fungi (2018 and 2019): host preparation/ inoculation techniques sessions. UCLouvain, Belgium.
- Student supervision of Flora Morelle, from the Faculté des bioingénieurs, UCLouvain (September to August 2017-2018). Title of her master thesis: «Impact d'un champignon mycorhizien à arbuscules dur la dynamique d'absorption du phosphore et la production de métabolites secondaires chez *Anchusa officinalis* (Boraginaceae)».
- Student supervision of Maria Miguel Serra Pires (October to June 2018-2019), Erasmus+ student from ITQB Universidade Nova de Lisboa, Portugal. Title of her master thesis: «Towards optimal production of secondary metabolites through association of Boraginaceae plants with arbuscular mycorrhizal fungi».
- Instructor of practical laboratory (March to May 2018) work with two different student groups of the Bachelor in Bioingénieur, UCLouvain (course LBIR1251 Biologie et physiologie végétale).

MICROMETABOLITE project's activities

MICROMETABOLITE project network meeting event and Network Wide Training on Project management, business development, IPR issues at the Austrian Institute of Technology GmbH, Tulln An Der Donau, Austria, November 8-10, 2017.

Network Wide Training on *ex-situ* conservation and cultivation of native Greek species, at the Hellenic Agricultural Organization-Demeter, Thessaloniki, Greece, April 24-26, 2018.

MICROMETABOLITE project network meeting event and summer school on Natural Products: Chemistry, Biological Activities & Technological Applications at the Aristotle University of Thessaloniki, Thessaloniki, Greece, April 26-29, 2018.

Summer school on *in vitro* culture of Arbuscular Mycorrhizal Fungi at UCLouvain, Louvain-la-Neuve, Belgium, May 12-15, 2019.

MICROMETABOLITE project network mid-term meeting event and evaluation, and Network Wide Training on isolation, identification and preservation of bacteria at the BCCM-LMG Bacteria Collection of Ghent University, Belgium, May 16-22, 2019.

Winter School on plant-associated microbiota and secondary metabolite production at the Austrian Institute of Technology GmbH, Tulln An Der Donau, Austria, December 6-10, 2019.

Network Wide Training on career aspects: How to become a well-trained, entrepreneurially minded and mobile researcher, on the *in vitro* culturing of plants, and on the registration of microbial products at the INOQ GmbH, Solkau, Germany, January 20-24, 2020.

School visit as Marie Curie Ambassador at the Athénée royal Andrée Thomas - ARAT-Forest, Bruxelles, March 5, 2020.

<u>Secondments during the MICROMETABOLITE project</u>

- Secondary metabolites extraction and analysis (HPLC-PDA-ELSD and HPTLC), and metabolite extraction *via* eco-friendly technologies and metabolome analysis training at the National & Kapodistrian University of Athens, June-July 2018, March and September 2019.

- E*x situ* and *in vitro* conservation and propagation of plants training at the Hellenic Agricultural Organization-Demeter, Thessaloniki, Greece, August 2019.
- RNA isolation and gene expression quantification, qPCR analysis and primers design training at the Austrian Institute of Technology GmbH, Tulln An Der Donau, Austria, August-September 2020.

REFERENCES

A. Hussein, R., A. El-Anssary, A., 2019. Plants Secondary Metabolites: The Key Drivers of the Pharmacological Actions of Medicinal Plants, in: F. Builders, P. (Ed.), Herbal Medicine. IntechOpen. https://doi.org/10.5772/intechopen.76139

Abu-Reidah, I.M., Arráez-Román, D., Al-Nuri, M., Warad, I., Segura-Carretero, A., 2019. Untargeted metabolite profiling and phytochemical analysis of Micromeria fruticosa L. (Lamiaceae) leaves. Food Chem. 279, 128–143. https://doi.org/10.1016/j.foodchem.2018.11.144

Abu-Reidah, I.M., Arráez-Román, D., Segura-Carretero, A., Fernández-Gutiérrez, A., 2013. Extensive characterisation of bioactive phenolic constituents from globe artichoke (Cynara scolymus L.) by HPLC–DAD-ESI-QTOF-MS. Food Chem. 141, 2269–2277. https://doi.org/10.1016/j.foodchem.2013.04.066

Agnolucci, M., Avio, L., Palla, M., Sbrana, C., Turrini, A., Giovannetti, M., 2020. Health-Promoting Properties of Plant Products: The Role of Mycorrhizal Fungi and Associated Bacteria. Agronomy 10, 1864. https://doi.org/10.3390/agronomy10121864

Ahmad, M., Leroy, T., Krigas, N., Temsch, E.M., Weiss-Schneeweiss, H., Lexer, C., Sehr, E.M., Paun, O., 2021. Spatial and Ecological Drivers of Genetic Structure in Greek Populations of Alkanna tinctoria (Boraginaceae), a Polyploid Medicinal Herb. Front. Plant Sci. 12, 706574. https://doi.org/10.3389/fpls.2021.706574

Ahmad, M., Varela Alonso, A., Koletti, A.E., Assimopoulou, A.N., Declerck, S., Schneider, C., Molin, E.M., 2022a. Transcriptional dynamics of Chitinophaga sp. strain R-73072-mediated alkannin/shikonin biosynthesis in Lithospermum officinale. Front. Microbiol. 13, 978021. https://doi.org/10.3389/fmicb.2022.978021

Ahmad, M., Varela Alonso, A., Koletti, A.E., Rodić, N., Reichelt, M., Rödel, P., Assimopoulou, A.N., Paun, O., Declerck, S., Schneider, C., Molin, E.M., 2022b. Dynamics of alkannin/shikonin biosynthesis in response to jasmonate and salicylic acid in Lithospermum officinale. Sci. Rep. 12, 17093. https://doi.org/10.1038/s41598-022-21322-0

Akiyama, K., Matsuzaki, K., Hayashi, H., 2005. Plant sesquiterpenes induce hyphal branching in arbuscular mycorrhizal fungi. Nature 435, 824–827. https://doi.org/10.1038/nature03608

Ali Akbar Safari Sinegani, Masomeh Elyasi Yeganeh, 2016. The occurrence of arbuscular mycorrhizal fungi in soil and root of medicinal plants in Bu-Ali Sina garden in Hamadan, Iran. Biol. J. Microorg. 5, 43–59.

Ali et al., 2014. The pharmacology of Anchusa Italica and Anchusa strigosa. A review. Int J Pharm Pharm Sci 6, 7–10.

Allkin, B., 2017. Useful Plants – Medicines: At Least 28,187 Plant Species are Currently Recorded as Being of Medicinal Use, in: Willis, K.J. (Ed.), State of the World's Plants 2017, Wellcome Trust–Funded Monographs and Book Chapters. Royal Botanic Gardens, Kew, London (UK).

A.M. Shohael, S.M. Khatun, M.F. Alam, K.Y. Paek, 2013. Effects of Murashige and Skoog medium strength on germination and secondary metabolites production of Eleutherococcus senticosus's somatic embryos in bioreactor. Int. J. Biosci. IJB 3, 155–163. https://doi.org/10.12692/ijb/3.3.155-163

Andrade, S.A.L., Malik, S., Sawaya, A.C.H.F., Bottcher, A., Mazzafera, P., 2013. Association with arbuscular mycorrhizal fungi influences alkaloid synthesis and accumulation in Catharanthus roseus and Nicotiana tabacum plants. Acta Physiol. Plant. 35, 867–880. https://doi.org/10.1007/s11738-012-1130-8

Arab, M.M., Yadollahi, A., Shojaeiyan, A., Shokri, S., Ghojah, S.M., 2014. Effects of nutrient media, different cytokinin types and their concentrations on in vitro multiplication of G×N15 (hybrid of almond×peach) vegetative rootstock. J. Genet. Eng. Biotechnol. 12, 81–87. https://doi.org/10.1016/j.jgeb.2014.10.001

Assimopoulou, A., Boskou, D, Papageorgiou, V. P., 2004. Antioxidant activities of alkannin, shikonin and Alkanna tinctoria root extracts in oil substrates. Food Chem. 87, 433–438. https://doi.org/10.1016/j.foodchem.2003.12.017

Auber, R.P., Suttiyut, T., McCoy, R.M., Ghaste, M., Crook, J.W., Pendleton, A.L., Widhalm, J.R., Wisecaver, J.H., 2020. Hybrid de novo genome assembly of red gromwell (Lithospermum erythrorhizon) reveals evolutionary insight into shikonin biosynthesis. Hortic. Res. 7, 82. https://doi.org/10.1038/s41438-020-0301-9

Avio, L., Turrini, A., Giovannetti, M., Sbrana, C., 2018. Designing the Ideotype Mycorrhizal Symbionts for the Production of Healthy Food. Front. Plant Sci. 9, 1089. https://doi.org/10.3389/fpls.2018.01089

Babula, P., Adam, V., Havel, L., Kizek, R., 2009. Noteworthy Secondary Metabolites Naphthoquinones – their Occurrence, Pharmacological Properties and Analysis. Curr. Pharm. Anal. 5, 47–68. https://doi.org/10.2174/157341209787314936

Bagheri, F., Tahvilian, R., Karimi, N., Chalabi, M., Azami, M., 2018. Shikonin Production by Callus Culture of Onosma bulbotrichom as Active Pharmaceutical Ingredient. Iran. J. Pharm. Res. IJPR 17, 495–504.

Bago, B., Azcon-Aguilar, C., Goulet, A., Piche, Y., 1998. Branched absorbing structures (BAS): a feature of the extraradical mycelium of symbiotic arbuscular mycorrhizal fungi. New Phytol. 139, 375–388. https://doi.org/10.1046/j.1469-8137.1998.00199.x

Bago, B., Pfeffer, P.E., Jehad Abubaker, Jeongwon Jun, Allen, J.W., Janine Brouillette, David D. Douds, Lammers, P.J., Shachar-Hill, Y., 2003. Carbon Export from Arbuscular Mycorrhizal Roots Involves the Translocation of Carbohydrate as Well as Lipid. Plant Physiol. 131, 1496–1507.

Bago, B., Pfeffer, P.E., Shachar-Hill, Y., 2000. Carbon Metabolism and Transport in Arbuscular Mycorrhizas. Plant Physiol. 124, 949–958. https://doi.org/10.1104/pp.124.3.949

Barros, L., Dueñas, M., Dias, M.I., Sousa, M.J., Santos-Buelga, C., Ferreira, I.C.F.R., 2013. Phenolic profiles of cultivated, in vitro cultured and commercial samples of Melissa officinalis L. infusions. Food Chem. 136, 1–8. https://doi.org/10.1016/j.foodchem.2012.07.107

Basiru, S., Mwanza, H.P., Hijri, M., 2020. Analysis of Arbuscular Mycorrhizal Fungal Inoculant Benchmarks. Microorganisms 9, 81. https://doi.org/10.3390/microorganisms9010081

Begum, N., Qin, C., Ahanger, M.A., Raza, S., Khan, M.I., Ashraf, M., Ahmed, N., Zhang, L., 2019. Role of Arbuscular Mycorrhizal Fungi in Plant Growth Regulation: Implications in Abiotic Stress Tolerance. Front. Plant Sci. 10, 1068. https://doi.org/10.3389/fpls.2019.01068

Bernardo, L., Carletti, P., Badeck, F.W., Rizza, F., Morcia, C., Ghizzoni, R., Rouphael, Y., Colla, G., Terzi, V., Lucini, L., 2019. Metabolomic responses triggered by arbuscular

mycorrhiza enhance tolerance to water stress in wheat cultivars. Plant Physiol. Biochem. 137, 203–212. https://doi.org/10.1016/j.plaphy.2019.02.007

Berruti, A., Lumini, E., Balestrini, R., Bianciotto, V., 2016. Arbuscular Mycorrhizal Fungi as Natural Biofertilizers: Let's Benefit from Past Successes. Front. Microbiol. 6. https://doi.org/10.3389/fmicb.2015.01559

Bonfante, P., Genre, A., 2015. Arbuscular mycorrhizal dialogues: do you speak 'plantish' or 'fungish'? Trends Plant Sci. 20, 150–154. https://doi.org/10.1016/j.tplants.2014.12.002

Boskovic, I., Đukić, D.A., Maskovic, P., Mandić, L., Perovic, S., 2018. Phytochemical composition and antimicrobial, antioxidant and cytotoxic activities of Anchusa officinalis L. extracts. Biologia (Bratisl.) 73, 1035–1041. https://doi.org/10.2478/s11756-018-0124-4

Bossard, E., Tsafantakis, N., Aligiannis, N., Fokialakis, N., 2022. A Development Strategy of Tailor-made Natural Deep Eutectic Solvents for the Enhanced Extraction of Hydroxynaphthoquinones from Alkanna tinctoria Roots. Planta Med. a-1738-5648. https://doi.org/10.1055/a-1738-5648

Brieudes, V., Angelis, A., Vougogiannopoulou, K., Pratsinis, H., Kletsas, D., Mitakou, S., Halabalaki, M., Skaltsounis, L., 2016a. Phytochemical Analysis and Antioxidant Potential of the Phytonutrient-Rich Decoction of Cichorium spinosum and C. intybus. Planta Med. 82, 1070–1078. https://doi.org/10.1055/s-0042-107472

Brieudes, V., Angelis, A., Vougogiannopoulou, K., Pratsinis, H., Kletsas, D., Mitakou, S., Halabalaki, M., Skaltsounis, L.A., 2016b. Phytochemical Analysis and Antioxidant Potential of the Phytonutrient-Rich Decoction of Cichorium spinosum and C. intybus. Planta Med. 82, 1070–1078. https://doi.org/10.1055/s-0042-107472

Brinckmann, J.A., Kathe, W., Berkhoudt, K., Harter, D.E.V., Schippmann, U., 2022. A New Global Estimation of Medicinal and Aromatic Plant Species in Commercial Cultivation and Their Conservation Status. Econ. Bot. 76, 319–333. https://doi.org/10.1007/s12231-022-09554-7

Brito, I., Goss, M.J., Alho, L., Brígido, C., van Tuinen, D., Félix, M.R., Carvalho, M., 2019. Agronomic management of AMF functional diversity to overcome biotic and abiotic stresses - The role of plant sequence and intact extraradical mycelium.

Fungal Ecol. 40, 72–81. https://doi.org/10.1016/j.funeco.2018.06.001

Brown, S.D., 1988. Chemometrics: A textbook. D. L. Massart. B. G. M. Vandeginste, S. N. Deming, Y. Michotte, and L. Kaufman, Elsevier, Amsterdam, 1988. ISBN 0-444-42660-4. Price Dfl 175.00. J. Chemom. 2, 298–299. https://doi.org/10.1002/cem.1180020409

Brundrett, M.C., Tedersoo, L., 2018. Evolutionary history of mycorrhizal symbioses and global host plant diversity. New Phytol. 220, 1108–1115. https://doi.org/10.1111/nph.14976

Bücking, H., Kafle, A., 2015. Role of Arbuscular Mycorrhizal Fungi in the Nitrogen Uptake of Plants: Current Knowledge and Research Gaps. Agronomy 5, 587–612. https://doi.org/10.3390/agronomy5040587

Bucking, H., Liepold, E., Ambilwade, P., 2012a. The Role of the Mycorrhizal Symbiosis in Nutrient Uptake of Plants and the Regulatory Mechanisms Underlying These Transport Processes, in: Dhal, N.K. (Ed.), Plant Science. InTech. https://doi.org/10.5772/52570

Bucking, H., Liepold, E., Ambilwade, P., 2012b. The Role of the Mycorrhizal Symbiosis in Nutrient Uptake of Plants and the Regulatory Mechanisms Underlying These Transport Processes, in: Dhal, N.K. (Ed.), Plant Science. InTech. https://doi.org/10.5772/52570

Bulgakov, V.P., Inyushkina, Y.V., Fedoreyev, S.A., 2012. Rosmarinic acid and its derivatives: biotechnology and applications. Crit. Rev. Biotechnol. 32, 203–217. https://doi.org/10.3109/07388551.2011.596804

Calonne-Salmon, M., Plouznikoff, K., Declerck, S., 2018. The arbuscular mycorrhizal fungus Rhizophagus irregularis MUCL 41833 increases the phosphorus uptake and biomass of Medicago truncatula, a benzo[a]pyrene-tolerant plant species. Mycorrhiza 28, 761–771. https://doi.org/10.1007/s00572-018-0861-9

Cameron, D.D., Neal, A.L., van Wees, S.C.M., Ton, J., 2013. Mycorrhiza-induced resistance: more than the sum of its parts? Trends Plant Sci. 18, 539–545. https://doi.org/10.1016/j.tplants.2013.06.004

Canellas, N.O.A., Olivares, F.L., Canellas, L.P., 2019. Metabolite fingerprints of maize and sugarcane seedlings: searching for markers after inoculation with plant growth-promoting bacteria

in humic acids. Chem. Biol. Technol. Agric. 6, 14. https://doi.org/10.1186/s40538-019-0153-4

Cardini, A., Pellegrino, E., Declerck, S., Calonne-Salmon, M., Mazzolai, B., Ercoli, L., 2021. Direct transfer of zinc between plants is channelled by common mycorrhizal network of arbuscular mycorrhizal fungi and evidenced by changes in expression of zinc transporter genes in fungus and plant. Environ. Microbiol. 23, 5883–5900. https://doi.org/10.1111/1462-2920.15542

Cartabia, A., Sarropoulou, V., Grigoriadou, K., Maloupa, E., Declerck, S., 2022. In vitro propagation of Alkanna tinctoria Tausch.: a medicinal plant of the Boraginaceae family with high pharmaceutical value. Ind. Crops Prod. 182, 114860. https://doi.org/10.1016/j.indcrop.2022.114860

Cartabia, A., Tsiokanos, E., Tsafantakis, N., Lalaymia, I., Termentzi, A., Miguel, M., Fokialakis, N., Declerck, S., 2021. The Arbuscular Mycorrhizal Fungus Rhizophagus irregularis MUCL 41833 Modulates Metabolites Production of Anchusa officinalis L. Under Semi-Hydroponic Cultivation. Front. Plant Sci. 12, 724352. https://doi.org/10.3389/fpls.2021.724352

Castillo, S., Gopalacharyulu, P.V., Yetukuri, L., Ore\vsič, M., 2011. Algorithms and tools for the preprocessing of LC–MS metabolomics data. Chemom. Intell. Lab. Syst. 108, 23–32.

Chajra, H., Salwinski, A., Guillaumin, A., Mignard, B., Hannewald, P., Duriot, L., Warnault, P., Guillet-Claude, C., Fréchet, M., Bourgaud, F., 2020. Plant Milking Technology—An Innovative and Sustainable Process to Produce Highly Active Extracts from Plant Roots. Molecules 25, 4162. https://doi.org/10.3390/molecules25184162

Charles Dorni, A.I., Amalraj, A., Gopi, S., Varma, K., Anjana, S.N., 2017. Novel cosmeceuticals from plants—An industry guided review. J. Appl. Res. Med. Aromat. Plants 7, 1–26. https://doi.org/10.1016/j.jarmap.2017.05.003

Chaudhary, V., Kapoor, R., Bhatnagar, A.K., 2008. Effectiveness of two arbuscular mycorrhizal fungi on concentrations of essential oil and artemisinin in three accessions of Artemisia annua L. Appl. Soil Ecol. 40, 174–181. https://doi.org/10.1016/j.apsoil.2008.04.003

Chen, K.-K., Xie, Z.-J., Dai, W., Wang, Q., 2017. A new oleanolic-type triterpene glycoside from *Anchusa italica*. Nat. Prod. Res. 31, 959–965. https://doi.org/10.1080/14786419.2016.1258557

Chen, M., Arato, M., Borghi, L., Nouri, E., Reinhardt, D., 2018. Beneficial Services of Arbuscular Mycorrhizal Fungi – From Ecology to Application. Front. Plant Sci. 9, 1270. https://doi.org/10.3389/fpls.2018.01270

Chenchouni, H., Mekahlia, M.N., Beddiar, A., 2020. Effect of inoculation with native and commercial arbuscular mycorrhizal fungi on growth and mycorrhizal colonization of olive (Olea europaea L.). Sci. Hortic. 261, 108969. https://doi.org/10.1016/j.scienta.2019.108969

Cho, J.-G., Cha, B.-J., Seo, W.-D., Jeong, R.-H., Shrestha, S., Kim, J.-Y., Kang, H.-C., Baek, N.-I., 2015. Feruloyl Sucrose Esters from Oryza sativa Roots and Their Tyrosinase Inhibition Activity. Chem. Nat. Compd. 51, 1094–1098. https://doi.org/10.1007/s10600-015-1500-8

Choi, J., Summers, W., Paszkowski, U., 2018. Mechanisms Underlying Establishment of Arbuscular Mycorrhizal Symbioses. Annu. Rev. Phytopathol. 56, 135–160. https://doi.org/10.1146/annurev-phyto-080516-035521

Chutia, R., Abel, S., Ziegler, J., 2019. Iron and Phosphate Deficiency Regulators Concertedly Control Coumarin Profiles in Arabidopsis thaliana Roots During Iron, Phosphate, and Combined Deficiencies. Front. Plant Sci. 10, 113. https://doi.org/10.3389/fpls.2019.00113

Chwil M., Weryszko-Chmielewska E., 2012. The structure of floral elements of Anchusa officinalis L. creating attractants for insects. Acta Agrobot. 62, 37–47.

Cioffi, G., Escobar, L.M., Braca, A., De Tommasi, N., 2003. Antioxidant Chalcone Glycosides and Flavanones from *Maclura* (*Chlorophora*) *t inctoria*. J. Nat. Prod. 66, 1061–1064. https://doi.org/10.1021/np030127c

Concannon, S., Ramachandran, V.N., Smyth, W.F., 2000. A study of the electrospray ionisation of selected coumarin derivatives and their subsequent fragmentation using an ion trap mass spectrometer. Rapid Commun. Mass Spectrom. 14, 1157–1166. https://doi.org/10.1002/1097-0231(20000730)14:14<1157::AID-RCM4>3.0.CO;2-V

Cook, S.D., 2019. An Historical Review of Phenylacetic Acid. Plant Cell Physiol. 60, 243–254. https://doi.org/10.1093/pcp/pcz004

Cornejo-Báez, A.A., Peña-Rodríguez, L.M., Álvarez-Zapata, R., Vázquez-Hernández, M., Sánchez-Medina, A., 2020. Chemometrics: a complementary tool to guide the isolation of

pharmacologically active natural products. Drug Discov. Today 25, 27–37. https://doi.org/10.1016/j.drudis.2019.09.016

Cranenbrouck, S., Voets, L., Bivort, C., Renard, L., Strullu, D.-G., Declerck, S., 2005. Methodologies for in Vitro Cultivation of Arbuscular Mycorrhizal Fungi with Root Organs, in: Declerck, S., Fortin, J.A., Strullu, D.-G. (Eds.), In Vitro Culture of Mycorrhizas, Soil Biology. Springer Berlin Heidelberg, Berlin, Heidelberg, pp. 341–375. https://doi.org/10.1007/3-540-27331-X_18

Csorba, C., Rodić, N., Zhao, Y., Antonielli, L., Brader, G., Vlachou, A., Tsiokanos, E., Lalaymia, I., Declerck, S., Papageorgiou, V.P., Assimopoulou, A.N., Sessitsch, A., 2022. Metabolite Production in *Alkanna tinctoria* Links Plant Development with the Recruitment of Individual Members of Microbiome Thriving at the Root-Soil Interface. mSystems 7, e00451-22. https://doi.org/10.1128/msystems.00451-22

Dattagupta, S., Zielinski, F., 2011. Symbiosis, in: Reitner, J., Thiel, V. (Eds.), Encyclopedia of Geobiology, Encyclopedia of Earth Sciences Series. Springer Netherlands, Dordrecht, pp. 866–870. https://doi.org/10.1007/978-1-4020-9212-1_228

De Klerk, G.-J., Brugge, J.T., Marinova, S., 1997. Effectiveness of indoleacetic acid, indolebutyric acid and naphthaleneacetic acid during adventitious root formation in vitro in Malus ‘Jork 9′. Plant Cell Tissue Organ Cult. 49, 39–44. https://doi.org/10.1023/A:1005850222973

Declerck, S., D’Or, D., Bivort, C., de Souza, F.A., 2004. Development of extraradical mycelium of Scutellospora reticulata under root-organ culture: spore production and function of auxiliary cells. Mycol. Res. 108, 84–92. https://doi.org/10.1017/S0953756203008761

Declerck, S., Fortin, J.A., Strullu, D.-G. (Eds.), 2005. In Vitro Culture of Mycorrhizas, Soil Biology. Springer Berlin Heidelberg, Berlin, Heidelberg. https://doi.org/10.1007/b138925

Dickson, S., 2004. The Arum-Paris continuum of mycorrhizal symbioses. New Phytol. 163, 187–200. https://doi.org/10.1111/j.1469-8137.2004.01095.x

Divito, E.B., Davic, A.P., Johnson, M.E., Cascio, M., 2012. Electrospray Ionization and Collision Induced Dissociation Mass Spectrometry of Primary Fatty Acid Amides. Anal. Chem. 84, 2388–2394. https://doi.org/10.1021/ac203158u

Dresler, S., Szymczak, G., Wójcik, M., 2017. Comparison of some secondary metabolite content in the seventeen species of the Boraginaceae family. Pharm. Biol. 55, 691–695. https://doi.org/10.1080/13880209.2016.1265986

Durán, A.G., Gutiérrez, M.T., Rial, C., Torres, A., Varela, R.M., Valdivia, M.M., Molinillo, J.M.G., Skoneczny, D., Weston, L.A., Macías, F.A., 2017. Bioactivity and quantitative analysis of isohexenylnaphthazarins in root periderm of two Echium spp.: E. plantagineum and E. gaditanum. Phytochemistry 141, 162–170. https://doi.org/10.1016/j.phytochem.2017.06.004

Eguchi, R., Ono, N., Hirai Morita, A., Katsuragi, T., Nakamura, S., Huang, M., Altaf-Ul-Amin, Md., Kanaya, S., 2019. Classification of alkaloids according to the starting substances of their biosynthetic pathways using graph convolutional neural networks. BMC Bioinformatics 20, 380. https://doi.org/10.1186/s12859-019-2963-6

El-Shazly, A., Wink, M., 2014. Diversity of Pyrrolizidine Alkaloids in the Boraginaceae Structures, Distribution, and Biological Properties. Diversity 6, 188–282. https://doi.org/10.3390/d6020188

Engskog, M.K.R., Haglöf, J., Arvidsson, T., Pettersson, C., 2016. LC–MS based global metabolite profiling: the necessity of high data quality. Metabolomics 12. https://doi.org/10.1007/s11306-016-1058-x

Ernst, M., Silva, D.B., Silva, R.R., Vêncio, R.Z.N., Lopes, N.P., 2014. Mass spectrometry in plant metabolomics strategies: from analytical platforms to data acquisition and processing. Nat. Prod. Rep. 31, 784. https://doi.org/10.1039/c3np70086k

Estrada, B., Aroca, R., Barea, J.M., Ruiz-Lozano, J.M., 2013. Native arbuscular mycorrhizal fungi isolated from a saline habitat improved maize antioxidant systems and plant tolerance to salinity. Plant Sci. 201–202, 42–51. https://doi.org/10.1016/j.plantsci.2012.11.009

Fadel, O., El Kirat, K., Morandat, S., 2011. The natural antioxidant rosmarinic acid spontaneously penetrates membranes to inhibit lipid peroxidation in situ. Biochim. Biophys. Acta BBA - Biomembr. 1808, 2973–2980. https://doi.org/10.1016/j.bbamem.2011.08.011

Feijen, F.A.A., Vos, R.A., Nuytinck, J., Merckx, V.S.F.T., 2018. Evolutionary dynamics of mycorrhizal symbiosis in land plant

diversification. Sci. Rep. 8, 10698. https://doi.org/10.1038/s41598-018-28920-x

Fenaille, F., Barbier Saint-Hilaire, P., Rousseau, K., Junot, C., 2017. Data acquisition workflows in liquid chromatography coupled to high resolution mass spectrometry-based metabolomics: Where do we stand? J. Chromatogr. A 1526, 1–12. https://doi.org/10.1016/j.chroma.2017.10.043

Feng, Z., Liu, X., Zhu, H., Yao, Q., 2020. Responses of Arbuscular Mycorrhizal Symbiosis to Abiotic Stress: A Lipid-Centric Perspective. Front. Plant Sci. 11, 578919. https://doi.org/10.3389/fpls.2020.578919

Fester, T., Fetzer, I., Buchert, S., Lucas, R., Rillig, M.C., Härtig, C., 2011. Towards a systemic metabolic signature of the arbuscular mycorrhizal interaction. Oecologia 167, 913–924. https://doi.org/10.1007/s00442-011-2037-6

Filipek, A., Wyszomierska, J., Michalak, B., Kiss, A.K., 2019. Syringa vulgaris bark as a source of compounds affecting the release of inflammatory mediators from human neutrophils and monocytes/macrophages. Phytochem. Lett. 30, 309–313. https://doi.org/10.1016/j.phytol.2019.02.008

Finimundy, T.C., Pereira, C., Dias, M.I., Caleja, C., Calhelha, R.C., Sokovic, M., Stojković, D., Carvalho, A.M., Rosa, E., Barros, L., Ferreira, I.C.F.R., 2020. Infusions of Herbal Blends as Promising Sources of Phenolic Compounds and Bioactive Properties. Molecules 25, 2151. https://doi.org/10.3390/molecules25092151

French, K.E., 2017. Engineering Mycorrhizal Symbioses to Alter Plant Metabolism and Improve Crop Health. Front. Microbiol. 8, 1403. https://doi.org/10.3389/fmicb.2017.01403

Frew, A., 2021. Contrasting effects of commercial and native arbuscular mycorrhizal fungal inoculants on plant biomass allocation, nutrients, and phenolics. PLANTS PEOPLE PLANET 3, 536–540. https://doi.org/10.1002/ppp3.10128

Fu, J.-Y., Zhao, H., Bao, J.-X., Wen, Z.-L., Fang, R.-J., Fazal, A., Yang, M.-K., Liu, B., Yin, T.-M., Pang, Y.-J., Lu, G.-H., Qi, J.-L., Yang, Y.-H., 2020. Establishment of the hairy root culture of Echium plantagineum L. and its shikonin production. 3 Biotech 10, 429. https://doi.org/10.1007/s13205-020-02419-7

Fu, W.-W., Shimizu, N., Dou, D.-Q., Takeda, T., Fu, R., Pei, Y.-H., Chen, Y.-J., 2006. Five New Triterpenoid Saponins from the

Roots of Platycodon grandiflorum. Chem. Pharm. Bull. (Tokyo) 54, 557–560. https://doi.org/10.1248/cpb.54.557

Fujita, Y., 1988. Shikonin: Production by Plant (Lithospermum erythrorhizon) Cell Cultures, in: Bajaj, Y.P.S. (Ed.), Medicinal and Aromatic Plants I, Biotechnology in Agriculture and Forestry. Springer Berlin Heidelberg, Berlin, Heidelberg, pp. 225–236. https://doi.org/10.1007/978-3-642-73026-9_11

Fusconi, A., 2014. Regulation of root morphogenesis in arbuscular mycorrhizae: what role do fungal exudates, phosphate, sugars and hormones play in lateral root formation? Ann. Bot. 113, 19–33. https://doi.org/10.1093/aob/mct258

Gaisser, S., Heide, L., 1996. Inhibition and regulation of shikonin biosynthesis in suspension cultures of Lithospermum. Phytochemistry 41, 1065–1072. https://doi.org/10.1016/0031-9422(95)00633-8

Galili, S., Amir, R., Galili, G., 2008. Genetic Engineering of Amino Acid Metabolism in Plants, in: Advances in Plant Biochemistry and Molecular Biology. Elsevier, pp. 49–80. https://doi.org/10.1016/S1755-0408(07)01003-X

Gamborg, O.L., Miller, R.A., Ojima, K., 1968. Nutrient requirements of suspension cultures of soybean root cells. Exp. Cell Res. 50, 151–158. https://doi.org/10.1016/0014-4827(68)90403-5

Garcés-Ruiz, M., Calonne-Salmon, M., Plouznikoff, K., Misson, C., Navarrete-Mier, M., Cranenbrouck, S., Declerck, S., 2017. Dynamics of Short-Term Phosphorus Uptake by Intact Mycorrhizal and Non-mycorrhizal Maize Plants Grown in a Circulatory Semi-Hydroponic Cultivation System. Front. Plant Sci. 8. https://doi.org/10.3389/fpls.2017.01471

Gaude, N., Bortfeld, S., Erban, A., Kopka, J., Krajinski, F., 2015a. Symbiosis dependent accumulation of primary metabolites in arbuscule-containing cells. BMC Plant Biol. 15, 234. https://doi.org/10.1186/s12870-015-0601-7

Gaude, N., Bortfeld, S., Erban, A., Kopka, J., Krajinski, F., 2015b. Symbiosis dependent accumulation of primary metabolites in arbuscule-containing cells. BMC Plant Biol. 15, 234. https://doi.org/10.1186/s12870-015-0601-7

Genre, A., Chabaud, M., Balzergue, C., Puech-Pagès, V., Novero, M., Rey, T., Fournier, J., Rochange, S., Bécard, G., Bonfante, P., Barker, D.G., 2013. Short-chain chitin oligomers from arbuscular mycorrhizal fungi trigger nuclear Ca^{2+} spiking in *Medicago truncatula* roots and their production is enhanced by

strigolactone. New Phytol. 198, 190–202. https://doi.org/10.1111/nph.12146

Genre, A., Chabaud, M., Faccio, A., Barker, D.G., Bonfante, P., 2008. Prepenetration Apparatus Assembly Precedes and Predicts the Colonization Patterns of Arbuscular Mycorrhizal Fungi within the Root Cortex of Both *Medicago truncatula* and *Daucus carota*. Plant Cell 20, 1407–1420. https://doi.org/10.1105/tpc.108.059014

Genre, A., Chabaud, M., Timmers, T., Bonfante, P., Barker, D.G., 2005. Arbuscular Mycorrhizal Fungi Elicit a Novel Intracellular Apparatus in *Medicago truncatula* Root Epidermal Cells before Infection. Plant Cell 17, 3489–3499. https://doi.org/10.1105/tpc.105.035410

Genre, A., Lanfranco, L., Perotto, S., Bonfante, P., 2020. Unique and common traits in mycorrhizal symbioses. Nat. Rev. Microbiol. 18, 649–660. https://doi.org/10.1038/s41579-020-0402-3

Gerardi, C., Mita, G., Grillo, E., Giovinazzo, G., Miceli, A., De Leo, P., 1998. Alkanna tinctoria T. (Alkanets): In Vitro Culture and the Production of Alkannin and Other Secondary Metabolites, in: Bajaj, Y.P.S. (Ed.), Medicinal and Aromatic Plants X, Biotechnology in Agriculture and Forestry. Springer Berlin Heidelberg, Berlin, Heidelberg, pp. 14–27. https://doi.org/10.1007/978-3-642-58833-4_2

Gianinazzi, S., Gollotte, A., Binet, M.-N., van Tuinen, D., Redecker, D., Wipf, D., 2010. Agroecology: the key role of arbuscular mycorrhizas in ecosystem services. Mycorrhiza 20, 519–530. https://doi.org/10.1007/s00572-010-0333-3

Giovannini, L., Palla, M., Agnolucci, M., Avio, L., Sbrana, C., Turrini, A., Giovannetti, M., 2020. Arbuscular Mycorrhizal Fungi and Associated Microbiota as Plant Biostimulants: Research Strategies for the Selection of the Best Performing Inocula. Agronomy 10, 106. https://doi.org/10.3390/agronomy10010106

Goddard, M.-L., Belval, L., Martin, I.R., Roth, L., Laloue, H., Deglène-Benbrahim, L., Valat, L., Bertsch, C., Chong, J., 2021. Arbuscular Mycorrhizal Symbiosis Triggers Major Changes in Primary Metabolism Together With Modification of Defense Responses and Signaling in Both Roots and Leaves of Vitis vinifera. Front. Plant Sci. 12, 721614. https://doi.org/10.3389/fpls.2021.721614

Goh, C.-H., Veliz Vallejos, D.F., Nicotra, A.B., Mathesius, U., 2013. The Impact of Beneficial Plant-Associated Microbes on Plant Phenotypic Plasticity. J. Chem. Ecol. 39, 826–839. https://doi.org/10.1007/s10886-013-0326-8

Gómez-García, R., Campos, D.A., Oliveira, A., Aguilar, C.N., Madureira, A.R., Pintado, M., 2021. A chemical valorisation of melon peels towards functional food ingredients: Bioactives profile and antioxidant properties. Food Chem. 335, 127579. https://doi.org/10.1016/j.foodchem.2020.127579

Gontier, E., Clément, A., Tran, T.L.M., Gravot, A., Lièvre, K., Guckert, A., Bourgaud, F., 2002a. Hydroponic combined with natural or forced root permeabilization: a promising technique for plant secondary metabolite production. Plant Sci. 163, 723–732. https://doi.org/10.1016/S0168-9452(02)00171-1

Gontier, E., Clément, A., Tran, T.L.M., Gravot, A., Lièvre, K., Guckert, A., Bourgaud, F., 2002b. Hydroponic combined with natural or forced root permeabilization: a promising technique for plant secondary metabolite production. Plant Sci. 163, 723–732. https://doi.org/10.1016/S0168-9452(02)00171-1

Goossens, J., Mertens, J., Goossens, A., 2016. Role and functioning of bHLH transcription factors in jasmonate signalling. J. Exp. Bot. erw440. https://doi.org/10.1093/jxb/erw440

Grzegorczyk-Karolak, I., Kuźma, Ł., Lisiecki, P., Kiss, A., 2019. Accumulation of phenolic compounds in different in vitro cultures of Salvia viridis L. and their antioxidant and antimicrobial potential. Phytochem. Lett. 30, 324–332. https://doi.org/10.1016/j.phytol.2019.02.016

Gupta, K., Garg, S., Singh, J., Kumar, M., 2014. Enhanced production of napthoquinone metabolite (shikonin) from cell suspension culture of Arnebia sp. and its up-scaling through bioreactor. 3 Biotech 4, 263–273. https://doi.org/10.1007/s13205-013-0149-x

Gutjahr, C., Parniske, M., 2013. Cell and Developmental Biology of Arbuscular Mycorrhiza Symbiosis. Annu. Rev. Cell Dev. Biol. 29, 593–617. https://doi.org/10.1146/annurev-cellbio-101512-122413

Halder, M., Sarkar, S., Jha, S., 2019. Elicitation: A biotechnological tool for enhanced production of secondary metabolites in hairy root cultures. Eng. Life Sci. 19, 880–895. https://doi.org/10.1002/elsc.201900058

Hammad, Y., Nalin, R., Marechal, J., Fiasson, K., Pepin, R., Berry, A.M., Normand, P., Domenach, A.-M., 2003. A possible role for phenyl acetic acid (PAA) on Alnus glutinosa nodulation by Frankia. Plant Soil 254, 193–205. https://doi.org/10.1023/A:1024971417777

Han, J., Weng, X., Bi, K., 2008. Antioxidants from a Chinese medicinal herb – Lithospermum erythrorhizon. Food Chem. 106, 2–10. https://doi.org/10.1016/j.foodchem.2007.01.031

Harbort, C.J., Hashimoto, M., Inoue, H., Niu, Y., Guan, R., Rombolà, A.D., Kopriva, S., Voges, M.J.E.E.E., Sattely, E.S., Garrido-Oter, R., Schulze-Lefert, P., 2020. Root-Secreted Coumarins and the Microbiota Interact to Improve Iron Nutrition in Arabidopsis. Cell Host Microbe 28, 825-837.e6. https://doi.org/10.1016/j.chom.2020.09.006

Hartmann, H.T., Hartmann, H.T. (Eds.), 2002. Plant propagation: principles and practices, 7th ed. ed. Prentice Hall, Upper Saddle River, N.J.

Hassani, D., Fu, X., Shen, Q., Khalid, M., Rose, J.K.C., Tang, K., 2020. Parallel Transcriptional Regulation of Artemisinin and Flavonoid Biosynthesis. Trends Plant Sci. 25, 466–476. https://doi.org/10.1016/j.tplants.2020.01.001

Heijden, M.G.A., Martin, F.M., Selosse, M., Sanders, I.R., 2015. Mycorrhizal ecology and evolution: the past, the present, and the future. New Phytol. 205, 1406–1423. https://doi.org/10.1111/nph.13288

Helsper, J.P., Loewus, F.A., 1982. Metabolism of l-Threonic Acid in *Rumex x acutus* L. and *Pelargonium crispum* (L.) L'Hér. Plant Physiol. 69, 1365–1368. https://doi.org/10.1104/pp.69.6.1365

Hill, E.M., Robinson, L.A., Abdul-Sada, A., Vanbergen, A.J., Hodge, A., Hartley, S.E., 2018. Arbuscular Mycorrhizal Fungi and Plant Chemical Defence: Effects of Colonisation on Aboveground and Belowground Metabolomes. J. Chem. Ecol. 44, 198–208. https://doi.org/10.1007/s10886-017-0921-1

Ho, C.S., Lam, C.W.K., Chan, M.H.M., Cheung, R.C.K., Law, L.K., Lit, L.C.W., Ng, K.F., Suen, M.W.M., Tai, H.L., 2003. Electrospray ionisation mass spectrometry: principles and clinical applications. Clin. Biochem. Rev. 24, 3–12.

Hopkins, W.G., Hüner, N.P.A., 2008a. Introduction to plant physiology, 4th ed. ed. John Wiley & Sons, Hoboken, NJ.

Hopkins, W.G., Hüner, N.P.A., 2008b. Introduction to plant physiology, 4th ed. ed. John Wiley & Sons, Hoboken, NJ.

Hussain, M., Qasim, M., Bamisile, B.S., Wang, L., 2017. Role of Saponins in Plant Defense against the Diamondback Moth, Plutella xylostella (L.) (preprint). BIOLOGY. https://doi.org/10.20944/preprints201706.0035.v1

Huu Tung, N., Du, G.-J., Wang, C.-Z., Yuan, C.-S., Shoyama, Y., 2013. Naphthoquinone Components from Alkanna tinctoria (L.) Tausch Show Significant Antiproliferative Effects on Human Colorectal Cancer Cells. Phytother. Res. 27, 66–70. https://doi.org/10.1002/ptr.4680

IJdo, M., Cranenbrouck, S., Declerck, S., 2011. Methods for large-scale production of AM fungi: past, present, and future. Mycorrhiza 21, 1–16. https://doi.org/10.1007/s00572-010-0337-z

Ivanova, M., Van Staden, J., 2011. Influence of gelling agent and cytokinins on the control of hyperhydricity in Aloe polyphylla. Plant Cell Tissue Organ Cult. PCTOC 104, 13–21. https://doi.org/10.1007/s11240-010-9794-5

Ivanova, M., van Staden, J., 2008. Effect of ammonium ions and cytokinins on hyperhydricity and multiplication rate of in vitro regenerated shoots of Aloe polyphylla. Plant Cell Tissue Organ Cult. 92, 227–231. https://doi.org/10.1007/s11240-007-9311-7

Jacott, C., Murray, J., Ridout, C., 2017. Trade-Offs in Arbuscular Mycorrhizal Symbiosis: Disease Resistance, Growth Responses and Perspectives for Crop Breeding. Agronomy 7, 75. https://doi.org/10.3390/agronomy7040075

Jakobsen, I., Hammer, E.C., 2015. Nutrient Dynamics in Arbuscular Mycorrhizal Networks, in: Horton, T.R. (Ed.), Mycorrhizal Networks, Ecological Studies. Springer Netherlands, Dordrecht, pp. 91–131. https://doi.org/10.1007/978-94-017-7395-9_4

Jakovljević Z. Dragana et al., 2016. The content of secondary metabolites and in vitro biological activity of Anchusa officinalis L. (Boraginaceae). Indian journal of traditional knowledge 15(4):587-593.

Jamshidi-Kia, F., Lorigooini, Z., Amini-Khoei, H., 2018. Medicinal plants: Past history and future perspective. J. Herbmed Pharmacol. 7, 1–7. https://doi.org/10.15171/jhp.2018.01

Javot, H., Penmetsa, R.V., Terzaghi, N., Cook, D.R., Harrison, M.J., 2007. A Medicago truncatula phosphate transporter indispensable for the arbuscular mycorrhizal symbiosis. Proc. Natl. Acad. Sci. 104, 1720–1725. https://doi.org/10.1073/pnas.0608136104

Ji, J., Feng, Q., Sun, H., Zhang, X., Li, X., Li, J., Gao, J., 2019. Response of Bioactive Metabolite and Biosynthesis Related Genes to Methyl Jasmonate Elicitation in Codonopsis pilosula. Molecules 24, 533. https://doi.org/10.3390/molecules24030533

Jiang, F., Zhang, L., Zhou, J., George, T.S., Feng, G., 2021. Arbuscular mycorrhizal fungi enhance mineralisation of organic phosphorus by carrying bacteria along their extraradical hyphae. New Phytol. 230, 304–315. https://doi.org/10.1111/nph.17081

Jiang, H., Yang, J., Zhang, W., Wang, Q., Du, Y., Sun, Q., Li, C., Xu, H., 2020. Characterisation of hederacoside C metabolites using ultrahigh-performance liquid chromatography quadrupole Orbitrap mass spectrometry based on automatic fragment ion search. Phytochem. Anal. 31, 395–407. https://doi.org/10.1002/pca.2908

Jiménez-Arias, D., García-Machado, F.J., Morales-Sierra, S., Luis, J.C., Suarez, E., Hernández, M., Valdés, F., Borges, A.A., 2019. Lettuce plants treated with L-pyroglutamic acid increase yield under water deficit stress. Environ. Exp. Bot. 158, 215–222. https://doi.org/10.1016/j.envexpbot.2018.10.034

Jung, S.C., Martinez-Medina, A., Lopez-Raez, J.A., Pozo, M.J., 2012a. Mycorrhiza-Induced Resistance and Priming of Plant Defenses. J. Chem. Ecol. 38, 651–664. https://doi.org/10.1007/s10886-012-0134-6

Jung, S.C., Martinez-Medina, A., Lopez-Raez, J.A., Pozo, M.J., 2012b. Mycorrhiza-Induced Resistance and Priming of Plant Defenses. J. Chem. Ecol. 38, 651–664. https://doi.org/10.1007/s10886-012-0134-6

Kameoka, H., Maeda, T., Okuma, N., Kawaguchi, M., 2019. Structure-Specific Regulation of Nutrient Transport and Metabolism in Arbuscular Mycorrhizal Fungi. Plant Cell Physiol. 60, 2272–2281. https://doi.org/10.1093/pcp/pcz122

Kapoor, R., Anand, G., Gupta, P., Mandal, S., 2017. Insight into the mechanisms of enhanced production of valuable terpenoids by arbuscular mycorrhiza. Phytochem. Rev. 16, 677–692. https://doi.org/10.1007/s11101-016-9486-9

Kara, Z., Arslan, D., Güler, M., Güler, Ş., 2015. Inoculation of arbuscular mycorrhizal fungi and application of micronized calcite to olive plant: Effects on some biochemical constituents of olive fruit and oil. Sci. Hortic. 185, 219–227. https://doi.org/10.1016/j.scienta.2015.02.001

Katoh, K., Standley, D.M., 2013. MAFFT Multiple Sequence Alignment Software Version 7: Improvements in Performance and Usability. Mol. Biol. Evol. 30, 772–780. https://doi.org/10.1093/molbev/mst010

Kaur, S., Campbell, B.J., Suseela, V., 2022. Root metabolome of plant–arbuscular mycorrhizal symbiosis mirrors the mutualistic or parasitic mycorrhizal phenotype. New Phytol. 234, 672–687. https://doi.org/10.1111/nph.17994

Kaur, S., Suseela, V., 2020. Unraveling Arbuscular Mycorrhiza-Induced Changes in Plant Primary and Secondary Metabolome. Metabolites 10, 335. https://doi.org/10.3390/metabo10080335

Keymer, A., Pimprikar, P., Wewer, V., Huber, C., Brands, M., Bucerius, S.L., Delaux, P.-M., Klingl, V., Röpenack-Lahaye, E. von, Wang, T.L., Eisenreich, W., Dörmann, P., Parniske, M., Gutjahr, C., 2017. Lipid transfer from plants to arbuscular mycorrhiza fungi. eLife 6, e29107. https://doi.org/10.7554/eLife.29107

Kheiri, A., Amini, S., Javidan, A.N., Saghafi, M.M., Khorasani, G., 2017. The effects of Alkanna tinctoria Tausch on split-thickness skin graft donor site management: a randomized, blinded placebo-controlled trial. BMC Complement. Altern. Med. 17, 253. https://doi.org/10.1186/s12906-017-1741-0

Khera, H.K., Singh, S.K., Mir, R., Singh, V.B. and S., 2017. A HR-MS Based Method for the Determination of Chorismate Synthase Activity [WWW Document]. Protein Pept. Lett. URL https://www.eurekaselect.com/148658/article (accessed 9.25.20).

Kilam, D., Sharma, P., Agnihotri, A., Kharkwal, A., Varma, A., 2017. Microbial Symbiosis and Bioactive Ingredients of Medicinal Plants, in: Varma, A., Prasad, R., Tuteja, N. (Eds.), Mycorrhiza - Eco-Physiology, Secondary Metabolites, Nanomaterials. Springer International Publishing, Cham, pp. 283–302. https://doi.org/10.1007/978-3-319-57849-1_16

Kim, H.K., Choi, Y.H., Verpoorte, R., 2010. NMR-based metabolomic analysis of plants. Nat. Protoc. 5, 536–549. https://doi.org/10.1038/nprot.2009.237

Kim, H.U., 2020. Lipid Metabolism in Plants. Plants 9, 871. https://doi.org/10.3390/plants9070871

Kim, K.H., Choi, S.U., Son, M.W., Lee, K.R., 2010. Two New Phenolic Amides from the Seeds of Pharbitis nil. Chem. Pharm. Bull. (Tokyo) 58, 1532–1535. https://doi.org/10.1248/cpb.58.1532

Klironomos, J.N., 2003. VARIATION IN PLANT RESPONSE TO NATIVE AND EXOTIC ARBUSCULAR MYCORRHIZAL FUNGI. Ecology 84, 2292–2301. https://doi.org/10.1890/02-0413

Kloppholz, S., Kuhn, H., Requena, N., 2011. A Secreted Fungal Effector of Glomus intraradices Promotes Symbiotic Biotrophy. Curr. Biol. 21, 1204–1209. https://doi.org/10.1016/j.cub.2011.06.044

Kobayashi, Y., Maeda, T., Yamaguchi, K., Kameoka, H., Tanaka, S., Ezawa, T., Shigenobu, S., Kawaguchi, M., 2018. The genome of Rhizophagus clarus HR1 reveals a common genetic basis for auxotrophy among arbuscular mycorrhizal fungi. BMC Genomics 19, 465. https://doi.org/10.1186/s12864-018-4853-0

Kokkoris, V., Stefani, F., Dalpé, Y., Dettman, J., Corradi, N., 2020. Nuclear Dynamics in the Arbuscular Mycorrhizal Fungi. Trends Plant Sci. 25, 765–778. https://doi.org/10.1016/j.tplants.2020.05.002

Koz, O., Pizza, C., Kırmızıgül, S., 2009. Triterpene and flavone glycosides from *Anchusa undulata* subsp. *hybrida*. Nat. Prod. Res. 23, 284–292. https://doi.org/10.1080/14786410802006140

Krüger, M., Krüger, C., Walker, C., Stockinger, H., Schüßler, A., 2012. Phylogenetic reference data for systematics and phylotaxonomy of arbuscular mycorrhizal fungi from phylum to species level. New Phytol. 193, 970–984. https://doi.org/10.1111/j.1469-8137.2011.03962.x

Krüger, M., Stockinger, H., Krüger, C., Schüßler, A., 2009. DNA-based species level detection of *Glomeromycota* : one PCR primer set for all arbuscular mycorrhizal fungi. New Phytol. 183, 212–223. https://doi.org/10.1111/j.1469-8137.2009.02835.x

Krzyżanowska-Kowalczyk, J., Pecio, Ł., Mołdoch, J., Ludwiczuk, A., Kowalczyk, M., 2018. Novel Phenolic Constituents of Pulmonaria officinalis L. LC-MS/MS Comparison of Spring and Autumn Metabolite Profiles, in: Molecules. https://doi.org/10.3390/molecules23092277

Kumar, A., B., A., 2011. Pyroglutamic acid: throwing light on a lightly studied metabolite. Curr. Sci. 102, 288–297.

Kuruuzum-Uz, A., Suleyman, H., Cadirci, E., Guvenalp, Z., Demirezer, L.O., 2012. Investigation on Anti-Inflammatory and Antiulcer Activities of Anchusa azurea Extracts and their Major Constituent Rosmarinic Acid. Z. Für Naturforschung C 67, 360–366. https://doi.org/10.1515/znc-2012-7-802

Lameira O.A., Pinto J.E.B.P., 2006. In vitro propagation of Cordia verbenacea (Boraginaceae). Rev. Bras. Plantas Med. 8, 102–104.

Laparre, J., Malbreil, M., Letisse, F., Portais, J.C., Roux, C., Bécard, G., Puech-Pagès, V., 2014. Combining Metabolomics and Gene Expression Analysis Reveals that Propionyl- and Butyryl-Carnitines Are Involved in Late Stages of Arbuscular Mycorrhizal Symbiosis. Mol. Plant 7, 554–566. https://doi.org/10.1093/mp/sst136

Le Pioufle, O., Ganoudi, M., Calonne-Salmon, M., Ben Dhaou, F., Declerck, S., 2019. Rhizophagus irregularis MUCL 41833 Improves Phosphorus Uptake and Water Use Efficiency in Maize Plants During Recovery From Drought Stress. Front. Plant Sci. 10, 897. https://doi.org/10.3389/fpls.2019.00897

Lee, J., Chan, B.L.S., Mitchell, A.E., 2017. Identification/quantification of free and bound phenolic acids in peel and pulp of apples (Malus domestica) using high resolution mass spectrometry (HRMS). Food Chem. 215, 301–310. https://doi.org/10.1016/j.foodchem.2016.07.166

Lehbili, M., Alabdul Magid, A., Kabouche, A., Voutquenne-Nazabadioko, L., Abedini, A., Morjani, H., Sarazin, T., Gangloff, S.C., Kabouche, Z., 2017. Oleanane-type triterpene saponins from Calendula stellata. Phytochemistry 144, 33–42. https://doi.org/10.1016/j.phytochem.2017.08.015

Li, W., Polachi, N., Wang, X., Chu, Y., Wang, Y., Tian, M., Li, D., Zhou, D., Zhou, S., Ju, A., Li, Y., Zhang, Y., Chen, M., Huang, L., Liu, C., 2018. A quality marker study on salvianolic acids for injection. Phytomedicine 44, 138–147. https://doi.org/10.1016/j.phymed.2018.02.003

Li, X., Yu, C., Sun, W., Liu, G., Jia, J., Wang, Y., 2004. Simultaneous determination of magnesium lithospermate B, rosmarinic acid, and lithospermic acid in beagle dog serum by liquid chromatography/tandem mass spectrometry. Rapid Commun. Mass Spectrom. 18, 2878–2882. https://doi.org/10.1002/rcm.1703

Liao, M., Li, A., Chen, C., Ouyang, H., Zhang, Y., Xu, Y., Feng, Y., Jiang, H., 2015. Systematic identification of shikonins and shikonofurans in medicinal Zicao species using ultra-high performance liquid chromatography quadrupole time of flight tandem mass spectrometry combined with a data mining

strategy. J. Chromatogr. A 1425, 158–172. https://doi.org/10.1016/j.chroma.2015.11.028

Liu, A.-H., Guo, H., Ye, M., Lin, Y.-H., Sun, J.-H., Xu, M., Guo, D.-A., 2007a. Detection, characterization and identification of phenolic acids in Danshen using high-performance liquid chromatography with diode array detection and electrospray ionization mass spectrometry. J. Chromatogr. A 1161, 170–182. https://doi.org/10.1016/j.chroma.2007.05.081

Liu, A.-H., Guo, H., Ye, M., Lin, Y.-H., Sun, J.-H., Xu, M., Guo, D.-A., 2007b. Detection, characterization and identification of phenolic acids in Danshen using high-performance liquid chromatography with diode array detection and electrospray ionization mass spectrometry. J. Chromatogr. A, 26th International Symposium on the Separation of Proteins, Peptides and Polynucleotides 1161, 170–182. https://doi.org/10.1016/j.chroma.2007.05.081

Lloyd, McCown, 1980. Commercially-feasible micropropagation of mountain laurel, Kalmia latifolia, by use of shoot-tip culture. Proc. Int. Plant Propag. Soc. 30, 421–437.

Lohse, S., Schliemann, W., Ammer, C., Kopka, J., Strack, D., Fester, T., 2005. Organization and Metabolism of Plastids and Mitochondria in Arbuscular Mycorrhizal Roots of *Medicago truncatula*. Plant Physiol. 139, 329–340. https://doi.org/10.1104/pp.105.061457

López-Ráez, J.A., Flors, V., García, J.M., Pozo, M.J., 2010. AM symbiosis alters phenolic acid content in tomato roots. Plant Signal. Behav. 5, 1138–1140. https://doi.org/10.4161/psb.5.9.12659

Lu, F.-C., Lee, C.-Y., Wang, C.-L., 2015. The influence of arbuscular mycorrhizal fungi inoculation on yam (*Dioscorea* spp.) tuber weights and secondary metabolite content. PeerJ 3, e1266. https://doi.org/10.7717/peerj.1266

Ludwig-Müller, J., 2010. Hormonal Responses in Host Plants Triggered by Arbuscular Mycorrhizal Fungi, in: Koltai, H., Kapulnik, Y. (Eds.), Arbuscular Mycorrhizas: Physiology and Function. Springer Netherlands, Dordrecht, pp. 169–190. https://doi.org/10.1007/978-90-481-9489-6_8

Luginbuehl, L.H., Menard, G.N., Kurup, S., Van Erp, H., Radhakrishnan, G.V., Breakspear, A., Oldroyd, G.E.D., Eastmond, P.J., 2017. Fatty acids in arbuscular mycorrhizal

fungi are synthesized by the host plant. Science 356, 1175–1178. https://doi.org/10.1126/science.aan0081

Lugon-Moulin, N., Ryan, L., Donini, P., Rossi, L., 2006. Cadmium content of phosphate fertilizers used for tobacco production. Agron. Sustain. Dev. 26, 151–155. https://doi.org/10.1051/agro:2006010

Luo, C., Zou, L., Sun, H., Peng, J., Gao, C., Bao, L., Ji, R., Jin, Y., Sun, S., 2020. A Review of the Anti-Inflammatory Effects of Rosmarinic Acid on Inflammatory Diseases. Front. Pharmacol. 11, 153. https://doi.org/10.3389/fphar.2020.00153

Luthfiana, N., Inamura, N., Tantriani, Sato, T., Saito, K., Oikawa, A., Chen, W., Tawaraya, K., 2021. Metabolite profiling of the hyphal exudates of Rhizophagus clarus and Rhizophagus irregularis under phosphorus deficiency. Mycorrhiza 31, 403–412. https://doi.org/10.1007/s00572-020-01016-z

Ma, L., Tang, L., Yi, Q., 2019. Salvianolic Acids: Potential Source of Natural Drugs for the Treatment of Fibrosis Disease and Cancer. Front. Pharmacol. 10, 97. https://doi.org/10.3389/fphar.2019.00097

Maeda, T., Kobayashi, Y., Kameoka, H., Okuma, N., Takeda, N., Yamaguchi, K., Bino, T., Shigenobu, S., Kawaguchi, M., 2018. Evidence of non-tandemly repeated rDNAs and their intragenomic heterogeneity in Rhizophagus irregularis. Commun. Biol. 1, 87. https://doi.org/10.1038/s42003-018-0094-7

Mahesh, A., Jeyachandran, R., 2013. Influence of plant growth regulators on micropropagation and *in vitro* flowering of *Trichodesma indicum* (Linn) R. Br. Plant Biosyst. - Int. J. Deal. Asp. Plant Biol. 147, 493–499. https://doi.org/10.1080/11263504.2012.727876

Mahroug, S., Burlat, V., St-Pierre, B., 2007. Cellular and sub-cellular organisation of the monoterpenoid indole alkaloid pathway in Catharanthus roseus. Phytochem. Rev. 6, 363–381. https://doi.org/10.1007/s11101-006-9017-1

Maillet, F., Poinsot, V., André, O., Puech-Pagès, V., Haouy, A., Gueunier, M., Cromer, L., Giraudet, D., Formey, D., Niebel, A., Martinez, E.A., Driguez, H., Bécard, G., Dénarié, J., 2011. Fungal lipochitooligosaccharide symbiotic signals in arbuscular mycorrhiza. Nature 469, 58–63. https://doi.org/10.1038/nature09622

Malik, S., Bhushan, S., Sharma, M., Ahuja, P.S., 2016. Biotechnological approaches to the production of shikonins: a critical review with recent updates. Crit. Rev. Biotechnol. 36, 327–340. https://doi.org/10.3109/07388551.2014.961003

Marchev, A.S., Yordanova, Z.P., Georgiev, M.I., 2020. Green (cell) factories for advanced production of plant secondary metabolites. Crit. Rev. Biotechnol. 40, 443–458. https://doi.org/10.1080/07388551.2020.1731414

Marleau, J., Dalpé, Y., St-Arnaud, M., Hijri, M., 2011. Spore development and nuclear inheritance in arbuscular mycorrhizal fungi. BMC Evol. Biol. 11, 51. https://doi.org/10.1186/1471-2148-11-51

Martin, K., 2003. Rapid in vitro multiplication and ex vitro rooting of Rotula aquatica Lour., a rare rhoeophytic woody medicinal plant. Plant Cell Rep. 21, 415–420. https://doi.org/10.1007/s00299-002-0547-8

McGonigle, T.P., Miller, M.H., Evans, D.G., Fairchild, G.L., Swan, J.A., 1990. A new method which gives an objective measure of colonization of roots by vesicular-arbuscular mycorrhizal fungi. New Phytol. 115, 495–501. https://doi.org/10.1111/j.1469-8137.1990.tb00476.x

Merrow, M., Spoelstra, K., Roenneberg, T., 2005. The circadian cycle: daily rhythms from behaviour to genes: First in the Cycles Review Series. EMBO Rep. 6, 930–935. https://doi.org/10.1038/sj.embor.7400541

Meselhy, M.R., Kadota, S., Tsubono, K., Kusai, A., Hattori, M., Namba, T., 1994. Shikometabolins A, B, C and D, novel dimeric naphthoquinone metabolites obtained from shikonin by human intestinal bacteria. Tetrahedron Lett. 35, 583–586. https://doi.org/10.1016/S0040-4039(00)75844-8

Miransari, M., 2017. Arbuscular Mycorrhizal Fungi and Heavy Metal Tolerance in Plants, in: Wu, Q.-S. (Ed.), Arbuscular Mycorrhizas and Stress Tolerance of Plants. Springer Singapore, Singapore, pp. 147–161. https://doi.org/10.1007/978-981-10-4115-0_7

Miransari, M., Bahrami, H.A., Rejali, F., Malakouti, M.J., 2008. Using arbuscular mycorrhiza to alleviate the stress of soil compaction on wheat (Triticum aestivum L.) growth. Soil Biol. Biochem. 40, 1197–1206. https://doi.org/10.1016/j.soilbio.2007.12.014

Mitter, B., Brader, G., Afzal, M., Compant, S., Naveed, M., Trognitz, F., Sessitsch, A., 2013. Advances in Elucidating Beneficial

Interactions Between Plants, Soil, and Bacteria, in: Advances in Agronomy. Elsevier, pp. 381–445. https://doi.org/10.1016/B978-0-12-407685-3.00007-4

Mitter, B., Pfaffenbichler, N., Sessitsch, A., 2016. Plant–microbe partnerships in 2020. Microb. Biotechnol. 9, 635–640. https://doi.org/10.1111/1751-7915.12382

M.K. Rai, J.S. Shanker, J. Uma, 2009. Shoot multiplication and plant regeneration of guava (Psidium guajava L.) from nodal explants of in vitro raised plantlets. J. Fruit Ornam. Plant Res. 17 (1), 29–38.

Mori, N., Nishiuma, K., Sugiyama, T., Hayashi, H., Akiyama, K., 2016. Carlactone-type strigolactones and their synthetic analogues as inducers of hyphal branching in arbuscular mycorrhizal fungi. Phytochemistry 130, 90–98. https://doi.org/10.1016/j.phytochem.2016.05.012

Mugford, S.T., Osbourn, A., 2012. Saponin Synthesis and Function, in: Bach, T.J., Rohmer, M. (Eds.), Isoprenoid Synthesis in Plants and Microorganisms. Springer New York, New York, NY, pp. 405–424. https://doi.org/10.1007/978-1-4614-4063-5_28

Muniz, B.C., Falcão, E.L., Monteiro, R. de P., Santos, E.L. dos, Bastos Filho, C.J.A., Silva, F.S.B. da, 2021. Acaulospora longula Spain & N.C. Schenck: A low-cost bioinsumption to optimize phenolics and saponins production in Passiflora alata Curtis. Ind. Crops Prod. 167, 113498. https://doi.org/10.1016/j.indcrop.2021.113498

Munkvold, L., Kjøller, R., Vestberg, M., Rosendahl, S., Jakobsen, I., 2004. High functional diversity within species of arbuscular mycorrhizal fungi. New Phytol. 164, 357–364. https://doi.org/10.1111/j.1469-8137.2004.01169.x

Murashige, T., Skoog, F., 1962. A Revised Medium for Rapid Growth and Bio Assays with Tobacco Tissue Cultures. Physiol. Plant. 15, 473–497. https://doi.org/10.1111/j.1399-3054.1962.tb08052.x

Naik, P.M., Al-Khayri, J.M., 2016. Abiotic and Biotic Elicitors–Role in Secondary Metabolites Production through In Vitro Culture of Medicinal Plants, in: Shanker, A.K., Shanker, C. (Eds.), Abiotic and Biotic Stress in Plants - Recent Advances and Future Perspectives. InTech. https://doi.org/10.5772/61442

Nairn, B.J., Furneaux, R.H., Stevenson, T.T., 1995. Identification of an agar constituent responsible for hydric control in

micropropagation of radiata pine. Plant Cell Tissue Organ Cult. 43, 1–11. https://doi.org/10.1007/BF00042665

Namdeo, A.G., 2018. Cultivation of Medicinal and Aromatic Plants, in: Natural Products and Drug Discovery. Elsevier, pp. 525–553. https://doi.org/10.1016/B978-0-08-102081-4.00020-4

Neelam, Khatkar, A., Sharma, K.K., 2020. Phenylpropanoids and its derivatives: biological activities and its role in food, pharmaceutical and cosmetic industries. Crit. Rev. Food Sci. Nutr. 60, 2655–2675. https://doi.org/10.1080/10408398.2019.1653822

Nisha, M.C., 2010. Effect of arbuscular mycorrhizal fungi on growth and nutrition of Wedilia chinensis (Osbeck) Merril. Indian J. Sci. Technol. 3, 676–678. https://doi.org/10.17485/ijst/2010/v3i6.23

Nomoto, Y., Sugimoto, S., Matsunami, K., Otsuka, H., 2013. Hirtionosides A–C, gallates of megastigmane glucosides, 3-hydroxyoctanoic acid glucosides and a phenylpropanoid glucoside from the whole plants of Euphorbia hirta. J. Nat. Med. 67, 350–358. https://doi.org/10.1007/s11418-012-0692-5

Oldroyd, G.E.D., 2013. Speak, friend, and enter: signalling systems that promote beneficial symbiotic associations in plants. Nat. Rev. Microbiol. 11, 252–263. https://doi.org/10.1038/nrmicro2990

Omar, M.B., Bolland, L., Heather, W.A., 1978. A permanent mounting medium for fungi. Stain Technol. 53, 293–294.

P. Hubert, J.J. Nguyen-Huu, B. Boulanger, E. Chapuzet, P. Chiap, N. Cohen, P.A.Compagnon, W. Dewé, M. Feinberg, M. Lallier, M. Laurentie, N. Mercie, G.Muzard, C. Nivet, L. Valat, 2003. Validation des procédures analytiques quantitatives, Harmonisation des démarches. S.T.P. Pharma Pratiques 13, 101–138.

Pal, M., Chaudhury, A., 2010. High frequency direct plant regeneration, micropropagation and Shikonin induction in Arnebia hispidissima. J. Crop Sci. Biotechnol. 13, 13–19. https://doi.org/10.1007/s12892-009-0127-3

Panchal, P., Miller, A.J., Giri, J., 2021. Organic acids: versatile stress-response roles in plants. J. Exp. Bot. 72, 4038–4052. https://doi.org/10.1093/jxb/erab019

Pandey, D.K., Kaur, P., Dey, A., 2018a. Arbuscular Mycorrhizal Fungi: Effects on Secondary Metabolite Production in Medicinal Plants, in: Gehlot, P., Singh, J. (Eds.), Fungi and Their Role in Sustainable Development: Current Perspectives. Springer

Singapore, Singapore, pp. 507–538. https://doi.org/10.1007/978-981-13-0393-7_28

Pandey, D.K., Kaur, P., Dey, A., 2018b. Arbuscular Mycorrhizal Fungi: Effects on Secondary Metabolite Production in Medicinal Plants, in: Gehlot, P., Singh, J. (Eds.), Fungi and Their Role in Sustainable Development: Current Perspectives. Springer Singapore, Singapore, pp. 507–538. https://doi.org/10.1007/978-981-13-0393-7_28

Papageorgiou, V., Assimopoulou, A., Ballis, A., 2008. Alkannins and Shikonins: A New Class of Wound Healing Agents. Curr. Med. Chem. 15, 3248–3267. https://doi.org/10.2174/092986708786848532

Papageorgiou, V.P., Assimopoulou, A.N., Couladouros, E.A., Hepworth, D., Nicolaou, K.C., 1999. The Chemistry and Biology of Alkannin, Shikonin, and Related Naphthazarin Natural Products. Angew. Chem. Int. Ed Engl. 38, 270–301. https://doi.org/10.1002/(SICI)1521-3773(19990201)38:3<270::AID-ANIE270>3.0.CO;2-0

Park, H.Y., Kim, D.H., Saini, R.K., Gopal, J., Keum, Y.-S., Sivanesan, I., 2019. Micropropagation and Quantification of Bioactive Compounds in Mertensia maritima (L.) Gray. Int. J. Mol. Sci. 20, 2141. https://doi.org/10.3390/ijms20092141

Park, H.Y., Kim, D.H., Sivanesan, I., 2017. Micropropagation of Ajuga species: a mini review. Biotechnol. Lett. 39, 1291–1298. https://doi.org/10.1007/s10529-017-2376-4

Park, Y.J., Seong, S.H., Kim, M.S., Seo, S.W., Kim, M.R., Kim, H.S., 2017. High-throughput detection of antioxidants in mulberry fruit using correlations between high-resolution mass and activity profiles of chromatographic fractions. Plant Methods 13, 108. https://doi.org/10.1186/s13007-017-0258-3

Parniske, M., 2008. Arbuscular mycorrhiza: the mother of plant root endosymbioses. Nat. Rev. Microbiol. 6, 763–775. https://doi.org/10.1038/nrmicro1987

Pedone-Bonfim, M.V.L., da Silva, F.S.B., Maia, L.C., 2015. Production of secondary metabolites by mycorrhizal plants with medicinal or nutritional potential. Acta Physiol. Plant. 37, 27. https://doi.org/decler

Peñuelas, J., Llusià, J., 1997. Effects of Carbon Dioxide, Water Supply, and Seasonality on Terpene Content and Emission by Rosmarinus officinalis. J. Chem. Ecol. 23, 979–993. https://doi.org/10.1023/B:JOEC.0000006383.29650.d7

Pereira-Caro, G., Ludwig, I.A., Polyviou, T., Malkova, D., García, A., Moreno-Rojas, J.M., Crozier, A., 2016. Identification of Plasma and Urinary Metabolites and Catabolites Derived from Orange Juice (Poly)phenols: Analysis by High-Performance Liquid Chromatography–High-Resolution Mass Spectrometry. J. Agric. Food Chem. 64, 5724–5735. https://doi.org/10.1021/acs.jafc.6b02088

Perić, M., Dmitrović, S., Živković, S., Filipović, B., Skorić, M., Simonović, A., Todorović, S., 2012. In Vitro Growth, Morphogenesis, and Acclimatization of Endangered Rindera umbellata (Waldst. & Kit.) Bunge. HortScience 47, 1123–1128. https://doi.org/10.21273/HORTSCI.47.8.1123

Pfaffl, M.W., 2001. A new mathematical model for relative quantification in real-time RT-PCR. Nucleic Acids Res. 29, 45e–445. https://doi.org/10.1093/nar/29.9.e45

Phulwaria, M., Shekhawat, N.S., 2013. An efficient in vitro shoot regeneration from immature inflorescence and ex vitro rooting of Arnebia hispidissima (Lehm). DC. - A red dye (Alkannin) yielding plant. Physiol. Mol. Biol. Plants 19, 435–441. https://doi.org/10.1007/s12298-013-0171-9

Pinheiro, J.C., Bates, D.M.,. Mixed-Effects Models in S and S-PLUS.

Pinson, B., Vaur, S., Sagot, I., Coulpier, F., Lemoine, S., Daignan-Fornier, B., 2009. Metabolic intermediates selectively stimulate transcription factor interaction and modulate phosphate and purine pathways. Genes Dev. 23, 1399–1407. https://doi.org/10.1101/gad.521809

Plouznikoff, K., Declerck, S., Calonne-Salmon, M., 2016. Mitigating Abiotic Stresses in Crop Plants by Arbuscular Mycorrhizal Fungi, in: Vos, C.M.F., Kazan, K. (Eds.), Belowground Defence Strategies in Plants, Signaling and Communication in Plants. Springer International Publishing, Cham, pp. 341–400. https://doi.org/10.1007/978-3-319-42319-7_15

Pluskal, T., Castillo, S., Villar-Briones, A., Orešič, M., 2010. MZmine 2: Modular framework for processing, visualizing, and analyzing mass spectrometry-based molecular profile data. BMC Bioinformatics 11, 395. https://doi.org/10.1186/1471-2105-11-395

Pozo, M.J., Azcón-Aguilar, C., 2007. Unraveling mycorrhiza-induced resistance. Curr. Opin. Plant Biol. 10, 393–398. https://doi.org/10.1016/j.pbi.2007.05.004

Pozo, M.J., Jung, S.C., López-Ráez, J.A., Azcón-Aguilar, C., 2010. Impact of Arbuscular Mycorrhizal Symbiosis on Plant Response to Biotic Stress: The Role of Plant Defence Mechanisms, in: Koltai, H., Kapulnik, Y. (Eds.), Arbuscular Mycorrhizas: Physiology and Function. Springer Netherlands, Dordrecht, pp. 193–207. https://doi.org/10.1007/978-90-481-9489-6_9

Priyadharsini, P., Muthukumar, T., 2015. Insight into the Role of Arbuscular Mycorrhizal Fungi in Sustainable Agriculture, in: Thangavel, P., Sridevi, G. (Eds.), Environmental Sustainability. Springer India, New Delhi, pp. 3–37. https://doi.org/10.1007/978-81-322-2056-5_1

Q.L. Liu, H. Ma, Y.M. Zheng, 2003. Tissue Culture of Flower. China Agriculture Press 55–56.

Quiroga, G., Erice, G., Aroca, R., Zamarreño, Á.M., García-Mina, J.M., Ruiz-Lozano, J.M., 2018. Arbuscular mycorrhizal symbiosis and salicylic acid regulate aquaporins and root hydraulic properties in maize plants subjected to drought. Agric. Water Manag. 202, 271–284. https://doi.org/10.1016/j.agwat.2017.12.012

Rat, A., Naranjo, H.D., Krigas, N., Grigoriadou, K., Maloupa, E., Alonso, A.V., Schneider, C., Papageorgiou, V.P., Assimopoulou, A.N., Tsafantakis, N., Fokialakis, N., Willems, A., 2021. Endophytic Bacteria From the Roots of the Medicinal Plant Alkanna tinctoria Tausch (Boraginaceae): Exploration of Plant Growth Promoting Properties and Potential Role in the Production of Plant Secondary Metabolites. Front. Microbiol. 12, 633488. https://doi.org/10.3389/fmicb.2021.633488

Ratnayake Bandara, B.M., Jayasinghe, L., Karunaratne, V., Wannigama, G.P., Kraus, W., Bokel, M., Sotheeswaran, S., 1989. Diploclisin, a bidesmosidic triterpenoid saponin from Diploclisia glaucescens. Phytochemistry 28, 2783–2785. https://doi.org/10.1016/S0031-9422(00)98088-9

Redecker, D., Schüßler, A., Stockinger, H., Stürmer, S.L., Morton, J.B., Walker, C., 2013. An evidence-based consensus for the classification of arbuscular mycorrhizal fungi (Glomeromycota). Mycorrhiza 23, 515–531. https://doi.org/10.1007/s00572-013-0486-y

Rillig, M.C., 2004. Arbuscular mycorrhizae, glomalin, and soil aggregation. Can. J. Soil Sci. 84, 355–363. https://doi.org/10.4141/S04-003

Rivero, J., Gamir, J., Aroca, R., Pozo, M.J., Flors, V., 2015. Metabolic transition in mycorrhizal tomato roots. Front. Microbiol. 6. https://doi.org/10.3389/fmicb.2015.00598

Romussi, G., Ciarallo, G., Falsone, G., Schneider, C., 1979. Inhaltsstoffe von Boraginaceae Triterpensaponine aus Anchusa officinalis L. Liebigs Ann. Chem. 1979, 2028–2035. https://doi.org/10.1002/jlac.197919791213

Romussi, G., Falsone, G., Wendisch, D., Parodi, B., 1984a. Inhaltsstoffe von Boraginaceae, 7. Anchusosid-8 und -9: Zwei neue Triterpensaponine ausAnchusa officinalis L. Liebigs Ann. Chem. 1984, 1869–1872. https://doi.org/10.1002/jlac.198419841113

Romussi, G., Falsone, G., Wendisch, D., Parodi, B., 1984b. Inhaltsstoffe von Boraginaceae, 7. Anchusosid-8 und -9: Zwei neue Triterpensaponine aus Anchusa officinalis L. Liebigs Ann. Chem. 1984, 1869–1872. https://doi.org/10.1002/jlac.198419841113

Ruiz-Lozano, J.M., Azcon, R., Palma, J.M., 1996. Superoxide dismutase activity in arbuscular mycorrhizal Lactuca sativa plants subjected to drought stress. New Phytol. 134, 327–333. https://doi.org/10.1111/j.1469-8137.1996.tb04637.x

Ruiz-Lozano, J.M., Porcel, R., Azcon, C., Aroca, R., 2012. Regulation by arbuscular mycorrhizae of the integrated physiological response to salinity in plants: new challenges in physiological and molecular studies. J. Exp. Bot. 63, 4033–4044. https://doi.org/10.1093/jxb/ers126

Sabih Ozer, M., Sarikurkcu, C., Tepe, B., Can, S., 2010. Essential oil composition and antioxidant activities of alkanet (Alkanna tinctoria subsp. tinctoria). Food Sci. Biotechnol. 19, 1177–1183. https://doi.org/10.1007/s10068-010-0168-x

Sahoo, N., Manchikanti, P., Dey, S., 2010. Herbal drugs: Standards and regulation. Fitoterapia 81, 462–471. https://doi.org/10.1016/j.fitote.2010.02.001

Saia, S., Ruisi, P., Fileccia, V., Di Miceli, G., Amato, G., Martinelli, F., 2015. Metabolomics Suggests That Soil Inoculation with Arbuscular Mycorrhizal Fungi Decreased Free Amino Acid Content in Roots of Durum Wheat Grown under N-Limited, P-Rich Field Conditions. PLOS ONE 10, e0129591. https://doi.org/10.1371/journal.pone.0129591

Sang Un Park, Md Romij Uddin, Hui Xu, Yong Kyoung Kim, 2008. Biotechnological applications for rosmarinic acid production in plant. African Journal of Biotechnology 7, 4959–4965.

Satish, C.J., Boskey, P., Renuka, J., 2014. Rapid in vitro multiplication and biological potentialities of Sericostoma pauciflorum stocks ex Wight. J. Med. Plants Res. 8, 45–51. https://doi.org/10.5897/JMPR11.1273

Sbrana, C., Avio, L., Giovannetti, M., 2014. Beneficial mycorrhizal symbionts affecting the production of health-promoting phytochemicals: General. ELECTROPHORESIS 35, 1535–1546. https://doi.org/10.1002/elps.201300568

Schenck, N.C., Smith, G.S., 1982. Additional New and Unreported Species of Mycorrhizal Fungi (Endogonaceae) from Florida. Mycologia 74, 77–92. https://doi.org/10.1080/00275514.1982.12021472

Schliemann, W., Ammer, C., Strack, D., 2008. Metabolite profiling of mycorrhizal roots of Medicago truncatula. Phytochemistry 69, 112–146. https://doi.org/10.1016/j.phytochem.2007.06.032

Schweiger, R., Baier, M.C., Persicke, M., Müller, C., 2014. High specificity in plant leaf metabolic responses to arbuscular mycorrhiza. Nat. Commun. 5, 3886. https://doi.org/10.1038/ncomms4886

Selosse, M.-A., Baudoin, E., Vandenkoornhuyse, P., 2004. Symbiotic microorganisms, a key for ecological success and protection of plants. C. R. Biol. 327, 639–648. https://doi.org/10.1016/j.crvi.2003.12.008

Selvi, F., Bigazzi, M., 1998. *Anchusa* L. and allied genera (*Boraginaceae*) in Italy. Plant Biosyst. - Int. J. Deal. Asp. Plant Biol. 132, 113–142. https://doi.org/10.1080/11263504.1998.10654198

Sengul, M., Yildiz, H., Gungor, N., Cetin, B., Eser, Z., Ercisli, S., 2009. Total phenolic content, antioxidant and antimicrobial activities of some medicinal plants. Pak. J. Pharm. Sci. 22, 102–106.

Sgherri, C., Cecconami, S., Pinzino, C., Navari-Izzo, F., Izzo, R., 2010. Levels of antioxidants and nutraceuticals in basil grown in hydroponics and soil. Food Chem. 123, 416–422. https://doi.org/10.1016/j.foodchem.2010.04.058

Shannon, P., Markiel, A., Ozier, O., Baliga, N.S., Wang, J.T., Ramage, D., Amin, N., Schwikowski, B., Ideker, T., 2003. Cytoscape: A Software Environment for Integrated Models of Biomolecular

Interaction Networks. Genome Res. 13, 2498–2504. https://doi.org/10.1101/gr.1239303

Sharma, R. A., Singh, B., Singh, D., Chandrawat, P., 2009. Ethnomedicinal, pharmacological properties and chemistry of some medicinal plants of Boraginaceae in India. J. Med. Plants Res. 3 (13), 1153–1175.

Sharma, S., Shahzad, A., 2013. Elicitation: An Alternative Approach Towards Commercialization of Secondary Metabolite Production, in: Shahid, Mohd., Shahzad, A., Malik, A., Sahai, A. (Eds.), Recent Trends in Biotechnology and Therapeutic Applications of Medicinal Plants. Springer Netherlands, Dordrecht, pp. 79–91. https://doi.org/10.1007/978-94-007-6603-7_4

Sharma, Y., Velamuri, R., Fagan, J., Schaefer, J., 2020. Full-Spectrum Analysis of Bioactive Compounds in Rosemary (Rosmarinus officinalis L.) as Influenced by Different Extraction Methods. Molecules 25, 4599. https://doi.org/10.3390/molecules25204599

Shi, X., Yang, Y., Ren, H., Sun, S., Mu, L. ting, Chen, X., Wang, Y., Zhang, Y., Wang, L. hong, Sun, C., 2020. Identification of multiple components in deep eutectic solvent extract of Acanthopanax senticosus root by ultra-high-performance liquid chromatography with quadrupole orbitrap mass spectrometry. Phytochem. Lett. 35, 175–185. https://doi.org/10.1016/j.phytol.2019.11.017

Shim, S.-W., Hahn, E.-J., Paek, K.-Y., 2003. In vitro and ex vitro growth of grapevine rootstock '5BB' as influenced by number of air exchanges and the presence or absence of sucrose in culture media. Plant Cell Tissue Organ Cult. 75, 57–62. https://doi.org/10.1023/A:1024695510994

Shimomura, K., Sudo, H., Saga, H., Kamada, H., 1991. Shikonin production and secretion by hairy root cultures of Lithospermum erythrorhizon. Plant Cell Rep. 10. https://doi.org/10.1007/BF00193142

Shoemaker, C.A., 1994. Plants and Human Culture. J. Home Consum. Hortic. 1, 3–7. https://doi.org/10.1300/J280v01n02_02

Shohael, A.M., Chakrabarty, D., Ali, M.B., Yu, K.W., Hahn, E.J., Lee, H.L., Paek, K.Y., 2006. Enhancement of eleutherosides production in embryogenic cultures of Eleutherococcus sessiliflorus in response to sucrose-induced osmotic stress.

Process Biochem. 41, 512–518. https://doi.org/10.1016/j.procbio.2005.09.005

Shtark, O.Y., Puzanskiy, R.K., Avdeeva, G.S., Yurkov, A.P., Smolikova, G.N., Yemelyanov, V.V., Kliukova, M.S., Shavarda, A.L., Kirpichnikova, A.A., Zhernakov, A.I., Afonin, A.M., Tikhonovich, I.A., Zhukov, V.A., Shishova, M.F., 2019. Metabolic alterations in pea leaves during arbuscular mycorrhiza development. PeerJ 7, e7495. https://doi.org/10.7717/peerj.7495

Silva, J.A.T. da, 2004. The effect of carbon source on in vitro organogenesis of chrysanthemum thin cell layers. Bragantia 63, 165–177. https://doi.org/10.1590/S0006-87052004000200002

Simpson, N.J.K., 2000. Solid-Phase Extraction, 0 ed. CRC Press. https://doi.org/10.1201/9780367802653

Singh, R.S., Gara, R.K., Bhardwaj, P.K., Kaachra, A., Malik, S., Kumar, R., Sharma, M., Ahuja, P.S., Kumar, S., 2010. Expression of 3-hydroxy-3-methylglutaryl-CoA reductase, p-hydroxybenzoate-m-geranyltransferase and genes of phenylpropanoid pathway exhibits positive correlation with shikonins content in arnebia [Arnebia euchroma (Royle) Johnston]. BMC Mol. Biol. 11, 88. https://doi.org/10.1186/1471-2199-11-88

Singh, Sharma, 2014. Antioxidant and antimicrobial activities of Arnebia hispidissima. Am J Adv Drug Deliv. 2(2).

Skoneczny, D., Weston, P., Zhu, X., Gurr, G., Callaway, R., Barrow, R., Weston, L., 2017. Metabolic Profiling and Identification of Shikonins in Root Periderm of Two Invasive Echium spp. Weeds in Australia. Molecules 22, 330. https://doi.org/10.3390/molecules22020330

Smith, S.E., Jakobsen, I., Gronlund, M., Smith, F.A., 2011. Roles of Arbuscular Mycorrhizas in Plant Phosphorus Nutrition: Interactions between Pathways of Phosphorus Uptake in Arbuscular Mycorrhizal Roots Have Important Implications for Understanding and Manipulating Plant Phosphorus Acquisition. PLANT Physiol. 156, 1050–1057. https://doi.org/10.1104/pp.111.174581

Smith, S.E., Read, D., 2008a. Mineral nutrition, toxic element accumulation and water relations of arbuscular mycorrhizal plants, in: Mycorrhizal Symbiosis. Elsevier, pp. 145–VI. https://doi.org/10.1016/B978-012370526-6.50007-6

Smith, S.E., Read, D.J., 2008b. Mycorrhizal symbiosis, 3. ed., Repr. ed. Elsevier/Acad. Press, Amsterdam.

Soleyman Dayani, Mohammad R. Sabzalian, 2017. Production of Secondary Metabolites in Medicinal Plants through Hydroponic Systems, in: Controlled Environment Agriculture. Nova Science Publishers, Inc.

Song, W., Zhuang, Y., Liu, T., 2020. Potential role of two cytochrome P450s obtained from Lithospermum erythrorhizon in catalyzing the oxidation of geranylhydroquinone during Shikonin biosynthesis. Phytochemistry 175, 112375. https://doi.org/10.1016/j.phytochem.2020.112375

Srinivasulu, C., Ramgopal, M., Ramanjaneyulu, G., Anuradha, C.M., Suresh Kumar, C., 2018. Syringic acid (SA) – A Review of Its Occurrence, Biosynthesis, Pharmacological and Industrial Importance. Biomed. Pharmacother. 108, 547–557. https://doi.org/10.1016/j.biopha.2018.09.069

Srinroch, C., Sahakitpichan, P., Chimnoi, N., Ruchirawat, S., Kanchanapoom, T., 2020. Phenolic glycosides from Magnolia figo. Phytochem. Lett. 37, 110–115. https://doi.org/10.1016/j.phytol.2019.09.008

Srivastava, S., Conlan, X.A., Cahill, D.M., Adholeya, A., 2016. Rhizophagus irregularis as an elicitor of rosmarinic acid and antioxidant production by transformed roots of Ocimum basilicum in an in vitro co-culture system. Mycorrhiza 26, 919–930. https://doi.org/10.1007/s00572-016-0721-4

Stamatakis, A., 2014. RAxML version 8: a tool for phylogenetic analysis and post-analysis of large phylogenies. Bioinformatics 30, 1312–1313. https://doi.org/10.1093/bioinformatics/btu033

St-Pierre, B., Vazquez-Flota, F.A., De Luca, V., 1999. Multicellular Compartmentation of *Catharanthus roseus* Alkaloid Biosynthesis Predicts Intercellular Translocation of a Pathway Intermediate. Plant Cell 11, 887–900. https://doi.org/10.1105/tpc.11.5.887

Strader, L.C., Bartel, B., 2011. Transport and Metabolism of the Endogenous Auxin Precursor Indole-3-Butyric Acid. Mol. Plant 4, 477–486. https://doi.org/10.1093/mp/ssr006

Stringer, K.A., McKay, R.T., Karnovsky, A., Quémerais, B., Lacy, P., 2016. Metabolomics and Its Application to Acute Lung Diseases. Front. Immunol. 7. https://doi.org/10.3389/fimmu.2016.00044

Stringlis, I.A., de Jonge, R., Pieterse, C.M.J., 2019. The Age of Coumarins in Plant–Microbe Interactions. Plant Cell Physiol. 60, 1405–1419. https://doi.org/10.1093/pcp/pcz076

Strullu-Derrien, C., Strullu, D.-G., 2007. Mycorrhization of fossil and living plants. Comptes Rendus Palevol 6, 483–494. https://doi.org/10.1016/j.crpv.2007.09.006

Stürmer, S.L., Bever, J.D., Morton, J.B., 2018. Biogeography of arbuscular mycorrhizal fungi (Glomeromycota): a phylogenetic perspective on species distribution patterns. Mycorrhiza 28, 587–603. https://doi.org/10.1007/s00572-018-0864-6

Su, W.W., Asali, E.C., Humphrey, A.E., 1994. Anchusa officinalis: Production of Rosmarinic Acid in Perfusion Cell Cultures, in: Bajaj, Y.P.S. (Ed.), Medicinal and Aromatic Plants VI. Springer Berlin Heidelberg, Berlin, Heidelberg, pp. 1–20. https://doi.org/10.1007/978-3-642-57970-7_1

Su, W.W., Lei, F., Kao, N.P., 1995. High density cultivation of Anchusa officinalis in a stirred-tank bioreactor with in situ filtration. Appl. Microbiol. Biotechnol. 44, 293–299. https://doi.org/10.1007/BF00169919

Sun, L., Fan, K., Wang, L., Ma, D., Wang, Y., Kong, X., Li, H., Ren, Y., Ding, Z., 2021. Correlation among Metabolic Changes in Tea Plant Camellia sinensis (L.) Shoots, Green Tea Quality and the Application of Cow Manure to Tea Plantation Soils. Molecules 26, 6180. https://doi.org/10.3390/molecules26206180

Sun, L., Lu, Y., Kronzucker, H.J., Shi, W., 2016. Quantification and enzyme targets of fatty acid amides from duckweed root exudates involved in the stimulation of denitrification. J. Plant Physiol. 198, 81–88. https://doi.org/10.1016/j.jplph.2016.04.010

Sun, X., Chen, W., Ivanov, S., MacLean, A.M., Wight, H., Ramaraj, T., Mudge, J., Harrison, M.J., Fei, Z., 2019. Genome and evolution of the arbuscular mycorrhizal fungus *Diversispora epigaea* (formerly *Glomus versiforme*) and its bacterial endosymbionts. New Phytol. 221, 1556–1573. https://doi.org/10.1111/nph.15472

Suttiyut, T., Auber, R.P., Ghaste, M., Kane, C.N., McAdam, S.A.M., Wisecaver, J.H., Widhalm, J.R., 2022. Integrative analysis of the shikonin metabolic network identifies new gene connections and reveals evolutionary insight into shikonin biosynthesis. Hortic. Res. 9, uhab087. https://doi.org/10.1093/hr/uhab087

T. Ezati, M.J. Marefatjoo, K. Haghbeen, R. Ahmmadkhaniha, 2015. Successful indirect regeneration of Arnebia pulchra (Roemer and Schultes) as medicinal plant. J. Med. Plants -Prod. 2, 233–242.

Taamalli, A., Arráez-Román, D., Abaza, L., Iswaldi, I., Fernández-Gutiérrez, A., Zarrouk, M., Segura-Carretero, A., 2015. LC-MS-based metabolite profiling of methanolic extracts from the medicinal and aromatic species Mentha pulegium and Origanum majorana. Phytochem. Anal. 26, 320–330. https://doi.org/10.1002/pca.2566

Taiz, L., Zeiger, E., 2010. Plant physiology, 5. ed. ed. Sinauer Assoc, Sunderland, Mass.

Takanashi, K., Nakagawa, Y., Aburaya, S., Kaminade, K., Aoki, W., Saida-Munakata, Y., Sugiyama, A., Ueda, M., Yazaki, K., 2019. Comparative Proteomic Analysis of *Lithospermum erythrorhizon* Reveals Regulation of a Variety of Metabolic Enzymes Leading to Comprehensive Understanding of the Shikonin Biosynthetic Pathway. Plant Cell Physiol. 60, 19–28. https://doi.org/10.1093/pcp/pcy183

Tamanna, N., Mahmood, N., 2014. Emerging Roles of Branched-Chain Amino Acid Supplementation in Human Diseases. Int. Sch. Res. Not. 2014, 1–8. https://doi.org/10.1155/2014/235619

Tang, C., Li, S., Wang, Y., Wang, X., 2020. Comparative genome/transcriptome analysis probes Boraginales' phylogenetic position, WGDs in Boraginales, and key enzyme genes in the alkannin/shikonin core pathway. Mol. Ecol. Resour. 20, 228–241. https://doi.org/10.1111/1755-0998.13104

Tanvir, R., Javeed, A., Rehman, Y., 2018. Fatty acids and their amide derivatives from endophytes: new therapeutic possibilities from a hidden source. FEMS Microbiol. Lett. 365. https://doi.org/10.1093/femsle/fny114

Tappeiner, J., Vasiliou, A., Ganzera, M., Fessas, D., Stuppner, H., Papageorgiou, V.P., Assimopoulou, A.N., 2014. Quantitative determination of alkannins and shikonins in endemic Mediterranean *Alkanna* species: Quantitative determination of alkannins and shikonins. Biomed. Chromatogr. 28, 923–933. https://doi.org/10.1002/bmc.3096

Tatsumi, K., Yano, M., Kaminade, K., Sugiyama, A., Sato, M., Toyooka, K., Aoyama, T., Sato, F., Yazaki, K., 2016. Characterization of Shikonin Derivative Secretion in Lithospermum erythrorhizon Hairy Roots as a Model of Lipid-

Soluble Metabolite Secretion from Plants. Front. Plant Sci. 7. https://doi.org/10.3389/fpls.2016.01066

Tedersoo, L., Bahram, M., Zobel, M., 2020. How mycorrhizal associations drive plant population and community biology. Science 367, eaba1223. https://doi.org/10.1126/science.aba1223

Tesfa, M., Admassu, B., 2016. In Vitro Rooting and Acclimatization of Micropropagated Elite Sugarcane (Saccharum officinarum L.)Genotypes - N52 and N53. J. Tissue Sci. Eng. 07. https://doi.org/10.4172/2157-7552.1000164

Tisserant, E., Malbreil, M., Kuo, A., Kohler, A., Symeonidi, A., Balestrini, R., Charron, P., Duensing, N., Frei dit Frey, N., Gianinazzi-Pearson, V., Gilbert, L.B., Handa, Y., Herr, J.R., Hijri, M., Koul, R., Kawaguchi, M., Krajinski, F., Lammers, P.J., Masclaux, F.G., Murat, C., Morin, E., Ndikumana, S., Pagni, M., Petitpierre, D., Requena, N., Rosikiewicz, P., Riley, R., Saito, K., San Clemente, H., Shapiro, H., van Tuinen, D., Becard, G., Bonfante, P., Paszkowski, U., Shachar-Hill, Y.Y., Tuskan, G.A., Young, J.P.W., Sanders, I.R., Henrissat, B., Rensing, S.A., Grigoriev, I.V., Corradi, N., Roux, C., Martin, F., 2013. Genome of an arbuscular mycorrhizal fungus provides insight into the oldest plant symbiosis. Proc. Natl. Acad. Sci. 110, 20117–20122. https://doi.org/10.1073/pnas.1313452110

Ton, J., Flors, V., Mauch-Mani, B., 2009. The multifaceted role of ABA in disease resistance. Trends Plant Sci. 14, 310–317. https://doi.org/10.1016/j.tplants.2009.03.006

Torres, Hilbert, Antolín, Goicoechea, 2019. Aminoacids and Flavonoids Profiling in Tempranillo Berries Can Be Modulated by the Arbuscular Mycorrhizal Fungi. Plants 8, 400. https://doi.org/10.3390/plants8100400

Toussaint, J.-P., 2007. Investigating physiological changes in the aerial parts of AM plants: what do we know and where should we be heading? Mycorrhiza 17, 349–353. https://doi.org/10.1007/s00572-007-0133-6

Toussaint, J.-P., Smith, F.A., Smith, S.E., 2007. Arbuscular mycorrhizal fungi can induce the production of phytochemicals in sweet basil irrespective of phosphorus nutrition. Mycorrhiza 17, 291–297. https://doi.org/10.1007/s00572-006-0104-3

Trépanier, M., Bécard, G., Moutoglis, P., Willemot, C., Gagné, S., Avis, T.J., Rioux, J.-A., 2005. Dependence of Arbuscular-Mycorrhizal Fungi on Their Plant Host for Palmitic Acid

Synthesis. Appl. Environ. Microbiol. 71, 5341–5347. https://doi.org/10.1128/AEM.71.9.5341-5347.2005

Trouvelot, S., HÃ©loir, M.-C., Poinssot, B., Gauthier, A., Paris, F., Guillier, C., Combier, M., TrdÃ¡, L., Daire, X., Adrian, M., 2014. Carbohydrates in plant immunity and plant protection: roles and potential application as foliar sprays. Front. Plant Sci. 5. https://doi.org/10.3389/fpls.2014.00592

Tsiokanos, E., Cartabia, A., Tsafantakis, N., Lalaymia, I., Termentzi, A., Miguel, M., Declerck, S., Fokialakis, N., 2022. The Metabolic Profile of Anchusa officinalis L. Differs According to Its Associated Arbuscular Mycorrhizal Fungi. Metabolites 12, 573. https://doi.org/10.3390/metabo12070573

Tsuzuki, S., 2016. Strigolactone-Induced Putative Secreted Protein 1 Is Required for the Establishment of Symbiosis by the Arbuscular Mycorrhizal Fungus Rhizophagus irregularis. Mol. Plant. Microbe Interact. v. 29, 277-286pp. 10. https://doi.org/10.1094/MPMI-10-15-0234-R

Turker, A.B. Yildirim, I. Taş, 2018. In vitro adventitious plant regeneration of Echium orientale L., an endemic plant: the evaluation of biological activities and phenolic content. Indian J. Biochem. Biophys 55 (4), 264–272.

Urbanek, H., Bergier, K., Saniewski, M., Patykowski, J., 1996. Effect of jasmonates and exogenous polysaccharides on production of alkannin pigments in suspension cultures of Alkanna tinctoria. Plant Cell Rep. 15, 637–641. https://doi.org/10.1007/BF00232468

Valdés, B., 2011. Boraginaceae. In: Euro+Med Plantbase: The information resource for Euro-Mediterranean plant diversity [WWW Document]. Httpww2bgbm OrgEuroPlusMed. URL (accessed 3.22.21).

Varela Alonso, A., Naranjo, H.D., Rat, A., Rodić, N., Nannou, C.I., Lambropoulou, D.A., Assimopoulou, A.N., Declerck, S., Rödel, P., Schneider, C., Willems, A., 2022. Root-associated bacteria modulate the specialised metabolome of Lithospermum officinale L. Front. Plant Sci. 13, 908669. https://doi.org/10.3389/fpls.2022.908669

Venturi, V., Keel, C., 2016. Signaling in the Rhizosphere. Trends Plant Sci. 21, 187–198. https://doi.org/10.1016/j.tplants.2016.01.005

Villas-Bôas, S.G., Mas, S., Åkesson, M., Smedsgaard, J., Nielsen, J., 2005. Mass spectrometry in metabolome analysis. Mass

Spectrom. Rev. 24, 613–646. https://doi.org/10.1002/mas.20032

Vincenti, F., Montesano, C., Di Ottavio, F., Gregori, A., Compagnone, D., Sergi, M., Dorrestein, P., 2020. Molecular Networking: A Useful Tool for the Identification of New Psychoactive Substances in Seizures by LC–HRMS. Front. Chem. 8, 572952. https://doi.org/10.3389/fchem.2020.572952

Voges, M.J.E.E.E., Bai, Y., Schulze-Lefert, P., Sattely, E.S., 2019. Plant-derived coumarins shape the composition of an *Arabidopsis* synthetic root microbiome. Proc. Natl. Acad. Sci. 116, 12558–12565. https://doi.org/10.1073/pnas.1820691116

Wagg, C., Jansa, J., Schmid, B., van der Heijden, M.G.A., 2011. Belowground biodiversity effects of plant symbionts support aboveground productivity: Biodiversity effects of soil symbionts. Ecol. Lett. 14, 1001–1009. https://doi.org/10.1111/j.1461-0248.2011.01666.x

Walker, C., 2005. A simple blue staining technique for arbuscular mycorrhizal and other root-inhabiting fungi. Inoculum 56.

Walker, C., Schüßler, A., Vincent, B., Cranenbrouck, S., Declerck, S., 2021a. Anchoring the species Rhizophagus intraradices (formerly Glomus intraradices). Fungal Syst. Evol. https://doi.org/10.3114/fuse.2021.08.14

Walker, C., Schüßler, A., Vincent, B., Cranenbrouck, S., Declerck, S., 2021b. Anchoring the species Rhizophagus intraradices (formerly Glomus intraradices) [WWW Document]. https://doi.org/10.3114/fuse.2021.08.14

Wang, E., Yu, N., Bano, S.A., Liu, C., Miller, A.J., Cousins, D., Zhang, X., Ratet, P., Tadege, M., Mysore, K.S., Downie, J.A., Murray, J.D., Oldroyd, G.E.D., Schultze, M., 2014. A H+-ATPase That Energizes Nutrient Uptake during Mycorrhizal Symbioses in Rice and *Medicago truncatula*. Plant Cell 26, 1818–1830. https://doi.org/10.1105/tpc.113.120527

Wang, M., Carver, J.J., Phelan, V.V., Sanchez, L.M., Garg, N., Peng, Y., Nguyen, D.D., Watrous, J., Kapono, C.A., Luzzatto-Knaan, T., Porto, C., Bouslimani, A., Melnik, A.V., Meehan, M.J., Liu, W.-T., Crüsemann, M., Boudreau, P.D., Esquenazi, E., Sandoval-Calderón, M., Kersten, R.D., Pace, L.A., Quinn, R.A., Duncan, K.R., Hsu, C.-C., Floros, D.J., Gavilan, R.G., Kleigrewe, K., Northen, T., Dutton, R.J., Parrot, D., Carlson, E.E., Aigle, B., Michelsen, C.F., Jelsbak, L., Sohlenkamp, C., Pevzner, P., Edlund, A., McLean, J., Piel, J., Murphy, B.T.,

Gerwick, L., Liaw, C.-C., Yang, Y.-L., Humpf, H.-U., Maansson, M., Keyzers, R.A., Sims, A.C., Johnson, A.R., Sidebottom, A.M., Sedio, B.E., Klitgaard, A., Larson, C.B., Boya P, C.A., Torres-Mendoza, D., Gonzalez, D.J., Silva, D.B., Marques, L.M., Demarque, D.P., Pociute, E., O'Neill, E.C., Briand, E., Helfrich, E.J.N., Granatosky, E.A., Glukhov, E., Ryffel, F., Houson, H., Mohimani, H., Kharbush, J.J., Zeng, Y., Vorholt, J.A., Kurita, K.L., Charusanti, P., McPhail, K.L., Nielsen, K.F., Vuong, L., Elfeki, M., Traxler, M.F., Engene, N., Koyama, N., Vining, O.B., Baric, R., Silva, R.R., Mascuch, S.J., Tomasi, S., Jenkins, S., Macherla, V., Hoffman, T., Agarwal, V., Williams, P.G., Dai, J., Neupane, R., Gurr, J., Rodríguez, A.M.C., Lamsa, A., Zhang, C., Dorrestein, K., Duggan, B.M., Almaliti, J., Allard, P.-M., Phapale, P., Nothias, L.-F., Alexandrov, T., Litaudon, M., Wolfender, J.-L., Kyle, J.E., Metz, T.O., Peryea, T., Nguyen, D.-T., VanLeer, D., Shinn, P., Jadhav, A., Müller, R., Waters, K.M., Shi, W., Liu, X., Zhang, L., Knight, R., Jensen, P.R., Palsson, B.Ø., Pogliano, K., Linington, R.G., Gutiérrez, M., Lopes, N.P., Gerwick, W.H., Moore, B.S., Dorrestein, P.C., Bandeira, N., 2016. Sharing and community curation of mass spectrometry data with Global Natural Products Social Molecular Networking. Nat. Biotechnol. 34, 828–837. https://doi.org/10.1038/nbt.3597

Wang, P., Yao, Z., Zhang, F., Shen, X., Dai, Y., Qin, L., Yao, X., 2015. Identification of metabolites of PSORALEAE FRUCTUS in rats by ultra performance liquid chromatography coupled with quadrupole time-of-flight tandem mass spectrometry analysis. J. Pharm. Biomed. Anal. 112, 23–35. https://doi.org/10.1016/j.jpba.2015.03.026

Wang, S., Alseekh, S., Fernie, A.R., Luo, J., 2019. The Structure and Function of Major Plant Metabolite Modifications. Mol. Plant 12, 899–919. https://doi.org/10.1016/j.molp.2019.06.001

Wang, S., Guo, L.P., Xie, T., Yang, J., Tang, J.F., Li, X., Wang, X., Huang, L.Q., 2014. Different secondary metabolic responses to MeJA treatment in shikonin-proficient and shikonin-deficient cell lines from Arnebia euchroma (Royle) Johnst. Plant Cell Tissue Organ Cult. PCTOC 119, 587–598. https://doi.org/10.1007/s11240-014-0558-5

Wang, W., Shi, J., Xie, Q., Jiang, Y., Yu, N., Wang, E., 2017. Nutrient Exchange and Regulation in Arbuscular Mycorrhizal

Symbiosis. Mol. Plant 10, 1147–1158. https://doi.org/10.1016/j.molp.2017.07.012

Wang, X., Larkins, B.A., 2001. Genetic Analysis of Amino Acid Accumulation in *opaque-2* Maize Endosperm. Plant Physiol. 125, 1766–1777. https://doi.org/10.1104/pp.125.4.1766

Wang, X., Lv, H., Sun, H., Liu, L., Sun, W., Cao, H., 2007a. Development of a rapid and validated method for investigating the metabolism of scoparone in rat using ultra-performance liquid chromatography/electrospray ionization quadruple time-of-flight mass spectrometry. Rapid Commun. Mass Spectrom. 21, 3883–3890. https://doi.org/10.1002/rcm.3296

Wang, X., Lv, H., Sun, H., Liu, L., Sun, W., Cao, H., 2007b. Development of a rapid and validated method for investigating the metabolism of scoparone in rat using ultra-performance liquid chromatography/electrospray ionization quadruple time-of-flight mass spectrometry. Rapid Commun. Mass Spectrom. 21, 3883–3890. https://doi.org/10.1002/rcm.3296

Wang, X., Yang, Y., Liu, X., Gao, X., 2020. Pharmacological properties of tanshinones, the natural products from Salvia miltiorrhiza, in: Advances in Pharmacology. Elsevier, pp. 43–70. https://doi.org/10.1016/bs.apha.2019.10.001

Waters, M.T., Gutjahr, C., Bennett, T., Nelson, D.C., 2017. Strigolactone Signaling and Evolution. Annu. Rev. Plant Biol. 68, 291–322. https://doi.org/10.1146/annurev-arplant-042916-040925

Weston, L.A., Ryan, P.R., Watt, M., 2012. Mechanisms for cellular transport and release of allelochemicals from plant roots into the rhizosphere. J. Exp. Bot. 63, 3445–3454. https://doi.org/10.1093/jxb/ers054

Weston, L.A., Skoneczny, D., Weston, P.A., Weidenhamer, J.D., 2015. Metabolic profiling: An overview - new approaches for the detection and functional analysis of biologically active secondary plant products.

Wewer, V., Brands, M., Dörmann, P., 2014. Fatty acid synthesis and lipid metabolism in the obligate biotrophic fungus *Rhizophagus irregularis* during mycorrhization of *Lotus japonicus*. Plant J. 79, 398–412. https://doi.org/10.1111/tpj.12566

Whiteside, M.D., Garcia, M.O., Treseder, K.K., 2012. Amino Acid Uptake in Arbuscular Mycorrhizal Plants. PLoS ONE 7, e47643. https://doi.org/10.1371/journal.pone.0047643

Widhalm, J.R., Dudareva, N., 2015. A Familiar Ring to It: Biosynthesis of Plant Benzoic Acids. Mol. Plant 8, 83–97. https://doi.org/10.1016/j.molp.2014.12.001

Wolfender, J.-L., Rudaz, S., Choi, Y.H., Kim, H.K., 2013. Plant metabolomics: from holistic data to relevant biomarkers. Curr. Med. Chem. 20, 1056–1090.

Worley, B., Powers, R., 2012. Multivariate Analysis in Metabolomics. Curr. Metabolomics 1, 92–107. https://doi.org/10.2174/2213235X11301010092

Wu, C.-H., Dewir, Y.H., Hahn, E.-J., Paek, K.-Y., 2006. Optimization of culturing conditions for the production of biomass and phenolics from adventitious roots ofEchinacea angustifolia. J. Plant Biol. 49, 193–199. https://doi.org/10.1007/BF03030532

Wu, F.-Y., Tang, C.-Y., Guo, Y.-M., Bian, Z.-W., Fu, J.-Y., Lu, G.-H., Qi, J.-L., Pang, Y.-J., Yang, Y.-H., 2017. Transcriptome analysis explores genes related to shikonin biosynthesis in Lithospermeae plants and provides insights into Boraginales' evolutionary history. Sci. Rep. 7, 4477. https://doi.org/10.1038/s41598-017-04750-1

Wu, H., Yu, X., Teixeira da Silva, J.A., Lu, G., 2011. Direct shoot induction of *Paeonia lactiflora* 'Zhong Sheng Fen' and rejuvenation of hyperhydric shoots. N. Z. J. Crop Hortic. Sci. 39, 271–278. https://doi.org/10.1080/01140671.2011.594445

Wu, Q.-S., Xia, R.-X., 2006. Arbuscular mycorrhizal fungi influence growth, osmotic adjustment and photosynthesis of citrus under well-watered and water stress conditions. J. Plant Physiol. 163, 417–425. https://doi.org/10.1016/j.jplph.2005.04.024

Wu, Q.-S., Zou, Y.-N., 2017. Arbuscular Mycorrhizal Fungi and Tolerance of Drought Stress in Plants, in: Wu, Q.-S. (Ed.), Arbuscular Mycorrhizas and Stress Tolerance of Plants. Springer Singapore, Singapore, pp. 25–41. https://doi.org/10.1007/978-981-10-4115-0_2

Wu, S.-J., Qi, J.-L., Zhang, W.-J., Liu, S.-H., Xiao, F.-H., Zhang, M.-S., Xu, G.-H., Zhao, W.-G., Shi, M.-W., Pang, Y.-J., Shen, H.-G., Yang, Y.-H., 2009. Nitric Oxide Regulates Shikonin Formation in Suspension-Cultured Onosma paniculatum Cells. Plant Cell Physiol. 50, 118–128. https://doi.org/10.1093/pcp/pcn178

Wu, Y.-H., Wang, H., Liu, M., Li, B., Chen, X., Ma, Y.-T., Yan, Z.-Y., 2021. Effects of Native Arbuscular Mycorrhizae Isolated on Root Biomass and Secondary Metabolites of Salvia miltiorrhiza

Bge. Front. Plant Sci. 12, 617892. https://doi.org/10.3389/fpls.2021.617892

Wu, Y.-T., Chen, Y.-F., Hsieh, Y.-J., Jaw, I., Shiao, M.-S., Tsai, T.-H., 2006. Bioavailability of salvianolic acid B in conscious and freely moving rats. Int. J. Pharm. 326, 25–31. https://doi.org/10.1016/j.ijpharm.2006.07.003

Xie, M.-M., Chen, S.-M., Zou, Y.-N., Srivastava, A.K., Rahman, M.M., Wu, Q.-S., Kuča, K., 2021. Effects of Rhizophagus intraradices and Rhizobium trifolii on growth and N assimilation of white clover. Plant Growth Regul. 93, 311–318. https://doi.org/10.1007/s10725-020-00689-y

Xie, W., Hao, Z., Zhou, X., Jiang, X., Xu, L., Wu, S., Zhao, A., Zhang, X., Chen, B., 2018. Arbuscular mycorrhiza facilitates the accumulation of glycyrrhizin and liquiritin in Glycyrrhiza uralensis under drought stress. Mycorrhiza 28, 285–300. https://doi.org/10.1007/s00572-018-0827-y

Xu, J., Aileni, M., Abbagani, S., Zhang, P., 2010. A reliable and efficient method for total rna isolation from various members of spurge family (Euphorbiaceae). Phytochem. Anal. 21, 395–398. https://doi.org/10.1002/pca.1205

Xue, L., Wang, E., 2020. Arbuscular mycorrhizal associations and the major regulators. Front. Agric. Sci. Eng. 7, 296. https://doi.org/10.15302/J-FASE-2020347

Yamamoto, H., Inoue, K., Li, S.-M., Heide, L., 2000. Geranylhydroquinone 3″-hydroxylase, a cytochrome P-450 monooxygenase from Lithospermum erythrorhizon cell suspension cultures. Planta 210, 312–317. https://doi.org/10.1007/PL00008139

Yaman, S. Uranbey, H.A, H.A. Ahmed, S. Özcan, O. Tugay, D. Başalma, 2019. Callus induction and regeneration of Alkanna orientalis var. orientalis and A. sieheana. Bangladesh J. Bot. 48 (3), 633–640.

Yan, Y., Tan, F., Miao, H., Wang, H., Cao, Y., 2019. Effect of Shikonin Against Candida albicans Biofilms. Front. Microbiol. 10, 1085. https://doi.org/10.3389/fmicb.2019.01085

Yang, C.-Q., Fang, X., Wu, X.-M., Mao, Y.-B., Wang, L.-J., Chen, X.-Y., 2012. Transcriptional Regulation of Plant Secondary Metabolism [F]. J. Integr. Plant Biol. 54, 703–712. https://doi.org/10.1111/j.1744-7909.2012.01161.x

Yang, Y., Ou, X., Yang, G., Xia, Y., Chen, M., Guo, L., Liu, D., 2017. Arbuscular Mycorrhizal Fungi Regulate the Growth and Phyto-

Active Compound of Salvia miltiorrhiza Seedlings. Appl. Sci. 7, 68. https://doi.org/10.3390/app7010068

Yazaki, K., 2017. Lithospermum erythrorhizon cell cultures: Present and future aspects. Plant Biotechnol. 34, 131–142. https://doi.org/10.5511/plantbiotechnology.17.0823a

Yazaki, K., Kunihisa, M., Fujisaki, T., Sato, F., 2002. Geranyl Diphosphate:4-Hydroxybenzoate Geranyltransferase fromLithospermum erythrorhizon. J. Biol. Chem. 277, 6240–6246. https://doi.org/10.1074/jbc.M106387200

Zare, K., Nazemiyeh, H., Movafeghi, A., Khosrowshahli, M., Motallebi-Azar, A., Dadpour, M., Omidi, Y., 2010. Bioprocess engineering of Echium italicum L.: induction of shikonin and alkannin derivatives by two-liquid-phase suspension cultures. Plant Cell Tissue Organ Cult. PCTOC 100, 157–164. https://doi.org/10.1007/s11240-009-9631-x

Zeng, Y., Guo, L.-P., Chen, B.-D., Hao, Z.-P., Wang, J.-Y., Huang, L.-Q., Yang, G., Cui, X.-M., Yang, L., Wu, Z.-X., Chen, M.-L., Zhang, Y., 2013a. Arbuscular mycorrhizal symbiosis and active ingredients of medicinal plants: current research status and prospectives. Mycorrhiza 23, 253–265. https://doi.org/10.1007/s00572-013-0484-0

Zeng, Y., Guo, L.-P., Chen, B.-D., Hao, Z.-P., Wang, J.-Y., Huang, L.-Q., Yang, G., Cui, X.-M., Yang, L., Wu, Z.-X., Chen, M.-L., Zhang, Y., 2013b. Arbuscular mycorrhizal symbiosis and active ingredients of medicinal plants: current research status and prospectives. Mycorrhiza 23, 253–265. https://doi.org/10.1007/s00572-013-0484-0

Zengin, G., Uysal, A., Diuzheva, A., Gunes, E., Jekő, J., Cziáky, Z., Picot-Allain, C.M.N., Mahomoodally, M.F., 2018. Characterization of phytochemical components of Ferula halophila extracts using HPLC-MS/MS and their pharmacological potentials: a multi-functional insight. J. Pharm. Biomed. Anal. 160, 374–382. https://doi.org/10.1016/j.jpba.2018.08.020

Zhang, D., Miyase, T., Kuroyanagi, M., Umehara, K., Noguchi, H., 1998. Oligosaccharide polyesters from roots of Polygala glomerata. Phytochemistry 47, 45–52. https://doi.org/10.1016/S0031-9422(97)00490-1

Zhang, H., Gong, C., Lv, L., Xu, Y., Zhao, L., Zhu, Z., Chai, Y., Zhang, G., 2009a. Rapid separation and identification of furocoumarins in *Angelica dahurica* by high-performance liquid

chromatography with diode-array detection, time-of-flight mass spectrometry and quadrupole ion trap mass spectrometry: Identification of furocoumarins in *Angelica dahurica*. Rapid Commun. Mass Spectrom. 23, 2167–2175. https://doi.org/10.1002/rcm.4123

Zhang, H., Gong, C., Lv, L., Xu, Y., Zhao, L., Zhu, Z., Chai, Y., Zhang, G., 2009b. Rapid separation and identification of furocoumarins in Angelica dahurica by high-performance liquid chromatography with diode-array detection, time-of-flight mass spectrometry and quadrupole ion trap mass spectrometry. Rapid Commun. Mass Spectrom. 23, 2167–2175. https://doi.org/10.1002/rcm.4123

Zhang, J., Zhou, J.-M., 2010. Plant Immunity Triggered by Microbial Molecular Signatures. Mol. Plant 3, 783–793. https://doi.org/10.1093/mp/ssq035

Zhang, N., Luo, J., Bhattacharya, D., 2017. Advances in Fungal Phylogenomics and Their Impact on Fungal Systematics, in: Advances in Genetics. Elsevier, pp. 309–328. https://doi.org/10.1016/bs.adgen.2017.09.004

Zhao, H., Chang, Q.S., Zhang, D.X., Fang, R.J., Zhao, H., Wu, F.Y., Wang, X.M., Lu, G.H., Qi, J.L., Yang, Y.H., 2015. Overexpression of LeMYB1 enhances shikonin formation by up-regulating key shikonin biosynthesis-related genes in Lithospermum erythrorhizon. Biol. Plant. 59, 429–435. https://doi.org/10.1007/s10535-015-0512-3

Zhao, Y., Cartabia, A., Lalaymia, I., Declerck, S., 2022. Arbuscular mycorrhizal fungi and production of secondary metabolites in medicinal plants. Mycorrhiza. https://doi.org/10.1007/s00572-022-01079-0

Zhu, X., Song, F., Liu, F., 2016. Altered amino acid profile of arbuscular mycorrhizal maize plants under low temperature stress. J. Plant Nutr. Soil Sci. 179, 186–189. https://doi.org/10.1002/jpln.201400165

Zou, A., Zhang, W., Pan, Q., Zhu, S., Yin, J., Tian, R., Gu, H., Wang, X., Qi, J., Yang, Y., 2011. Cloning, characterization, and expression of LeEIL-1, an Arabidopsis EIN3 homolog, in Lithospermum erythrorhizon. Plant Cell Tissue Organ Cult. PCTOC 106, 71–79. https://doi.org/10.1007/s11240-010-9895-1

Zubek, S., Błaszkowski, J., Mleczko, P., 2011. Arbuscular mycorrhizal and dark septate endophyte associations of medicinal plants.

Acta Soc. Bot. Pol. 80, 285–292. https://doi.org/10.5586/asbp.2011.033

Zubek, S., Nobis, M., Błaszkowski, J., Nowak, A., Majewska, M.L., Bąba, W., 2016. Arbuscular mycorrhiza and fungal root endophytes of weeds in an altitudinal gradient in the Pamir Alai Mountains of Central Asia. Plant Biosyst. - Int. J. Deal. Asp. Plant Biol. 150, 161–170. https://doi.org/10.1080/11263504.2014.990944

Zubek, S., Rola, K., Szewczyk, A., Majewska, M.L., Turnau, K., 2015. Enhanced concentrations of elements and secondary metabolites in Viola tricolor L. induced by arbuscular mycorrhizal fungi. Plant Soil 390, 129–142. https://doi.org/10.1007/s11104-015-2388-6